

RUSSIAN GEOGRAPHICAL SOCIETY

FACULTY OF GEOGRAPHY,
LOMONOSOV MOSCOW STATE UNIVERSITY

INSTITUTE OF GEOGRAPHY,
RUSSIAN ACADEMY OF SCIENCE

Vol. 11

2018

No. 01

GEOGRAPHY

ENVIRONMENT

SUSTAINABILITY

Special Issue: Pan-Eurasian
Experiment (PEEX)

Issue Guest Editors: Sergey Dobrolyubov,
Natalia Chubarova, Veli-Matti Kerminen

EDITORIAL BOARD

EDITORS-IN-CHIEF:

Kasimov Nikolay S.

Lomonosov Moscow State University,
Faculty of Geography, Russia

Kotlyakov Vladimir M.

Russian Academy of Sciences
Institute of Geography, Russia

DEPUTY EDITORS-IN-CHIEF:

Solomina Olga N.

Russian Academy of
Sciences, Institute of
Geography, Russia

Tikunov Vladimir S.

Lomonosov Moscow
State University, Faculty of
Geography, Russia

Vandermotten Christian

Université Libre de Bruxelles
Belgium

Chalov Sergei R. (Secretary-General)

Lomonosov Moscow State University,
Faculty of Geography, Russia

Baklanov Alexander

World Meteorological Organization,
Switzerland

Baklanov Petr Ya.

Russian Academy of Sciences,
Pacific Institute of Geography, Russia

Chubarova Natalya E.

Lomonosov Moscow State University,
Faculty of Geography, Russia

De Maeyer Philippe

Ghent University,
Department of Geography, Belgium

Dobrolyubov Sergey A.

Lomonosov Moscow State University,
Faculty of Geography, Russia

Haigh Martin

Oxford Brookes University,
Department of Social Sciences, UK

Gulev Sergey K.

Russian Academy of Sciences,
Institute of Oceanology, Russia

Guo Huadong

Chinese Academy of Sciences,
Institute of Remote Sensing and Digital
Earth, China

Jarsjö Jerker

Stockholm University, Department of
Physical Geography and Quaternary
Geography, Sweden

Kolosov Vladimir A.

Russian Academy of Sciences,
Institute of Geography, Russia

Konečný Milan

Masaryk University,
Faculty of Science, Czech Republic

Kroonenberg Salomon

Delft University of Technology, Department
of Applied Earth Sciences, The Netherlands

Kulmala Markku

University of Helsinki, Division of
Atmospheric Sciences, Finland

Malkhazova Svetlana M.

Lomonosov Moscow State University,
Faculty of Geography, Russia

Meadows Michael E.

University of Cape Town, Department of
Environmental and Geographical Sciences
South Africa

Nefedova Tatyana G.

Russian Academy of Sciences,
Institute of Geography, Russia

O'Loughlin John

University of Colorado at Boulder,
Institute of Behavioral Sciences, USA

Pedroli Bas

Wageningen University,
The Netherlands

Radovanovic Milan

Serbian Academy of Sciences and Arts,
Geographical Institute "Jovan Cvijić",
Serbia

Sokratov Sergei A.

Lomonosov Moscow State University,
Faculty of Geography, Russia

Tishkov Arkady A.

Russian Academy of Sciences,
Institute of Geography, Russia

Wuyi Wang

Chinese Academy of Sciences,
Institute of Geographical Sciences and
Natural Resources Research,
China

Zilitinkevich Sergey S.

Finnish Meteorological Institute,
Finland

ASSOCIATE EDITORS:

Maslakov Alexey A.,

Litovchenko Daria K.

CONTENTS

GEOGRAPHY

- Hanna K. Lappalainen, Nuria Altimir, Veli-Matti Kerminen, Tuukka Petäjä, Risto Makkonen, Pavel Alekseychik, Nina Zaitseva, Irina Bashmakova, Joni Kujansuu, Antti Lauri, Päivi Haapanala, Stephany B. Mazon, Alla Borisova, Pavel Konstantinov, Sergej Chalov, Tuomas Laurila, Eija Asmi, Heikki Lihavainen, Jaana Bäck, Michael Arshinov, Alexander Mahura, Steven Arnold, Timo Vihma, Petteri Uotila, Gerrit de Leeuw, Ilmo Kukkonen, Svetlana Malkhazova, Veli-Pekka Tynkkynen, Irina Fedorova, Hans-Christian Hansson, Sergey Dobrolyubov, Vladimir Melnikov, Gennady Matvienko, Alexander Baklanov, Yrjö Viisanen, Nikolay Kasimov, Huadong Guo, Valery Bondur, Sergej Zilitinkevich, Markku Kulmala**
PAN-EURASIAN EXPERIMENT (PEEX) PROGRAM: AN OVERVIEW OF THE FIRST 5 YEARS IN OPERATION AND FUTURE PROSPECTS 6
- Anatoly V. Gavrilov, Elena I. Pizhankova**
DYNAMICS OF PERMAFROST IN THE COASTAL ZONE OF EASTERN-ASIAN SECTOR OF THE ARCTIC 20
- Vadim Yu. Grigoriev, Natalia L. Frolova**
TERRESTRIAL WATER STORAGE CHANGE OF EUROPEAN RUSSIA AND ITS IMPACT ON WATER BALANCE 38
- Nikolay S. Kasimov, Vladimir M. Kotlyakov, Dmitry N. Krasnikov, Alexander N. Krayukhin, Vladimir S. Tikunov**
NATIONAL ATLAS OF THE ARCTIC 51

CONTENTS

ENVIRONMENT

Vladimir S. Kazantsev, Liudmila A. Krivenok, Maria Yu. Cherbunina

METHANE EMISSIONS FROM THERMOKARST LAKES
IN THE SOUTHERN TUNDRA OF WESTERN SIBERIA 58

**Natalia Chubarova, Alexey Poliukhov, Marina Shatunova, Gdaliy Rivin, Ralf Becker,
Stefan Kinne**

CLEAR-SKY RADIATIVE AND TEMPERATURE EFFECTS
OF DIFFERENT AEROSOL CLIMATOLOGIES IN THE COSMO MODEL 74

**Natalia Pankratova, Andrey Skorokhod, Igor Belikov, Nikolai Elansky, Vadim Rakitin,
Yury Shtabkin, Elena Berezina**

EVIDENCE OF ATMOSPHERIC RESPONSE TO METHANE
EMISSIONS FROM THE EAST SIBERIAN ARCTIC SHELF 85

**Stanislav Myslenkov, Alisa Medvedeva, Victor Arkhipkin, Margarita Markina,
Galina Surkova, Aleksey Krylov, Sergey Dobrolyubov, Sergey Zilitinkevich,
Peter Koltermann**

LONG-TERM STATISTICS OF STORMS IN THE BALTIC, BARENTS
AND WHITE SEAS AND THEIR FUTURE CLIMATE PROJECTIONS 93

Natalia Shabanova, Stanislav Ogorodov, Pavel Shabanov, Alisa Baranskaya

HYDROMETEOROLOGICAL FORCING OF WESTERN
RUSSIAN ARCTIC COASTAL DYNAMICS: XX-CENTURY HISTORY
AND CURRENT STATE 113

Alexander Mahura, Iraxte Gonzalez-Aparacio, Roman Nuterman, Alexander Baklanov

SEASONAL IMPACT ANALYSIS ON POPULATION DUE
TO CONTINUOUS SULPHUR EMISSIONS FROM SEVERONIKEL
SMELTERS OF THE KOLA PENINSULA 130

CONTENTS

SUSTAINABILITY

**Sergey N. Bobylev, Olga Yu. Chereshnya, Markku Kulmala,
Hanna K. Lappalainen, Tuukka Petäjä, Svetlana V. Solov'eva,
Vladimir S. Tikunov, Veli-Pekka Tynkkynen**

INDICATORS FOR DIGITALIZATION OF SUSTAINABLE
DEVELOPMENT GOALS IN PEEEX PROGRAM 145

**Svetlana M. Malkhazova, Varvara A. Mironova, Dmitry S. Orlov,
Olga S. Adishcheva**

INFLUENCE OF CLIMATIC FACTOR ON NATURALLY DETERMINED
DISEASES IN A REGIONAL CONTEXT 157

Lassi Heininen

ARCTIC GEOPOLITICS FROM CLASSICAL TO CRITICAL APPROACH –
IMPORTANCE OF IMMATERIAL FACTORS 171

Disclaimer:

The information and opinions presented in the Journal reflect the views of the authors and not of the Journal or its Editorial Board or the Publisher. The GES Journal has used its best endeavors to ensure that the information is correct and current at the time of publication but takes no responsibility for any error, omission, or defect therein.

Hanna K. Lappalainen^{1,2,10*}, Nuria Altimir¹, Veli-Matti Kerminen¹, Tuukka Petäjä^{1,10, 16}, Risto Makkonen¹, Pavel Alekseychik¹, Nina Zaitseva³, Irina Bashmakova¹, Joni Kujansuu^{1,16}, Antti Lauri¹, Päivi Haapanala¹, Stephany B. Mazon¹, Alla Borisova¹, Pavel Konstantinov⁴, Sergej Chalov⁴, Tuomas Laurila², Eija Asmi², Heikki Lihavainen², Jaana Bäck¹, Michael Arshinov⁵, Alexander Mahura¹, Steven Arnold⁶, Timo Vihma², Petteri Uotila¹, Gerrit de Leeuw², Ilmo Kukkonen¹, Svetlana Malkhazova⁴, Veli-Pekka Tynkkynen⁷, Irina Fedorova⁸, Hans-Christian Hansson⁹, Sergey Dobrolyubov⁴, Vladimir Melnikov^{10,11}, Gennady Matvienko⁵, Alexander Baklanov¹², Yrjö Viisanen², Nikolay Kasimov⁴, Huadong Guo¹³, Valery Bondur¹⁴, Sergej Zilitinkevich^{1,2,4,10,15} and Markku Kulmala^{1,10}

¹Institute for Atmospheric and Earth System Research INAR / Physics, Faculty of Science, University of Helsinki, Helsinki, Finland

²Finnish Meteorological Institute, Helsinki, Finland

³Dept. of Earth Sciences, Russian Academy of Sciences, Russia

⁴Faculty of Geography, Lomonosov Moscow State University, Moscow, Russia

⁵Institute of Atmospheric Optics, Russian Academy of Sciences, Tomsk, Russia

⁶Institute for Climate and Atmospheric Science, School of Earth and Environment, University of Leeds, UK

⁷Aleksanteri Institute, Department of Social Research, University of Helsinki, Helsinki, Finland

⁸Institute of Earth Science, OSL, Arctic and Antarctic Research Institute, St. Petersburg State University, St. Petersburg, Russia

⁹Dept. of Environmental Science and Analytical Chemistry, Stockholm University, Sweden

¹⁰Department of Cryosphere, Tyumen State University, Tyumen, Russia

¹¹Tyumen Scientific Center, Siberian Branch, Russian Academy of Science, Tyumen Russia

¹²World Meteorological Organization, Geneva, Switzerland

¹³Institute of Remote Sensing and Digital Earth, Chinese Academy of Sciences, Beijing, China

¹⁴AEROCOSMOS Research Institute for Aerospace Monitoring, Moscow, Russia

¹⁵Department of Radiophysics, Nizhny Novgorod State University, Nizhny Novgorod, Russia

¹⁶Joint international research Laboratory of Atmospheric and Earth System sciences (JirLATEST), Nanjing University, Nanjing, China

* **Corresponding author:** hanna.k.lappalainen@helsinki.fi

PAN-EURASIAN EXPERIMENT (PEEX) PROGRAM: AN OVERVIEW OF THE FIRST 5 YEARS IN OPERATION AND FUTURE PROSPECTS

ABSTRACT. The Pan-Eurasian Experiment (PEEX) program was initiated as a bottom-up approach by the researchers coming from Finland and Russia in October 2012. The PEEX China kick off meeting was held in November 2013. During its five years in operation, the program has established a governance structure and delivered a science plan for the Northern Eurasian region. PEEX has also introduced a concept design for a modelling platform and ground-based in situ observation systems for detecting land-atmosphere and ocean-atmosphere interactions. Today, PEEX has an extensive researcher's network representing research communities coming from the Nordic countries, Russia and China. PEEX is currently carrying out its research activities on a project basis, but is looking for more coordinated funding bases, especially in Russia and in China. The near-future challenge in implementing the PEEX research agenda is to achieve a successful integration and identification of the methodological approaches of the socio-economic research to environmental sciences. Here we give insight into these issues and provide an overview on the main tasks for the upcoming years.

KEY WORDS: multidisciplinary approach, multiscale research, global grand challenges, arctic-boreal environment, observation networks, modelling platform, land-atmosphere interactions, the Arctic Ocean

CITATION: Hanna K. Lappalainen, Nuria Altimir, Veli-Matti Kerminen, Tuukka Petäjä, Risto Makkonen, Pavel Alekseychik, Nina Zaitseva, Irina Bashmakova, Joni Kujansuu, Antti Lauri, Päivi Haapanala, Stephany B. Mazon, Alla Borisova, Pavel Konstantinov, Sergej Chalov, Tuomas Laurila, Eija Asmi, Heikki Lihavainen, Jaana Bäck, Michael Arshinov, Alexander Mahura, Steven Arnold, Timo Vihma, Petteri Uotila, Gerrit de Leeuw, Ilmo Kukkonen, Svetlana Malkhazova, Veli-Pekka Tynkkynen, Irina Fedorova, Hans-Christian Hansson, Sergey Dobrolyubov, Vladimir Melnikov, Gennady Matvienko, Alexander Baklanov, Yrjö Viisanen, Nikolay Kasimov, Huadong Guo, Valery Bondur, Sergej Zilitinkevich and Markku Kulmala (2018) Pan-Eurasian Experiment (PEEX) Program: An overview of the first 5 years in operation and future prospects. *Geography, Environment, Sustainability*, Vol.11, No 1, p. 6-19
DOI-10.24057/2071-9388-2018-11-1-6-19

INTRODUCTION

The Pan-Eurasian Experiment (PEEX) Program (www.atm.helsinki.fi/peex/) is an international, multidisciplinary, multiscale bottom-up initiative. The precursor idea of PEEX, first called as "Pan-Siberian Experiment", was released in 2011. The importance of the

Siberia region and its boreal (taiga) forests in the climate system was introduced by Kulmala et al. (2011), who emphasized biogenic volatile organic compound (BVOC) emissions from the boreal forest, their connection to secondary aerosol formation process and aerosols in the cloud formation processes and in turn their effect on the radiation balance on

the Earth surface. Thus, the first idea was to organize a measurement program for aerosols, greenhouse gases (GHG) and BVOCs. It was also discussed that such type of program could serve as a starting point for establishing a more coherent, coordinated observation network extending from Scandinavia to China and with the focus on the understanding processes in the land- atmosphere interface. In 2012, this idea expanded to cover the whole Northern Eurasian geographical domain and evolved into PEEEX (Kulmala et al. 2011; Lappalainen et al. 2014, 2015).

GOVERNANCE

The promoter institutes of the PEEEX Program have been the University of Helsinki (UHEL) and Finnish Meteorological Institute in Finland (FMI), Institute of Geography of the Moscow State University, AEROCOSMOS, and Institute of Atmospheric Optics (Siberian branch, the Russian Academy of Sciences (SB RAS)) in Russia, Institute of Remote Sensing and Digital Earth (RADI) of the Chinese Academy of Sciences (CAS) and Institute for Climate and Global Change Research of Nanjing University in China. The program governance and communications are coordinated by the PEEEX Offices in Helsinki (PEEX Headquarters), in Moscow, in Beijing and in Nanjing. One of the main tasks of the PEEEX Headquarters is to coordinate information flows and distribute information at different scales. In 2018, the PEEEX office network is expected to expand and new offices or local contact points will be established in Russia in cities of Vladivostok and Tyumen. The upcoming challenge will be the training of the new PEEEX science officers to act as local contact points and to establish fluent information flows within the network. The Program Steering Committee consists of internationally recognized central scientists and research directors in their fields, who are overseeing and discussing the position of PEEEX program in the international research and research infrastructure landscape. At an institutional level, the collaboration within PEEEX is typically initiated by signing a Memorandum of Understanding (MoU) with the PEEEX program. Up to this date, we have signed PEEEX-oriented Memorandum of Understanding (MoUs) with 30 and 5 universities or research institutes in Russia and China, respectively.

As a whole, the PEEEX researchers' network includes approximately 4000 researchers from 20 countries in Europe, Russia and China. The network is currently dominated by the experts representing the atmospheric sciences. The near-future challenge in implementing the PEEEX research agenda is the identification and integration of the socio-economic and marine researchers into the PEEEX research community at a larger scale. The PEEEX science conferences are the main forum for the research community to share their scientific outcomes. For the 3rd Science Conference (held in Moscow, September 2017), altogether 181 abstracts were submitted; of which 113 (63%) represented atmospheric sciences, 24 (13%) ocean sciences, and 44 (24%) socio-economics disciplines, including political and epidemiological sciences, research infrastructures (12; 7%), and university science oriented education (5; 3%).

In addition to the organization of the conferences, the work of the PEEEX working groups (WG) is facilitated by organizing working group meetings. So far, the Modelling-Platform (MP) WG and the Infrastructure WG have been the most active and their work has been mainly focused on the concept design of the modelling platform and on establishing the PEEEX in-situ observation network in Russia. For example, the MP Working Group has almost 100 members from European, Russian, and Chinese institutions including international organizations (ECMWF, WMO) covering different multi-scales and types of models (in total more than 30 models). MP webpages at: <https://www.atm.helsinki.fi/peex/index.php/modelling-platform> introduces the modelling platform overview, list of modelling tools and demonstrations, information on past meetings and sessions.

New working groups and community based activity as bottom-up activities are foreseen on topics like "environmental change and epidemics" and "connecting social parameters to atmospheric emissions".

PEEX Headquarters is coordinating the PEEEX network at different levels (researchers, institutes and organizations) and the governance activities together with other offices in Russia and in China. This activity is facilitated by different tools such as a website (www.atm.helsinki.fi/peex/), e-news-letter,

e-mailing lists, social media (Twitter has #PEEX hashtag), organization of conferences, conference sessions, meetings and forums (e.g. 1st Sofia Earth Forum in Helsinki, 2016). During 2012-2017, we have organized altogether 7 meetings and 3 science conferences (Helsinki - 2015, Beijing - 2016, Moscow - 2017). Starting from January 2017, PEEX has joined the U-Arctic community of 170 Arctic universities; and PEEX acts as an "Arctic-Boreal Hub", which is one of the U-Arctic Thematic networks (www.uarctic.org/organization/thematic-networks/arctic-boreal-hub). The Arctic-Boreal Hub network expands the PEEX approach into a circumpolar context and opens up connection points with the US and Canadian research communities. One practical example of this activity was the ARCTIC Fluxes – CRAICC/CRUCIAL (Critical steps in understanding land surface – atmosphere interactions: from improved knowledge to socioeconomic solutions) workshop (February 2017, Hyytiälä, Finland) which was attended by 71 participant from Canada, USA, Europe and Russia. As a whole, the PEEX network is open for new researchers and organizations representing different scientific disciplines to join in and is especially interested in strengthening the role of social and socio-economic sciences within this community.

RESEARCH

The main scientific mission of the PEEX program is to understand large-scale feedbacks and interactions between the land-atmosphere-ocean continuum in the changing climate of northern high latitude and in China (Kulmala et al. 2016, Lappalainen et al. 2016). The PEEX Science Plan (Lappalainen et al. 2015; http://www.atm.helsinki.fi/peex/images/PEEX_Science_Plan.pdf) addresses the scientific aims and large-scale research questions of the program (Fig. 1). The focal points in the PEEX research are e.g. on the net effects of various feedback mechanisms connecting the biosphere, atmosphere and human activities. These feedbacks can either hinder or speed up the climate change. Such feedbacks stem from higher temperature and increased concentration of GHG in the future. The climate change and associated feedbacks lead to further consequences, such as permafrost thawing, land cover changes, increased dissolved organic carbon content in freshwaters, acidification of the Arctic Ocean, increased photosynthetic activity, elevated GHG uptake by terrestrial ecosystems, increased BVOCs emissions, changes in secondary aerosol production, changes in cloud processes and their effects on the radiation budget as well as precipitation.

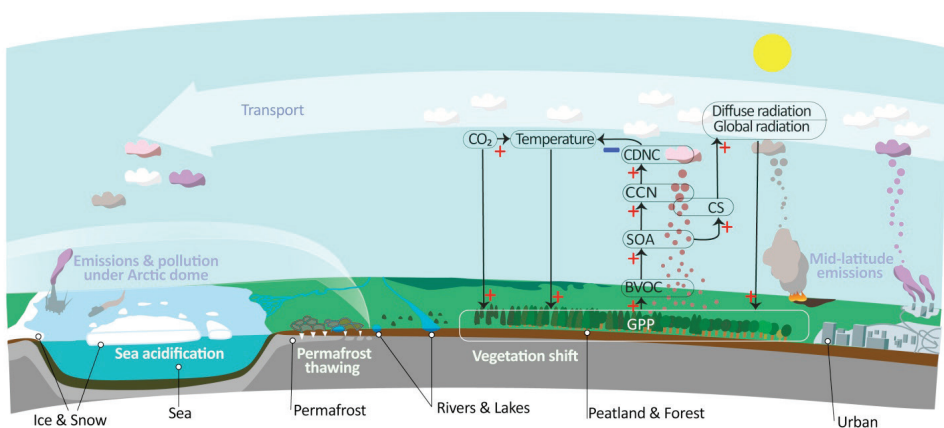


Fig. 1. Overview of the PEEX research domain, which extends over the Eurasian region, from Arctic to Boreal and Temperate zones. The figure lists key processes that drive the research focuses and the variety of site types that come under study. As an example of feedback process, the COBACC (Continental Biosphere Atmosphere Cloud Climate; Kulmala et al. 2014) feedback mechanism is superposed on the elements of the landscape, evidencing the width of the scale coverage required for its observation

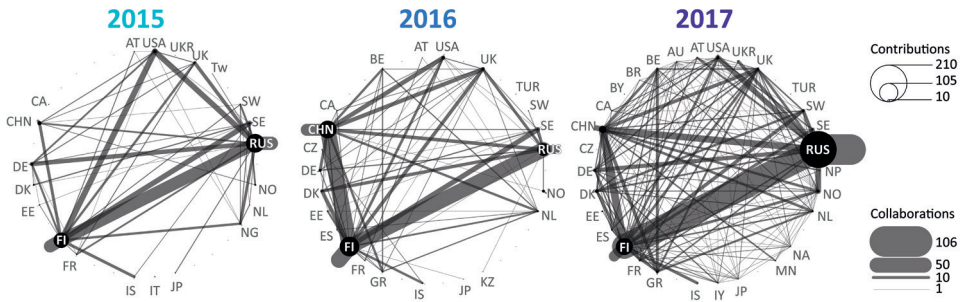


Fig. 3. Degree of participation and the amount of collaboration in the works included in the PEEX conference proceedings, by country. The amount of contributions shows the total times per year that a certain country appears in the affiliation lists. The number of collaborations refers to the times certain two countries are sharing co-authorship. The lines connecting two countries refer to the between-country collaboration, within-country collaborations (that is, different institutes from the same country in the same work) is represented by the lines that go outwards

RESEARCH INFRASTRUCTURE

Arctic – boreal infrastructure and common data formats

The main strategic challenge of the PEEX program is to initiate a comprehensive and coordinated research infrastructure in collaboration with the main partners in Russia and China. There is an urgent need for comprehensive, coordinated in-situ observations over the Arctic and Northern

Eurasian region detecting different fluxes, emissions and concentrations on greenhouse gases and atmospheric compounds between different Earth surfaces and atmosphere (Fig. 4). In situ observations are providing complementary information to the satellite observations, which provide an overview on a large spatial scale, and both information flows are used together with modeling to create a complete understanding of the processes over the PEEX study area.

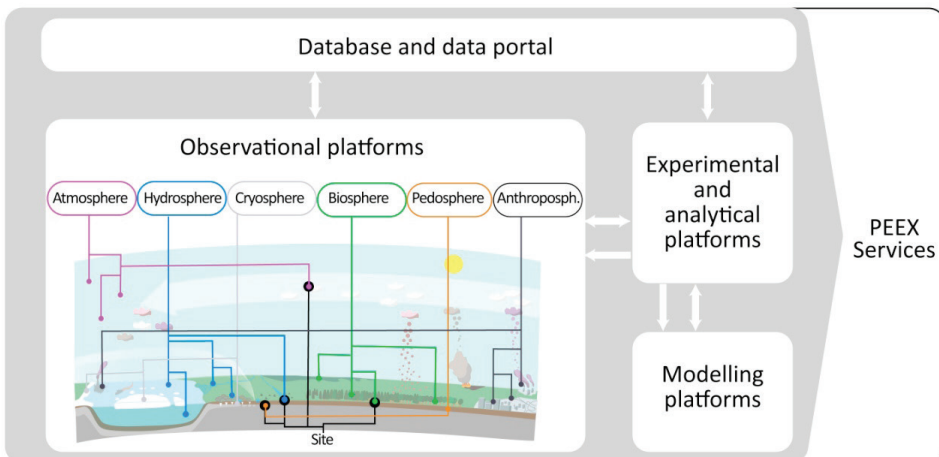


Fig. 4. Overview of the infrastructure conceptual framework. The observational platforms are highly distributed covering all compartments of the system so that multitude of variables are measured for the same compartments and multiple of compartments are measured at one same site. The future task is to establish connections and information flows between each platforms and, in the end, provide atmospheric and environmental real time data for different national early warning systems

The PEEEX land-ecosystem in-situ network will be built upon complementary approaches. The coordination and upgrading of the existing station activities and establishing new SMEAR (Stations for Measuring Earth surface - Atmosphere Relations) -type stations will be based on a SMEAR concept (Hari et al. 2016). The principles of the PEEEX in-situ observation network, also as a part of the global observatory, were introduced by Hari et al. (2016) and Kulmala et al. (2016). In reference to the "coordination and upgrading of the existing stations" in Russia, the collection of the preliminary information of the existing station activities started in 2012. The first inventory on more than 200 in situ stations operating in the Arctic and Subarctic Eurasian regions was conducted by the Russian Academy of Sciences (RAS) and Moscow State University together with the University of Helsinki (Alekeychik et al. 2016). Based on the first inventory, we are currently collecting more detailed information, termed "station metadata" here. The station metadata includes detailed descriptions of variables from atmospheric and ecosystem (soil-forest-lake-urban-peatland-taiga) measurements and from the observation site itself. This enables the categorization of the stations in a systematic manner, and it will provide tools to connect them to international observation networks, such as WMO-Global Atmospheric Watch Program, China Ecosystem Network (CERN) and global SMEAR network, and to carry out standardization work towards common data formats. Based on this work, PEEEX will also publish a station e-catalog, which will give information on the on-going measurements and contact points and will initiate research collaboration between the research groups.

One of the most important relevant PEEEX research infrastructure activity, focused mainly on Arctic regions, just started under the ERAPLANET (The European network for observing our changing planet) project (www.era-planet.eu) Horizon-2020 project (the Strand-4) "Integrative and Comprehensive Understanding on Polar Environments (iCUPE, www.atm.helsinki.fi/icupe) and is led by University of Helsinki. The core idea of iCUPE is the development of novel, integrated, quality-controlled

and harmonized in-situ observations and satellite data in the polar areas, including also data products for the end users.

In terms of the Arctic marine environment, the most relevant observations for PEEEX will be collected from regions of the Russian Arctic, and in particular, the Siberian coastal regions. For this, good quality data on the current state and change of hydrography, sea ice and marine biology are needed. This is issue addressed by the PEEEX marine concept, which is, similarly to the SMEAR measurement concept for the land-atmosphere surfaces, based on a hierarchical station network, but affected by the practical challenges in making long-term observations in and over the sea. The processes to be studied include the sea ice thermodynamics and dynamics, ocean heat and freshwater budgets, ocean circulation and hydrography, waves and tides, ocean chemistry and ecosystems, atmospheric heat and moisture budgets, synoptic-scale cyclones and Polar lows, troposphere-stratosphere coupling, atmospheric boundary-layer processes, as well as aerosols and clouds (Vihma et al. 2014). An essential aspect of the development and operation of the PEEEX marine component is its close linkage to the PEEEX land-atmosphere component. Only in this way important research challenges related to the coastal processes, such as river freshwater and heat fluxes, melting of the subsea permafrost and the erosion of shoreline, can be adequately addressed.

The development of the PEEEX research infrastructure concepts and identification of the research needs are also connected to the EU Horizon2020-BG-09 "Integrated Arctic Observation Systems" (INTAROS; 2016-2021; www.intaros.eu) project coordinated by the Nansen Environmental and Remote Sensing Center, Norway; and it contributes to the Arctic Council's Sustainable Arctic Observation Systems Network (SAON).

Modelling Platform

The purpose of the PEEEX Modelling Platform (MP) is to support the PEEEX observational system and to answer the PEEEX scientific

Table 1. Examples of relevant PEEX hydrospheric research topics and their key gaps.

Research topic	Key issues
Seasonal tidal maps for the Siberian Arctic	The lack of marine observations limits the validity of current maps: need for more measurement sites.
CO ₂ fluxes through the atmosphere-ocean interface	Large observational uncertainties exist, e.g. in terms wind velocity at high latitudes. New high resolution reanalysis products are likely a part of the solution.
Global eddy-resolving ocean model	Southern Ocean eddies have large impacts on the World Ocean circulation with decadal oceanic signals propagating to the North Atlantic sub-polar gyre, and occasionally to the Arctic Ocean. Hence, one should ideally have a global eddy-resolving ocean model to derive oceanic boundary conditions for Arctic climate simulations.
Freeze-up and melt times of Siberian lakes	Very relevant for the Northern Eurasian region and could be used to build a map of observed regional climatic trends and variability. The map could be complemented spatially with remote sensed data.
Long time series constructed from river catchment flow data	River runoff data could provide long-term time series of variability for many climatic zones. They could also be used to estimate transports of carbon and chemical fluxes. However, river regulation may affect the quality of time series.
Methane emissions from tundra lakes	Are not well studied and the existing data have high uncertainties. Furthermore, climatic change affects the fluxes. To obtain a more comprehensive view, emissions from wetlands and peats should be included. Existing measurement time series need to be maintained. Combination with remote sensing measurements would provide an extended spatial coverage. Short targeted field campaigns are also necessary, and could be associated with the PEEX education component.

questions, which requires a hierarchy and a framework of modern multi-scale models for different elements of the Earth system integrated with the observation system. The PEEX-MP provides a seamless approach that considers several dimensions of the coupling between temporal and spatial scales, a wide range of processes, Earth system components, types of observations and modelling tools, user-oriented integrated systems and impact based forecasts and services (Baklanov et al. 2017). In particular, the temporal scales are ranging from minutes (e.g. nowcasting) to decadal and centennial (climate change), while the spatial scales are varying from the regional to a global scale (downscaling and upscaling). Processes can be of physical, chemical, biological, social or some other

character, and they can be occurring in the atmosphere, hydrosphere, pedosphere, biosphere or in other environments. The PEEX-MP models will be validated and constrained by available in-situ and remote sensing data of various spatial and temporal scales.

The MP will be based on a seamless modelling framework from nano-scale modelling to global Earth System Models (ESMs). It will also introduce community-based services for data mining and for demonstrating air pollution events at regional scales. One of the large-scale components of PEEX-MP consists of the EC-Earth ESM (www.ec-earth.org), which combines all relevant PEEX elements (atmosphere-ocean-sea-ice) on the global scale. Downscaling approach is

realized with the Enviro-HIRLAM (seamless online integrated coupled meteorology-chemistry-aerosols) modelling system, which can be subsequently run on hemispheric-regional-subregional-urban scales by producing simultaneously 3D meteorology and atmospheric composition (Baklanov et al. 2017). For example, for large eddy simulations (LES), the UCLALES-SALSA (Tonttila et al. 2017), PALM, and LESNIC models can be used for large scale applications with sectional aerosol module included, for simulations of atmospheric and oceanic flows, and for simulation of stably stratified planetary boundary layer, respectively (Esau 2014).

The overall list of MP models is available at <https://www.atm.helsinki.fi/peex/index.php/modelling-tools-demonstration>, where each model has a short description and information on available modes for the model runs, components and processes, which are covered by the model and corresponding list of references. A series of models/ modules is available in PEEEX-MP framework. These models can be used to simulate organic compounds, sulfuric acid and aerosols; surface energy in urban or natural environments and water balance; tropospheric gas-phase and aerosol physical and chemical processes at multiple scales; atmosphere-vegetation interactions; coupling of the atmosphere, ocean and land surface through the exchange of energy, momentum, water and important trace gases; and coupling of the ocean and sea ice at various scales. There are also process-based models for simulating methane emissions from natural/ managed wetlands; crop photosynthesis, respiration and other processes involved in crop growth and carbon/ nitrogen dynamics in soils; hydro-biogeochemical gaseous carbon and nitrogen emissions and hydrologic nitrogen losses from a catchment; biosphere-atmosphere-hydrosphere exchange processes at site, local, and regional scales, etc. Finally, there are MP models in support of research on atmospheric circulation and composition from global to local scales; inverse modeling of GHG emissions; atmospheric transport, dynamics, dispersion and deposition at global-hemispheric-

regional-other scales for air pollution and climatic environmental studies; and inverse modeling with data assimilation framework.

The key issues for the PEEEX modelling framework are anthropogenic emissions; permafrost effects; carbon dioxide and methane; ecosystem carbon cycle; short lived pollutants and climate forcers; BVOC emissions; forest fires and their effects; aerosol formation in Arctic and Siberia; aerosol radiative forcing; air pollution - ecosystem feedbacks; dynamics of ocean and sea ice; and high impact events.

EDUCATION

Within PEEEX we have recognized the need of discipline-tied fundamental education as a backbone for multidisciplinary research. However, also shift towards multidisciplinary in education is imperative for a successful career in climate and global change science (Nordic Climate Change Research 2009). Based on the experiences in educating several generations of students during the past 20 years in the Nordic research community, we have developed a model to improve the learning outcomes in multidisciplinary atmospheric sciences. The model is a result of work including pedagogical experiments, utilization of modern technologies (Junninen et al. 2009), workshops for teachers and supervisors and, most importantly, organizing a long series of multidisciplinary hands-on research-intensive short courses for graduate students.

During the last 5 years, Division of Atmospheric Sciences of University of Helsinki has been coordinating the following international environmental-education projects responding to new challenges posed by PEEEX an funded by the EU-Commission: TEMPUS 159352-FI-JPHES "Development of qualification framework in meteorology" (2010-2013); Erasmus+ 561975-EPP-1-2015-1-FI-EPPKA2-CBHE-JP "Adaptive learning environment for competence in economic and societal impacts of local weather, air quality and climate (2015-2018, www.e-impact.net).

The PEEX community has been actively involved in organizing special events, such as Young Scientist Summer Schools (YSSS); research training intensive courses on modelling, observations and data analysis; and the series of education workshops in the framework of InterCarto conferences. During such events, young researchers have the opportunity to attend lectures and participate in practical exercises showing their personal skills in doing research. For that, for example, practical exercises are developed as independent small-scale research projects (Mahura et al. 2012). Such approach is problem-based learning (Duch et al. 2001). The schools were organized in 2008, 2011 and 2014 in Zelenogorsk, Russia (led by NordForsk NetFAM; netfam.fmi.fi), in Odessa, Ukraine (led by NordForsk MUSCATEN; muscaten.ut.ee), and in Aveiro, Portugal (by EU COST Action EuMetChem; eumetchem.info; Baklanov, 2017). The main focus of these schools was on-online integrated modelling of meteorological and chemical transport processes for weather, air quality, and climate applications.

Besides the YSSSs, the Nordic research community has run a dedicated multidisciplinary master's programme ABS (Atmosphere-Biosphere Studies) continuously since 2006. A special feature of the ABS programme is the continuous series of short research-intensive interdisciplinary courses. Five to ten such courses are currently given every year.

The PEEX partners are setting up new programs as well. Recent examples of these are POMOR, a master's program for applied and marine sciences at St. Petersburg State University, Russia; CORELIS, Cold Regions Environmental Landscapes Integrated Science program; and the Russian-Chinese MSc program in hazard hydrological events. Furthermore, there have been projects to foster Russian-Nordic collaboration in developing education, such as the Nordic-Russian University Network for Successful Cooperation in Higher Environmental Education and the Nordic-Russian Virtual University Campus for Higher Environmental Education. The NordForsk-funded CRUCIAL project paves way for the multidisciplinary

PEEX education activities. The EU-funded ECOIMPACT Erasmus+ program project (e-impact.net/en) is developing sectoral courses in a personal learning environment. Earlier, the PEEX community carried out two TEMPUS projects, COMBAT-METEO and QUALIMET.

The PEEX education roadmap includes the following main components: (i) labeled and themed research-intensive international interdisciplinary short courses; (ii) introduction of a dedicated Pan-Eurasian mobility programme for MSc and PhD students and postdocs; (iii) development of new educational tools based on pedagogical research done in the PEEX community; (iv) development of joint online courses and massive open online courses (MOOCs); (v) sharing good practices and benchmarking done in dedicated PEEX education workshops; and (vi) encouraging partners to seek for bilateral funding to develop education and to increase mobility.

CONCLUSIONS

As a whole, the Pan-Eurasian Experiment is an active contributor and a collaborator in the international research and research infrastructure landscape. The main international partners and collaborators are the Future Earth and Future Earth iLEAPS, Arctic Council AMAP and SAON WGs, GEO – GEOSS Cold regions (PEEX - the in situ observations activity), U-Arctic, IIASA and WMO GAW program. PEEX is also closely connected to International Eurasian Academy – European Center and the DBAR (Digital Belt and Road) Initiative, which are interested to provide a big data platform on Earth observation from China and countries along the new Silk Road - Belt and Road area. PEEX has released a program agenda and is currently finalizing the conceptual design of PEEX-relevant research infrastructures. The program is currently calling for financial support from the European Union, Russian and Chinese basic funding organizations to implement the program at a large scale. The implementation of the PEEX program would make significant impact on the sustainable development of the Northern societies and China.

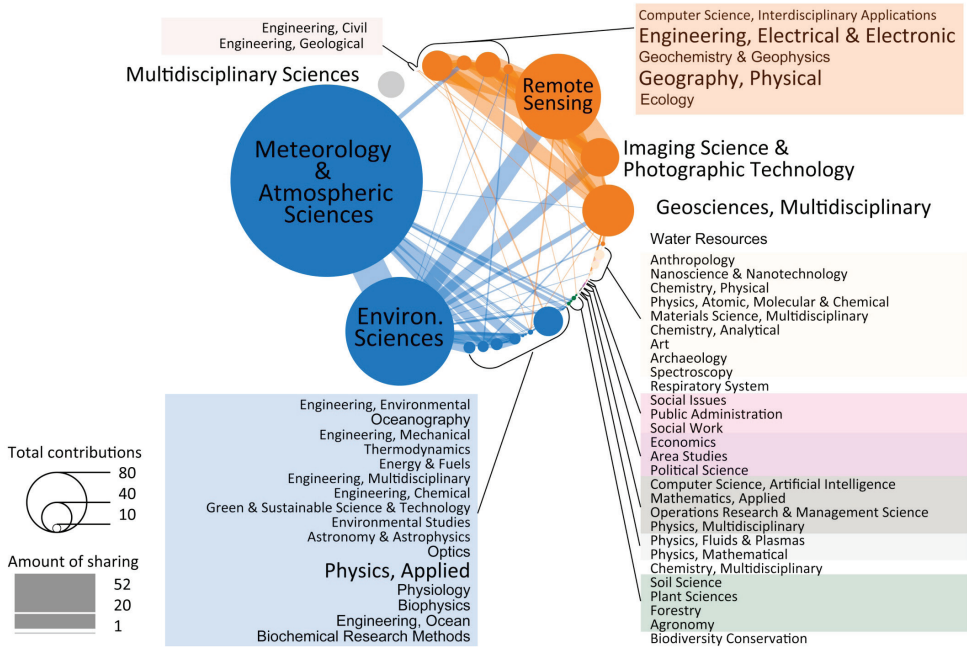


Fig. 5. Future potential of the research community in different scientific disciplines could be demonstrated by the published papers between 2012 and present for 8 active PEEEX researchers. Data mined from Web-of-Science Classification of “Research areas” according to Web-of-Science, “Research areas” is an attribute to the journal where the paper was published. A journal can belong to more than one Research area

ACKNOWLEDGEMENTS

A major part of the PEEEX Preparatory Phase work in years 2010–2017 has been based on the in-kind contribution of several European, Russian and Chinese research institutes via supporting active participation to the PEEEX meetings, conference organized in Helsinki, Moscow, Hyytiälä, Saint Petersburg and Beijing. In addition we would like acknowledge the following support or funding from the following bodies: Finnish Cultural Foundation, Grant: Prof. Markku

Kulmala “International Working Groups”; Russian Mega-Grant No. 11.G34.31.0048 (University of Nizhny Novgorod), Academy of Finland contract 259537, Beautiful Beijing (Finland- China collaboration project) funded by TEKES, EU project InGOS and the NordForsk Nordic Centre of Excellence of CRAICC (no 26060), Nordforsk CRAICC-PEEX (amendment to contact 26060) and Nordforsk CRUCIAL-project active in 2016-2017. ERAPLANET iCUPE, Academy of Finland (FCOE), European Commission (ACTRIS). ■

REFERENCES

- Alekseychik P, Lappalainen H.K., Petäjä T., Zaitseva N., Heimann H., Laurila T., Lihavainen H., Asmi E., Arshinov M., Shevchenko V., Makshtas A., Dubtsov S., Mikhailov E., Lapshina E., Kirpotin S., Kurbatova Yu., Ding A., Guo H., Park S., Lavric J.V, Reum F., Panov A., Prokushkin A., and Kulmala M. (2016). Ground-based station network in Arctic and Subarctic Eurasia: an overview. *J. Geography Environment Sustainability*, No 2, pp. 75-88.
- Arneth A., Harrison S. P., Tsigaridis K., Menon S., Bartlein P. J., Feichter H., Korhola A., Kulmala M., O'Donell D., Schurgers G., Sorvari S., Vesala T., and Zaehle S. (2010). Terrestrial biogeochemical feedbacks in the climate system: from past to future. *Nat. Geosci.*, 3, pp. 525–532.
- Baklanov A. (2017). Overview of the European framework for online integrated air quality and meteorology modelling (EuMetChem). *Atmospheric Chemistry and Physics*, doi:10.5194/acp-special_issue370-preface.
- Baklanov A., Smith Korsholm U., Nuterman R., Mahura A., Sass B., Rasmussen A., Zakey A., Kaas E., Kurganskiy A., Sorensen B., and González-Aparicio I. (2017). The Enviro-HIRLAM online integrated meteorology–chemistry modelling system: strategy, methodology, developments, and applications. *Geosci. Model Dev. Discuss.* 10.5194/gmd-2016-319.
- Duch B. J., Groh S. E. and Allen D. E. (2001). *The Power of Problem-Based Learning*. Stylus Publishing, Sterling, VA, U.S.A.
- Esau I. (2004). Simulation of Ekman Boundary Layers by Large Eddy Model with Dynamic Mixed Subfilter Closure. *Environmental Fluid Mechanics* 4: 273–303.
- Hari P., Petäjä T., Bäck J., Kerminen V-M., Lappalainen H.K. Vihma T., Laurila T., Viisanen Y., Vesala T., and Kulmala M. (2016). Conceptual design of a measurement network of the global change. *Atmos. Chem. Phys.*, 16, pp. 1017-1028.
- Hari P., Andreae M. O., Kabat P., and Kulmala M. (2009). A comprehensive network of measuring stations to monitor climate change. *Boreal Environ. Res.*, 14, pp. 442–446.
- Hari P. and Kulmala M. (2005). Stations for Measuring Ecosystem – Atmosphere Relations (SMEAR II). *Boreal Environ. Res.*, 10, pp. 315–322.
- Junninen H., Lauri A., Keronen P., Aalto P., Hiltunen V., Hari P., and Kulmala M. (2009). Smart-SMEAR: on-line data exploration and visualization tool for SMEAR stations. *Boreal Environment Research*, 14, pp. 447–457.
- Kulmala M., Nieminen T., Nikandrova A., Lehtipalo K., Manninen H. E., Kajos M.K., Kolari P., Lauri A., Petäjä T., Krejci R., Hansson H-C., Swietlicki E., Lindroth A., Christensen T.R., Arneth A., Hari P., Bäck J., Vesala T., and Kerminen V-M. (2014). CO₂-induced terrestrial climate feedback mechanism: From carbon sink to aerosol source and back. *Boreal Environment Research* 19 (suppl. B): pp. 122–131.
- Kulmala M., Lappalainen H.K., Petäjä T., Kerminen V-M., Viisanen Y., Matvienko G., Melnikov V., Baklanov A., Bondur V., Kasimov N., and Zilitinkevich S. (2016). Pan-Eurasian Experiment (PEEX) Program: Grant Challenges in the Arctic-boreal context. *J. Geography Environment Sustainability*, 2, pp. 5–18, DOI:http://dx.doi.org/10.15356/2071-9388_02v09_2016_01.

Kulmala M., Lappalainen H.K., Petäjä T., Kerminen V-M., Viisanen Y., Matvienko G., Melnikov V., Baklanov A., Bondur V., Kasimov N., and Zilitinkevich S. (2016). Pan-Eurasian Experiment (PEEX) Program: Grant Challenges in the Arctic-boreal context. *J. Geography Environment Sustainability*, 2, pp. 5-18.

Kulmala M., Lappalainen H.K., Petäjä T., Kurten T., Kerminen V-M., Viisanen Y., Hari P., Bondur V., Kasimov N., Kotlyakov V., Matvienko G., Baklanov A., Guo H., Ding A., Hansson H-C., and Zilitinkevich S. (2015). Introduction: The Pan-Eurasian Experiment (PEEX) – multi-disciplinary, multi-scale and multi-component research and capacity building initiative. *Atmos. Chem. Phys.*, 15, 13085-13096, doi:10.5194/acp-15-13085-2015.

Lappalainen H.K., Petäjä T., Kujansuu J., Kerminen V-M., Shvidenko A., Bäck J., Vesala T., Vihma T., De Leeuw G., Lauri A., Ruuskanen T., Lapshin V.B., Zaitseva N., Glezer O., Arshinov M., Spracklen D.V., Arnold S.R., Juhola S., Lihavainen H., Viisanen Y., Chubarova N., Chalov S., Filatov N., Skorokhod A., Elansky N., Dyukarev E., Esau I., Hari P., Kotlyakov V., Kasimov N., Bondur V., Matvienko G., Baklanov A., Mareev E., Troitskaya Y., Ding A., Guo H., Zilitinkevich S., and Kulmalas M. (2014). Pan Eurasian Experiment (PEEX) - A research initiative meeting the Grand Challenges of the changing environment of the Northern Pan-Eurasian arctic-boreal areas. *Geography, Environment, Sustainability*, 7(2):13-48.

Lappalainen H.K., Kulmala M., and Zilitinkevich S. (2015). Pan-Eurasian Experiment (PEEX) Science Plan. Helsinki 2015. ISBN 978-951-51-0587-5 (printed).

Nordic Climate Change Research (2009). NordForsk Policy Briefs 2009-8. Mandag Morgen.

Tonttila J., Maalick Z., Raatikainen T., Kokkola H., Kühn T., and Romakkaniemi S. (2017). UCLALES-SALSA v1.0: a large-eddy model with interactive sectional microphysics for aerosol, clouds and precipitation. *Geosci. Model Dev.*, 10, 169-188, <https://doi.org/10.5194/gmd-10-169-2017>.

Received on December 12th, 2017

Accepted on March 1st, 2018



Hanna K. Lappalainen, PhD, Pan-Eurasian Experiment (PEEX) Program Secretary General, works currently at PEEX Headquarters, at the University of Helsinki, Institute for Atmospheric and Earth System Research (INAR). She has a long-term experience of coordinating large-scale research projects and funding applications and has been working as a research coordinator and a science coordinator of large scale projects at the Finnish Centre of Excellence in Physics, Chemistry, Biology and Meteorology of Atmospheric Composition and Climate Change (2012-2013). Since 2014 Lappalainen has been a representative of Finland in the Sustainable Arctic Observing Network (SAON) Data working group, a Future Earth - iLEAPS Steering Group Member and starting from 2017 as a national delegate of the International Arctic Science Committee (ISAC) - The International Science Initiative in the Russian Arctic (ISIRA). She obtained her PhD. from the Department of Biological and Environmental Sciences, University of Helsinki, Finland and has been engaged in analysis of the atmospheric concentration of the Biogenic Volatile Organic Compounds (BVOCs) and plant phenological time series and modelling.

Anatoly V. Gavrilov¹, Elena I. Pizhankova^{1*}

¹Lomonosov Moscow State University, Faculty of Geology, Moscow, Russia;

* **Corresponding author:** pijankova@yandex.ru

DYNAMICS OF PERMAFROST IN THE COASTAL ZONE OF EASTERN-ASIAN SECTOR OF THE ARCTIC

ABSTRACT. The study summarizes results on the cryogenic dynamics in the coastal zone. The paper shows that ongoing climate warming and shrinking of ice extent of the Arctic seas triggers both thermogenic and cryogenic processes at the same time. The first group includes thermal abrasion, thermal denudation, degradation of submarine permafrost, and the second one is the syncryogenesis of the new-formed coastal-marine sediments. The first group results in an increase of the retreat rate of coasts, the second results in the islands formation on banks and shallows where the domination of bottom thermal abrasion and deepening of the sea bottom has been taken place previously. Arguments for stamukhas and cryogenesis role in islands formation are presented.

KEY WORDS: coastal zone, coast retreat, degradation of submarine permafrost, coastal-marine sedimentation, formation of permafrost, stamukhas

CITATION: Anatoly V. Gavrilov, Elena I. Pizhankova (2018) Dynamics of permafrost in the coastal zone of eastern-asian sector of the arctic. *Geography, Environment, Sustainability*, Vol.11, No 1, p. 20-37

DOI-10.24057/2071-9388-2018-11-1-20-37

INTRODUCTION

Studies of coastal dynamics in cryolithozone are often conducted disregarding the processes along the submarine near shore zone. However, changes of above-water part of coastal zone (onshore) are determined by changes of its underwater part (offshore) (Zenkovich, 1962; Are, 2012). The variations of hydrometeorological parameters have definite impact on the changes of the both parts of coastal zone triggering the changes in other components of natural environment. Thus, at the end of 20th Century – in the beginning of 21th Century there the decreasing of ice coverage of the Arctic Seas and longer ice-free period can be observed, along with the increasing of mean annual air temperatures. The mentioned

above changes lead to the increasing of retreat rates of icy shores. Simultaneously, the temperature of bottom water is increasing that causes further degradation of permafrost that slides into submarine conditions. Both processes facilitate the increasing percentage of suspension and melted sediments at the submarine near shore zone. This, in turn, stimulates sedimentation here and on the nearby seabed.

Recent permafrost dynamics in the coastal zone is determined by climate and sedimentation in the late Pleistocene and Holocene. In the cold period of the Late Pleistocene, syncryogenic deposits of the Ice Complex (IC) were formed at the drained shelf and the coastal lowlands of the Eastern sector of the Eurasian Arctic. These deposits

make up the upper 30-50m of the Late Pleistocene accumulative coastal plain. They are characterized by volumetric ice content of 70-95% and thick ice wedges. In the Holocene, as the result of destruction of IC by lake thermokarst, the syncryogenic deposits of the Alas Complex were formed. They are also of high ice content (60-70%) and contain ice wedges. They both compose the significant part of the shores of the Laptev and East-Siberian Seas. The vulnerability of icy deposits towards the thermal influence causes the shores retreat as a result of thermal abrasion and thermal denudation, and then, the degradation of offshore permafrost. These processes determine the environmental conditions at the coastal zone of the East-Arctic seas.

At the same time, coastal-marine sedimentation and emergence of recent permafrost often exist at the coastal zone. As a result, the coastal zone is the particular place on the Eastern sector of Eurasian Arctic shelf where there are widely spread multidirectional cryogenic processes under natural conditions. Their characteristics in connection the sea ice coverage and climate changes in the second part of the 20th Century and the beginning of the 21st Century is the matter of consider in this paper.

MATERIALS AND METHODS

The study area covers the coastal zone of the Laptev Sea and western part of the East-Siberian Sea (Fig. 1).

The study of coastal dynamics of eastern part of Russian Arctic has been constantly conducted since the late 60s – the mid-70s of the 20th Century (Grigoriev 1966; Molochushkin 1970; Are 1980; etc.). It became of special importance at the end of 20th Century – in the beginning of 21st Century (Coastal ... 1984; Are 1985, 2012; Novikov 1984; Grigoriev 1993, 2008; Grigoriev et al. 2006; Razumov 1996, 2010; Dynamics ... 1998; etc.). From the mid-1990s to the present time the coastal zone research is being carried out with the participation of German scientists (Overduin et al. 2007, 2013; Rachold et al. 2007; Junker et al. 2008; Günther et al. 2013, 2015; etc.) within the framework of Russian–German collaboration. Now field instrumental methods are being replaced by studies with using multi-temporal remote sensing data more and more often (Pizhankova and Dobrynina 2010; Pizhankova 2011, 2016; Günther 2013, 2015; Lantuit 2011; etc.). Such studies are more effective, especially for considerable length of coastlines. We resolve the problem of shores survey with application of space

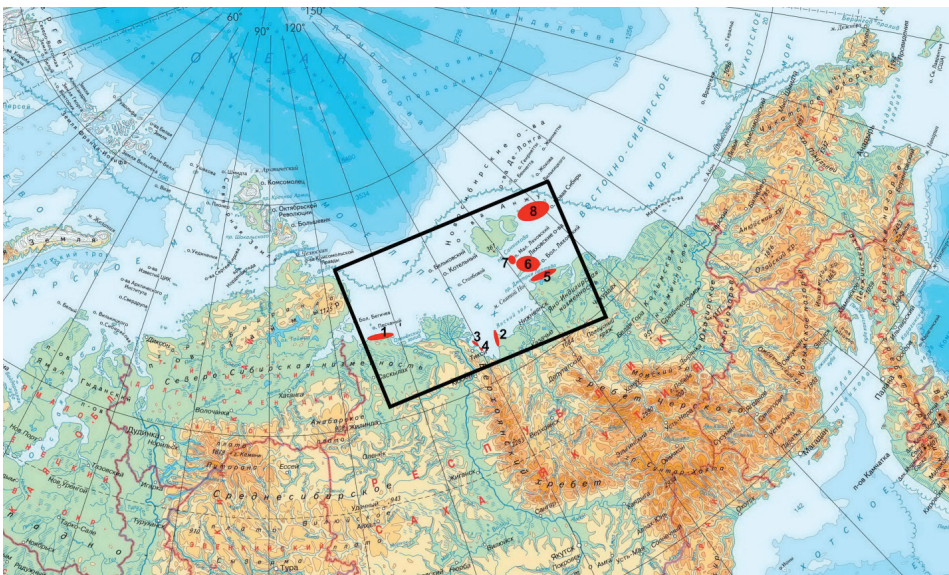


Fig. 1. The research area. Numbers indicate the sites for which the coastal dynamics were studied using remote sensing data

imagery of medium resolution (Landsat-7, 8) with overlapped archival aerial photography of the Novosibirskiye Islands with the aim to investigate the spatial patterns of their dynamics. Such surveys were conducted for the New Siberia Island (Dobrynin et al. 2005), the Bolshoy and Maliy Lyakhovsky Islands (Pizhankova and Dobrynina 2010; Pizhankova 2011). There was revealed the acceleration of coastal retreat rate for the region of Dmitry Laptev Strait in the 20st Century (Pizhankova 2016). ScanEx Image Processor and MapInfo Professional were used in the survey. Almost 1,000 km of shores was studied using remote sensing data.

The study of cryogenesis of offshore sediments is associated closely with the study of spread and depth of permafrost table. This study conducted with the help of drilling profiles was initiated in 1950s. Permafrost studies and geothermal monitoring in boreholes were carried out in various regions of submarine coastal zone of the East-Siberian Arctic in 1960-1980s, for the purposes of geological survey, search for and exploration of mineral resources. The work was accompanied by a complex of laboratory studies of sediments. They were conducted in the area of the Tiksi Bay and Muostakh Island, the Vankina and Sellyakhskaya Bays, the coastal zone of the Novosibirsk Islands, the mouths of the rivers (Grigoriev 1966; Molochushkin 1969, 1970, 1973; Are 1980, 2012; Zhigarev 1981, 1997; Zhigarev and Plakht 1977; Fartyshev 1993; Fartyshev et al. 1983; Neizvestnov 1980, 1999; Soloviev 1981; Soloviev et al. 1987; etc.). In 1970 Molochushkin E.N. (1973) sampled bottom sediments with a vibration-based piston tube in the interval from 10 to 40 m isobaths for the first time. These works were continued in the 21st Century (Grigoriev 2008).

Since 1970s, mathematical modeling started to apply in studies of distribution, thickness and evolution of permafrost (Romanovskii et al. 2006; Gavrilov 2008; Nicol'sky et al. 2012). These results supplemented the drilling data on the submarine permafrost degradation from the top by data on their degradation from the bottom.

Echolocation at shallow depths was carried out within the framework of Russian-German scientific collaboration. In 2003 and 2005, two very informative meridian cross-sections were established from the Mamontov Klyk Cape to open sea (Grigoriev 2008; Junker et al. 2008).

The mathematical simulation of the permafrost current state for the East Siberian shelf was carried out on the basis of the latest achievements in paleogeography and software implementing the solution of the Stefan task under various conditions (Romanovskii et al. 2006).

The electronic archives of Arctic and Antarctic Research Institute (AARI) (<http://www.aari.nw.ru/projects/ECIMO/>) and the All-Russia Research Institute for Hydro- and Meteorological Information — the World Data Center (ARRIHMI – WDC) (<http://aisori.meteo.ru/ClimateR>) serve as the important source of information about the changes in ice cover and climate of the East-Arctic Seas.

THE MAIN FACTORS OF THE COASTAL CRYOGENIC DYNAMICS

As mentioned above, the high ice content of the main relief-forming complexes (Ice and Alas Complexes) is due to the history of its development. The latter is also related closely to the geological-tectonic structure and location of the research area in the eastern most continental high-latitude part of the Arctic. It was the Late Cenozoic subsidence and climate continental conditions that led to the underground freezing of the region in the Late Pleistocene. At that time glaciers were forming in the western sector of the Eurasia. They melted away 17-15 ka BP (Hughes et al. 2016), while the ground ice of the Eastern sector still exists. This one determines the increased rates of coastal retreat and seabed deepening. The geological and tectonic structure determines the direction of contemporary vertical movements, the composition and ice content of the deposits in the wave action zone, and the height of the cliffs. These factors determine the general direction of the cryogenic dynamics in the coastal zone, as well as the specific spatial confinement of processes and their rates.

Another group of factors is presented by the hydrological and climatic conditions. They include the duration of ice-free period, currents, the strength and direction of winds and wind-induced surges, the sum of positive air temperatures, the distribution of snow accumulation, the radiation-heat balance of the coastal outcrops surface, and the features of surface runoff in the coastal zone.

Both groups of factors determine coastal retreat under the influence of thermal abrasion and thermal denudation. The mechanism of coastal erosion depends on the structure of the cliffs. The first (block) mechanism is most typical for shores of 8-12 m height, predominantly inherent to Alas Complex. At the cliff bottom, the sea produces wave-cut niches with a depth of up to 10-15 m. The overlying deposits break down along the cracks, and then the sea washes them away (Fig. 2).

The second type of destruction was observed on the shores of more than 15-20 m height, composed of deposits of Ice Complex. They are characterized by the formation of thermo-cirques (Fig. 3) with ice cliffs at the top (so-called "kygams")

and thermo-terraces at the base. Thermo-terraces form when the kygams retreat at a rate exceeding the rate of thermal abrasion. The retreat of such shores is due to the thermal denudation of icy cliffs under the influence of air temperatures, solar radiation and atmospheric precipitation, as well as coastal erosion of thermo-terraces.

The third type of shore destruction is typical for marine and alluvial-marine terraces less than 3-4 m height. Thermo-abrasive niches do not form there. The deposits thaw down to the water's edge and the debris are washed away by the sea.

Detail studies, conducted by international groups (Günther 2013, 2015; Lantuit 2011) on many sections of the retreating Laptev Sea coasts using remote data (Mamontov Klyk, Buor-Khaya, Bykovsky Peninsula, Muostah Island, Oyogos Yar, Fig. 1), showed significant variations in values of retreat rates (Table 1). However, they were not always able to reveal the significant factors that affect these variations. It should be noted that this was also hampered because of different averaging period used in these studies.



Fig. 2. The block collapse mechanism of coastal erosion. Southern shore of the Laptev Sea, 2010. Photo by A. Dereviagin



Fig. 3. Coastal erosion with forming the thermal cirques. Southern shore of the Laptev Sea, 2007. Photo by A. Dereviagin

The role of individual factors was the most fully determined for the Lyakhovsky Islands (Pizhankova and Dobrynina 2010; Pizhankova 2011). The most important factors were the following: neotectonic position of the coast, which determines the structure of the coastal section; the depth of the submarine near shore zone, the presence of shoals and foreshores; exposure of the coast through the intensity of storm surges; the presence of alongshore currents; the effect of solar radiation and the nature of snow accumulation (the formation of snowpacks on leeward shores); the regime of surface runoff contributing to the change in the ice situation in the near shore zone.

Thermal denudation in our studies was taken into account only for the Ice Complex shores, where it can be characterized on the basis of interpretation of medium-scale space imagery. For the Lyakhovsky Islands, there was revealed that the nature of the appearance and the parameters of thermal denudation are significantly various for the shores of different exposures. Both thermal abrasion and thermal denudation are proved to be more rapid on the shores up to the water's edge (and below) entirely composed of the Ice Complex, while the coasts with the ice-less quaternary deposits, underlying Ice Complex, retreat slower (in 1.2 times or more). For the first of them, the rate of

thermal denudation in 1.4 times exceeds the speed for the latter. This is not only due to the corresponding difference in the rates of thermal abrasion, but also, apparently, to the more significant influence of the radiation-heat balance on the large cliffs that are entirely composed of the Ice Complex.

We analyzed the changes of the Arctic ice coverage and climate warming from the 40s-20s of the 20th century to 2014 and their role in increasing of the coast retreat rates (Pizhankova 2016). This analysis showed that until 2000 the fluctuations in ice cover, with the exception of the explicit maximum of the 1960s in the Kara Sea, are weakly exposed: the ice coverage fluctuates around the average value for the period from the beginning of observations to 2000. And for the period after 2000, the common feature for all the seas is steady and rather sharp reduction in ice coverage up to values significantly below average figures. Fig. 4 shows data on the ice coverage for the Laptev Sea and the western part of the East Siberian Sea.

In our opinion, that is why it is advisable to use remote sensing data obtained in 2000 or a little earlier in order to measure the rates of coast retreat of different sections along the Arctic shores and compare them with data for previous and subsequent years.

Table 1. Information of the coastal retreat of the Laptev and East Siberian Seas, obtained in the early 21st century by use of remote sensing data

№	Name and location of the shore		Coast retreat rate, m / year	Measurement period	The source of information
1	Mamontov Klyk		2,1± 1,2	1965-2011	Günther et al. 2013
			4,6± 1.2	2007(2009) -2011	
2	Buor-Khaya		0,5± 0,4	1965-2011	
			1,2± 0,7	2007(2009) -2011	
3	Bykovsky Peninsula		0,6	1951-2006	Lantuit et al. 2011
4	Muostah Island		1,8± 1,3	1951- 2013	Günther et al. 2015
			3,4± 2,7	2010 -2013	
5	Oyogos Yar		3,2± 1,1	1965-2011	Günther et al 2013
			8,3± 2,8	2007(2009) -2011	
			2,4	1951- 1999	Pizhankova 2016
			3,4	1999 -2013	
6	Bolshoy Lyakhovsky Island	South coast	3,4	1951- 2001	Pizhankova and Dobrynina 2010; Pizhankova 2016
			7,7	2000 -2013	
		West coast	4,3	1951- 2001	
			9,4	2000 -2013	
		Northeast coast	2,7	1951- 2001	
			4,2	2000 -2013	
7	Maliy Lyakhovsky Island	Southeast coast	2,1	1951- 2001	Pizhankova and Dobrynina 2010
8	New Siberia Island	North coast	1,5	1952- 2002	Dobrynin et al. 2005; Gavrilov et al. 2012
		South coast	2,5		
		Southeast coast	4,1		
		East coast	3,6		
		West coast	2,3		

The study of multi-temporal remote sensing data (1951~2000 and 2000-2013) showed that reduction of sea ice coverage after 2000 (and correspondingly an increase in ice-free period duration) led to a significant increase in the rates of shore retreat in the 21st century (Fig. 5). The scale of the increase (in 1.5-2 and more times) is clearly visible in Fig. 6.

Similar results were obtained for the western and eastern shores of Bolshoy Lyakhovsky Island and the Shore Oyogos Yar. In the papers of Günther et al. (2013, 2015) in the short-term observations of 2007-2011 and 2010-2013 (see Table 1), there is also an increase of retreat rates, although it should be noted that Are (1980) pointed to the effect of higher values of retreat rates obtained during measurements in a short period.

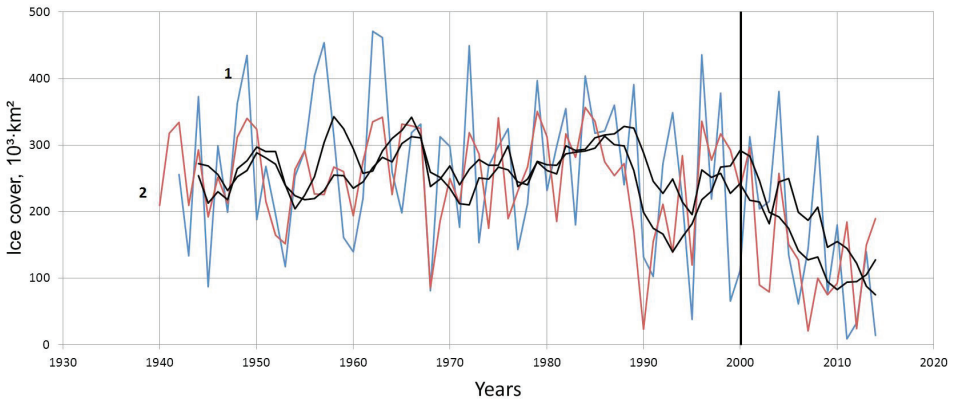


Fig. 4. Ice coverage dynamics of the Laptev Sea (1) and the western part of the East Siberian Sea (2) (august) and the trend curves based on averaging results for a five-year period

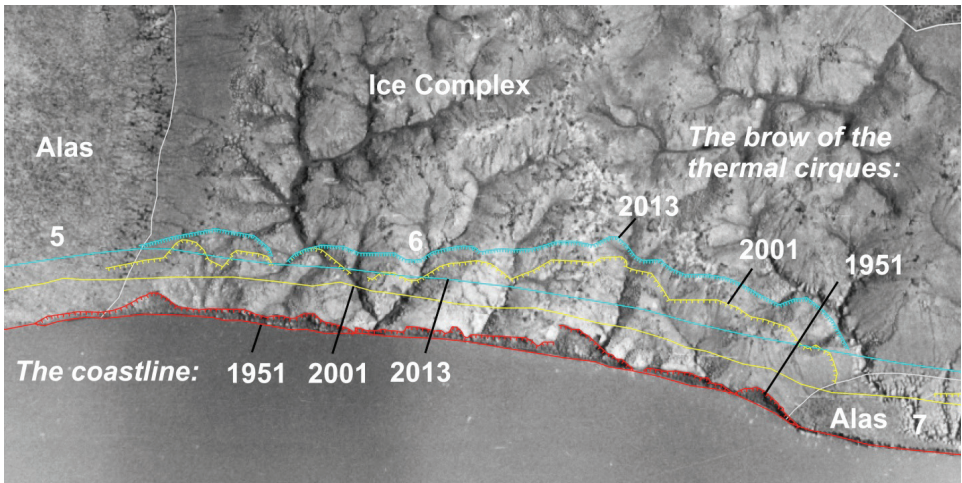


Fig. 5. The coastal dynamics of the southern coast of the Bolshoy Lyakhovsky Island. 5, 6, 7 – segment numbers for which the retreat rates have been calculated. Air photo of 1951

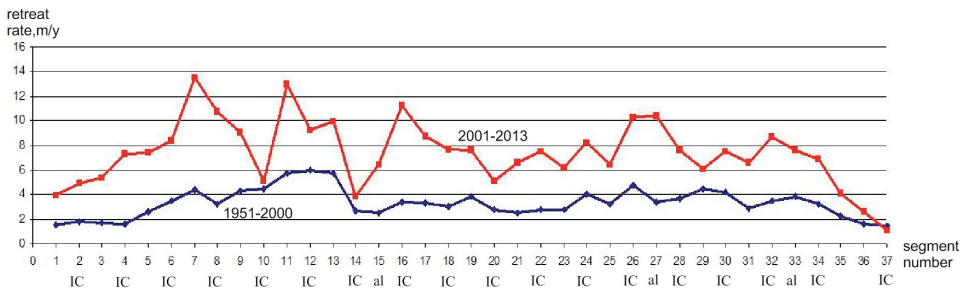


Fig. 6. Changes in the retreat rates for different segments of the southern coast of Bol. Lyakhovsky Island. The length of the coast is 70 km. IC – segments of the Ice Complex; al – segments of alluvial deposits; no letter indications – segments of the Alas Complex (Pizhankova, 2016)

Data based on comparison of different positions of coastlines of the Novosibirskiye Islands and the southern coast of the Dm. Laptev Strait (Pizhankova and Dobrynina 2010; Gavrilov et al. 2012; Pizhankova 2016), have shown that for 50 years (from 1951 to 2000) the total area of the washed out coasts was: 27.2 km² for the Bolshoy Lyakhovsky Island, 1.7 km² for the Malyi Lyakhovsky Island, 12.4 km² for Oyogos Yar, and 36 km² for the New Siberia Island. Over the past 13 years (from 2001 to 2013), they were enlarged by 10.3 km² of the coast of Bolshoy Lyakhovsky and 6.5 km² of the Oyogos Yar. The average retreat rates were 3.2 m/y for the period up to 2000 and 6.4 m/year from 2000 to 2013 for all the eroded coasts of this region. Thus, the retreat rates in 1.3-2.9 times increased in 2000-2013 in comparison with the period 1951-1999. The rate of thermal denudation increasing was not that much dramatic - by 1.7-1.9 times (Pizhankova 2011, 2016). In our opinion, this shows that the influence of reducing ice coverage on the shore retreat process is more dramatic than the influence of increasing air temperatures.

DEGRADATION OF PERMAFROST UNDER SUBMARINE CONDITIONS CAUSED BY COASTAL RETREAT

The transition of permafrost from subaerial to submarine conditions (from onshore to offshore) simultaneously increases the average annual temperature of sediment surface from -11...-15 to -0.5...+0.5°C. This triggers the degradation of newly formed submarine frozen ground. This degradation is represented by the transformation of ice-bonded permafrost into ice-bearing permafrost (ice-bearing permafrost in the crystal lattice contain together with ice unfrozen water), and then thawing. The submarine permafrost thaws from the top as well as from its bottom as it acquires a gradientless temperature profile. Thawing from the top is due to salinization of sediments, which lowers the freezing-melting point, and high temperature of the bottom water. The latter factor is due to summer radiative warming.

Dependence of bottom water temperature from air temperature determines the

relationship of submarine permafrost degradation with climate dynamics. The rate of degradation from top can be judged according to drilling profiles from the coast towards the sea for the Muostakh Island, the Bykovsky Peninsula and the Mamontov Klyk (Grigoriev 2008; Overduin 2016). The highest rate of permafrost table lowering was fixed for the period 1983 - 2013/2014 along the profile of Muostakh Island. For the subsea Ice Complex, the rate was 13.5-18.5 cm/year, and for its underlying deposits - 6 cm/year. If we take into account that on the average 1/3 thawed sediments separating the permafrost table from the seafloor are excited by waves (Are 2012), then the rate of degradation is 28 cm/year for the first case and 9 cm/year for the second one. However, such velocities are the maximum and are observed in the first years and decades. The rates for the periods of thousands of years are estimated at least lower by an order of magnitude. Thus, at Mamontov Klyk, thawing of 35 m of top of permafrost occurred for at least 2500 years at the site of the borehole most remote from the shore (11.5 km), so the average speed was 1.9 cm / year (Grigoriev 2008). The thawing time duration was calculated basing on the current rate of shore retreat. Meanwhile, his reconstruction shows a lower retreat rate in the past, especially in the Little Ice Age. It was 3-4 times slower (Razumov and Grigoriev 2017). Therefore, the average rate of permafrost degradation from the top should be considered substantially lower than the indicated value, and its duration was longer.

When studying the degradation of submarine permafrost by drilling methods, thawing from the bottom is not usually considered. Meanwhile, its contribution into the general permafrost degradation is not only comparable with the degradation from the top, but also can exceed it. This is evidenced by the results of mathematical simulation. The decrease in the permafrost thickness from the bottom varies from 1.5 to 3 cm/year and depends on the density of the geothermal flux. The first value corresponds to a flux density of 50 mW/m², the second one is to 75 mW/m² (Romanovskii et al. 2006; Gavrilov 2008). The region of the Bykovsky Peninsula and Muostakh Island belongs to

the Ust-Lena rift, for which the second value should be taken. Thus, the rate of permafrost degradation from the bottom can be at least two or more times higher than the rate of degradation from the top.

RECENT FORMATION AND FREEZING OF COASTAL-MARINE SEDIMENTS

The coastal-marine sedimentation was studied in the region of the Lyakhovsky Islands using remote sensing data. These studies have shown that the coast increment occurs in the areas of tectonic uplift, and due to the input of a significant volume of solid runoff to the coastal zone. In this case, spits, bars and foreshores are formed in the places where the capacitance of landshore drift decreases. Subsequently, the submarine coastal slope turns into beach level, and with the continuation of sedimentation - to the march level.

Studies indicated that the increment of shores is the most typical for Malyi Lyakhovsky Island. The northern, western and northeastern coasts of this island are accreted because of the formation of beaches and marches; the southern and southwestern ones are due to the formation of spits. The accretion of the spit on the southern coast of the island is quite

pronounced, the extension of the coast to the sea averaged about 70 m for the 6 km section of the spit for 50 years.

On the Bolshoy Lyakhovsky Island, the shore accretion is typical for the north-northeastern coastal areas and for the areas adjacent to the east of the Kigilyakh Peninsula, where the accumulation occurs through the filling an incoming angle of a coast contour. Accreting spits subsequently form the surface of terraces, which stepwise rise up to the root slope (Fig. 7). The total area of the shore increment was 1.8 km² for Bolshoy Lyakhovsky Island and 1.6 km² for Malyi Lyakhovsky Island for 50 years (from 1951 to 2000) (Pizhankova and Dobrynina 2010)

Coastal-marine buildings are characterized by explicit variability in the coastline. This is particularly evident in the dynamics of the areas of Sellyach and Ebelyach foreshores, the dimensions of which are measured by many tens of kilometers. The western parts of these foreshores are washed away; the sediments are transported and deposited in the east. Debris of the Late Pleistocene Ice Complex, which is affected by thermo-abrasion and thermo-denudation, is the main source of their formation, as in the case of the Lyakhovsky Islands. The sediments of the foreshores usually consist of saline

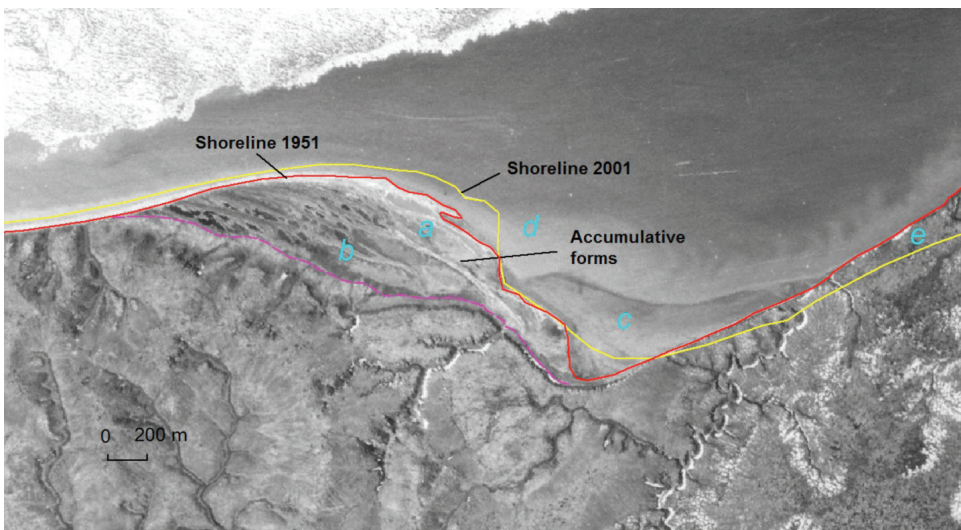


Fig. 7. Accumulative relief forms of Bolshoy Lyakhovsky Island: above sea water ones: a - recent (1950-2001), b - recent and Holocene; underwater forms: c - recent; d - formed in the past. The retreat of the shore - e. Air photo of 1951

aleurites, silty material, and fine dust sands. In Vankina Bay, recent syncryogenic submarine permafrost is estimated as 25 m thick (Zhigarev and Plakht 1974). They generally merge with the underlying permafrost relict layers.

The formation of coastal-marine sediments is accompanied by its syncriogenesis. This is evidenced by the numerous islands located to west of the Lena delta. These are elevated fragments of bars bordering the delta for many tens of kilometers. The largest of them is a chain of islands stretching along the western coast of the Arga-Muora Ceese Island. The Aeros'yemki and Samoleta Islands can also be the same elevated parts of bars, formed several thousand years ago. The remains of the eroded parts of the delta are in close proximity to them.

Contemporary activation of sedimentation in shallow waters is quite interesting. It is identified due to the new formation of the islands in recent years. Yaya Island

at Vasilyevskaya Bank was revealed in aerovisual observations (Gukov 2014; Fig. 8). The Island Zatoplyayemyy, in 60 km east of the Lena delta and the Neizvestnyye Islands near the southeastern shore of Bunge Land were recently marked on topographic maps.

The way of formation of such islands is disputed. In our opinion, ice hummocks locating on the ground - stamukhas, most likely facilitate their formation. This is consistent with available data (Fig. 9). For three decades of visual ice reconnaissance surveys, according to incomplete data, 2086 stamukhas were found in the Laptev Sea (Gorbunov et al. 2008) and 7962 stamukhas in the East Siberian Sea (Gorbunov et al. 2007).

In summer, as sea is cleared from the ice, warmed bottom water on shallows induces thawing of bottom sediments, which turn to be mobile. Accumulation occurs under wind surges and storms, when the thawed sediments are stored around stamukhas



Fig. 8. The Yaya Island appeared at Vasilyevsky Bank and discovered in 2013. Photo by Pavel S. Sayapin (<https://commons.wikimedia.org/w/index.php?curid=30168239>)

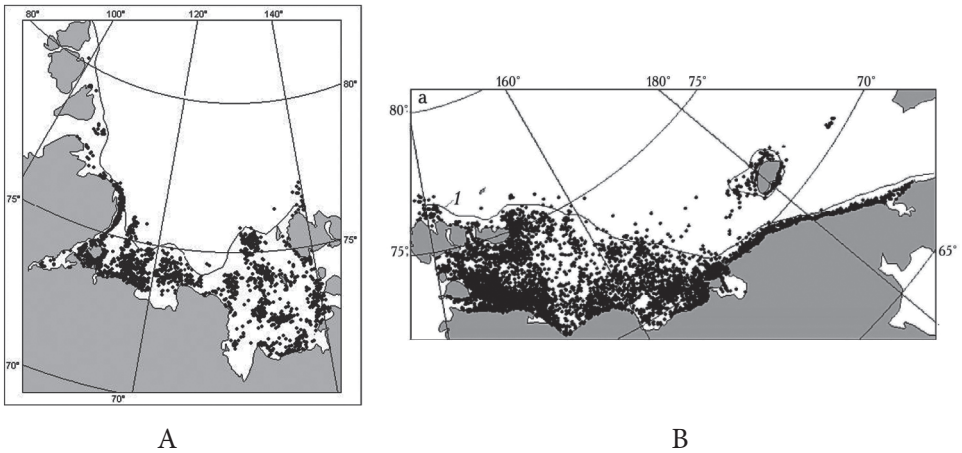


Fig. 9. The average long-term position of the stamukhas (black dots) and the fast ice border (black line) in the Laptev Sea (a) and East Siberian Sea (b) (Gorbunov et al. 2007, 2008)

adfreezing with the bottom near the coastline. Stamukhas melts at the end of summer, and the accumulative formation remains in the shape of atoll, which was frozen in next winter. Freezing is facilitated by the fact that the bottom sediments located at the site of the stamukhas after their melting may be low or non-saline.

Freezing plays a key role in formation of such islands in the process of sedimentation. Freezing fixes them for a long time. Indeed, on shallows, the summer radiation warming of the bottom water and ice play an important role in the formation of the average annual temperatures of bottom permafrost (Zhigarev 1981, 1997). There are three sea depths intervals, 0...2-2.5 m; 2.5...6-8 m and more than 6-8 m. The first one corresponds to the thickness of the seasonal ice cover in the Laptev and East Siberian Seas at 70-76° N. This is the fast ice zone. Here, intensive conductive cooling of the bottom deposits occurs through the ice adfreezing with the bottom during the long winter time. Despite the summer warming of the bottom water up to 10-14°C, the annual sums of winter negative temperatures exceed the sum of summer positive temperatures, especially significantly near the sea edge. Therefore, the deposits freeze if the rising surface of coastal-marine accumulation falls into the upper part of the interval of isobaths of 2.5 to 0 m. According to the data obtained for Vankina Bay (72°N, Katasonov and Pudov 1972, Molochushkin 1973), the forming average

annual temperature of bottom sediments is -10...-11.5°C. On foreshores, near the coasts of the Lyakhovsky Islands (74°N), where the temperature of the subaerial permafrost is -12...-15°C (Geocryology of the USSR, 1989), the temperature of bottom sediments in the fast ice zone is even lower.

The depth interval from 2.5 to 6-8 m is also significant. In the conditions of contemporary warming, the bottom water here has a positive average annual temperature, causing the existence of thawed and seasonally thawing sediments freely transporting by the waves. This interval of depths within the underwater elevations is a supplier of terrigenous material to accrete their tops and form islands. Below these depths, negative mean annual temperatures of the bottom water and bottom deposits are mainly formed (Zhigarev 1981; Grigoriev and Razumov 2005; Are 2012).

Sedimentation and formation of islands in the shallows also occurred in the past. The topographic maps of the 1950-80 period show several islands, a shape of which is completely similar or close to that shown in Fig. 8. These are Islands Peschanyy (Fig. 10), Nanosnyy. A shape of an atoll is rather unusual for islands of the Arctic seas. The possibility of their formation according to the pattern described above seems very plausible due to the constant presence of stamukhas throughout the summer.

Яндекс

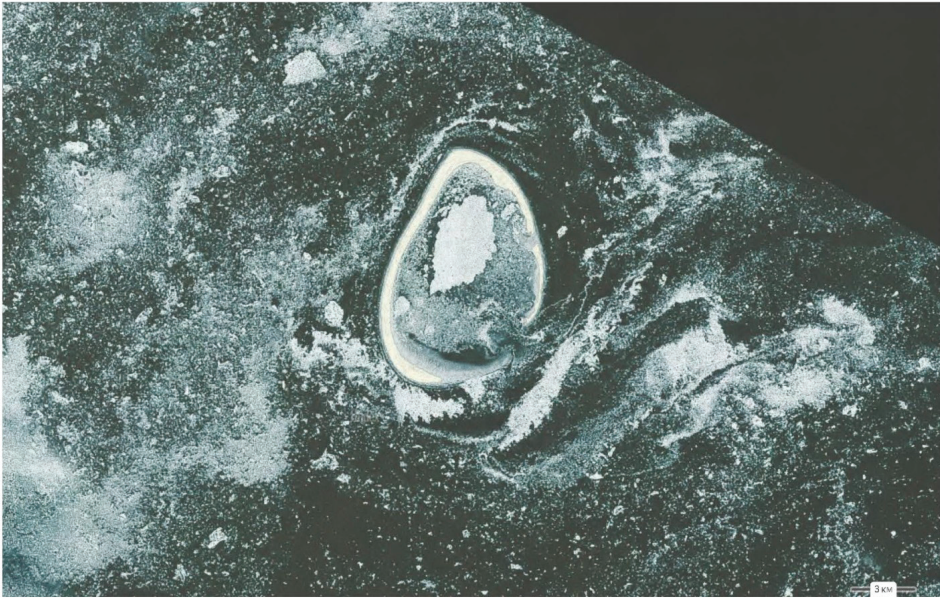


Fig. 10. Peschany Island

(<https://yandex.ru/maps/?clid=2220323-129&win=196&ll=116.290258%2C74.310081&z=10&l=sat>)

The possibility of a present formation of islands and frozen ground, in our opinion, is closely related to warming and an increase in the duration of ice-free period. During the 19th and 20th centuries, the relicts islands of the Late Pleistocene Ice Complex were continuously destroyed, disappeared, and the shallows that they inherited were deepened (Gavrilov et al. 2003; Dudarev et al. 2003). However, according to the hydrographic monitoring of the Pacific Oceanological Institute, FEB RAS (Dudarev et al. 2003, 2008, 2015), the constant deepening of the Semenovskaya, Vasilievskaya and other shoals in the seas of Eastern Siberia, that occurred in the past, was replaced by the stabilization of their depths and even the formation of islands. In our opinion, the change in the orientation of lithomorphogenesis in shallow waters was caused by the increase of contemporary warming scale. Warming causes an increase in the volume of sedimentary material as a result of accelerating of coastal retreat and intensification of bottom erosion. The duration of the ice-free period, the wave length, the frequency and the strength of storms, and the wind-induced surges has increased. The large-scale increase in the

volume of terrestrial material and wave energy in conditions when stamukhas exist up to freezing-over results in accumulation of sediments along their perimeter. The freezing of accumulated sediments preserves the formed islands.

CONCLUSIONS

1. The coastal zone of the East Asian sector of the Arctic is the area with highly dynamic permafrost environment. On the one hand, here the onshore permafrost is transformed into degrading offshore permafrost, and, on the other hand, modern submarine and subaerial syncryogenic permafrost are under formation.

2. The high activity of cryogenic (primarily thermogenic) processes in the coastal zone of study area is due to the participation of ice-rich syncryogenic deposits of the Late Pleistocene Ice Complex and the Holocene Alas Complex in its structure. The main processes are thermal erosion, thermal denudation causing a rapid coastal retreat, and degradation of the submarine permafrost.

3. The current decrease in the sea ice cover (an increase in an ice-free period) and climate warming result in an increase in the retreat rate of studied coast sections by 1.3-2.9 times in the 21st century compared with the second half of the 20th century. The rate of thermal denudation increased by 1.7-1.9 times during this time.
4. Degradation of the offshore permafrost from the top is caused by salinization of bottom sediments, their high ice content, and high annual average temperatures of the bottom water. Dependence of the bottom water temperature on air temperature allows us to assume higher rates of this process in the 21st century. The average rate of permafrost degradation from the top may be 1.5-2 cm/year, and from the bottom - 1.5-3 cm/year.
5. Contemporary accumulation and freezing of coastal-marine sediments occur in the areas of modern uplifts and where the coastline features contribute to sedimentation. Seasonal freezing first and then perennial freezing begins when the rising accumulation surface falls within a depth interval of 2-2.5 to 0 m and occurs through fast ice.
6. The large-scale increase in wave energy and in the amount of sediments coming from the coastal and bottom thermal abrasion, owing to the increasing duration of ice-free period, leads to a distinctly pronounced activation of sedimentation. The sedimentation occurs on banks and shallows, where, from the depths of 1-1.5 m, there is the possibility of fixing its results by freezing.
7. The activation of sedimentation in the shallows and the numerous stamukhas located in the zone of fast ice show the pattern of the formation of the islands around them. Stamukhas thaw shortly before freeze-up, and accumulative formations in a shape of an atoll are fixed by freezing. One of these islands – Yaya – was recently formed at Vasilyevskaya Bank. Similar islands were also formed in the past and designated on published topographic maps. ■

REFERENCES

- Are F.E. (1980). Thermal abrasion of sea shores. Moscow: Nauka, 160 p. (in Russian).
- Are F.E. (1985). Basics of forecasting of coastal thermal abrasion. Novosibirsk: Nauka, 172 p. (in Russian with English summary).
- Are F.E. (1998). Thermal abrasion of the Laptev Sea shores and its contribution to the sea sediment balance. *Kriosfera Zemli*. vol. II, No. 1, pp. 55-61. (in Russian with English summary).
- Are F.E. (2012). Coastal erosion of the arctic lowlands, Novosibirsk: Academic Publishing House "Geo", 2012, 291p. (in Russian with English summary).
- Coastal processes in the permafrost zone (1984). Novosibirsk: Nauka, 135 p. (in Russian).
- Dynamics of the Arctic coasts of Russia (1998). Moscow: MSU, 248 p. (in Russian).
- Dobrynin D.V., Pizhankova E.I., Tumskoy V.E. and Rivkin F.M. (2005). The coastal dynamics of New Siberia Island based on the comparison of multitemporal remote sensing materials// *Materials of the Third Conference of Russian Geocryologists*. vol. III, ch. 6, Moscow: MSU, pp. 76-82. (in Russian).
- Dudarev O.V., Botsul A.I., Semiletov I.P. and Charkin A.N. (2003). Modern sedimentation within the near-coastal shelf cryolithic zone of the Dmitriy Laptev Strait of the East Siberian Sea. *Pacific Geology*. vol. 22, № 1. pp. 51-60. (in Russian with English summary).

Dudarev O.V., Charkin A.N., Semiletov I.P., Shilo I.N., Salyuk A.N. and Spivak E.A. (2008). About the current state of subsea island relics on the East Siberian shelf. *Doklady Earth Sciences*. vol. 419, pp. 225-261. (in Russian with English summary).

Dudarev O.V., Charkin A.N., Semiletov I.P., Pipko I.I., Pugach S.P., Chernykh D.V., Shakhova N.E. and Sergienko V.I. (2015). Peculiarities of the present-day morpholithogenesis on the Laptev Sea Shelf: Semenovskaya shoal (Vasema Land). *Doklady Earth Sciences*. vol. 462. № 1. pp. 510-516. doi: 10.7868/S0869565215140194.

Fartyshev A.I., Shamshurin V.Yu. and Uritskiy V.F. (1983). The permafrost-geothermal conditions of the North-Lyakhovsky shelf of the East Siberian Sea. *Thermophysical studies of the cryolithozone of Siberia*. Novosibirsk: Nauka, pp.111-126. (in Russian).

Fartyshev A.I. (1993). Features of the coastal-shelf cryolithozone of the Laptev Sea. Novosibirsk: Nauka, 135 p. (in Russian).

Gavrilov A.V., Romanovskii N.N., Romanovsky V.E., Hubberten H.-W. and Tumskey V.E. (2003). Reconstruction of Ice Complex Remnants on the Eastern Siberian Arctic Shelf. *Permafrost and Periglacial Processes*, 14, pp. 187-198.

Gavrilov A.V. (2008). Cryolithozone of the Eastern Siberia Arctic shelf (current state and history of development in the Middle Pleistocene-Holocene). Abstract Doctor of Geological and Mineralogical Sciences. Moscow: MSU, 48 p. (in Russian).

Gavrilov A.V., Pizhankova E.I., Derevyagin A.YU. and Chizhov A.B. (2012). Ecologically adverse Natural processes of the Northern Yakutia coastal accumulative plains. *Proceedings of the Tenth International Conference on Permafrost Salekhard, Yamal-Nenets Autonomous District, Russia, June 25–29, Vol. 3 (Contributions in Russian)* pp. 97-100 (in Russian).

Geocryology of the USSR. Eastern Siberia and the Far East (1989). Moscow: Nedra, 515 p. (in Russian).

Gorbunov Yu.A., Losev S.M. and Dyment L.N. (2007). Stamukhas of the East Siberian and Chukchi Seas. *Materials of glaciological research*, vol. 102, pp. 41 – 47. (in Russian with English summary).

Gorbunov Yu.A., Losev S.M. and Dyment L.N. (2008). Stamukhas of the Laptev Sea. *Probl. Arctic and Antarctic*, No. 2 (79), pp. 111-116. (in Russian with English summary).

Grigoriev M.N. (1993). Cryomorphogenesis of the estuary region of the Lena river. *Yakutsk. Permafrost Institute SB RAS*, 176 p. (in Russian).

Grigoriev M.N. (2008). Cryomorphogenesis and lithodynamics of the coastal-shelf zone of the Eastern Siberia seas. Abstract ... Doctor of Geographical Sciences. Yakutsk, 38 p. (in Russian).

Grigoriev M.N. and Razumov S.O. (2005). Distribution and evolution of subaquatic permafrost in the coastal-shelf zone of the Laptev and East-Siberian seas as a consequence of long-term transformation of the coastal zone//Modern geodynamics and dangerous natural processes in Central Asia. Irkutsk: Institute of the Earth's Crust, SB RAS, ch. 2, pp. 136-155. (in Russian).

Grigoriev M.N., Razumov S.O., Kunitzkiy V.V., Spektor V.B. (2006) Dynamics of the Russian East Arctic Sea coast: major factors, regularities and tendencies. *Kriosfera Zemli*, vol. X, № 4, pp. 74–94. (in Russian with English summary).

Grigoriev N.F. (1966). Permafrost of the Primorsky zone of Yakutia. Moscow: Nauka, 180 p. (in Russian).

Gukov A.Yu. (2014). Island discovered in the 21st century. Geography and ecology in the school of the XXI century, № 2, pp. 14-18. (in Russian).

Günther, F., Overduin, P. P., Sandakov, A. V., Grosse, G., and Grigoriev, M. N. (2013). Short- and long-term thermo-erosion of ice-rich permafrost coasts in the Laptev Sea region. *Biogeosciences*, 10, 4297–4318, doi:10.5194/bg-10-4297-2013.

Günther F., Overduin P. P., Yakshina I. A., Opel T., Baranskaya A. V., and Grigoriev M. N. (2015). Observing Muostakh disappear: permafrost thaw subsidence and erosion of a ground-ice-rich island in response to arctic summer warming and sea ice reduction. *The Cryosphere*, 9, 151–178, www.the-cryosphere.net/9/151/2015/ doi:10.5194/tc-9-151-2015.

Hughes A.L.C., Gyllencreutz R., Lohne Ø. S., Mangerud J. and Svendsen J. I. (2016). The last Eurasian ice sheets – a chronological database and time-slice reconstruction, DATED-1. *Boreas*, January 2016, Volume 45, Issue 1 (pp. 1–45), doi: 10.1111/bor.12142.

Junker R., Grigoriev M.N. and Kaul N. (2008). Non-contact infrared temperature measurements in dry permafrost boreholes. *J. Geophys. Res.*, 2008, vol. 113, No. B04102.

Katasonov E.M. and Pudov G.G. (1972). Cryolithological studies in the area of the Vankina Bay of the Laptev Sea //Permafrost studies, vol. XII, MSU, pp. 130-136. (in Russian).

Lantuit H., Atkinson D., Overduin P. P., Grigoriev M.N., Rachold, V., Grosse, G. & Hubberten, H.-W. (2011). Coastal erosion dynamics on the permafrost-dominated Bykovsky Peninsula, north Siberia, 1951-2006. *Polar Research*, 30, 7341, doi:10.3402/polar.v30i0.7341.

Molochushkin E.N. (1969). On the nature of the heat exchange of water and bottom rocks in the coastal zone of the Laptev Sea. *Questions of the geography of Yakutia*. Yakutsk, pp.121-126. (in Russian).

Molochushkin E.N. (1970). Thermal regime of rocks in the southeastern part of the Laptev Sea. Abstract of the Dissert ... Candidate of Geographical Sciences. Moscow: MSU, 20 p. (in Russian).

Molochushkin E.N. (1973). Influence of thermal abrasion on the temperature of permafrost in the coastal zone of the Laptev Sea. *Proceedings of II Intern. Conf. on permafrost*, issue 2. Yakutsk, pp. 52-57. (in Russian).

Neizvestnov Ya.V. (1980). Engineering geology of the Arctic Shelf zone of the USSR Abstract ... Doctor of Geological and Mineralogical Sciences. Leningrad, 31 p. (in Russian).

Neizvestnov Ya.V. (1999). Hydrogeology. Explanatory note to the geological map of the USSR, scale 1: 1 000 000 (new series), sheet S-53-55 (Novosibirsk Islands). Leningrad: VSEGEI, pp.139-146. (in Russian).

Nicolsky D.J., Romanovsky V.E., Romanovskii N.N., Kholodov A. L., Shakhova N. E., Semiletov I. P. (2012). Modeling sub-sea permafrost in the East Siberian Arctic Shelf: The Laptev Sea Region. *J. Geophys. Res.*, 117, F03028, doi:10.1029/2012JF002358.

Novikov V.N. (1984). Morphology and dynamics of the Vankina Bay shores of the Laptev Sea. *Coastal processes in the permafrost zone*. Novosibirsk: Nauka, pp. 20–28. (in Russian).

Overduin, P. P., Hubberten, H.-W., Rachold, V., Romanovskii, N. N., Grigoriev, M. N., and Kasymkaya, M. (2007). The evolution and degradation of coastal and offshore permafrost in the Laptev and East Siberian Seas during the last climatic cycle, in: *Coastline Changes: Interrelation of Climate and Geological Processes*, vol. 426, edited by: Harff, J., Hay, W., and Tetzlaff, D., The Geological Society of America, Boulder, CO, 97–111, doi:10.1130/2007.2426(07).

Overduin P.P., Strzelecki M.C., Grigoriev M.N. Couture N. Lantuit H. St-Hilaire-Gravel D. Gunther F. and Wetterich S. (2013). Coastal changes in the Arctic, Geological Society of London Special Publications, 388, pp. 103-129, doi: 10.1144/SP388.13.

Overduin, P. P., Wetterich, S., Günther, F., Grigoriev, M. N., Grosse, G., Schirrmeister, L., Hubberten, H.-W., and Makarov, A. (2016). Coastal dynamics and submarine permafrost in shallow water of the central Laptev Sea, East Siberia. *The Cryosphere*, 10, pp. 1449-1462. <https://doi.org/10.5194/tc-10-1449-2016>.

Pizhankova E.I. (2011). Termodenudation in the coastal zone of the Lyakhovsky Islands (interpretation of aerospace images). *Kriosfera Zemli*, vol.XV, № 3, pp. 61-70. (in Russian with English summary).

Pizhankova E.I. (2016). Modern climate change at high latitudes and its influence on the coastal dynamics of the Dmitriy Laptev Strait area. *Earth`s Cryosphere*, vol. XX, No. 1, pp. 46–59.

Pizhankova E.I. and Dobrynina M.S. (2010). The dynamics of the Lyakhovsky Islands coastline (results of aerospace image interpretation). *Kriosfera Zemli*, vol. XVI, № 4, pp. 66-79. (in Russian with English summary).

Rachold, V., Bolshiyarov, D. Y., Grigoriev, M. N., Hubberten, H.-W., Junker, R., Kunitsky, V. V., Merker, F., Overduin, P., and Schneider, W. (2007). Nearshore arctic subsea permafrost in transition, *Eos T. Am. Geophys. Un.*, 88, 149–150, doi:10.1029/2007EO130001.

Razumov S.O. (1996). Dynamics of marine thermoabrasive shores in connection with the peculiarities of permafrost-climatic conditions (on the example of the Kolyma Bay of the East Siberian Sea). Abstract of the Dissert ... Candidate of Geographical Sciences. Yakutsk, 24 p. (in Russian).

Razumov S.O. (2007). Modeling and forecasting of icy coasts dynamics of the eastern Arctic seas of Russia. Abstract ... Doctor of Geographical Sciences. Yakutsk, 52 p. (in Russian).

Razumov S.O. (2010). Permafrost as a Factor of Coastal Zone Dynamics in the East Arctic Seas of Russia. *Oceanology*, vol. 50, № 2, pp. 285-291 (in Russian with English summary).

Razumov S.O. and Grigoriev M.N. (2017). Modeling of coastal dynamics of the Laptev and East Siberian seas in the second half of Holocene. *Kriosfera Zemli*, vol. XXI, No. 1, pp. 32–40. DOI: 10.21782/EC2541-9994-2017-1(32-40) (in Russian with English summary).

Romanovskii N.N., Eliseeva A.A., Gavrilov A.V., Tipenko G.S. and Hubberten H.-W. (2006). The long-term dynamics of the permafrost and gas hydrate stability zone on rifts of the East Siberian Arctic shelf (report 2). *Kriosfera Zemli*, vol. X, № 1, pp. 29-38. (in Russian with English summary).

Soloviev V.A. (1981). Forecast of the distribution of the relict subaquatic frozen zone (on the example of the Eastern Arctic seas). *Cryolithozone of the Arctic shelf*. Yakutsk: Permafrost Institute SB RAS, pp. 28-38. (in Russian).

Soloviev V.A., Ginsburg G.D., Telepnev E.V. and Mikhalyuk Yu.N. (1987). Cryogeothermy and hydrates of natural gas in the bowels of the Arctic Ocean. Leningrad: PGO Sevmorgeology, 151 p. (in Russian).

Zenkovich V.P. (1962). Fundamentals of the theory of the sea coast development. Moscow: Publishing House of the Academy of Sciences of the USSR, 710 p. (in Russian).

Zhigarev L.A. (1981). Regularities of the development of the Arctic basin cryolithozone. Cryolithozone of the Arctic shelf. Yakutsk: Permafrost Institute SB RAS. pp. 4-17. (in Russian).

Zhigarev L.A. (1997). Oceanic cryolithozone. Moscow: MSU, 318 p. (in Russian).

Zhigarev L.A. and Plakht I.R. (1974). Features of the structure, distribution and formation of the subaquatic cryogenic stratum. Problems of cryolithology, vol. IV. Moscow: MSU, pp. 115-124 (in Russian).

Zhigarev L.A. and Plakht I.R. (1977). Permafrost and perennial-cooled rocks of the Vankina Bay. Geographical problems of the study of the North. Moscow: MSU, pp. 136-142 (in Russian).

aisori.meteo.ru, (2015). Specialized arrays for climate research [Online]. Available at: <http://aisori.meteo.ru/ClimateR> [Accessed 24 Nov. 2015].

aari.nw.ru, (2015). Arctic and Antarctic Research Institute [Online]. Available at: <http://www.aari.nw.ru/projects/ECIMO/> [Accessed 4 Feb. 2015].

commons.wikimedia.org, (2017). Wikimedia Commons [Online]. Available at: <https://commons.wikimedia.org/w/index.php?curid=30168239> [Accessed 9 Oct. 2017].

yandex.ru, (2017). Yandex Maps [Online]. Available at: <https://yandex.ru/maps/?clid=2220323-129&win=196&ll=116.290258%2C74.310081&z=10&l=sat> [Accessed 9 Oct. 2017].

Received on November 1st, 2017

Accepted on March 1st, 2018



Anatoly V. Gavrilov, D.Sc. in Geological - Mineralogical Sciences, Leading Researcher at the Laboratory of the geological environment and the relationship of surface and underground waters of the Faculty of Geology Lomonosov Moscow State University. His scientific interests are issues of regional and historical geocryology, paleogeography and aerospace research of cryosphere. Areas of his research are the coastal lowlands and mountain structures of the Northeast of Russia, South Yakutia, the North of Transbaikalia, the shelf of the Arctic seas. Gavrilov Anatoly V. is the author of more than 150 works, including the Geocryological map of the USSR scale 1: 2 500 000 and nine monographs.



Elena I. Pizhankova, Ph.D. in Geological-Mineralogical Sciences, Senior Researcher at the Laboratory of the geological environment and the relationship of surface and underground waters of the Faculty of Geology Lomonosov Moscow State University. Her scientific interests are issues of regional and historical geocryology and the remote sensing of permafrost and periglacial processes. The main area of her research are Northern and Southern Yakutia, Pechora Lowland, the coastal zone of the Laptev and East Siberian seas. She is author of about 90 publications and numerous reports.

Vadim Yu. Grigoriev^{1*}, Natalia L. Frolova²

¹Water problems institute of Russian Academy of Science, Lomonosov Moscow State University, Moscow, Russia

²Land hydrology department Lomonosov Moscow State University, Moscow, Russia;

* **Corresponding author:** vadim308g@mail.ru

TERRESTRIAL WATER STORAGE CHANGE OF EUROPEAN RUSSIA AND ITS IMPACT ON WATER BALANCE

ABSTRACT. Terrestrial water storage has a significant impact on the water balance of river basins. The analysis of its changes in the European part of Russia (EPR) using the GRACE (Gravity Recovery and Climate Experiment) data showed that its reduction was approximately 150 mm for 2002-2015 for the south of EPR, especially the Don basin, which is caused rather by a decline in the storages of surface and ground waters then to changes in soil waters. Quasilinear relation between the values of terrestrial water storages and a river runoff for the period of a summer low water level for a number of rivers has been revealed.

KEY WORDS: GRACE, water balance, European Russia, soil water content.

CITATION: Vadim Yu. Grigoriev, Natalia L. Frolova (2018) Terrestrial water storage change of European Russia and its impact on water balance. *Geography, Environment, Sustainability*, Vol.11, No 1, p. 38-50

DOI-10.24057/2071-9388-2018-11-1-38-50

INTRODUCTION

In 1896 A. Penk proposed the equation of the water balance of a river basin for long-term period. E. V. Oppokov in 1904 proposed the equation of the water balance of a river basin for some period as the sum of precipitation (P), evaporation (E), a river and underground runoff (R), and a terrestrial water storage change ($TWSC$) equal to zero in its most general form (Babkin and Vuglinsky 1982)

$$P_t - E_t - R_t \pm TWSC_t = 0 \quad (1)$$

where t indicates some time interval. Further in the text this index is omitted.

The total terrestrial water storages (TWS) are the storages of surface and ground waters in all aggregate states. As a rule, individual TWS components are of interest. Thus, the snow water equivalent (SWE) is one of the key predictors of spring high water runoff and the maximum values of a water flow for the rivers with a cold climate. The risk of hydrological drought depends on groundwater storages. The soil water content (SWC) largely determines the nature of the interaction of the atmosphere with the underlying surface (Kumar et al. 2016), and is also a factor in the formation of the maximum runoff. Terrestrial water storage change $TWSC$ is the difference between end-of-period and beginning-of-period TWS .

There are several methods to determine the value of *TWSC*. One of them used in the GRACE (Gravity Recovery and Climate Experiment) project is based on the impact of water mass redistribution on the Earth's gravitational field. The basis of the GRACE system is 2 satellites equipped with microwave range finders, star cameras, accelerometers and GPS signal receivers (Zotov et al. 2015). A component due to a change in *TWS* is obtained using the models of circulation of the atmosphere and the ocean, as well as the dynamics of the earth's crust from the Earth's gravitational field. Thus, the obtained data on a *TWS* change are a solution to an inverse regularization problem. Since the solution to this problem is unstable, the final result depends on a method for solving the problem. There are two main approaches to solving this problem. The first is in the form of Stokes coefficients, global, the solution is sought for the entire land. The second is in the form of mascons, local, the solution is sought for each local area, for example 3° hexagons (Save et al. 2016). The result of the calculation presents an anomaly of terrestrial water storage (not its absolute value) *TWSA*, for any period, most often in one month.

GRACE data are used in meteorology to validate a reanalysis (Springer et al. 2017) and improve a surface air temperature forecast (Lin et al. 2016), and in glaciology to validate and calibrate the melting of a seasonal snow cover and glaciers (Wahr et al. 2016; Chen et al. 2017a; Schlegel et al. 2016). The use of GRACE data in hydrology is mainly limited to the issues of water runoff estimation, although there is an example of their use for studying the dynamics of river sediments (Liu et al. 2016). The study of a river runoff using GRACE is concentrated in two main trends: 1) the calculation of various components of water balance using remote sensing data (RSD) and a weather reanalysis using the water balance equation; 2) the assimilation of GRACE data into hydrological models and LSM (land surface model). The first trend appeared first of all. An unknown member of water balance (usually a river runoff) is calculated therein from the known values of the remaining terms. Despite the low accuracy of such calculations in comparison with the measurements or

simulation results, they make it possible to estimate it for large areas there are few measurement data for (Li et al. 2016; Lorenz et al. 2014) or they are not publicly available (North Korea (Seo and Lee 2017)). Due to the rough spatial resolution of GRACE data, the calculation of a river runoff directly from the changes in channel storages, without using other RSD, is only possible on the Amazon River, the largest river (Eom et al. 2017). In a number of cases, such as the dynamics of the level of the Caspian Sea (Chen et al. 2017b), the world ocean (Chambers et al. 2017), the water resources of arid lands (Deng and Chen 2017; Forootan et al. 2017, Frolova et al. 2017) and wetlands (Xie et al. 2016), *TWSC* is precisely of interest. If the dynamics of water storages varies significantly in different reservoirs in a basin, it is possible to split *TWSC* into separate components using a spectral analysis (Andrew et al. 2017).

The first study within the framework of the second trend is (Zaitchik et al. 2008), where the GRACE data were used to improve the reproducibility of the flood in the Mississippi basin in June, 2008. The assimilation of measurement data into a model is based on the Bayesian approach, when the measurement data are used to find the posterior probability distribution function (PDF) of the model parameters. In the case of a nonlinear system, which is a hydrological cycle, there is no analytical solution, and a numerical solution is required. A group of variational methods and statistical sequential analysis methods can be distinguished from them (Khaki et al. 2017). The former are little used due to their laboriousness. The latter are mainly an ensemble Kalman filter, both a deterministic and stochastic one, an ensemble Kalman smoother, a particle filter and a non-Gaussian rank histogram filter (Khaki et al. 2017). Together with the GRACE data, other RSDs, such as SMOS (soil water content) and MODIS (snow cover area) can be assimilated into a model. The experience of GRACE data assimilation showed that the decrease in the error in reproducing ground water storages and the soil water content in a layer of several dozen centimeters was the greatest (Tian et al. 2017; Khaki et al. 2017; Kumar et al. 2016; Tangdamrongsub et al. 2017) - by 15-30%. Especially important is the assimilation of GRACE data when there

is a change in basin water storages as a result of anthropogenic activity (pumping out) that is not taken into account in a model, although this is what may lead to the appearance of pseudotrends for other parameters (Giroto et al. 2017). The use of GRACE can also improve the reproducibility of snow water equivalents, mainly in high latitudes and highland areas (Tibet). This is due to a relatively low quality of the input meteorological information in these areas (a sparse observation network and systematic errors) that is often the main source of model errors. In addition, GRACE errors do not depend on such factors as the forest coverage, height and structure of the snow cover that are critical for a microwave survey (Zhang and Yang 2016; Lin et al. 2016; Forman et al. 2012). For water flow rates and evaporation, the change in the accuracy of calculation, when using GRACE, is generally insignificant, and can give both a positive and negative effect.

The question of an impact of total of water storages on the remaining components of water balance (P, E, R) has been considered for a long time. The relation between modulus of flow Q and TWS may be written as (Klemes 1974; Klemes 1978).

$$Q = a(TWS)^c \quad (2)$$

where a and c are coefficients, Q – modulus of flow ($(m^3/s)/km^2$). The power dependence for some assumptions about the similarity of a river network can be obtained from a kinematic wave equation for a slope runoff (Dolgonosov 2008), moreover, the exponent can be in the range from 1.5 to 3 depending on the preferred type of a runoff (1.5 for a turbulent and 3 for a laminar one). The value of the autocorrelation coefficient, the dispersion of a river runoff and the correlation coefficient between precipitation and a river runoff depend on the dependence $R = f(TWS)$ (Frolov 2011; Frolov 2014).

The paper aims at analyzing a change in TWS in the European part of Russia (EPR) for 2002–2015 and studying the relation between terrestrial water storages and a river runoff.

MATERIALS AND METHODS

The source of the GRACE data was the site (JPL GRACE data) that contains the processing materials of a geophysical institute (GFZ, Potsdam, Germany), the Center for Space Research (CSR, Austin, the USA) and the Jet Propulsion Laboratory (JPL, Pasadena, the USA). The values of terrestrial water storages were calculated as the average values between the blocks of these three centers. As it is shown, the arithmetic mean between these 3 archives has the smallest error compared to each of the archives individually (Sakumura et al. 2014). The data has a resolution of 1° in latitude and longitude and 1 month in time (monthly averages). There are gaps in the GRACE data series, which is due to the deterioration of batteries on satellites and the ability to maintain the required voltage only for certain orbital parameters (<https://grace.jpl.nasa.gov>). Thus, there are 19 gaps in the series from April 2002 to January 2017, i.e. the actual length of a series is 159 months. 13 passes refer to the period after 2010. For the same reason, the measurements for some months have a reduced accuracy. The lowered accuracy is also characteristic for the data for 2002, which is due to the incompletely adjusted operation of all devices in the first months of the operation of satellites. Due to the presence of gaps in the data, the period of 2002–2015 was used for calculating the minimum annual water storages, and the period of 2003–2015 was used for the maximum annual water storages.

Materials on the regime snow-measuring surveys for 284 routes on EPR for 1966–2015 were taken from the site meteo.ru. The study also used the data of a ERA-Interim reanalysis (Albergel et al. 2012) on a soil water content. The expedited data for 0, 6, 12 and 18 hours were used to calculate the average monthly values (at the levels of 0–7 cm, 7–28 cm, 28–100 cm and 100–289 cm). ERA-Interim covers the period from 1979 to 2017 with a resolution of about 0.75° in latitude and longitude. The data for 31 gauging stations were used to calculate the average monthly runoff (Table. 1)

Table 1. Parameters from the power function (2), linear function (3) and their accuracy (4) in each of the 31 river basins using TWSA to calculate river discharge

river basin	area, th. km ²	power function				linear function			
		D, %	err _{ref} %	a	c	D, %	err _{ref} %	a _{lin} ·10 ⁹ , 1/s	b·10 ³ , m ³ / (s·km ²)
Samara -Kargala	29.6	73.5	21.2	5.7*10 ⁻¹¹	2.93	68.1	25.6	12.1	-2.49
N. Dvina-Abramkovo	220	63.9	13.9	5.57*10 ⁻⁸	2.06	65.0	13.7	44.9	-6.32
Mezen - Bolshaya Pyssa	16.1	41.3	27.5	2*10 ⁻⁹	2.77	41.2	26.7	104	-17.0
Pechora-Troitsko-Pechorsk	35.6	34.1	23.0	9.07*10 ⁻⁶	1.33	35.0	22.6	81	-6.36
N. Dvina -Ust Pinega	350	75.3	13.7	5.06*10 ⁻⁹	2.51	75.9	13.0	59.3	-9.54
Pechora - Oksino	310	47.7	15.5	1.05*10 ⁻⁵	1.32	48.3	15.3	87.3	-6.19
Mezen - Malonikolskaya	56.4	55.0	22.7	4.95*10 ⁻¹⁰	3.00	53.4	23.3	102	-17.5
Pechora - Ust -Tsilma	250	41.7	19.0	1.19*10 ⁻⁵	1.27	42.2	18.7	71.7	-4.64
Neva-Novosaratovka	280	24.8	11.6	2.99*10 ⁻⁵	1.00	31.2	11.0	20.6	2.99
Volga - Staritsa	21.1	38.9	33.2	1.18*10 ⁻⁸	2.24	39.4	34.8	37	-6.91
Oka - Kaluga	54.9	68.6	10.7	1.03*10 ⁻⁶	1.39	67.4	10.9	12.9	-0.964
Oka - Polovskoe	99	68.2	13.4	1.14*10 ⁻⁶	1.41	66.7	13.8	15.6	-1.11
Oka - Murom	190	81.3	9.3	2.12*10 ⁻⁶	1.27	80.4	9.5	11.9	-0.641
Oka-Gorbatov	240	68.5	10.9	1.53*10 ⁻⁶	1.33	67.5	11.0	13.4	-0.877
Moksha-Shevelevsky Maidan	28.6	59.8	11.1	5.21*10 ⁻⁶	1.00	59.8	10.9	5.2	0.055
Kama-Gayna	27.4	55.3	19.2	2.36*10 ⁻⁸	2.19	55.4	19.8	43.2	-6.62
Kama-Bandug	46.3	61.4	28.3	2.09*10 ⁻¹⁰	3.00	56.6	31.0	51.8	-9.78
Vyatka - Rabino	30.9	39.4	21.9	3.47*10 ⁻⁶	1.48	39.2	22.2	75.7	-6.90
Chusovaya-Lyamino	21.5	63.6	31.4	2.31*10 ⁻¹⁰	3.00	53.1	37.0	68.1	-14.0
Belaya-Sterlitamak	21	44.2	20.6	4.82*10 ⁻⁷	1.47	42.5	20.8	9.75	-0.786
Belaya Ufa	100	38.4	18.9	7.7*10 ⁻⁶	1.07	38.4	18.9	11.9	-0.164
Belaya -Birsk	120	50.9	17.1	2.43*10 ⁻⁶	1.26	50.3	17.3	13.4	-0.742
Vyatka-Ustyevskaya	16.5	37.5	34.0	1.84*10 ⁻¹⁰	3.00	32.4	35.9	41.8	-7.38
Vyatka - Kirov	48.3	55.3	20.8	6.42*10 ⁻¹⁰	2.75	51.5	22.7	34.3	-5.90
Vyatka-Kotelniki	72	56.3	15.5	2.82*10 ⁻⁸	2.07	55.0	16.1	24.5	-3.51
Vyatka-Arkul'	96.9	50.8	20.7	3.18*10 ⁻⁸	2.05	49.8	21.2	25	-3.62
Vyatka - Vyatskie Polyany	120	50.5	15.6	3.3*10 ⁻⁷	1.66	48.8	15.9	22.1	-2.28
Don-Zadonsk	31.1	44.8	13.0	9.6*10 ⁻⁶	1.00	53.3	11.9	6.89	0.983
Don - Liski	69.5	78.9	8.8	6.3*10 ⁻⁶	1.00	78.9	8.9	6.25	0.021
Don-Kazanskaya	100	82.0	10.5	5.92*10 ⁻⁷	1.39	80.8	10.9	7.74	-0.652
Don-Belyaevskaya	200	89.0	7.4	1.03*10 ⁻⁶	1.27	88.6	7.7	6	-0.382

Revealing a relation between TWS and the modulus of flow (Q) using the GRACE data in the form of a power dependence that has a physical basis (Dolgonosov 2008; Frolov 2011, 2014) is complicated by the fact that it is not the absolute amount of water in the basin that the available TWS values express, but its anomaly ($TWSA$), relative to the average value for any period taken as zero. As a result, the $TWSA$ values are negative for some months. To avoid this, the minimum value for the entire observation period was subtracted and 200 mm was added for each basin from the $TWSA$ series. To construct the dependences, we used both a power function (2), and a linear one

$$Q = a_{lin} TWSA + b \quad (3)$$

Where a_{lin} is a coefficient (1/1000 s). The use of a linear function instead of a power one can be permissible with sufficiently small changes in TWS , due to the differentiation of the latter (Frolov 2011). In addition, application of a linear function allows the use of the water storage anomalies instead of their absolute values, because the dependences obtained will differ only by a constant. The smoothed average monthly values of Q and $TWSA$ (using the moving average method with a window width of two months) from July to October were used as the data to construct the dependence. In order to evaluate the accuracy of the dependences obtained, we used such parameters as the determination coefficient (D) and the mean absolute relative error (err_{rel}) expressed as

$$err_{rel} = \sum_{i=1}^n |(Q_{obs,i} - Q_{cal,i}) * 100 / Q_{cal,i}| / n \quad (4)$$

where $Q_{obs,i}$ is a measured modulus of flow value for i month and $Q_{cal,i}$ is a calculated modulus of flow for i month.

RESULTS AND DISCUSSION

In the second half of the 20th century, there was an increase in terrestrial water storages in EPR, both due to the growth of SWC , and the rise of the groundwater level. On average for EPR, the growth of SWC can be estimated as 50 mm in the last decade of September. The data of water balance

stations indicate an increase in the level of ground waters over the period of 1950-1990 (Water Resources of ... 2008). The main growth was in the mid-1970s and it was 50-130 cm by the early 1990s. Since the average active porosity in EPR is about 15% in the first hydrodynamic zone (with a capacity of about 100 m in EPR), it is possible to estimate approximately a change in groundwater storages by 100 mm. However, a decrease in water storages could be in deeper aquifers, especially where depression pits are formed, the largest of which are in the Central Federal District (Dzhamalov et al. 2015). On the other hand, in the second half of the 20th century, a lot of water storages were created in EPR, which not only increased the total water storages of the area by themselves, but also led to a local rise in the groundwater level. The maximum snow water equivalent changed insignificantly for the period of 1966-2002, having grown for the field routes and decreasing for the forest ones.

The GRACE data indicate a change in $TWSA$ in EPR for 2002-2015 already. The months of the minimum ($TWSA_{min}$) and the maximum ($TWSA_{max}$) annual water storages were calculated for this period to analyze the seasonal movement of $TWSA$. Clear zoning is noted both for the time of the maximum and the minimum water storages anomaly. The earliest $TWSA_{min}$ are formed in the far north - in August (and in July in some places). For the Upper Volga and Kama basins, $TWSA_{min}$ can already be noted in September. South of 53°, $TWSA_{min}$ are noted in October. It is characteristic up to 50° N that as moving from the north-east to the south-west of the area, the time of $TWSA_{max}$ formation shifts from later dates (May) to earlier ones (March). The fact that $TWSA_{max}$ are later again south of 50° is due to lack of a sufficiently strong stable snow cover in the region (on the lowland and in the foothills), which would determine the peak of the maximum water storages as the peak of the maximum water storages in the snow.

$TWSA_{min}$ (the minimum monthly average value of $TWSA$ for the year) hardly changed in the north for the period of 2002-2015 (Fig. 1a). The growth of more than 5 mm/year is only noted in the northwest (in places)

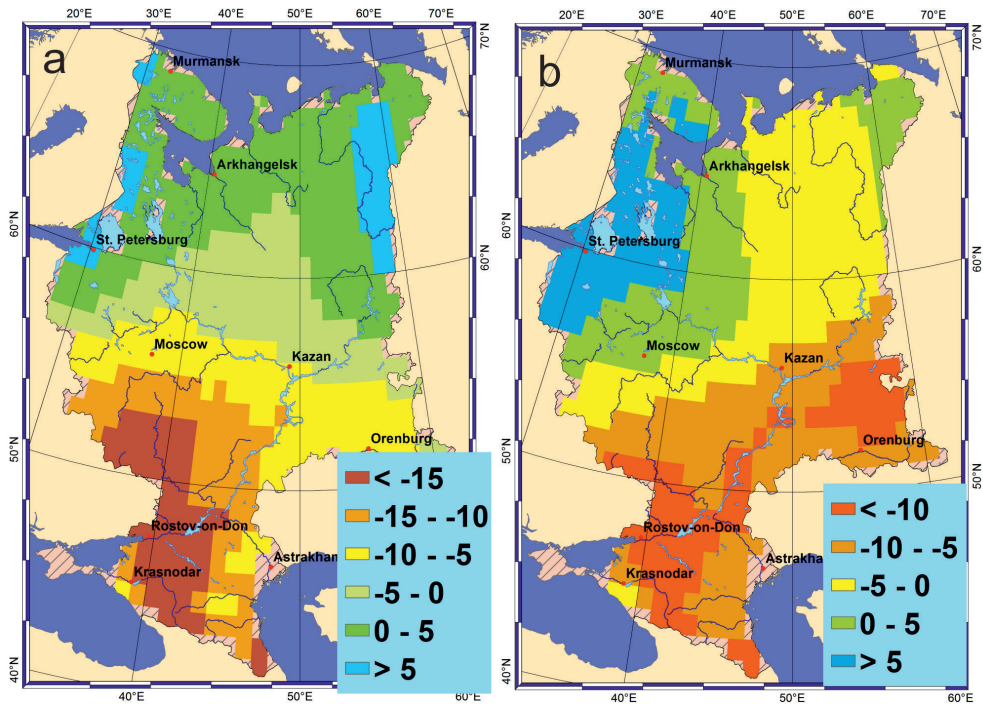


Fig. 1. Linear trend coefficient of the minimum (a) and maximum (b) water storages anomaly for 2002-2015, mm/year (according to GRACE)

and in the northeast (mainly in the Pechora basin). There was a slight decrease in water storages, within 10 mm/year, for the basins of the Kama, the Ural, the Upper Volga and especially the Oka River. The most significant decrease was in the Don basin (to a lesser extent, in the Koper and Medveditsa basin) and the Kuban basin, where linear trend coefficient or average rate of change it exceeded 15 mm/year.

The change in $TWSA_{max}$ was not so significant - the positive trends do not exceed 10 mm/year and the negative ones - 15 mm/year (Fig. 1b). An increase in $TWSA_{max}$ is noted practically for the whole northwest of EPR. The areas of a decrease in the maximum water storages, as well as the minimum ones, are located in the south of EPR. At the same time, for $TWSA_{max}$ in contrast to $TWSA_{min}$ the decrease in the Kama and Ural basins (more than 10 mm/year) is comparable to that of the Don and Kuban basins.

In general, there were not any $TWSA$ changes over the period from 2002 to 2015, although the years with the minimum $TWSA$ values

(2010, 2011 and 2014) refer to the second half of the period. In the Don basin, which underwent the most significant changes in $TWSA$, there was a decrease in $TWSA$ in 2007-2010. Further on, the decline almost ceased, but the growth did not change either. The lowest water storages in the Don basin were in 2015, when their $TWSA_{max}$ was at a level of $TWSA_{min}$ for 2002-2007. The situation in the Oka basin is similar to that in the Don basin. However, the value of $TWSA$ has started to grow again there since 2010, having reached its maximum in 2013, when the water storages in the basin were at a level of 2002-2007. But in 2014 and 2015 there was a sharp decrease again. The minimum values of $TWSA_{max}$ were in 2015. The changes in the northern catchments areas were smaller, and they were not unidirectional. A period of a decline in 2002-2006, of a rise in 2006-2007, then a decline from 2007 to 2012 again and a rise to 2016 can be noted for the Pechora basin. The situation with the Northern Dvina River is the same. A growth in 2002-2004 has been noted in the basin of the Neva River (the area of the Ladoga and Onega lakes was not taken into account when calculating

TWSA). There were no directed multi-year changes for the rest of the time.

In order to identify the storages used (groundwater, SWC or SWE) let us consider the dynamics of the first two storages. The maximum snow water equivalent closely related to the formation of the maximum water storages did not change in total over the period from 2002 to 2015 (Fig. 2).

On average for the field routes (Fig. 2a), the growth of SWE was only 0.04 mm/year. A decrease in SWE within 1-5 mm/year is noted for the north of EPR. At the same time, there is a growth, within 1-5 mm/year as well, in the south, especially in the basin of the Volga River. For most of the forest routes (70%), located mainly in the north of EPR, a decrease in SWE on average by 3 mm/year is typical. For some of those forest routes where there is a growth in SWE (mainly in the south of EPR), it averages 1.3 mm/year. Thus, a decrease in the maximum $TWSA$ in the south of EPR is not related with a reduction in SWE . A slight decrease in TWS in

the north-east of the EPR (<5 mm/year) may be caused by a decrease in SWE . The near-zero SWE change in the north-west of EPR could not cause a growth in TWS (>5 mm/year) in this area.

The pattern of a change in the maximum and minimum water storages in the soil (Fig. 3) is close to that for $TWSA$ - minor changes in the north and a decrease in the south.

The reduction in the minimum annual water storages in the soil (SWC_{min}), in the areas of the maximum decline in $TWSA_{min}$, does not exceed 5 mm/year. Thus, the negative trend of $TWSA_{min}$ for the Don basin of no more than 30% is due to a decrease in SWC_{min} . The remainder is probably related with a reduction in the storage of the surface (ponds and reservoirs) and ground waters. The rate of a decline in the maximum annual water storages (SWC_{max}) in the soil is already significantly higher, and it accounts for more than 50-70% of the negative trend of $TWSA_{max}$ for the Don and Lower Volga River and the Caucasus region. The most

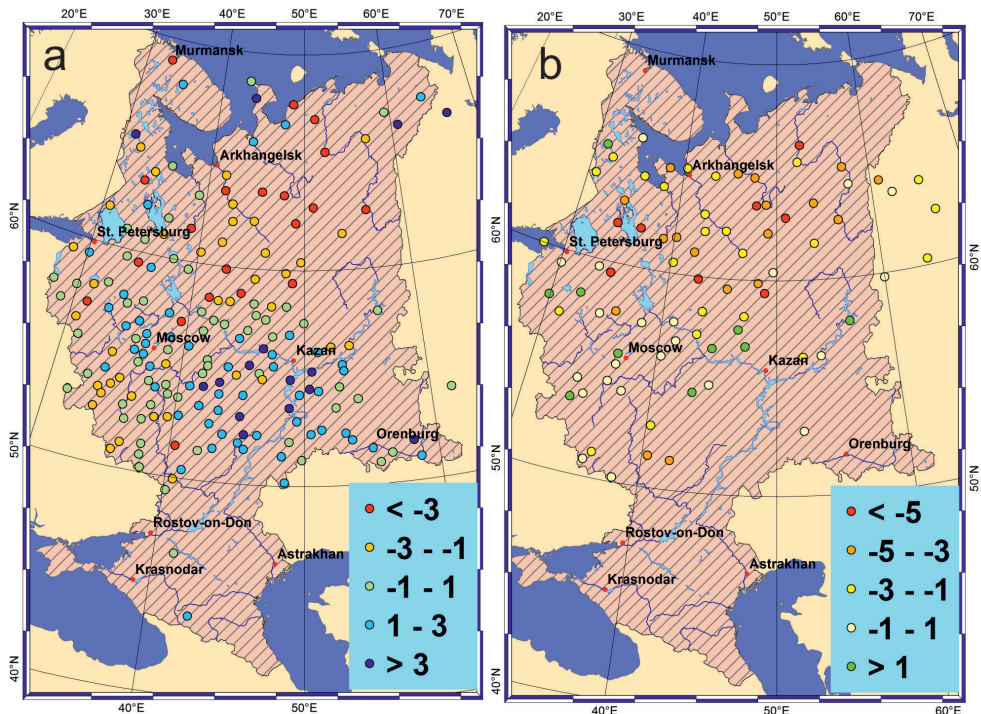


Fig. 2. Linear trend coefficient of the maximum winter values of SWE for field (a) and forest (b) routes for 2002-2015, mm/year (according to the ground-based measurements)

significant discrepancy in the dynamics of SWCmax and TWSAmax is in the basin of the Ural and partly of the Kama River, where there is practically no change in SWCmax with a decrease in TWSAmax at a rate of about 10 mm/year. The conclusion that the decline in TWSA in the southern part of EPR had an impact not only on soil waters, but also surface and ground waters, is indirectly confirmed by the fact that the impact of the initial soil moistening conditions on its subsequent dynamics affects a time interval of not more than 4-6 months (Demchenko and Kislov 2010), which is not enough to form a long period of a decline in water storages under conditions of a relatively stationary climate. The recent studies have also shown the significant values of correlation coefficients (0.46-0.83) of TWSA with a groundwater level for a number of wells in EPR (Savin et al. 2016).

The comparison of the accuracy of the obtained dependences $Q=f(TWSA)$ in the form of a power (2) and a linear (3) function showed close results. Thus, the power dependences

showed $D=56.2$ ($err_{rel}=18.1\%$), and the linear ones - 55.4 ($err_{rel}=18.7\%$) on average for 31 stations for the summer low water level period (July–October). The highest values of D and the minimum err_{rel} were obtained for the sections of the Don River - Khutor Belyaevsky, the Don River - Stanitsa Kazanskaya and the Oka River - Murom, where D exceeded 80% and err_{rel} is less than 10%. One of the reasons for the most satisfactory approximation for these sections is a significant, in comparison with the rivers of the north of EPR, range of TWSA that exceeds the error of TWSA estimation by 5-10 times. The catchment areas positively correlate with the values D of the dependences obtained ($r=0.18$ for power and 0.25 for linear dependences) and negatively with err_{rel} ($r=-0.51$ for power and -0.53 for linear dependences), which is caused by a decrease in GRACE errors with an increase in the averaging area. The only catchment area with a shift of 1 month (TWSA is used as a predictor for Q), where the approximation accuracy has increased, is the catchment area of the Neva River, which may be related with a longer basin lag.

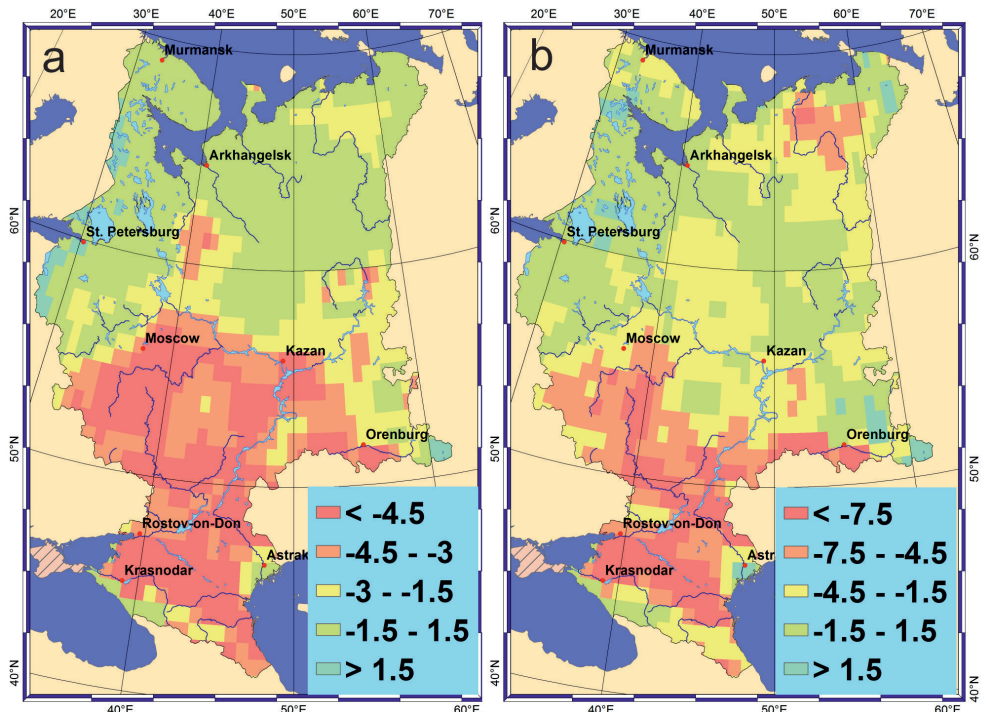


Fig. 3. Linear trend coefficient of the minimum (SWCmin) (a) and maximum (SWCmax) (b) soil water contents for 2002-2015, mm/year (according to the ERA-Interim reanalysis data)

The parameter a_{lin} in the formula (3) determines how much the runoff value increases with an increase in $TWSA$ by 1 mm. The higher a_{lin} , the lower the water-retaining capacity of a catchment area, the lower the runoff autocorrelation coefficient and the lower its inertia (Frolov 2014). Therefore, the variability of terrestrial water storages (σ_{TWS}) will be lower for the catchment areas with high a_{lin} values. Thus, when using a logarithmic dependence, the determination coefficient between σ_{TWS} and a_{lin} was more than 83% (Fig. 4).

Such a dependence (Fig. 4) makes it possible to calculate a river runoff value (relative to its average long-term value) only in terms of water storages, the a_{lin} parameter can be obtained from a dependence on σ_{TWS} . However, the value of σ_{TWS} contains both the natural variability of TWS and the error of its estimation, which prevents the construction of a reliable dependence of σ_{TWS} on a_{lin} . Also a_{lin} is a constant value only in a certain range of TWS oscillations.

CONCLUSION

A number of papers were written during the functioning of the GRACE system (April 2002 - August 2017) that demonstrated the usefulness of data on terrestrial water storages for solving various problems of hydrology and other related areas.

With the development of methods for processing satellite gravimetry data, as well as an increase in their accuracy due to the emergence of new models of atmosphere and ocean circulation (Dobslaw et al. 2017) and the launch of new satellites in 2018 (GRACE Follow-On), their scope of application in hydrology will extend.

The analysis of a change in $TWSA$ in EPR, beginning with the second half of the 20th century, according to literature data and the GRACE data, has shown that the growth of TWS in EPR in the second half of the 20th century was replaced by a decline for the southern half of EPR in the 21st century, which was the most significant in the Don basin, where the rate of a decline is 14 mm/year for 2002-2015. There were no significant changes for the northern half of EPR. It has been revealed that there is a close relation between the value of terrestrial water storages and the water flow rate in the period of a summer low water level, which can be approximated by a linear dependence. The obtained dependences can be used to calculate a river runoff and its probability distribution function.

ACKNOWLEDGEMENTS

The study was supported by RSF grants (Project No. 14-17-00155-P - analysis of meteorological information; project No.

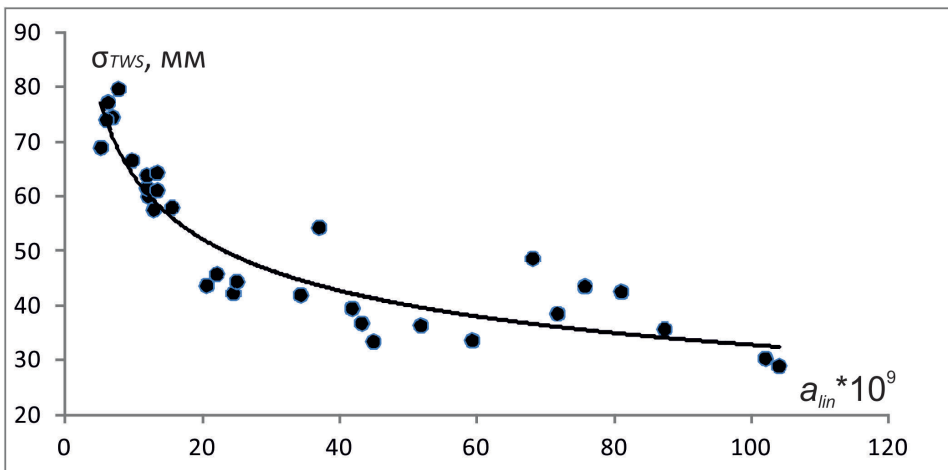


Fig. 4. Dependence of the mean-square deviation of the monthly mean values of TWSA for July-October on the proportionality coefficient between TWSA and a river runoff for 31 catchment areas

14-37-00038-P - statistical analysis), RFBR (projects No. 16-55-52008 MNT_a - flow calculations, No. 16-05-00753 A - GRACE data processing, No. 17-05-41030 RGO_a - cartographic processing). ■

REFERENCES

Albergel C., De Rosnay P., Balsamo G., Isaksen L., Muñoz-Sabater J. (2012). Soil Moisture Analyses at ECMWF: Evaluation Using Global Ground-Based In Situ Observations. *Journal of Hydrometeorology*, 13(5), pp. 1442-1460. DOI: <https://doi.org/10.1175/JHM-D-11-0107.1>.

Andrew, R., Guan, H., Batelaan, O. (2017). Estimation of GRACE water storage components by temporal decomposition. *Journal of Hydrology*, 552, pp. 341-350. DOI: <https://dx.doi.org/10.1016/j.jhydrol.2017.06.016>.

Babkin V.I., Vuglinsky V.S. (1982). Water balance of river basins. Leningrad: Hydrometeoizdat (in Russian).

Chambers D. P., Cazenave A., Champollion N., Dieng H., Llovel W., Forsberg R., Schuckmann K., Wada Y. (2017). Evaluation of the Global Mean Sea Level Budget between 1993 and 2014. *Surveys in Geophysics*. 38(1), pp. 309-327. DOI: <http://dx.doi.org/10.1007/s10712-016-9381-3>.

Chen X., Long D., Hong Y., Zeng C., Yan D. (2017 a). Improved modeling of snow and glacier melting by a progressive two-stage calibration strategy with GRACE and multisource data: How snow and glacier meltwater contributes to the runoff of the Upper Brahmaputra River basin? *Water Resour. Res.*, 53(3), pp. 2431-2466. DOI:10.1002/2016WR019656.

Chen J.L., Wilson C. R., Tapley B. D., Save H., Cretaux J. F. (2017 b). Long-term and seasonal Caspian Sea level change from satellite gravity and altimeter measurements. *Journal of Geophysical Research - Solid Earth*, 122(3), pp. 2274-2290. DOI: <https://dx.doi.org/10.1002/2016jb013595>.

Demchenko P. F., Kislov A. V. (2010). Stochastic Dynamics of Natural Objects. Brownian Motion and Geophysical Applications. Moscow: GEOS. (in Russian).

Deng H., Chen Y. (2017). Influences of recent climate change and human activities on water storage variations in Central Asia. *Journal of Hydrology*, 544, pp. 46-57. DOI: <https://dx.doi.org/10.1016/j.jhydrol.2016.11.006>.

Dobslaw H., Bergmann-Wolf I., Dill R., Poropat L., Thomas M., Dahle C., Esselborn S., König R., Flechtner F. (2017). A new high-resolution model of non-tidal atmosphere and ocean mass variability for de-aliasing of satellite gravity observations: AOD1B RL06. *Geophysical Journal International*, 211(1), pp. 263-269. DOI: <https://dx.doi.org/10.1093/gji/ggx302>.

Dolgonosov B. M. (2009). Nonlinear dynamics of ecological and hydrological processes. Moscow: LIBROKOM, p. 440. (in Russian).

Dzhamalov R. G., Frolova N. L., Kireeva M. B., Rets E. P., Safronova T. I., Bugrov A. A., Telegina A. A., Telegina E. A. (2015). Modern resources of underground and surface waters of the European Russia: formation, distribution, use. Moscow: GEOS, p. 315. (in Russian).

Eom J., Seo K.-W., Ryu D. (2017). Estimation of Amazon River discharge based on EOF analysis of GRACE gravity data. *Remote Sens. Environ.*, 191, pp. 55-66. DOI: <https://dx.doi.org/10.1016/j.rse.2017.01.011>.

Forman B. A., Reichle R. H., Rodell M. (2012). Assimilation of terrestrial water storage from GRACE in a snow-dominated basin. *Water Resour. Res.*, 48(1), W01507. DOI: 10.1029/2011WR011239.

Forootan E., Safari A., Mostafaie A., Schumacher M., Delavar M., Awange J. L. (2016). Large-Scale Total Water Storage and Water Flux Changes over the Arid and Semiarid Parts of the Middle East from GRACE and Reanalysis Products. *Surveys in Geophysics*, 38(3), pp 591-615. DOI: <https://dx.doi.org/10.1007/s10712-016-9403-1>.

Frolov A. V. (2011). Discrete dynamic-stochastic model of long-term river runoff variations. *Water Resources*, 38(5), pp. 583-592. DOI: 10.1134/S0097807811040051.

Frolov A. V. (2014). Estimation of the statistical characteristics of long-term fluctuations in evaporation from large river catchments. *Doklady Earth Sciences*, 458(1), pp. 1183-1186. DOI: 10.1134/S1028334X1409027X.

Frolova N., Belyakova P., Grigoriev V., Sazonov A., Zotov L. V., Jarsjö J. (2017). Runoff fluctuations in the Selenga river basin. *Regional Environmental Change*, 17(7), pp. 1965–1976. DOI: <https://doi.org/10.1007/s10113-017-1199-0>.

Giroto M., De Lannoy G. J. M., Reichle R. H., Rodell M., Draper C., Bhanja S. N., Mukherjee A. (2017). Benefits and pitfalls of GRACE data assimilation: A case study of terrestrial water storage depletion in India. *Geophys. Res. Lett.*, 44(9), pp. 4107–4115. DOI:10.1002/2017GL072994.

<https://grace.jpl.nasa.gov> (2017). JPL data page. [online]. Available at: <https://grace.jpl.nasa.gov/data/grace-months/>. [Accessed 20 Oct. 2017].

Khaki M., Hoteit I., Kuhn M., Awange J., Forootan E., van Dijk A., Schumacher M., Pattiaratchi C. (2017). Assessing sequential data assimilation techniques for integrating GRACE data into a hydrological model. *Advances in Water Resources*, 107, pp. 301-316. <https://dx.doi.org/10.1016/j.advwatres.2017.07.001>.

Klemes V. (1974). The Hurst phenomenon— a puzzle? *Water Resources Research*, 10(4), pp. 675-688.

Klemes V. (1978). Physically based stochastic hydrologic analysis, *Advances in Hydroscience*, 11, 285–356.

Klemes, V. (1978), Physically based stochastic hydrologic analysis, *Adv. Hydrosci.*, 11, 285–356.

Klemes, V. (1978), Physically based stochastic hydrologic analysis, *Adv. Hydrosci.*, 11, 285–356.

Kumar S. V., Zaitchik B. F., Peters-Lidard C. D. et al. (2016). Assimilation of Gridded GRACE Terrestrial Water Storage Estimates in the North American Land Data Assimilation System. *Journal of Hydrometeorology*, 17(7), pp. 1951-1972. DOI: <https://dx.doi.org/10.1175/jhm-d-15-0157.1>.

Li Q., Zhong B., Luo Z. C., Yao C. L. (2016). GRACE-based estimates of water discharge over the Yellow River basin. *Journal of Geodesy and Geodynamics*, 7(3), pp. 187-193. DOI: <https://dx.doi.org/10.1016/j.geog.2016.04.007>.

Lin P., Wei J., Yang Z.-L., Zhang Y., Zhang K. (2016). Snow data assimilation-constrained land initialization improves seasonal temperature prediction. *Geophysical Research Letters*, 43(21), 11,423-11,432. DOI: 10.1002/2016GL070966.

Liu Y. C., Hwang C. W., Han J. C., Kao R., Wu C. R., Shih H. C., Tangdamrongsub N. (2016). Sediment-Mass Accumulation Rate and Variability in the East China Sea Detected by GRACE. *Remote Sensing*, 8(9), 777. DOI: <https://dx.doi.org/10.3390/rs8090777>.

Lorenz C., Kunstmann H., Devaraju B., Tourian M.J., Sneeuw N., Riegger N. (2014). Large-Scale Runoff from Landmasses: A Global Assessment of the Closure of the Hydrological and Atmospheric Water Balances. *Journal of Hydrometeorology*, 15(6), pp. 2111-2139. DOI: 10.1175/JHM-D-13-0157.1.

Naydenov V. I. (2004). *Nonlinear dynamics of surface waters*. Moscow: Nauka, p. 318 (in Russian).

Sakumura C., Bettadpur S., Bruinsma S. (2014). Ensemble prediction and intercomparison analysis of GRACE time-variable gravity field models. *Geophys. Res. Lett.* 41(5). pp. 1389-1397. DOI:10.1002/2013GL058632

Save H., Bettadpur S., Tapley B. D. (2016). High-resolution CSR GRACE RL05 mascons. *Journal of Geophysical Research-Solid Earth*, 121(10), pp. 7547-7569. DOI: <https://dx.doi.org/10.1002/2016jb013007>.

Savin I.Y., Markov M. L., Ovechkin S.V., Isaev V. A. (2016). Trend in total terrestrial water storage at the European Russia detected based on GRACE DATA. *Bulletin of V.V. Dokuchaev Soil Science Institute*, 82, pp. 28-41. (in Russian with English abstract and title). DOI: 10.19047/0136-1694-2016-82-28-41.

Schlegel N. J., Wiese D. N., Larour E. Y., Watkins M. M., Box J. E., Fettweis X., van den Broeke M. R. (2016). Application of GRACE to the assessment of model-based estimates of monthly Greenland Ice Sheet mass balance (2003-2012). *Cryosphere*, 10(5), pp. 1965-1989. DOI: <https://dx.doi.org/10.5194/tc-10-1965-2016>.

Seo J. Y., Lee S.-I. (2017). Total discharge estimation in the Korean Peninsula using multi-satellite products. *Water*, 9(7), 532. DOI: <https://dx.doi.org/10.3390/w9070532>.

Shiklomanov I. A. (ed.). *Water resources of Russia and their use*. (2008). St. Petersburg: State Hydrological Institute (in Russian)

Springer A., Eicker A., Bettge A., Kusche J., Hense A. (2017). Evaluation of the Water Cycle in the European COSMO-REA6 Reanalysis Using GRACE. *Water*, 9(4), 289. DOI:10.3390/w9040289.

Tangdamrongsub N., Steele-Dunne S. C., Gunter B. C., Ditmar P. G., Sutanudjaja E. H., Sun Y., Xia T., Wang Z. (2017). Improving estimates of water resources in a semi-arid region by assimilating GRACE data into the PCR-GLOBWB hydrological model. *Hydrol. Earth Syst. Sci.*, 21(4), pp. 2053-2074. DOI: <https://doi.org/10.5194/hess-21-2053-2017>.

Tian S., Tregoning P., Renzullo L. J., van Dijk A., Walker J. P., Pauwels V. R. N., Allgeyer S. (2017). Improved water balance component estimates through joint assimilation of GRACE water storage and SMOS soil moisture retrievals. *Water Resour. Res.*, 53(3), pp. 1820-1840. DOI:10.1002/2016WR019641.

Wahr J., Burgess E., Swenson S. (2016). Using GRACE and climate model simulations to predict mass loss of Alaskan glaciers through 2100. *Journal of Glaciology*, 62(234), pp. 623-639. DOI: <https://dx.doi.org/10.1017/jog.2016.49>.

Xie Z. Y., Huete A., Ma X., Restrepo-Coupe N., Devadas R., Clarke K., Lewis M. (2016). Landsat and GRACE observations of arid wetland dynamics in a dryland river system under multi-

decadal hydroclimatic extremes. *Journal of Hydrology*, 543, pp. 818-831. DOI: <https://dx.doi.org/10.1016/j.jhydrol.2016.11.001>.

Zaitchik B. F., Rodell M., Reichle R. H. (2008). Assimilation of GRACE Terrestrial Water Storage Data into a Land Surface Model: Results for the Mississippi River Basin. *Journal of Hydrometeorology*, 9(3), pp. 535-548. DOI: 10.1175/2007JHM951.1

Zhang Y. F., Yang Z. L. (2016). Estimating uncertainties in the newly developed multi-source land snow data assimilation system. *Journal of Geophysical Research-Atmospheres*, 121(14), pp. 8254-8268. DOI: <https://dx.doi.org/10.1002/2015jd024248>.

Zotov L., Frolova N., Grigoriev V., Kharlamov M. (2015). Application of the satellite system of the Earth's gravity field measurement (GRACE) for the evaluation of water balance in river catchments. *Moscow University Herald. Geography*, (4), pp. 27-33. (in Russian with English abstract).

Received on December 6th, 2017

Accepted on March 1st, 2018



Vadim Yu. Grigoriev, junior researcher at Water problems institute of Russian Academy of Science.



Natalia L. Frolova, DSc in Geography, Professor of the Department of Hydrology of the Lomonosov Moscow State University. Member of the IAHS, a Member of the Hydrological Commission of the International Geographical Union. Scientific interests: estimates and forecast of river flow, dangerous hydrological processes, and mountain hydrology.

**Nikolay S. Kasimov^{1*}, Vladimir M. Kotlyakov², Dmitry N. Krasnikov³,
Alexander N. Krayukhin³, Vladimir S. Tikunov¹**

¹Faculty of Geography, Lomonosov Moscow State University

²Institute of Geography, Russian Academy of Sciences

³Joint-Stock Company "Roscartography"

*Corresponding author: nskasimov@mail.ru

NATIONAL ATLAS OF THE ARCTIC

ABSTRACT. The National Atlas of the Arctic is a set of spatio-temporal information about the geographic, ecological, economic, historical-ethnographic, cultural, and social features of the Arctic compiled as a cartographic model of the territory. The Atlas is intended for use in a wide range of scientific, management, economic, defense, educational, and public activities. The state policy of the Russian Federation in the Arctic for the period until 2020 and beyond, states that the Arctic is of strategic importance for Russia in the 21st century. A detailed description of all sections of the Atlas is given. The Atlas can be used as an information-reference and educational resource or as a gift edition.

KEY WORDS: GRACE, Arctic, Atlas, concept, structure, outcomes

CITATION: Nikolay S. Kasimov, Vladimir M. Kotlyakov, Dmitry N. Krasnikov, Alexander N. Krayukhin, Vladimir S. Tikunov (2018) National atlas of the Arctic. *Geography, Environment, Sustainability*, Vol.11, No 1, p. 51-57

DOI-10.24057/2071-9388-2018-11-1-51-57

INTRODUCTION

This modern large-formate encyclopedic edition reflects the results of the Arctic studies of recent decades, which allowed accumulating unique information on a global scale. The Atlas represents a reference source and a scientific folio and, at the same time, it is a colorful album. In addition to maps, the Atlas contains illustrations, diagrams, graphs, schematic drawings, and tables. Each map is accompanied by a text description. The Atlas helps its readers to gain critical insight and understand the importance of the Arctic region for Russia and the world as a whole. The Atlas includes maps related to general Arctic problems, the Russian Arctic, and the regional issues. This edition represents the most complete modern body of knowledge of the region. The cross-border and interdisciplinary

nature of the Atlas will allow its readers to draw new conclusions and take into account those relationships that are not visible from the point of view of individual branches of science or spheres of activity; it will facilitate the new ideology of industrial revival of the region while preserving its nature.

The characteristic features of the Arctic zone of the Russian Federation, which influence the national policy in this region, are:

a) extreme natural and climatic conditions, including permanent ice cover and drifting ice in the Arctic seas;

b) focal character of industrial and economic development of territories and low population density;

c) remoteness from the main industrial centers, high resource intensity, and dependence of economic activities and livelihood of the population on fuel, food, and essential goods from other regions of Russia;

d) low stability of environmental systems determining the biological stability and climate of the Earth and their vulnerability to even minor anthropogenic influences.

Solutions to the problems of sustainable development of the Arctic zone of the Russian Federation in the context of the national interests and international dialogue, preservation of the environment, and development of Arctic natural resources require creation of a new integrated cartographic work — the National Atlas of the Arctic.

The Atlas is based on the concept outlined in the “National Atlas of the Arctic: Structure and Development Stages” (Kasimov et al. 2015). The main positions of this concept incorporated in the Atlas are as follows. Organizational and coordination work on the Atlas was made by the Joinet-Stock Company “Roscartography”.

CONCEPT OF THE ATLAS

The Atlas is an information-reference resource containing the most current and detailed data. In essence, it is a transboundary database that addresses the tasks of developing the region and preserving its biological diversity. The Atlas is not just a system for providing information to different social groups and the entire population of the region, but a system of information integration, which influences territorial management towards the optimal solution of the regional problems. It is designed not only to propagate the ideas of nature conservation, but also to emphasize the dependence of quality of life on quality of the natural environment and to offer environmentally sound management methods and environmental technologies.

The Atlas is an educational resource, i.e., a reference manual for all levels of education, from schools and universities to public and state organizations, professional schools, refresher courses, etc. The material integrates a highly advanced science and a clear presentation. In a highly understandable way it describes the indigenous population's traditions of careful treatment of nature. Tourist maps of the Atlas serve as guides to the Arctic, showing its landscape and ethnocultural diversity.

The Atlas is published as a gift edition; its design allows considering it as a general cultural asset that follows the best traditions of Russian cartography as exemplified by the “Atlas of the Arctic” (1985); “Atlas of Snow and Ice Resources of the World” (1997); “Ecological Atlas of Russia” (2002, 2017); “Atlas of the Russian Arctic in the 21st Century ...” (2013); “National Atlas of Russia” (2004-2008); and other works. A wide distribution of the Atlas will help maintain and develop the image of the Arctic as a global and the Russian national asset.

The Atlas presents in an optimal way the degree of study of the Arctic, its environmental problems, and the state of rare and endangered species; it also describes ethnic groups and their cultures. Russia differs from many circumpolar countries in that its Arctic territories are more populated and much more strongly involved in the economic life of the country. Therefore, much attention is paid to the problems of nature management — economic management and its consequences.

The scale of pollution of these territories is astonishing. Only in the Novaya Zemlya archipelago, 130 atomic explosions were conducted in 1955-1990. In the Barents and Kara Seas, there are flooded reactors from Soviet nuclear submarines. Numerous items have been abandoned on the islands of Franz Josef Land — nearly 250 thousand barrels with 40-60 thousand tons of oil products, about a million of empty barrels, and various equipment (airplanes, radar stations, vehicles and structures). In the

Severny Harbor, where ships carrying out northern deliveries for military and civil needs moored, the total area polluted with waste is about 100 hectares. A special section of the Atlas comprehensively characterizes the environmental ills of the Arctic and discusses environmentally protective measures to address these problems. The description of potentially dangerous objects of the Arctic will be of interest to companies that conduct economic activities in the region.

One of the characteristic features of the Atlas is that all its sections contain maps with environmental content. The Atlas targets solutions to the problems of sustainable development of the region. Its task is to overcome the disconnect between the main information flows and the decision-making process, to create an information and analytical base for solving an array of problems. The creation of such an atlas will provide the basis for the scientific substantiation of the strategic planning of the socio-economic development of the Arctic zone of the Russian Federation and ensure the national security of Russia.

SCIENTIFIC FOUNDATIONS OF ATLAS

In order to design and create the National Atlas of the Arctic at high scientific and methodological levels that incorporate modern scientific achievements, a number of requirements have been met; these

requirements were formed in the practice of cartographic research. The Atlas is a body of information and knowledge accumulated to date in the course of long-term and comprehensive study of the Arctic region and a means of research and development strategy.

The Atlas utilizes the latest scientific and methodological achievements of the complex of modern subject sciences (geography, biology, ecology, and history) and cartography, while preserving continuity with the best examples of the national and international cartographic works. The Atlas is part of the information system of the Arctic region of Russia; it is designed and functions as the system's constantly updated cartographic and geographic component.

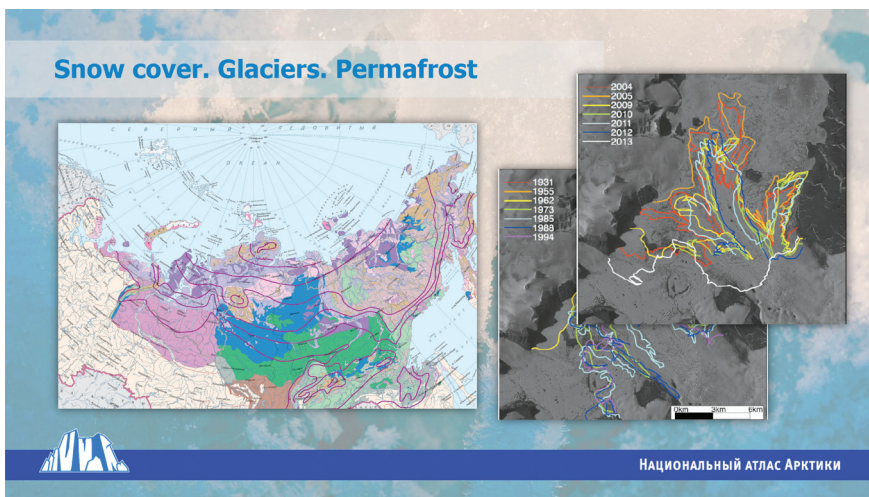
The Atlas can address multi-purpose goals; its content is versatile. It is thematically complete, geographically specific and detailed; it possesses internal unity (complementarity, consistency, and comparability of maps), scientific validity, modernity, clarity, and accessibility.

The Atlas reflects the features of the natural environment, the resource potential, the current state of society and the economy, and the level and direction of the socio-economic development of the Arctic region. Much attention is paid to the

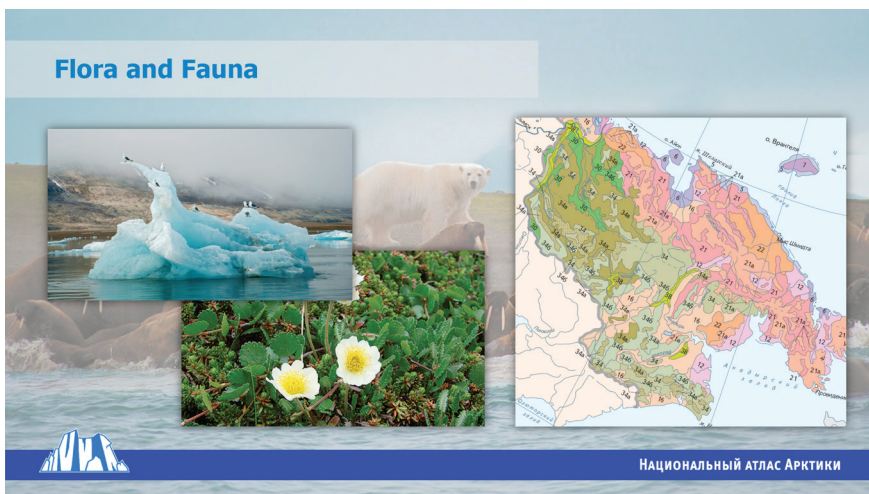
(a)



(b)



(c)



(d)



comparative representation of a number of indicators characterizing the region.

The Atlas contains topics that reveal the main problems of the modern development of the Arctic, e.g., ensuring sustainable development of the region, preserving the resource potential, solving environmental problems and the problems of social infrastructure development, accelerating economic development, etc Fig. 1.

The variety of thematic maps and their large number require that different thematic sections be balanced among themselves in terms of the number of maps, their scales, levels of generalization, and other characteristics. When possible, the maps display phenomena in their dynamics and historical developmental context, which allows for a deeper understanding of the current processes and a forecast of their development features.

Mapping in the Atlas is realized on four spatial levels, each utilizing the appropriate scales and layouts (overall Arctic, Russian, regional, and local). All levels are closely linked.

The content of the maps is based on modern scientific approaches (integrated, system, inventory-resource, regional,

estimated-forecast, geo-engineering, ecological-geographic, historical, and comparative-geographic).

Cartographic objects and phenomena and their states and interrelations are evaluated and represented on three levels of generalization: analytical (mapping of "homogeneous" objects in one system of indicators), integrated (mapping of several interrelated phenomena or their elements, each in its own system of indicators), and synthetic (mapping of selected complex objects with integral characteristics).

PUBLICATION OUTCOMES

The Atlas targets primarily three groups of users: 1) decision-makers; 2) teachers and students; and 3) professionals in various fields of science, economics, culture, health care, etc. For decision-makers, the reference nature of the Atlas will serve as a cross-border database necessary for the development and preservation of the region. The Atlas will not be just a system for providing information for various social groups, but a system of information interaction and influence on the management of the territory towards its optimization.

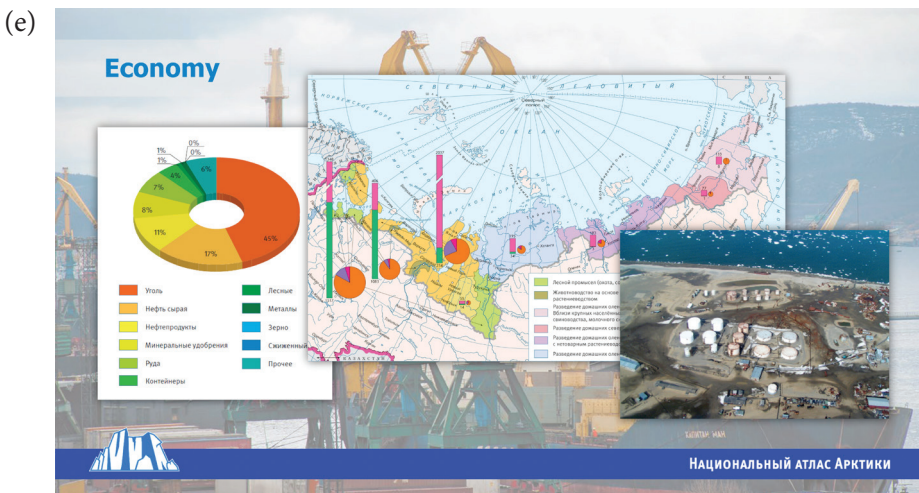


Fig. 1. Sample maps pages of the National Atlas of the Arctic: a – geological structure; b – Snow cover, glaciers, permafrost; c- Flora and Fauna; d – Population; e - Economy

Scientific Outcomes

The publication of the Atlas sets certain research tasks. The Atlas is not so much the statement of the existing order of things and the static reproduction of the realities of the Arctic region. Its purpose is to represent the dynamic nature of the region, because it is in the dynamics of relations that the significance of the region is recognized.

Public Importance

The Atlas describes the various features and prospects of the Arctic. The Atlas not only propagates the ideas of nature conservation, but it reveals the dependence of quality and diversity of life on quality and diversity of its natural environment and offers environmentally sound management practices and technologies. The presentation of the material combines a high scientific level and a clear language. The Atlas will be an important channel for interdisciplinary discussions for the broadest range of professionals.

Publication Impact

The full-color and richly illustrated edition of the Atlas can become a reference source for thousands of people — students of schools and colleges, scientists, teachers, and business and industry community. Its English edition will have a significant impact on the business climate in favor of rapprochement and cooperation between participants of political, economic, and cultural activities.

The National Atlas of the Arctic will serve as the scientific substantiation of strategic planning for the social and economic development of the Arctic zone of the Russian Federation towards strengthening Russia's leading positions in the Arctic.

Supplementary

Supplementary material, including list of maps of the Atlas is available at: <https://ges.rgo.ru/jour/manager/files/Supplementarymaterials.pdf>

REFERENCES

Atlas of the Arctic (1985). Moscow, GUGK (Chief Directorate of Geodesy and Cartography under the Council of Ministers of the USSR), 204 p.

Atlas of Snow and Ice Resources of the World (1997). Moscow, Institute of Geography, Russian Academy of Sciences, 264p.

Atlas of the Russian Arctic in the 21st Century: Natural Conditions and Risks of Development (2013). Moscow, 144p.

Ecological Atlas of Russia (2002). Moscow, 128p.

Ecological Atlas of Russia (2017). Moscow, 510p.

Kasimov N.S., Kotlyakov V.M., Chilingarov A.N., Krasnikov D.N., Tikunov V.S. (2015). National Atlas of the Arctic: Structure and Development Stages. Ice and Snow, 1 (129), pp. 4-14.

National Atlas of Russia; Moscow, Roskartografiya (2004-2008): Vol. 1 — General characteristics of the territory, Moscow, Roskartografiya (2004), 495 p; Vol. 2 — Nature. Ecology. Moscow, Roskartografiya (2007) 495 p; Vol. 3 — Population. Economy. Moscow, Roskartografiya, (2008) 495 p; Vol. 4 — History. Culture. Moscow, Roskartografiya, (2008), 495 p.



Professor, full member of Russian Academy of Sciences **Nikolay S. Kasimov**, is Head of the Department of Landscape Geochemistry and Soil Geography since 1987; since 2015 he is the President of the Faculty of Geography, Lomonosov Moscow State University. His current research interests are: landscape geochemistry, paleoecology. He is the author of about 300 scientific works, including: Landscape Geochemistry of Steppe and Desert Landscapes, 1988; Ecogeochemistry of Urban Landscapes, 1995 (author and editor); Landscape Geochemistry, 1999 (co-author A.I. Perel'man); Oil and Environment of Kaliningrad Region, 2008 (author and editor); Landscape Ecogeochemistry, 2013.

Vladimir S. Kazantsev^{1*}, Liudmila A. Krivenok^{1,2}, Maria Yu. Cherbunina³

¹ A.M. Obukhov Institute of Atmospheric Physics Russian Academy of Sciences, Moscow, Russia

² Institute of Forest Science, Russian Academy of Sciences, Uspenskoe, Russia

³ Lomonosov Moscow State University, Moscow, Russia

* **Corresponding author:** kazantsev@ifaran.ru

METHANE EMISSIONS FROM THERMOKARST LAKES IN THE SOUTHERN TUNDRA OF WESTERN SIBERIA

ABSTRACT. Lakes are an important natural source of methane – significant greenhouse gas of the modern atmosphere. Monitoring of methane emission from lakes of northern territories is needed to update the available estimates of CH₄ emission intensity into the atmosphere and to obtain multi-year series of observations. Field measurements of diffuse methane fluxes were carried out on lakes at different stages of thermokarst process located in Yamalo-Nenets Autonomous District (Western Siberia, Russia) during summer 2016 using static chamber method. Some statistical characteristics of measured fluxes were calculated (medians vary from 0.46 to 0.93 mgC-CH₄·m⁻²·h⁻¹), as well as annual diffuse emissions from studied lakes, which values are determined by the area of the lake's water surface. Daily dynamics of methane fluxes were defined and approximation of fluxes with simple model was done, major factors are temperatures of lake bottom and of the surface air layer.

KEY WORDS: Greenhouse gases, fluxes, methane, freshwater ecosystems, polar regions

CITATION: Vladimir S. Kazantsev, Liudmila A. Krivenok, Maria Yu. Cherbunina (2018) Methane emissions from thermokarst lakes in the southern tundra of Western Siberia. *Geography, Environment, Sustainability*, Vol.11, No 1, p. 58-73
DOI-10.24057/2071-9388-2018-11-1-58-73

INTRODUCTION

Methane (CH₄), which is a trace gas of the modern atmosphere, is one of the most important greenhouse gases. One molecule has an impact on the climate 28–34 times greater than CO₂ using a 100-year horizon (IPCC 2013). This, together with feedback mechanism between annual global temperature and CH₄ emission contributing to rapid release of methane from natural

sources under climate warming causes the importance of methane studying (O'Connor et al. 2010).

According to assessment given in (Kirschke et al. 2013) the global annual methane emission from natural sources for 2000-2009 varies from 238 to 484 TgCH₄·year⁻¹ and is equal to 44–57% of total methane emission. In the third place among them are lakes with contribution from 10 to 50 TgCH₄·year⁻¹

(Anderson et al. 2010). Thermokarst lakes of Western Siberia tundra zone are of special interest because of their poor exploration degree due to the inaccessibility of the sites and response of subarctic regions to climate change (Pavlov and Malkova 2009).

A characteristic hydrological feature of Western Siberia is the exceptional abundance of lakes. It is associated with a flat topography and aquiclude that occurs close to the surface because of wide permafrost spreading in the northern part of the plain (Shvareva 1963). The total area of lakes in the southern tundra is 8.8 thousands km², which is 5% of the total area of the subzone of the southern tundra of Western Siberia (Golubyatnikov and Kazantsev 2013; Golubyatnikov et al. 2015). The boundaries of the southern tundra zone were taken according to (Gvozdetskiy et al. 1973; Liss et al. 2001).

The activity of methane-producing Archaea is regulated by several factors, one of them is the bottom sediment temperature (Schulz et al. 1997). In turn, the temperature of the lake bottom is influenced to a certain extent by the climatic features of the studied region.

The issue of monitoring the lakes as a source of methane of the northern territories of Western Siberia still remains unsolved – previous measurements in this area (Glagolev et al. 2010a; Golubyatnikov and Kazantsev 2013) including small number of lakes (10 objects in total) were conducted

in summer season 2009–2010. So further studies are needed to update the available estimates of CH₄ emission from tundra lakes into the atmosphere, as well as to obtain multi-year series of observations.

The aim of our work was to study diffuse fluxes of methane from the lakes of the southern tundra of Western Siberia, to identify factors that affect the emission intensity and to estimate the annual diffuse emission of methane from lakes of different stages of the thermokarst process. In this paper we focused on the study of the diffuse emission of methane at open water period.

STUDY AREA

Field studies of methane fluxes from lakes were carried out from June 27 to July 4, 2016 in the key site «Jarneto» (67.37°N, 78.60°E) 12 km to the southwest from the settlement Tazovsky (Yamalo-Nenets Autonomous District) located in the natural zone of the southern tundra (Fig. 1).

Territory is characterized by moderate continental to continental climate with long severe winter and short cool summer. A characteristic feature of the climate is its significant variability over the years (Vasilevskaya et al. 1986). The average annual air temperature in the zone of the southern tundra in 2016 was -4.9°C, the average air temperature in July and January was 18.6°C and -19.9°C, respectively. The duration of the frost-free period is 116

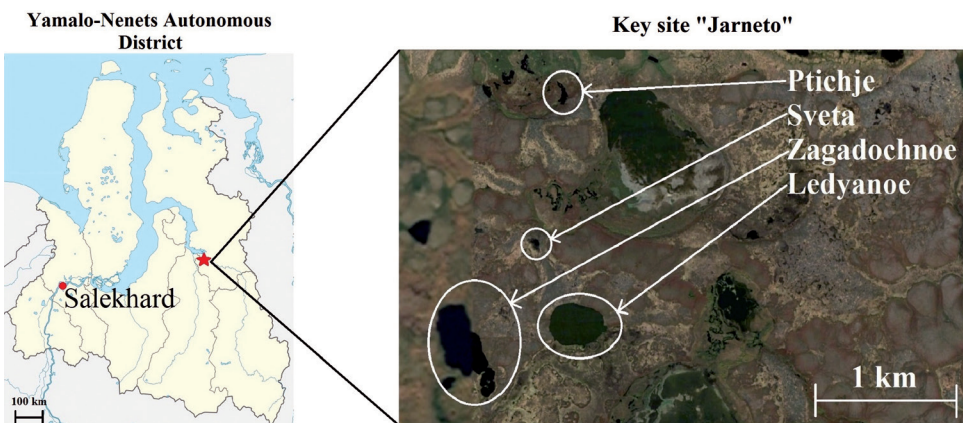


Fig.1. Location of the study site (based on (openstreetmap.org; maps.google.com))

Table 1. Characteristics of studied lakes

Lake	Coordinates, degrees		Area, m ²
	N	E	
Ledyanoe	67.3695	78.6112	≈ 91400
Zagadochnoe	67.3683	78.5925	≈ 131000
Ptichje	67.3841	78.6093	≈ 5100
Sveta	67.3748	78.6044	≈ 1800

days, the amount of precipitation is 384 mm·year⁻¹, the duration of the period with a stable snow cover is 205 days (rp5.ru).

The terrestrial ecosystems of the study area consist of shrubby-lichen tundra in watershed areas and oligotrophic and meso-oligotrophic bogs on slopes and lowland areas according to the classification (Liss et al. 2001). Besides there are khasyreys that are large depressions of the ground surface caused by draining of thermokarst lake.

The study site is located in the northern part of the Pur-Taz interfluvium in the zone of continuous permafrost with high ice content (Firsov et al. 1989). According to (Kravtsova 2009), this area belongs to the zone of ubiquitous distribution of medium and large thermokarst lakes of modern and late Holocene thermokarst in peatlands and mineral soils. The studied lakes are located on the third terrace, composed of ice-covered lake-alluvial sediments of the Upper Quaternary age. The satellite images show a polygonal frozen cracks that confirms thermokarst formation of the lakes due to thawing of the underground ice. The location of frozen soils upper boundary under thermokarst forms are the following: within the limits of small lake water bodies (diameter less than 0.1 km), the thickness of talik zones is from 3 to 80 m, under larger lakes – the thickness of taliks is more than 100 m, and under lake basins over 1 km mainly through taliks were formed (Andrianov et al. 1989).

The studied lakes differ in the stage of the thermokarst process. Ledyanoe and Zagadochnoe lakes are in the active phase of destruction of icy margins (Fig. 2), which is a sign of active thermokarst processes and

the growth of the lake depression. Ptichje lake is characterized by the initial stage of shallowing, bogging along the shoreline (Fig. 3). Lake Sveta is at the final stage of the thermokarst lake, characterized shallow depth, widespread bogging and weediness of waters (Fig. 4). Some characteristics of studied lakes are given in Table 1.

MATERIALS AND METHODS

The measurements of CH₄ flux were performed using the static chamber method following the methodology described in (Glagolev et al. 2010b). Plexiglass chambers (40 cm × 40 cm × 40 cm) covered with reflecting fabric and floats of four plastic bottles with a capacity of 2 liters were used (Fig. 5). Chambers were dipped into the water with their lower facet being 4 cm below the surface. The period of exposure was 30 min during which 4 gas samples were taken in 50 ml three-component syringes. The air samples were transferred to hermetically sealed glass bottles by displacing the concentrated sodium chloride solution. The temperature was measured at the surface of the lake and at the bottom (thermal sensors «Thermochron» DS 1922L, Maxim Integrated, USA), the wind speed, air temperature and atmospheric pressure at 5 cm above the lake surface (portable weather station Skywatch GEOS N11, JDC Electronic SA, Switzerland) were observed. All these variables along with the depth of the lake were registered at each measurement point. Samples of bottom sediments were taken from Ptichje lake. The methane fluxes measurements for diurnal dynamics on Ledyanoe lake were made in duplicate once every two hours. Table 2 gives a more detailed description of fluxes measurement points.



Fig. 2. Lake Ledyanoe



Fig. 3. Lake Ptichje



Fig. 4. Lake Sveta



Fig. 5. Floating chambers

Table 2. Points of methane fluxes measurements (2016 year)

Date	Lake	Lake part	Water depth, cm	Number of measurements	Time of measurements
27.06	Ledyanoe	center	170	8	16:34–20:05
02.07	Ledyanoe	between center and shore	170	8	16:03–18:18
02.07	Ledyanoe	shore	50	8	19:44–21:34
03.07-04.07	Ledyanoe	shore	75	23	14:17–12:37 (diurnal dynamics)
28.06	Zagadochnoe	center	150	8	14:32–18:53
29.06	Zagadochnoe	between center and shore	140	7	12:37–15:14
29.06	Zagadochnoe	shore	60	8	16:23–18:42
30.06	Sveta	center	90	8	12:09–14:26
30.06	Sveta	shore	82	8	15:43–17:59
01.07	Ptichje	center	120	8	14:05–16:22
01.07	Ptichje	shore, deep place	170	8	17:15–19:23

The methane concentrations in the samples were determined by gas chromatography on a Chromatec-Crystal 5000.2 instrument (ZAO Khromatek, Yoshkar-Ola) with a flame ionization detector. Each sample of gas from a syringe was analyzed three times. The volume of the sampler (loops) is 0.250 ml. The length of the chromatographic column is 3 m, the diameter is 2 mm, the adsorbent is Hayesep-N 80/100. The column temperature is 60°C, the temperature of the flame ionization detector is 150°C. As the carrier gas, nitrogen (99.999%) is used at a flow rate of 30 ml·min⁻¹. The flow rate of hydrogen – 20 ml·min⁻¹, air – 200 ml·min⁻¹. Calibration of the chromatograph was carried out using calibration gas mixtures with the following methane concentrations: 0.49 ± 0.07 ppm, 5.3 ± 0.5 ppm, 10.3 ± 0.6 ppm, 100 ± 5 ppm (OAO Monitoring, St. Petersburg).

Organic carbon concentrations in sediments were determined in the laboratory of UNESCO Chair on Environmental Dynamics and Global Climate Change (Yugra State

University) using an EA-3000 analyzer (EuroVector, Italy) by combustion in a catalyst tube in excess of oxygen and helium current. Gas separation was produced in a packed chromatography column and the detection of a signal on a thermal-conductivity detector. Calibration was produced by two standards: acetanilide (C=71.09%, N=10.36%, H=6.71%) and atropine (C=70.56%, N=4.84%, H=8.01%) using a linear calibration method.

The values of fluxes were calculated by the linear regression method with weights for positive values and nonlinear with weights for negative values (Glagolev et al. 2010b).

With the KSDENSITY function from the Statistic Toolbox of Matlab 7.10.0 (MathWorks, USA), probability density functions for methane fluxes were calculated for each lake. The weights of the variables were determined in inverse proportional to the square of the standard deviation corresponding to the measurement, according to (Rumshisky

1971); the kernel type (normal) and the smoothing width correspond to the default ones. Boundaries, on which the probability density was reconstructed, were chosen in accordance with arguments in (Krivenok et al. 2014): the interval $[\min(x_i - w_p); x_{\max} + v]$ was taken, where x_i is measured methane flux, w_i is corresponding error value, i is the index number of measurement (varies from 1 to n), n is the number of measurements; $v = 5 \cdot (x_{\max} - x_{\min}) / (n - 1)$, x_{\min} and x_{\max} are the minimum and maximum values of measured methane fluxes (according to Stephanyuk's empirical formula, (Vapnik et al. 1984)). For more details on the construction of probability distributions in application to methane fluxes, we refer to (Glagolev and Sabrekov 2008).

For checking of the measured methane fluxes accordance with lognormal distributions the Anderson-Darling test with 0.05 significance level from the Statistic Toolbox of Matlab was used.

The annual diffuse emission of methane was calculated using the methodology of the «standard model» (Glagolev 2008). According to this methodology, the annual diffuse methane emission was calculated as product of the following parameters: 1) area of the lake water surface; 2) the period of diffuse methane emission; 3) characteristic values of methane fluxes (the medians of the measured methane fluxes on each lake) taken by constants during the entire emission period. 95% confidence interval was given as an error of the medians according to (GOST R ISO 16269-7-2004 2004).

The period of diffuse methane emission in 2016 is calculated according to the methodology outlined in (Suvorov and Glagolev 2007). In this work, the period of methane emission (PME) is defined as the duration of the summer-autumn period multiplied by the empirically selected coefficient. The date of a stable transition of the average daily air temperature through 10°C is taken as the beginning of the summer-autumn period. The date of a stable transition of the average daily air temperature through 0°C is taken for

the end of it. According to the Tazovsky meteorological station (rp5.ru) in 2016, the summer-autumn period lasted from June 9 to October 3 (117 days). The empirical coefficient required for the calculation of the PME was assumed to be 1.147. This value was obtained by dividing the PME values given in (Glagolev, 2008) to the duration of the summer-autumn period according to the data of (Shvareva 1963) – reference which was indicated in the original publication when describing the PME calculation method. So the duration of PME in the southern tundra in 2016 was selected as 134 days.

Approximation for the daily dynamics of methane fluxes was conducted by the following equation (we were inspired by (Juutinen et al. 2004) for choosing this form of dependence):

$$F = b_1 + b_2 T_{air} \cdot \sin\left(\left[\pi \cdot (b_3 - h) / 24\right]^2\right)$$

where F – CH₄ fluxes (mgC-CH₄·m⁻²·h⁻¹), b_1 , b_2 and b_3 – parameters, T_{air} – air temperature (°C), h – running hour, corresponding to the mid-exposure time (hh.hh, integer and decimal fraction).

The determination of parameters was carried out in the program STATISTICA 7.0 (StatSoft, USA) using the method of least squares, also weights of the variable F (determined in this case in inverse proportional to the corresponding standard deviation) were taken into account. Parameters were determined with their standard errors, p-level < 0.05.

The quality of the approximation is indicated by the value of the Theil divergence coefficient, which varies from 0 with a complete coincidence to 1 with a very poor coincidence of the measured and modeled data (Theil 1971).

RESULTS AND DISCUSSION

Following results of field measurements were obtained in 2016: 47 values of methane fluxes from Ledyanoe lake, 16 from lakes Ptichje and Sveta and 23 values from lake Zagadochnoe. The median

Table 3. Statistical characteristics of methane fluxes from the studied lakes of the southern tundra of Western Siberia

Lake	Number of samples	Methane fluxes, mgC-CH ₄ ·m ⁻² ·h ⁻¹				
		I quartile	Median	III quartile	Lower limit of 95% confidence interval	Upper limit of 95% confidence interval
Ledyanoe	47	0.30	0.46	0.79	0.33	0.67
Zagadochnoe	23	0.48	0.59	1.16	0.48	0.86
Sveta	16	0.76	0.93	1.01	0.65	1.12
Ptichje	16	0.16	0.50	2.14	0.16	3.59

values and quartiles were calculated (Table 3). Medians of the methane fluxes from lakes Ledyanoe, Zagadochnoe and Ptichje are approximately 0.5 mgC-CH₄·m⁻²·h⁻¹, whereas the median of the methane fluxes from Sveta lake is almost twice higher – 0.96 mgC-CH₄·m⁻²·h⁻¹. Probability density functions of methane fluxes for each of the lakes are shown at Fig. 6 a-c.

Probability distributions of methane fluxes from lakes Ledyanoe and Ptichje (Fig. 6 a, b) both have main peaks, which fall on the values 0.25 and 0.10 mgC-CH₄·m⁻²·h⁻¹ respectively, Zagadochnoe lake (Fig. 6 a) has peak at 0.48 mgC-CH₄·m⁻²·h⁻¹ and another small one near 0.14 mgC-CH₄·m⁻²·h⁻¹. The distribution of methane fluxes from lake Sveta (Fig. 6 c) has two peaks, one is near 0.25 mgC-CH₄·m⁻²·h⁻¹, the other is 0.94 mgC-CH₄·m⁻²·h⁻¹.

The Anderson-Darling test does not reject the null hypothesis that measured methane fluxes values for lakes Ledyanoe and Ptichje are from lognormal distributions.

Generally, the lognormal form is quite typical for probability density distributions of the methane fluxes (similar types of distributions could be seen in (Panikov 1995; Smagin et al. 2003; Glagolev and Suvorov 2008). The reason of this phenomenon is described, for example, at (Glagolev and Sabrekov 2008), since it is known that the lognormal value is obtained as the result of multiple multiplications of independent quantities (Borovikov 2001). That means if the studied process is the result of the

combined action of several independent processes, then the observed distribution of the random variable is lognormal. This is true for methane emission that consists of the production of CH₄ by microorganisms-methanogens, transport from the place of formation to the surface and consuming by methanotrophs and is influenced by multiple environmental factors (Chanton et al. 1992; Glagolev et al. 2008). With the combined effect of all processes, a distribution close to the lognormal distribution is obtained.

As we can see, on some graphs there are more than one peak. The point is that nowadays the issue of probability distributions errors calculation is not developed completely, particularly Matlab does not have means to estimate these errors. So we can not be confident whether the first (smaller one) peak for Zagadochnoe lake shows real feature of studied ecosystem and not the artifact of mathematical processing of experimental data. But if it is not an artifact and bimodality of methane fluxes probability distribution is a result of natural processes, extrema could be caused by different environmental conditions between measurement points. As for the Sveta lake, it should be mentioned, that there were two measurement points and we can see two major peaks on the graph. This example once again illustrates the fact that it is not correct to use the arithmetic mean of methane fluxes sampling as the distribution of initial data is not normal in most cases (Glagolev and Suvorov 2008; Taylor 1985).

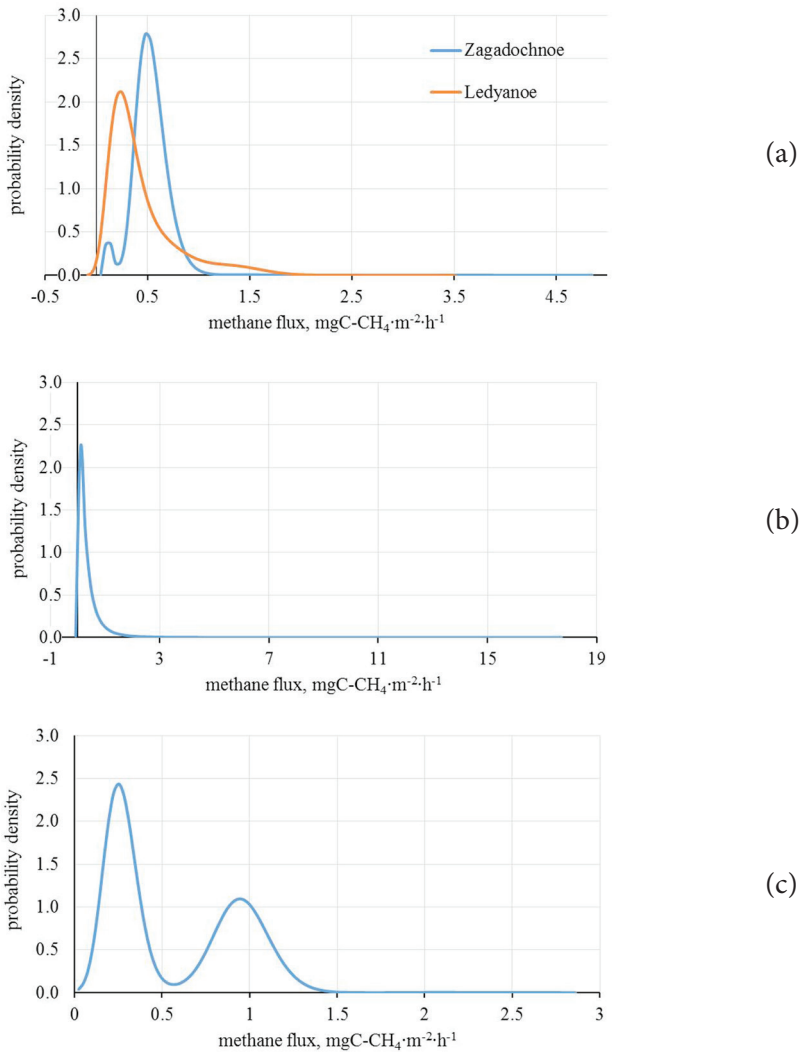


Fig. 6. Probability distributions of methane fluxes from lakes: a) Zagadochnoe and Ledyanoe, b) Ptichje, c) Sveta

We compared the data we obtained with the results of other researchers who conducted similar studies of lakes in various natural zones of Western Siberia (Table 4). Here we should make a restriction that the comparison is not absolutely strict, since the emission of methane is affected by a large number of different factors, the influence of which we can not fully take into account. In the first approximation, we assume that the change of natural zones is an integral factor in relation to most factors that affect methane emission.

As far as we know the first results on emission of methane from the tundra lakes of Western Siberia were published in (Glagolev et al. 2010a). Similar studies (Sabrekov et al. 2011), were conducted in the area of Tazovsky and Gyda (Yamalo-Nenets Autonomous District, Russia). The lakes described in this work, according to our data, are of thermokarst origin, not wetland lakes, as they are classified in the source (one of the authors of this article personally carried out measurements of methane from these lakes). Methane fluxes from the lakes in this research, with the exception of lake Ptichje, exceed the

Table 4. Emission of methane from the lakes of the natural zones of Western Siberia, $\text{mgC-CH}_4 \cdot \text{m}^{-2} \cdot \text{h}^{-1}$

Zone	Objects	I quartile	Median	III quartile	Comment	Reference
Southern tundra	Thermokarst lakes	0.32	0.61	0.97	Generalized statistical characteristics are given (calculated from all measured values of methane fluxes)	Current research
Southern tundra	Wetland lakes	0.34	0.64	1.07		Glagolev et al. 2010a
Tundra	Thermokarst lakes	0.15	0.27	0.57		Sabrekov et al. 2011
Forest tundra	Wetland lakes	–	0.17	–	Recalculated from $5.3 \text{ mgCH}_4 \cdot \text{m}^{-2} \cdot \text{d}^{-1}$	Repo et al. 2007
North taiga	Wetland lakes	-0.01	0.10	0.31		Sabrekov et al. 2013
Middle taiga	Wetland lakes		0.13		Recalculated from $4.1 \text{ mgCH}_4 \cdot \text{m}^{-2} \cdot \text{d}^{-1}$	Repo et al. 2007
Middle taiga	Small wetland lake	–	0.75	–	Recalculated from $24 \text{ mgCH}_4 \cdot \text{m}^{-2} \cdot \text{d}^{-1}$	Repo et al. 2007
Middle taiga	Lakes of different types		0.23			Sabrekov et al. 2013
Middle taiga	Wetland lakes	0.18	0.49	2.15		Sabrekov et al. 2013
Southern taiga	Lakes of different types	–	3.08	–	Recalculated from $4.1 \text{ mgCH}_4 \cdot \text{m}^{-2} \cdot \text{d}^{-1}$	Sabrekov et al. 2017
Southern taiga	Wetland lakes	3.21	17.94	77.76		Sabrekov et al. 2013
Forest-steppe	Wetland lakes	97.93	125.55	145.92	Quartiles calculated from 4 values	Glagolev et al. 2009

indicated values. This can be explained by the fact that the values of methane from lakes located on the boundary of the typical and arctic tundra were included in the data set (Sabrekov et al. 2011), where the emission is expected to be lower than from the lakes of the southern tundra due to the lower speed of the methanogenesis process.

The methane emissions for thermokarst lakes with three different ages in (Desyatkin 2009) are compared for Eastern Siberia (Central Yakutia) region. Results show the highest emission at «mature alas» stage and the lowest – at «tyympy» one. The stages are named according to the regional classification (Soloviev 1959), where «tyympy» corresponds to the stage of the primary thermokarst lake, and «mature alas» is the stage of lake draining with starting the freezing of the alas depression. Therefore the values of methane fluxes at the primary stage of forming the young thermokarst basin («dyuedya» stage) were comparable with the stage of mature alas. There is an analogy with our studied lakes. Thus, Ledyanoe and Zagadochnoe lakes, which are in the active phase of development, have the values of the methane fluxes 2 times smaller than Sveta lake, that goes through the final stage of development of the thermokarst lake, that is close to the results for Central Yakutia (Destyakin 2009). Nevertheless, Ptichje lake occupies an intermediate position in the development course (going through the initial stage of shallowing), but has the values of methane fluxes equal to Ledyanoe and Zagadochnoe lakes, although the intermediate results are anticipated from the above concept. This can be explained by the fact that lake Ptichje has the largest spread of fluxes values, which is associated with a strong spatial heterogeneity of the methane emission intensity caused by the initial stage of the lake evolution, when some measurements were carried out on a site with developing bogging and others on the open water.

Lakes Ptichje and Sveta can be correlated with wetland lakes according to bottom substrate, that is nutrient medium for

methane-producing Archaea, as Ptichje lake sediments contain 10-20% of carbon.

The medians of methane fluxes measured in wetland lakes are reduced in the forest-tundra zone in comparison with tundra lakes and reach a minimum in the north-taiga zone. Further, the values of methane fluxes from wetland lakes increase southward. Thus, methane fluxes from tundra wetland lakes are quantitatively comparable to methane fluxes from more southern middle-taiga wetland lakes. This can be seen as a contradiction, since it is logical to expect an increase in methane emissions from more southern wetlands due to an increase in the intensity of biological processes, in particular, methanogenesis. This phenomenon, as well as the minimum values of methane fluxes from the north taiga wetlands can be explained by a small number of measurements that indicates the need for more detailed studies of methane emissions from lakes of different natural zones of Western Siberia. Besides, in (Glagolev et al. 2009), rather large values of methane fluxes from the wetland lakes of the forest-steppe zone are given. Most likely these values are due to the fact that the researcher was standing on the floating mat and bubbling methane was released, so the methane concentration in the chamber and, correspondingly, the value of the diffuse methane fluxes were overestimated. It should be also mentioned, that in personal communication first author of the article (Sabrekov et al. 2017) explained, that methane flux value of $3.08 \text{ mgC-CH}_4 \cdot \text{m}^{-2} \cdot \text{h}^{-1}$ (Table 4) from southern taiga lakes corresponds to total (diffuse plus bubble) methane fluxes. We agree with the suggestion of anonymous reviewer of current article about the increase of bubble CH_4 flux intensity from lakes in southern taiga zone and more southerly regions. Thus, values of methane fluxes for southern taiga and forest steppe are caused both by diffusive and bubble mechanisms of CH_4 transport, whereas for northwardly lakes – mostly by diffuse transport mechanism.

On the basis of measured values of methane emission for each lake, an annual emission was calculated (Table 5).

Table 5. Estimation of annual diffuse methane emissions, kgC-CH₄·year⁻¹

Lake	The annual diffuse emission	Lower limit of 95% confidence interval	Upper limit of 95% confidence interval
Ledyanoe	135	97	197
Ptichje	8	3	59
Sveta	5	4	6
Zagadochnoe	249	203	363

The annual emission of methane from lakes varies by almost two orders of magnitude from 5 kgC-CH₄·year⁻¹ for lake Sveta to 249 kgC-CH₄·year⁻¹ for lake Zagadochnoe. This is primarily due to a significant difference in the areas of the water surface of lakes, whereas the difference in methane fluxes from each lake is insignificant.

Daily dynamics of methane fluxes

The daily dynamics of methane emissions was measured at lake Ledyanoe during the period from 3 to 4 July 2016 (Fig. 7 a). The given plot of the daily dynamics of methane fluxes values has two minimums with an interval of approximately 12 hours: 4 am and 16 pm for shallow

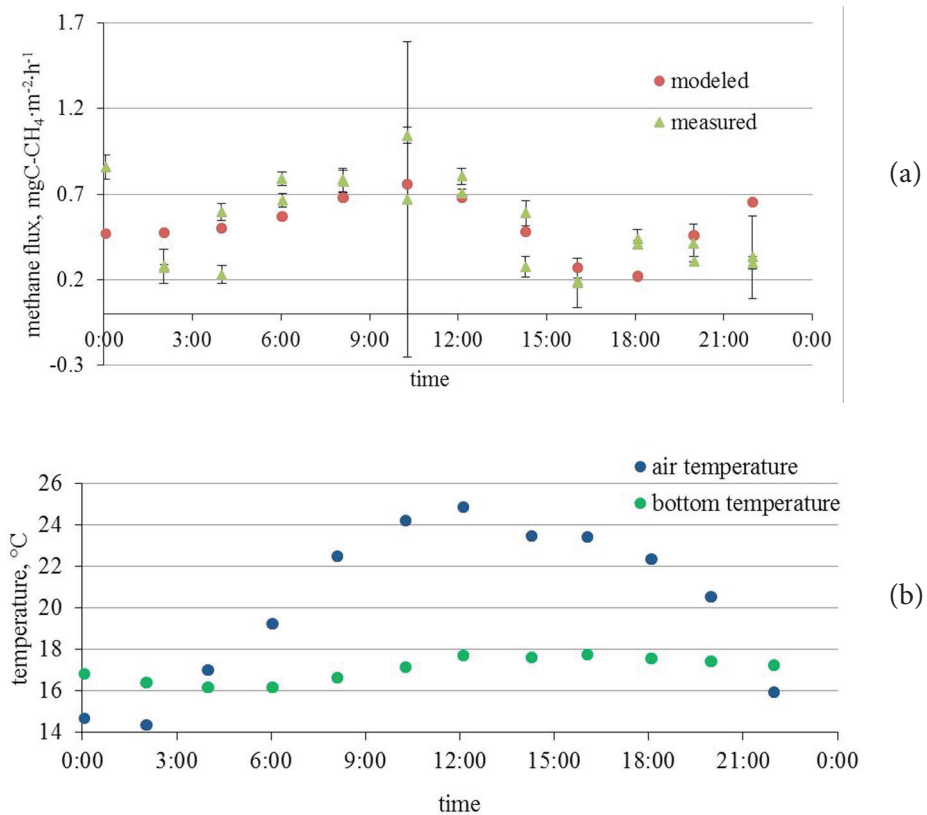


Fig. 7. a) The daily dynamics of methane fluxes for the shallow waters of lake Ledyanoe (July 3–4, 2016). Error bars are for standard deviation. b) Temperatures of lake bottom and air at the surface of the lake

waters of lake Ledyanoe. The only clearly expressed emission maximum is about 10 am.

Thus we obtained the equation (air temperature ranges from 14.4 to 24.9°C) with the following form:

$$F = (0.47 \pm 0.01) + (0.012 \pm 0.001) \cdot T_{air} \cdot \sin\left[\pi \cdot (1.14 \pm 0.11 - h) / 24\right]^2$$

For this model Theil divergence coefficient value is 0.03 without contribution of the original data errors and 0.18 with them.

The temperature of the lake bottom correlates nonlinearly with the air temperature T_{air} and with the time of day (Fig. 7 b). The presence of correlations between temperatures is evidenced by the value of the nonparametric rank correlation coefficient of Spearman equal to 0.63. A nonparametric correlation criterion was chosen in view of the fact that the relationship between the variables is nonlinear as advised at (Borovikov 2001).

CONCLUSION

Based on the above results, we made the following conclusions.

Medians of diffuse methane fluxes for the studied thermokarst lakes of the southern tundra vary from 0.46 to 0.93 mgC-CH₄·m⁻²·h⁻¹. The fluxes values from

two of studied lakes are of lognormal distributions according to the Anderson-Darling test.

The intensity of methane emission in the shallow part of lakes depends on the temperature of the surface air layer. Due to daily natural fluctuations in air temperature, the daily dynamics of methane emission intensity is also observed.

The annual diffuse emission of methane from the studied thermokarst lakes varies from a few to hundreds of kilograms of methane per year and first of all is determined by the area of the lake's water surface.

This work can be considered as a special case of research in major issue of Western Siberia tundra lakes as a source of methane.

ACKNOWLEDGMENTS

Authors are grateful to the reviewers for valuable advice and comments that have significantly improved the article. This work was supported by the RFBR grant № 16-35-00097 «Estimating the methane flux into the atmosphere from southern tundra lakes in Western Siberia» and the RFBR grant № 14-05-00193 «Estimating the intensity of methane flux into the atmosphere from ecosystems of the northern region in Western Siberia». ■

REFERENCES

- Anderson B., Bartlett K., Frolking S., Hayhoe K., Jenkins J. and Salas W. (2010). Methane and nitrous oxide emissions from natural sources. Washington DC: US EPA.
- Andrianov V., Voitsekhovskaya I., Grechishev S., Krishchuk L., Nevecherya V., Stremyakov A., Uvarkin Yu., Shamanova I., Sheshin Yu. and Shur Yu. (1989). Conditions of development and expansion of cryogenic geological processes and phenomena. In E.D. Ershov, ed., *Geokriologia SSSR. Zapadnaya Sibir'*. Moscow: Nedra, pp. 135-155. (in Russian).
- Borovikov V. (2001). STATISTICA: art of computer data processing. For professionals. St. Petersburg: Piter. (in Russian).
- Chanton J., Martens C., Kelley C., Crill P. and Showers W. (1992). Methane transport mechanisms and isotopic fractionation in emergent macrophytes of an Alaskan tundra lake. *Journal of Geophysical Research: Atmospheres*, 97(D15), pp. 16681-16688. DOI: 10.1029/90JD01542.
- Desyatkin A., Takakai F., Fedorov P., Nikolaeva M., Nikolaev A., Hatano R. and Desyatkin R. (2009). Methane emission at taiga alar ecosystems of Central Yakutia. *Nauka i obrazovanie*, 3, pp. 72-76. (in Russian).
- Firsov N., Anan'eva G., Dubrovin V. and Ukraintseva N. (1989). Ust'purovsko-Tazovsky region. In E.D. Ershov, ed., *Geokriologia SSSR. Zapadnaya Sibir'*. Moscow: Nedra, pp. 247-251. (in Russian).
- Glagolev M. (2008). The emission of methane: ideology and methodology of «standard model» for Western Siberia. *Environmental Dynamics and Global Climate Change*. S1. pp. 176-190. (in Russian).
- Glagolev M. and Sabrekov A. (2008). Reconstruction of probability density distribution by histogram method in soil science and ecology. *Environmental Dynamics and Global Climate Change*, S1, pp. 55-83. (in Russian).
- Glagolev M. and Suvorov G. (2008). Wetlands in the problem of methane as greenhouse gas: what was investigated and what is forthcoming?. *Interactive journal of ecological soil science*, 2(8), pp. 19-43. (in Russian).
- Glagolev M., Golovatskaya E. and Shnyrev N. (2008). Greenhouse gas emission in West Siberia. *Contemporary Problems of Ecology*, 1(1), pp. 136-146. DOI: 10.1134/S1995425508010165.
- Glagolev M., Kleptsova I., Filippov I., Kazantsev V. and Maksyutov Sh. (2010a). Methane emission from West Siberian tundra mires. *Tomsk State Pedagogical University Bulletin*, 3(93), pp. 78-86. (in Russian).
- Glagolev M., Kleptsova I., Kazantsev V., Filippov I., Machida T. and Maksyutov Sh. (2009). Methane emission from typical peatland landscapes of Western Siberia forest-steppe: for «standard model» Bc5. *Tomsk State Pedagogical University Bulletin*, 11(89), pp. 198-206. (in Russian).
- Glagolev M., Sabrekov A. and Kazantsev V. (2010b). Physicochemistry and biology. Methods of gas exchange measurements at soil – atmosphere border. Tomsk: TGPU. (in Russian).
- Golubyatnikov L. and Kazantsev V. (2013). Contribution of tundra lakes in Western Siberia to the atmosphere methane budget. *Izvestiya, Atmospheric and Oceanic Physics*, (49)4, pp. 395-403, DOI: 10.1134/S000143381304004X.

Golubyatnikov L., Zarov E., Kazantsev V., Filippov I. and Gavrilov G. (2015). Analysis of landscape structure in the tundra zone for Western Siberia based on satellite data *Izvestiya. Atmospheric and Oceanic Physics*, 51(9), pp. 969-978.

GOST R ISO 16269-7-2004 (2004). Statistical interpretation of data — Part 7: Median — Estimation and confidence intervals (IDT). Moscow: Izdatel'stvo standartov. (in Russian).

Gvozdet'skiy N., Krivolut'skiy A. and Makunina A. (1973). Scheme of physico-geographical regionalization of the Tyumen region. In N.A. Gvozdet'skiy, ed., *Fiziko-geograficheskoye rayonirovaniye Tyumenskoy oblasti*, 1st ed. Moscow: MGU, pp. 9-27. (in Russian).

IPCC (2013). *Climate Change 2013: The Physical Science Basis. Contribution of Working Group I to the Fifth Assessment Report of the Intergovernmental Panel on Climate Change*. Stocker, T.F., D. Qin, G.-K. Plattner, M. Tignor, S.K. Allen, J. Boschung, A. Nauels, Y. Xia, V. Bex and P.M. Midgley (eds). Cambridge University Press, Cambridge, United Kingdom and New York, NY, USA. 1535 p.

Juutinen S., Alm J., Larmola T., Saarnio S., Martikainen P. and Silvola J. (2004). Stand-specific diurnal dynamics of CH₄ fluxes in boreal lakes: Patterns and controls. *Journal of Geophysical Research: Atmospheres*, 109, DOI: 10.1029/2004JD004782.

Kirschke S., Bousquet P., Ciais P., Saunois M., Canadell J., Dlugokencky E., et al. (2013). Three decades of global methane sources and sinks. *Nature Geoscience*, 6(10), pp. 813-823. DOI: 10.1038/ngeo1955.

Kravtsova V. and Bystrova A. (2009). Changes in thermokarst lake size in different regions of Russia for the last 30 years. *Earth's Cryosphere*, 13(2), pp. 16-26. (in Russian).

Krivenok L., Glagolev M., Fastovets I., Smolentsev B. and Maksyutov S. (2014). Methane fluxes from south tundra ecosystems of West Siberia. *Environmental Dynamics and Global Climate Change*, 5(1), pp. 26-42. (in Russian).

Liss O., Abramova L., Avetov N., Berezina N., Inisheva L., Kurnishkova T., Sluka Z., Tolpysheva T. and Shvedchikova N. (2001). *Wetland systems of Western Siberia and their environmental significance*. Tula: Grif i Ko. (in Russian).

maps.google.com, (2018). Google maps. [online] Available at: <https://maps.google.com> [Accessed 01 Jan. 2018].

O'Connor F., Boucher O., Gedney N., Jones C., Folberth G., Coppel R., Friedlingstein P., Collins W., Chappellaz J., Ridley J. and Johnson, C. (2010). Possible role of wetlands, permafrost, and methane hydrates in the methane cycle under future climate change: A review. *Reviews of Geophysics*, 48(4). DOI: 10.1029/2010RG000326.

openstreetmap.org, (2018). OpenStreetMap. [online] Available at: <https://openstreetmap.org> [Accessed 01 Jan. 2018].

Panikov N. (1995). Taiga wetlands – global source of atmospheric methane. *Priroda*, 6, pp. 14-25. (in Russian).

Pavlov A. and Malkova G. (2009). Small-scale mapping of trends of the contemporary ground temperature changes in the Russian north. *Earth's Cryosphere*, 13(4), pp. 32-39 (in Russian).

Repo M., Huttunen J., Naumov A., Chichulin A., Lapshina E., Bleuten W. and Martikainen P. (2007). Release of CO₂ and CH₄ from small wetland lakes in western Siberia. *Tellus B*, 59(5), pp. 788-796. DOI: 10.1111/j.1600-0889.2007.00301.x.

rp5.ru, (2017). RP5 Official Website. [online] Available at: <https://rp5.ru> [Accessed 27 Oct. 2017].

Rumshiskyi L. (1971). Mathematical processing of experiment results. Moscow: Nauka. (in Russian).

Sabrekov A., Glagolev M., Kleptsova I. and Maksyutov S. (2011). CH₄ emission from West Siberia tundra mires. *Environmental Dynamics and Global Climate Change*, 2(1). (in Russian).

Sabrekov A., Glagolev M., Kleptsova I., Machida T. and Maksyutov S. (2013). Methane emission from mires of the West Siberian taiga. *Eurasian soil science*, 46(12), pp. 1182-1193.

Sabrekov A., Runkle B., Glagolev M., Terentieva I., Stepanenko V., Kotsyurbenko O., Maksyutov S. and Pokrovsky O. (2017). Variability in methane emissions from West Siberia's shallow boreal lakes on a regional scale and its environmental controls. *Biogeosciences*, 14(15), pp. 3715-3742.

Schulz S., Matsuyama H. and Conrad R. (1997). Temperature dependence of methane production from different precursors in a profundal sediment (Lake Constance). *FEMS Microbiology Ecology*, 22(3), pp. 207-213. DOI: 10.1111/j.1574-6941.1997.tb00372.x.

Shvareva Yu. (1963). *Klimat [Climate]*. In G.D. Rihter and V.I. Orlov, ed., *Zapadnaya Sibir*. Moscow: Izdatel'stvo AN SSSR, pp. 70-99. (in Russian).

Smagin A., Glagolev M., Suvorov G. and Shnyrev N. (2003). Methods for studying gas fluxes and the composition of soil air in field conditions using a portable PGA-7 gas analyzer. *Moscow University Soil Science Bulletin*, 58(3), pp. 26-35.

Soloviev P. (1959). Permafrost of northern part of Lena-Amga interfluve area. Moscow: Izdatel'stvo AN SSSR. (in Russian).

Suvorov G. and Glagolev M. (2007). The duration of «active methane emission period». *Bolota i biosfera: Sbornik materialov Shestoi Nauchnoi Shkoli (10-14 sentyabrya 2007 g.)*. pp. 270-274 (in Russian).

Taylor D. (1985). *Introduction to error theory*. Moscow: Mir. (in Russian).

Theil H. (1971). *Economic forecasts and policy*. Moscow: Statistica. (in Russian).

Vapnik V., Glazkova T., Koshcheev V., Mikhal'skiy A. and Chervonenkis A. (1984). *Algorithms and programs for dependencies lifting*. Moscow: Nauka. (in Russian).

Vasilevskaya V., Ivanov V. and Bogatirev L. (1986). *Soils of Western Siberia north*. Moscow: Izdatel'stvo MGU. (in Russian).

Vladimir S. Kazantsev graduated from Moscow State University, Soil science faculty. PhD in biology (2013). Researcher of Laboratory of mathematical ecology A.M. Obukhov Institute of Atmospheric Physics RAS. Research interests: arctic lakes and wetlands as source of greenhouse gases.



Liudmila A. Krivenok is a junior researcher at Laboratory of Mathematical Ecology in Institute of Atmospheric Physics RAS and a PhD student at Institute of Forest Science RAS. She graduated from Moscow State University, faculty of soil science with specialization in soil physics. Her current focus of research is on various ecosystems (wetlands, peatlands, lakes) of different Russian natural zones as a source of greenhouse gases methane and carbon dioxide.



Maria Yu. Cherbunina is a research engineer at geocryological department of Lomonosov Moscow State University. Her field of research is gas and microorganisms in frozen soils. She is involved in several projects on gas and organic matter content in permafrost zone- in Central Yakutia and Western Siberia, field work, field course on methods in engineering-geological, hydrogeological and geocryological studies and teaching a course on geocryology.

**Natalia Chubarova^{1*}, Aleksei Poliukhov^{1,2}, Marina Shatunova²,
Gdaliy Rivin^{1,2}, Ralf Becker³, Stefan Kinne⁴**

¹Faculty of Geography, Moscow State University, Moscow, Russia

²Hydrometeorological Centre of Russia, Moscow, Russia

³Deutscher Wetterdienst, Meteorologisches Observatorium Lindenberg/Mark,
Tauche, Germany

⁴Max Planck Institute for Meteorology, Hamburg, Germany

* **Corresponding author:** natalia.chubarova@gmail.com

CLEAR-SKY RADIATIVE AND TEMPERATURE EFFECTS OF DIFFERENT AEROSOL CLIMATOLOGIES IN THE COSMO MODEL

ABSTRACT. We estimated the effects of the different aerosol climatologies in the COSMO mesoscale atmospheric model using long-term aerosol measurements and the accurate global solar irradiance observations at ground at the Moscow State University Meteorological Observatory (Russia) and Lindenberg Observatory (Germany) in clear sky conditions. The differences in aerosol properties have been detected especially during winter months. There is a better agreement of MACv2 aerosol climatology with measurements for Moscow conditions compared with Tegen aerosol climatology. However, we still have a systematical negative bias of about 2-3% in global solar irradiance at ground for both sites. A noticeable sensitivity of air temperature at 2 meters to the net radiation changes of about 1°C per 100 Wm⁻² due to aerosol has been evaluated, which approximately is around -0.2 – -0.3°C, when accounting for real aerosol properties.

KEY WORDS: aerosol, radiative processes, COSMO model, aerosol climatologies, temperature effects, AERONET.

CITATION: Natalia Chubarova, Aleksei Poliukhov, Marina Shatunova, Gdaliy Rivin, Ralf Becker, Stefan Kinne (2018) Clear-Sky Radiative And Temperature Effects Of Different Aerosol Climatologies In The Cosmo Model. *Geography, Environment, Sustainability*, Vol.11, No 1, p. 74-84

DOI-10.24057/2071-9388-2018-11-1-74-84

INTRODUCTION

Aerosol is one of the key factors, which has a significant influence on scattering and absorption of solar irradiance in the atmosphere and on climate (Boucher et al. 2013). Due to large variation in its composition aerosol may have different optical properties. The uncertainty in aerosol properties of the atmosphere affects the accuracy of radiative flux simulation and may provide significant errors in evaluating different parameters in numerical weather prediction (NWP) models (Tanre et al. 1984; Ritter and Geleyn 1992).

There are several approaches to account for aerosol properties in the models: to compute directly their properties or to use various aerosol climatologies. The first approach is computationally very time consuming and need exact data on emission rates of different aerosol precursors, which are often unavailable. Therefore, the second approach (the application of aerosol climatologies) is usually applied in the different atmospheric models. One of the well-known atmospheric models is the COSMO (Consortium for Small-scale MOdeling) model, which is widely used in different countries for the operational weather forecasting and climate modelling (www.cosmo-model.org).

Different aerosol climatologies optionally can be used in the COSMO model. The Tanre aerosol climatology (Tanre et al. 1984) is characterized by large biases compared with the observations. Another aerosol climatology is a well-known Tegen aerosol dataset (Tegen et al. 1997), which is usually applied in the model computations. Since recent time a new aerosol MACv2 (Max Planck Institute Aerosol Climatology version 2) climatology developed by Kinne et al. (2013) is also available as the input aerosol dataset in the COSMO model. However, the quality of the Tegen and MACv2 aerosol climatologies has not been thoroughly tested using long-term ground-based aerosol datasets. Therefore, the main objectives of the study were the following:

1. To evaluate the uncertainties of Tegen and MACv2 aerosol climatologies against long-

term aerosol datasets at the Moscow State University Meteorological Observatory (MSU MO, Russia) and Lindenberg Observatory (LO, Germany) and to estimate the radiative effects of these uncertainties for clear sky conditions.

2. To test radiative simulations in COSMO model against radiative density flux measurements (global solar irradiance) at both sites in cloudless situations.

3. To estimate temperature effects of aerosol properties using COSMO model.

We would like to emphasize that since the locations of the sites are inside the Eurasian continent, the obtained results concern mainly the effects of continental aerosols.

MATERIALS AND METHODS

The COSMO model is a non-hydrostatic mesoscale atmospheric model (Doms et al. 2011a; Doms et al. 2011b). In Russian Federation it is being utilized in operational mode as a COSMO-Ru configuration (Rivin et al. 2015). Model has been actively developed during last several years. However, the methods implemented for radiation transfer calculations and the corresponding databases remained unchanged. An algorithm of radiation transfer calculation is based on the two-stream approach and takes into account the extinction by atmospheric gases (H_2O , CO_2 , O_3 , O_2 , CH_4), clouds and aerosols. Radiation transfer equation is solved for several spectral intervals: 3 within solar and 5 within thermal part of spectrum (Ritter and Geleyn, 1992). Prognostic or diagnostic model variables determine optical properties of atmospheric layers. Content of water vapor and cloud liquid/ice water, as well as air temperature are prognostic variables while ozone, carbon dioxide and aerosols contents are specified according to the prescribed climatological values. As it was already mentioned two variants of aerosol climatology (Tanre et al. 1984, Tegen et al. 1997) can be chosen for simulations in the COSMO model, but recently the new MACv2 aerosol climatology has been also implemented within the framework of the international

$T^2(RC)^2$ (Testing and Tuning of Revised Cloud Radiation Coupling, 2015-2019) project.

In the Tegen climatology the optical properties of 5 aerosol types (sea salt, soil dust, organic, black carbon, sulfate aerosol) are considered. The climatology has monthly temporal resolution and $4^\circ \times 5^\circ$ horizontal spatial resolution. The MACv2 climatology takes into account for the recent developments in aerosol modelling and experimental data and is a combination of the model ensemble data and observations. It provides all necessary aerosol input parameters for the radiative computations in different spectral intervals for fine and coarse aerosol modes. It is also possible to retrieve an anthropogenic aerosol mode from this climatology. MACv2 aerosol climatology has monthly temporal resolution and provides $1^\circ \times 1^\circ$ spatial fields.

Testing the aerosol climatologies was made against long-term aerosol datasets at the MSU MO (www.momsu.ru) and Lindenberg observatory (<https://rcccm.dwd.de/EN/aboutus/locations/observatories/mol/mol.html>). The MSU MO site (thereafter, Moscow) is a part of AERONET (Aerosol Robotic NETwork) network (Holben et al. 1998) and the aerosol dataset applied in the study includes the continuous long-term measurements over 2001 – 2014 period (version 2.0, level 2.0) with additional cloud screening and NO_2 correction according to the approach described in (Chubarova et al. 2016). At the Lindenberg Observatory (thereafter, Lindenberg) the AERONET site has been in operation only since 2013. Therefore, for increasing the volume of data for the statistical analysis we also included the aerosol dataset obtained there from Precision Filter Radiometer (PFR) aerosol sun photometers measurements over the 2003-2013 period.

We used radiative measurements by Kipp&Zonen CNR-4 net radiometer at Moscow and by the BSRN (Baseline Surface Radiation Network) type of radiative instruments – at Lindenberg. We focused mainly on the measurements of global solar irradiance. However, for obtaining surface albedo we also used reflected shortwave irradiance. Water vapor retrievals were also obtained using AERONET algorithm at 940 nm channel. In addition, we used upper – air soundings (temperature, water vapor) at both sites as well as ozonezone dataset - at Lindenberg. At Moscow air temperature measurements at 2 meters were analyzed using routine observations and Vaisala automatic weather station. At Lindenberg the data from the automatic weather station were used. In order to reveal clear sky situations we used hourly visual observations at both sites. The data were chosen over the snowless period during 2014-2015 when the absence of cloudiness was recorded both in observations and COSMO model output for more than 5-hour continuous series. As a result, for Moscow we identified 11 days and for Lindenberg – 6 days with these conditions. In overall, 103 cases of one-hour global solar irradiance averages supported with different meteorological and aerosol datasets were used in the comparisons.

RESULTS AND DISCUSSION

Analysis of aerosol climatologies

Long-term measurements of different aerosol properties using AERONET at the Moscow MSU MO and AERONET/PFR data at the Lindenberg Observatory provide a testbed for comparisons of the aerosol climatologies. Fig. 1 demonstrates seasonal changes in main aerosol radiative parameters (aerosol optical thickness at 550nm (AOT), single scattering albedo (SSA), and factor of asymmetry ASY^1) obtained from the aerosol climatologies and long-term observations

¹AOT is determined as $AOT = -\cos Z_0 \ln \frac{S_\lambda}{S_{0\lambda}}$, where Z_0 -zenith angle, S_λ - spectral direct irradiance, $S_{0\lambda}$ -spectral direct irradiance at the TOA. $SSA_\lambda = \beta_{sc\lambda} / \beta_{ext\lambda}$ where $\beta_{ext\lambda}$ -extinction coefficient, $\beta_{sc\lambda}$ -scattering coefficient (1/cm). $g = \frac{1}{2} \int_{-1}^1 \cos \theta P(\theta) d(\cos \theta)$, where θ is the scattering angle, $P(\theta)$ is the aerosol phase function;

at both sites. We used median values in measurement dataset to avoid the bias due to fire smoke aerosol, which dominated in Moscow region in some months of 2002 and 2010. One can see an overestimation of MACv2 and Tegen climatologies in most months for both sites. For Moscow conditions the AOT seasonal cycle in Tegen climatology is characterized by much less seasonal variations (variation coefficient, VC=14%), while MACv2 climatology has similar seasonal changes compared with the observations which in turn have the highest variations (respectively VC=26% and VC=34%). However, in winter months the AOT even in MACv2 climatology is higher than the observed data. Presumably, it is due

to cloud contamination effect which does not fully accounted while compiling the model and standard AERONET observations in MACv2 dataset (see the discussion on the quality of standard V2 AERONET version in (Chubarova et al. 2016)). In addition, in the MACv2 climatology there is a shift of local AOT minimum from June to May.

For Lindenberg both climatologies have much smaller seasonal changes compared with observations and significantly overestimate AOT. Variation coefficients are similar for all datasets: 20%, 18% and 21% respectively. Single scattering albedo (SSA) obtained from aerosol climatologies is in a good agreement with the observations

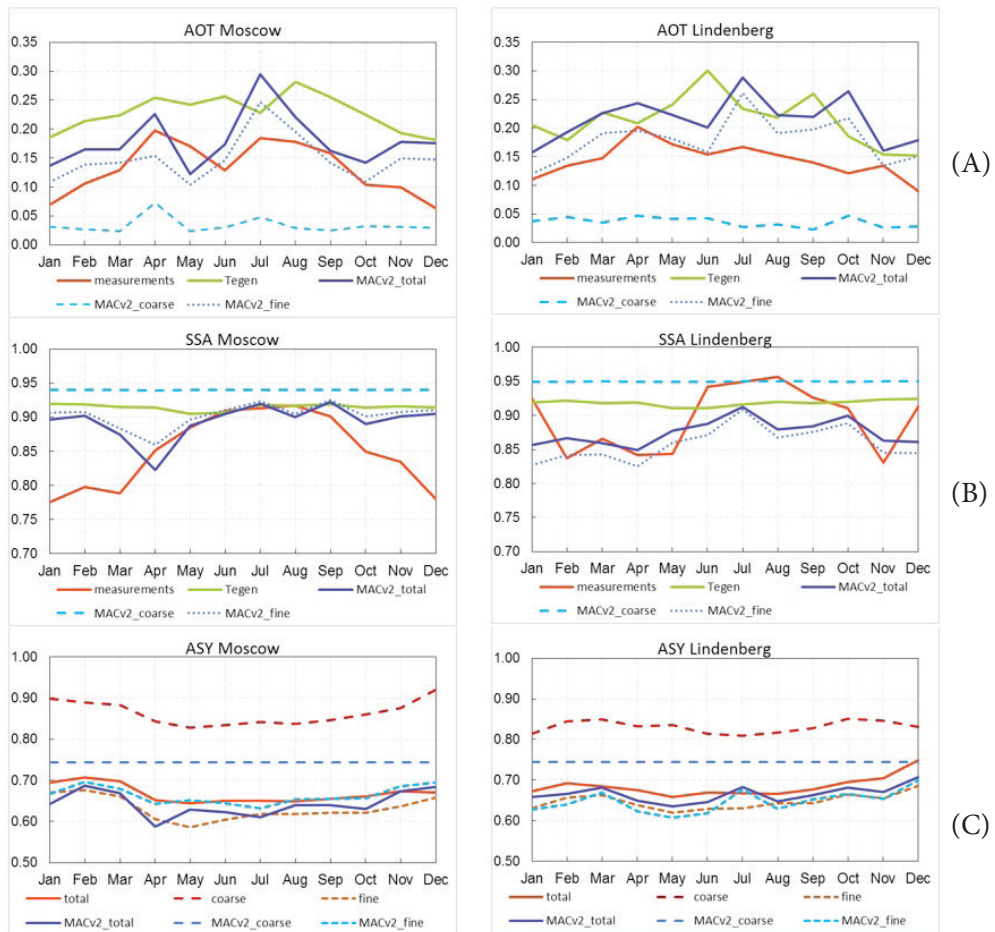


Fig. 1. Monthly variability in aerosol optical thickness at 550 nm (AOT) (a), single scattering albedo (SSA) (b) and asymmetry factor (ASY) (c) according to different aerosol climatologies for Moscow and Lindenberg

during warm period (Fig. 1b). However, in winter one can see its noticeable overestimation in both climatologies (note, that we use final calibrated SSA data at level 1.5 due to the lack of statistics at level 2, but the quality of these data has been thoroughly tested). We should note that at both sites SSA values from Tegen climatology practically do not vary throughout a year, while MACv2 SSA variations are closer to the observed values. Asymmetry factor from MACv2 also demonstrates a satisfactory agreement with the observations (Fig. 1c). However, for the coarse aerosol mode in real conditions it is much higher than that in MACv2 climatology. Since a fraction of this aerosol mode is small this inconsistency does not affect the total values of asymmetry factor, which agree well with the observations.

Using the obtained aerosol parameters from the climatologies and the observations we calculated global solar irradiance (Q) at ground and the corresponding difference ($\Delta Q = Q_{\text{climatology}} - Q_{\text{obs}}$) (Fig. 2). Radiative simulations were fulfilled using a modified CLIRAD radiative transfer code (Tarasova and Fomin, 2005) for noon conditions for the central day of a month. For Moscow (Fig. 2a) for the Tegen climatology Q values are underestimated on $11\text{--}26 \text{ W/m}^2$ while for MACv2 the difference ΔQ varies from -23 to $+4 \text{ W/m}^2$. Annual mean difference for the MACv2 climatology is closer to the observations than that for the Tegen climatology (-10.8 W/m^2 compared with -17.3 W/m^2).

For Lindenberg both climatologies provide underestimation of global solar irradiance of about 10 W/m^2 for annual means compared with the Q values simulated with the aerosol input parameters taken from observations. Both of them have lower solar irradiance for almost all months mainly due to the overestimated AOT . At the same time, for the Tegen climatology in April and November in conditions with only small AOT overestimation ($\Delta AOT = 0.01\text{--}0.02$) we observe even positive bias in solar irradiance ($1\text{--}2 \text{ W/m}^2$) due to the large difference in SSA. For these months Tegen climatology provides much higher SSA values (0.92) compared with the observations (0.85). Note, that in Tegen climatology 10–20 % of aerosol optical thickness over Europe relates to black carbon aerosol, that should significantly increase the absorption especially in visible spectrum. However, this is not enough to explain the lower SSA values observed at Moscow site, which probably occur due to smaller aerosol size.

Comparisons of global solar irradiance

The comparisons between simulated and observed global solar irradiance datasets were fulfilled for different aerosol conditions and solar zenith angles. The examples of the diurnal cycles of simulated and observed Q values for a particular day in Moscow and Lindenberg are shown in Fig. 3. One can see that for both sites the observations of global irradiance are higher than the COSMO

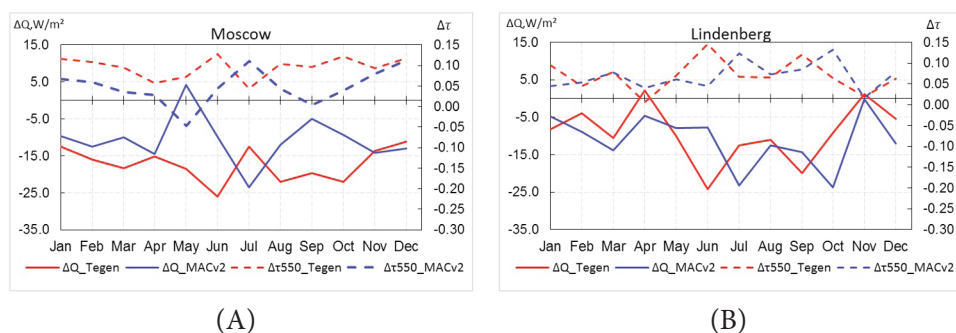


Fig. 2. The difference in monthly mean aerosol optical thickness compared with long-term aerosol measurements and absolute difference in global solar irradiance computed with different aerosol climatologies against simulations with the observed aerosol parameters for Moscow (a) and Lindenberg (b). Simulations were made for local noon

model simulations for both climatologies mainly due to overestimating in their AOT values. These results are in agreement with those obtained using the CLIRAD radiative transfer simulations with different aerosol datasets (see Fig.2). The overall differences in AOT for the selected clear sky cases and in global shortwave irradiance Q are shown in Fig.4 for both sites. The application of MACv2 climatology provides better agreement: the difference ΔAOT decreases from -0.16 to -0.12 for Moscow and from -0.23 to -0.14 for Lindenberg. These differences are statistically significant at $\alpha = 0.05$. However, the overestimation of AOT is still large. This positive bias results in the underestimation by 2-3 % in global solar irradiance simulated

by COSMO radiative algorithm for both aerosol climatologies. The differences in dQ/Q % between the climatologies are not statistically significant. We should note that the relative difference (dQ/Q) should be much higher, however, the old radiative scheme used in COSMO model is responsible for the 5 % positive bias in radiative simulations (Poliukhov et al. 2017a). The exact radiative transfer simulations would have the overall bias of about 7-8 % for the same cases.

Temperature effects

The instant temperature effects of aerosol were analyzed using different COSMO model

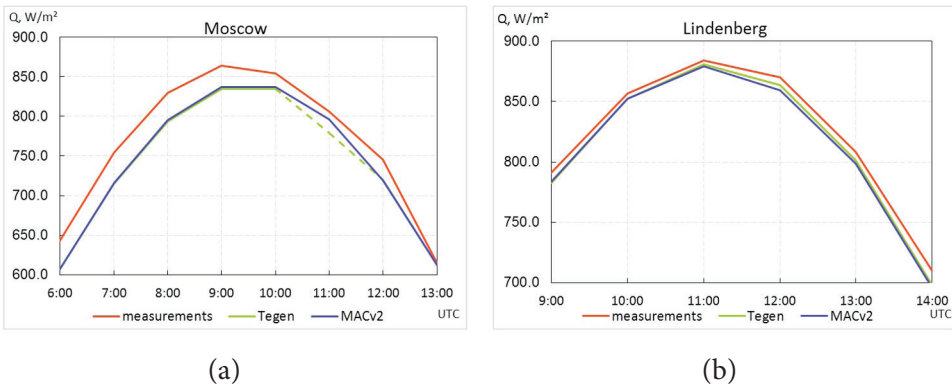


Fig. 3. The examples of diurnal cycle in the global solar irradiance (Q) from the measurement data and COSMO model with different (Tegen and MACv2) aerosol datasets in clear sky conditions in Moscow (04.07.2015) (a) and Lindenberg (02.07.2015) (b)

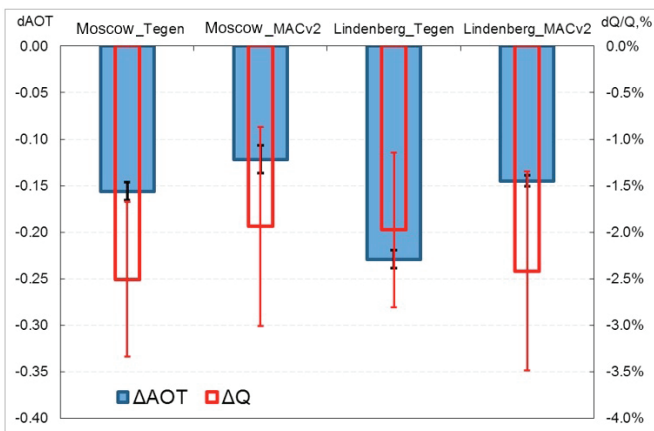


Fig. 4. The mean difference in aerosol optical thickness at 550nm ($\Delta AOT = AOT_{obs} - AOT_{model}$) and in global solar irradiance $dQ/Q = (Q_{model} - Q_{obs}) / Q_{obs}$ % according to COSMO model runs and observations at Moscow and Lindenberg. Clear sky conditions

runs with different aerosol climatologies and with zero aerosol conditions for the same clear sky days which are used in the analysis. Since aerosol over continental Europe is characterized by weak absorption in visible spectral range it should provide the negative effect on temperature at ground level. To account the changes in all the aerosol properties (AOT, SSA, factor of asymmetry) we chose net shortwave irradiance at ground as an aggregated characteristic. Net shortwave radiation is the difference in downwelling and upwelling shortwave irradiance and it also accounts for surface albedo effects, which play, however, minor role in our snowless conditions. We analyzed the dependence of difference in air temperature at 2 meters (ΔT) simulated in conditions with and without aerosols to the corresponding difference in net radiation (ΔB) to estimate the temperature sensitivity to aerosol. The results are shown in Fig. 5a. The negative values in net radiation at ground level due to aerosol provide negative effects on temperature difference. The difference in temperature should reach zero when $\Delta B=0$ in conditions with zero AOT.

For Moscow and Lindenberg we obtained a pronounced statistically significant dependence which provides similar aerosol temperature effects. For Moscow this effect is about $0.8 \pm 0.2^\circ\text{C}$ per 100 W/m^2 , which is in agreement with our previous estimates (Poliukhov et al. 2017b), and for Lindenberg

this value is about $1.0 \pm 0.3^\circ\text{C}$ per 100 W/m^2 with correlation coefficients $r=0.5-0.6$. The observed deviations may occur due to some slight variations in other parameters (water vapor, differences in profiles, etc.) in COSMO model runs.

Another testing was made using similar approach but in comparisons with observations. In this case we should have much more deviations due to the influence of the uncertainty in actual atmospheric parameters which may differ from the simulated ones. Fig. 5b demonstrates the difference between the observed and simulated temperature at 2 meters (ΔTr) as a function of the difference between observed and simulated net radiation (ΔBr). We obtained the same tendency with the increase of positive temperature shift with positive bias in net radiation, which is mainly a function of aerosol loading. The gradients are similar to those obtained in the previous pure model experiment (see Fig. 5a). These results confirm the pronounced temperature sensitivity to aerosol loading via its influence on net radiation at ground.

For estimating typical aerosol temperature effects for Moscow and Lindenberg, the changes in net radiation due to the changes in corresponding aerosol properties against aerosol-free conditions should be used. These temperature effects comprise about $-0.2 - -0.3^\circ\text{C}$ for typical aerosol over these sites.

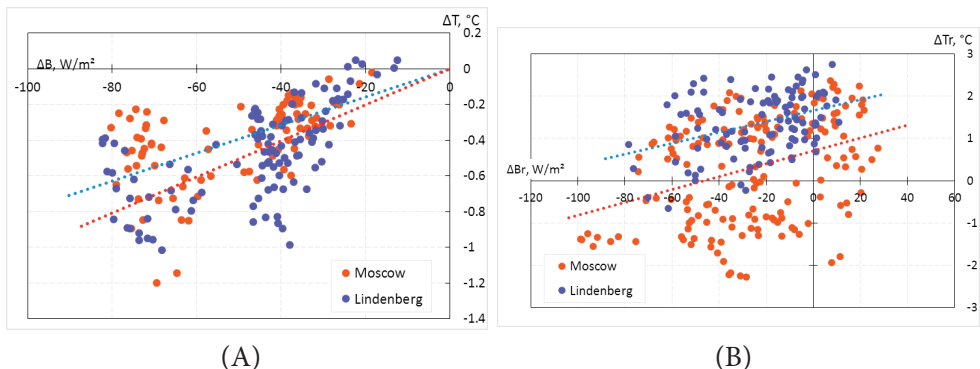


Fig. 5. The sensitivity of temperature at 2 meters to the shortwave net radiation changes. a) Temperature variations versus the changes in shortwave net radiation simulated by COSMO model with and without aerosol; b) Difference between the observed and simulated temperature as a function of the difference between the observed and simulated shortwave net radiation

CONCLUSIONS

The application of the new MACv2 climatology in COSMO model in comparison with the Tegen climatology allowed us to evaluate the uncertainties in radiative fluxes and temperature at 2 meters for the cloudless atmosphere over the continental area in Central and Eastern Europe.

The comparisons with long-term aerosol measurements revealed some deficiency in MACv2 climatology in winter months and the bias in May-June local AOT maxima. The Tegen climatology was characterized by much higher values than the observations and does not reproduce the existing seasonal cycle in different characteristics.

The results obtained for two sites (Moscow, Russia and Lindenberg, Germany) have revealed the same tendency of the AOT overestimation in both aerosol climatologies (with smaller difference for the new MACv2 climatology) and in the corresponding differences of global solar irradiance between the model simulations and observations.

Using both model and measurement datasets we showed that MACv2 climatology provides better agreement with observations in Moscow. However, still the difference with observations

was not small that resulted in systematical negative bias of about 2-3 % in global solar irradiance at ground estimated in the model.

The analysis of aerosol temperature effects in the model has revealed the sensitivity of temperature at 2 meters to the changes in net radiation at ground due to aerosol of about 0.8-1°C per 100 W/m². The existence of this dependence was confirmed by the comparisons between the simulated data and observations.

Hence, we can state that continental type of aerosol causes a pronounced temperature effect, and therefore the application of accurate aerosol may improve the temperature forecast in COSMO model. This could be possible via application and further development of COSMO-ART (Aerosols and Reactive Trace Gases) or CAMS (Copernicus Atmosphere Monitoring Service) aerosol forecast schemes.

ACKNOWLEDGMENTS

This study is being fulfilled within the framework of the COSMO Priority Project - T²(RC)² - Testing & Tuning of Revised Cloud Radiation Coupling. This research was supported by the RSF grant # 18-17-00149.

REFERENCES

Boucher O., Randall D., Artaxo P., Bretherton C., Feingold G., Forster P., Kerminen V.-M., Kondo Y., Liao H., Lohmann U., Rasch P., Satheesh S.K., Sherwood S., Stevens B., and Zhang X.Y. (2013). Clouds and Aerosols. In: T.F. Stocker, ed., *Climate Change 2013: The Physical Science Basis*. Contribution of Working Group I to the Fifth Assessment Report of the Intergovernmental Panel on Climate Change 1st ed. New York, Cambridge University Press, pp 571-659.

Chubarova N. Y., Poliukhov A. A., and Gorlova I. D. (2016). Long-term variability of aerosol optical thickness in Eastern Europe over 2001–2014 according to the measurements at the Moscow MSU MO AERONET site with additional cloud and NO₂ correction. *Atmospheric Measurement Techniques*, 9(2), pp. 313-334.

Doms G. and Baldauf M. (2011a). A Description of the Nonhydrostatic Regional COSMO model. Part I: Dynamics and Numerics. Consortium for Small-Scale Modelling, Deutscher Wetterdienst (DWD).

Doms G., Foerstner J., Heise E., Herzog H.-J., Mironov D., Raschendorfer M., Reinhardt T., Ritter B., Schrodin R., Schulz J.-P., and Vogel G. (2011b). A Description of the Nonhydrostatic Regional

COSMO-Model. Part II: Physical Parameterization. Consortium for Small-Scale Modelling, Deutscher Wetterdienst (DWD).

Holben B.N., Eck T.F., Slutsker I., Tanre D., Buis J.P., Setzer A., Vermote E., Reagan J.A., Kaufman Y., Nakajima T., Lavenu F., Jankowiak I., and Smirnov A. (1998). AERONET—A federated instrument network and data archive for aerosol characterization. *Remote sensing of environment*, 66(1), pp 1-16.

Polukhov A.A., Chubarova N.Y., Rivin G.S., Shatunova M.V. and Tarasova T.A. (2017a). Assessment of the clear sky radiation simulated using COSMO model based on precise calculation and observation in Moscow. *Proceedings of Hydrometcentre of Russia*. 364. pp.38-52.

Poliukhov A., Chubarova N., Kinne S., Rivin G., Shatunova M., and Tarasova T. (2017b). Comparison between calculations of shortwave radiation with different aerosol datasets and measured data at the MSU MO (Russia). *AIP Conference Proceeding*. 1810(1), p. 100006.

Tanré D., Geleyn J. F., and Slingo J. M. (1984). First results of the introduction of an advanced aerosol-radiation interaction in the ECMWF low resolution global model. *Aerosols and their climatic effects*, pp 133-177.

Tarasova T. A. and Fomin B. A. (2007). The use of new parameterizations for gaseous absorption in the CLIRAD-SW solar radiation code for models. *Journal of Atmospheric and Oceanic Technology*, 24(6), pp. 1157-1162.

Tegen I., Hollrig P., Chin M., Fung I., Jacob D., and Penner J. (1997). Contribution of different aerosol species to the global aerosol extinction optical thickness: Estimates from model results. *Journal of Geophysical Research: Atmospheres*, 102(D20), pp 23895-23915.

Received on November 1st, 2017

Accepted on March 1st, 2018



Natalia Chubarova is a professor at the Department of Meteorology and Climatology, Faculty of Geography of Moscow State University. Her scientific interests lie in the field of atmospheric physics and concern the studies of radiative processes in the atmosphere. A particular attention in her work is paid to the analysis of biologically active UV radiation and atmospheric aerosols. She has published about 100 papers in per-reviewed journals and 15 monographs.



Aleksei Poliukhov is a PD student at the Faculty of Geography of Moscow State University. He has obtained the Master's degree in 2017. His main research directions include atmospheric aerosols and radiation transfer in atmospheric models.



Marina Shatunova is a Leading Researcher at Laboratory of limited area NWP of Hydrometeorological Research Center of Russia. Her tasks include the development and maintenance COSMO-Ru system for numerical weather prediction and concern atmospheric physics modelling.



Gdaliy Rivin is a professor at the Department of Meteorology and Climatology, Faculty of Geography of Moscow State University and Head of Numerical Weather Forecasts Laboratory, Hydrometcenter of Russia. His scientific interests lie in the field of numerical weather prediction. He has published about 100 papers in per-reviewed journals and 4 monographs.



Ralf Becker is a scientist at the Meteorological Observatory Lindenberg of German Weather Service. He is responsible for sunphotometric aerosol measurements at the GAW associate stations Lindenberg, Zingst and Zugspitze (Germany). His work is on sunphotometer instrument intercomparison and experimental broadband irradiation profiling.



Stefan Kinne is a scientist at the Max-Planck Institute for Meteorology in Hamburg Germany. He specializes in atmospheric radiative transfer, both theoretical work and applications for climate. In recent years he got increasingly involved with tropospheric aerosol and in that context with also with evaluations of complex models (by co-organizing AeroCom activities), assessment work on remote sensing (as global data on aerosol but also clouds and radiation), and oceanic reference data (by supplying staff and instruments on German Research vessels).

Natalia Pankratova^{1*}, Andrey Skorokhod¹, Igor Belikov¹, Nikolai Elansky¹, Vadim Rakitin¹, Yury Shtabkin¹, Elena Berezina¹

¹A.M. Obukhov Institute of Atmospheric Physics of Russian Academy of Sciences, Moscow, Russia

* **Corresponding author:** pankratova@ifaran.ru

EVIDENCE OF ATMOSPHERIC RESPONSE TO METHANE EMISSIONS FROM THE EAST SIBERIAN ARCTIC SHELF

ABSTRACT. Average atmospheric methane concentration (CH_4) in the Arctic is generally higher than in other regions of the globe. Due to the lack of observations in the Arctic there is a deficiency of robust information about sources of the methane emissions. Measured concentrations of methane and its isotopic composition in ambient air can be used to discriminate sources of CH_4 . Here we present the results of measurements of the atmospheric methane concentration and its isotope composition ($\delta^{13}\text{C}_{\text{CH}_4}$) in the East Siberian Arctic Seas during the cruise in the autumn 2016. Local sections where the concentration of methane in the near-water layer of the atmosphere reaches 3.6 ppm are identified. The measurements indicated possibility of formation of high methane peaks in atmospheric surface air above the East Siberian Arctic Shelf (ESAS) where methane release from the bottom sediments has been assumed.

KEYWORDS: atmospheric methane, methane emissions, Arctic, sub-sea permafrost, warming, shipborne measurements, atmospheric surface layer, East Siberian Arctic Shelf

CITATION: Natalia Pankratova, Andrey Skorokhod, Igor Belikov, Nikolai Elansky, Vadim Rakitin, Yury Shtabkin, Elena Berezina (2018) Evidence Of Atmospheric Response To Methane Emissions From The East Siberian Arctic Shelf. *Geography, Environment, Sustainability*, Vol.11, No 1, p. 85-92
DOI-10.24057/2071-9388-2018-11-1-85-92

INTRODUCTION

Methane (CH_4) is a second greenhouse gas after carbon dioxide which atmospheric concentration has increased by 150% since pre-industrial times (IPCC, 2013). However, the CH_4 global warming potential is approximately 28 times higher than that of CO_2 over a 100-year frame (Myhre et al. 2013). It accounts for 20% of the global radiative forcing of well-mixed greenhouse gases (Quay et al. 1999; Dlugokencky et al. 2014).

As is thought, methane contributes greatly to warming in the Arctic region, which is characterized by abundant methane sources such as, for example, wetlands of the northern Eurasia, shelf areas of the Arctic seas (Shakhova et al. 2014), gas combustion (Stohl et al. 2005), and anthropogenic emissions. It is assumed that the influence of methane sources on the climate of the region should progressively increase with temperature growth in the Arctic (Shakhova et al. 2015).

Sub-sea permafrost and hydrates in the shelf regions of the seas of the Eastern Arctic are significant methane pool and potentially can be large source of atmospheric methane emissions (Berchet et al. 2015). A significant number of localized seeps of methane in offshore regions of the East Arctic seas have been found (Shakhova et al. 2015; Thornton et al. 2016), but the quantity and quality of the available experimental data is currently insufficient to obtain stable estimates of CH_4 emissions into the air above-sea layer, which are still very contradictory (Berchet et al. 2015; Shakhova et al. 2014). The evidence of methane release from the ESAS bottom layers have been previously reported (Thornton et al. 2016; Shakhova et al. 2010), while the ability of benthic methane to penetrate into the atmosphere had not yet been proven. Satellite measurements of the surface methane concentration cover the whole Earth but do not have sufficient accuracy. Very little data are available for the isotope $\delta^{13}\text{C}_{\text{CH}_4}$ in methane, which provides information on sources of methane in the atmosphere (Warwick et al. 2016; Fisher et al. 2011). Thus, it is very important to expand the experimental studies of methane concentrations in the Arctic to check whether methane released from

the seawater into the atmosphere. Present work is continuing the Arctic methane study started during previous observation campaign of 2015 described in (Skorokhod et al. 2016).

MATERIALS AND METHODS

Atmospheric CH_4 mixing ratio and changes in the $^{13}\text{C}:^{12}\text{C}$ ratio in CH_4 (reported a changes relative to a reference ratio and denoted as $\delta^{13}\text{C}_{\text{CH}_4}$) were measured from aboard the research vessel (RV) Akademik M.A. Lavrentiev from 23 September to 3 November 2016 in the Laptev, East Siberian and Chukchi Seas and as well as the North Pacific and the Sea of Japan (see Fig. 1). The measurements were performed using a Cavity-Ring-Down Spectrometer (CRDS) from Picarro™ (model G2132-i). Together with methane concentrations of other trace gases (CO_2 , NO , NO_2 , O_3) were measured.

CRDS (G2132i) allows to measure the methane concentration in the range from 1800 to 12000 ppb with an error of less than 5 ppb, and the value of $\delta^{13}\text{C}_{\text{CH}_4}$ with an error of less than 1 ‰. The camera experiments showed that the intrinsic noise of the device did not exceed the indicated error values.

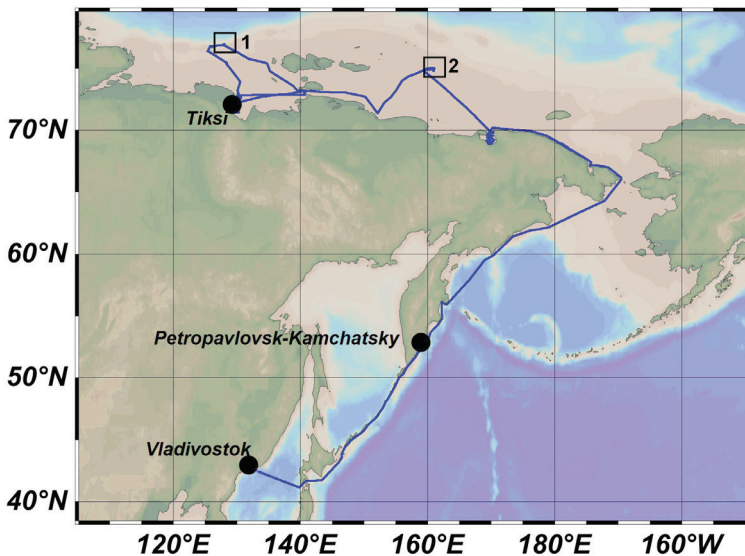


Fig. 1. The route of R/V Akademik M.A. Lavrentiev, Tiksi - Vladivostok, 24.09-03.11.2016. The areas with the high methane concentration are in the frames. 1 - corresponds to the Laptev sea polygon with CH_4 maximum (2.133 ppm); 2 - CH_4 maximum in the East Siberian sea (3.537 ppm)

Calibrations of the CRDS (G2132i) were carried out according to the secondary standard, which was a 1-liter compressed air cylinder provided by the Norwegian Institute for Air Research (NILU) with known values of methane and $\delta^{13}\text{C}_{\text{CH}_4}$ concentrations. The relative error of this measurement did not exceed 0.03% for methane and 0.1% for $\delta^{13}\text{C}_{\text{CH}_4}$. The secondary standard was calibrated by primary standard known as NOAA04 (Dlugokencky et al. 2005) for CH_4 , while calibration for $\delta^{13}\text{C}_{\text{CH}_4}$ was made by method described in (Fisher et al. 2006).

Calibrations of the G2132i were carried out with a period of 1-2 months, immediately before and after the ship campaign. The scheme of the experimental setup and the calibration results are shown in Fig. 2. All obtained values differ within error of the CRDS, indicated in its technical specification (5 ppb). A special study of the short-period drift of the instrument readings showed that the root-mean-square deviation of the instrument readings did not exceed 0.05% within a time period of 10-20 minutes. All the observational data were recalculated in accordance with the obtained calibration coefficients, and a series of data were averaged over the intervals of 1 min and 10 min.

During the ship campaign, the air was sampled from the inlet at the front of the deck at height of 11 meters above sea level. The length of the pipeline was 30 m, and the inner diameter was 10 mm with air flow rate of 3 litres min^{-1} . Such arrangement of the air intake allows minimizing the perturbations of the airflow by the vessel during air sampling (Edson et al. 1998). The diesel fuel used by ship engine does not contain methane, though it contains hydrocarbons, such as, for example, cetane and alpha-methylnaphthalene-an aromatic hydrocarbon. If smoke from ship chimney occurs into the G2132-i air intake, hydrocarbons may distort the methane concentration value. Thus, to exclude the influence of the ship itself, data on the CO_2 concentration were analyzed. CH_4 data, which were corresponding to a high concentration of CO_2 , were excluded from analyses.

The measurements were carried out in the autumn period, when advection of cold air occurred on the coast of the Arctic seas, and a snow cover began to form. During the cruise the temperature was lower than 0°C coastal zone was under the snow cover. Under these conditions, the mainland natural sources of methane were not active.

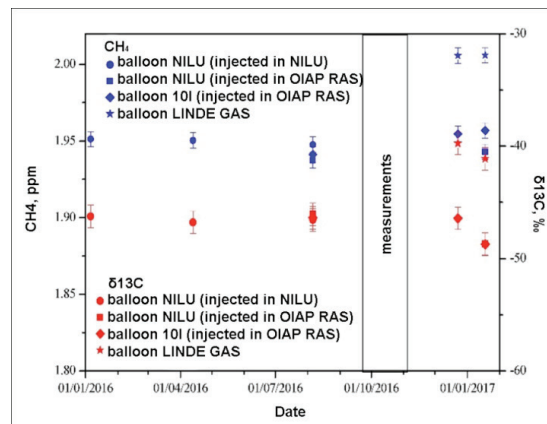
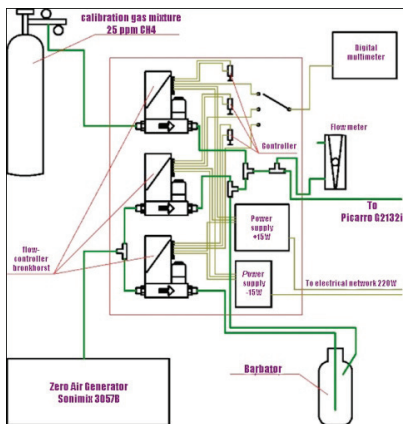


Fig. 2. a - Schematic diagram of the experimental setup for calibration of the CRDS (G2132i) with different humidity of the analyzed air, b - Calibration results for the CRDS (G2132i) before and after the campaign

It was confirmed by the wind direction analysis. The frequency of wind direction were calculated for four sectors (316-45, 46-135, 136-225, 226-315 degrees) for the Laptev, the East-Siberian and the Chukchi seas and the mean CH_4 concentration for each sector was obtained. There is no significant dependence of the methane concentration on the direction of the wind in the seas of the Eastern Arctic - difference between the mean methane concentrations calculated for the each sector is less than 1 %.

RESULTS AND DISCUSSION

Table 1 gives the statistical characteristics of the results of observations for the Laptev and East Siberian seas, calculated with averaging of 1 minute. As follows from these data, in general, the methane content in the near-surface air of the seas of the Eastern Arctic and in the northern Pacific regions is very uniform in October (the standard deviation of the series is about 0.02 ppm) and stably exceeds the average global value characteristic for this period.

At the same time, in the Laptev and the East-Siberian seas, localized areas with a high concentrations of methane in the above-sea air have been identified (Fig. 3). Of greatest interest are the so-called methane-emission polygons described in (Shakhova et al. 2014). One of these polygons was located approximately at the coordinates of 75° N and 160° E (Fig. 4). The vessel was there from October 11 to October 13, 2016. Figure 3 shows the graph of the dependence of the methane concentrations on time according to the measurements by the G2132i instrument with averaging of 10 seconds. As can be seen from the graph, the

concentration of methane above the water surface is characterized by a large number of peaks by the value of 2.0-2.2 ppm and more. From the board of the vessel raising of methane bubbles from the water was visually detected. According to sonar data from the vessel, methane bubbles came directly from the bottom, as the depth in the observation area reached 45-50 meters.

Information on $\delta^{13}\text{C}_{\text{CH}_4}$ is important for identifying sources of atmospheric methane in the Arctic (Quay et al. 1999; Fisher et al. 2011). The average value of $\delta^{13}\text{C}_{\text{CH}_4}$ for well-mixed atmospheric air is about -47.1 ‰, but it strongly depends on the season and latitude (Rigby et al. 2012). Our results show the average $\delta^{13}\text{C}_{\text{CH}_4}$ value -49.86 ‰ for Laptev and East Siberian seas.

Arctic wetlands are characterized by values of $\delta^{13}\text{C}_{\text{CH}_4}$ within -69 ÷ -60 ‰ (Fisher et al. 2011), methane emissions from fossil fuel vary from -50 ‰ to 26 ‰. Biomass burning gives $\delta^{13}\text{C}_{\text{CH}_4}$ in the range of -18 ÷ -30 ‰ (Rigby et al. 2012). The $\delta^{13}\text{C}$ composition of methane for methane hydrate emission has a magnitude $-50 \pm 3\%$ (Dlugokencky et al. 2011). The average $\delta^{13}\text{C}_{\text{CH}_4}$ over the seep polygon was -51.16 ‰ that corresponds to this magnitude. Herewith the standard Keeling plot analysis (Fisher et al. 2011; Pataki et al. 2003) shows the inconclusive result, that prevents clear determination of CH_4 source.

The presence of methane concentration peaks generated by the release of methane bubbles to the surface causes a slight increase in CH_4 average concentration in the surface air above the seeps.

Table 1. Statistical characteristics of 1-min data sets of the methane concentrations and $\delta^{13}\text{C}_{\text{CH}_4}$ measured over the Laptev and the East-Siberian Seas in autumn of 2016

Parameter	Laptev Sea		East-Siberian Sea	
	$\delta^{13}\text{C}_{\text{CH}_4}$ ‰	CH_4 ppm	$\delta^{13}\text{C}_{\text{CH}_4}$ ‰	CH_4 ppm
Minimum	-57.12	1.938	-54.86	1.935
Maximum	-44.10	2.133	-46.96	3.537
Mean	-49.59	1.962	-50.12	1.958
Standard deviation	1.46	0.015	1.2	0.024

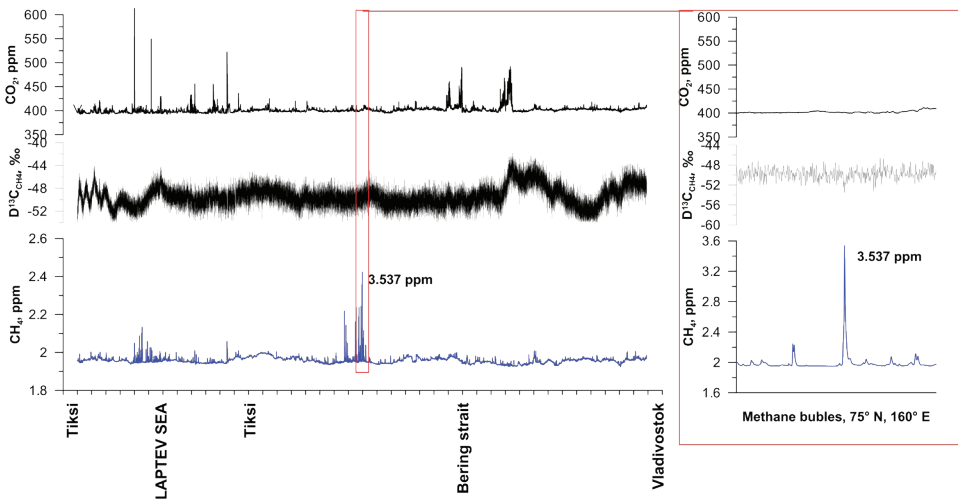


Fig. 3. Observed CH₄ and CO₂ concentration and δ¹³C_{CH₄} during the ship campaign of R/V 'Akademik M.A. Lavrentiev' (24 Sept– 02 Nov 2016). Scaling up CH₄ peak for methane emission polygon (of 75° N and 160° E) is shown in the frame on the right

Thus, the average daily methane concentration level on the seep polygon (October 12) is by few percent higher than the average daily methane concentration outside of this polygon (October 10 and 14). It is comparable with regional variations in the average daily concentration (for example, on October 9, when the vessel was near of Kolyma delta). However, the AIRS data Level 2 show the area with the excess total CH₄ content which can be connected with releasing of the methane from the sea water to the surface air (see Fig. 4). One can notice relatively slight decrease of δ¹³C_{CH₄} opposite the highest methane peaks (see

Fig. 3). This can be explained by similar isotopic signatures of ambient air and air from hydrates (Fisher et al. 2011) that makes application of isotopic analyses methods (like Keeling plot) for seeping regions not clear (Skorokhod et al. 2016).

CONCLUSIONS

Our measurements of CH₄ in the atmosphere across ESAS during September and October 2016 in general show stable CH₄ and δ¹³C_{CH₄} concentrations in the surface air. However, the possibility of CH₄ high peak (up to 3.54 ppm according to our measurements)

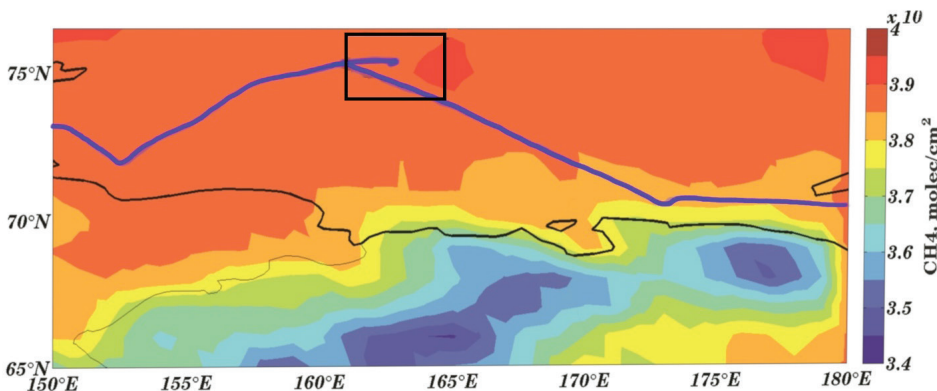


Fig. 4. Average CH₄ Total column over the East Siberian Sea for October 2016 and the route of R/V 'Akademik M.A. Lavrentiev' with marked polygon of seep measurements (black square). AIRS level 3 v6 ascending data with the spatial resolution 1°x1° were used. Data available on <https://airs.jpl.nasa.gov/>

formation in the atmospheric air above the ESAS in the areas of methane seeps was indicated. These enhancements cannot be associated with air pollution (including influence ship emissions) and terrestrial methane sources, which were likely to be inactive during the ship campaign. Therefore, the performed measurements were likely to be the first direct evidence of atmospheric response of benthic methane escape into the atmosphere in the Arctic.

On base of these data, it is difficult to assess real amount of methane released from the Arctic seas into the atmosphere. Meteorological conditions were not favorable to methane accumulation within the boundary layer. On the contrary, strong winds and unstable stratification led to fast dissipation of released methane. One can assume nevertheless that those methane emissions are significant enough to make quite stable footprint on maps built from satellite data. Thus, satellite data of AIRS (Atmospheric Infrared Sounder) steadily show an increased total methane content

in the vertical column of the atmosphere in the area corresponding to the seep area. For instance, in October, 2016 CH₄ total column exceeded 3.90×10^{19} mol/cm² inside the polygon comparing to 3.85×10^{19} mol/cm² out of it (see Fig. 4).

The local peaks of atmospheric methane in this region is a strong indication in favor of the hypothesis that the ESAS shelf is a potential significant source of atmospheric methane. But further studies are needed to clarify the quantitative characteristics of this source nowadays and in the future.

ACKNOWLEDGEMENTS

We are grateful to the crew of the V/R «Academik M.A. Lavrentiev» and to the staff of the Il'ichev Pacific Oceanological Institute RAS, and personally to Prof. Igor Semiletov for organizing the expedition and comprehensive support for the measurement. The work was supported by the Russian Science Foundation (grant № 14-47-00049). ■

REFERENCES

- Berchet A., Bousquet P., Pison I., Locatelli R., Chevallier F., Paris J.-D., Dlugokencky E. J., Laurila T., Hatakka J., Viisanen Y., Worthy D. E. J., Nisbet E., Fische, R., France J., Lowry D., Ivakhov V., and Hermansen O. (2016). Atmospheric constraints on the methane emissions from the East Siberian Shelf, *Atmos. Chem. Phys.*, 16, 4147-4157, doi:10.5194/acp-16-4147-2016.
- Dlugokencky E.J., R.C. Myers P.M. Lang, K.A. Masarie, A.M. Crotwell, K.W. Thoning, B.D. Hall, J.W. Elkins, and L.P. Steele (2005), Conversion of NOAA CMDL atmospheric dry air methane mole fractions to a gravimetrically-prepared standard scale, *J. Geophys. Res.*, 110, D18306, doi : 10.1029/2005JD006035.
- Dlugokencky E. J., Nisbet E. G., Fisher R. E., and Lowry D. (2011), Global atmospheric methane: Budget, changes, and dangers, *Philos. Trans. R. Soc. London, Ser. A.*, 369, pp. 2058–2072.
- Edson J. B., Hinton A. A., Prada K. E., Hare J. E., and Fairall C. W. (1998). Direct covariance flux estimates from mobile platforms at sea, *J. Atmos. Oceanic Technol.*, 15, 547–562, doi:10.1175/1520-0426
- Fisher R., Lowry D., Wilkin O., Sriskantharajah S., Nisbet E.G. (2006). High-precision, automated stable isotope analysis of atmospheric methane and carbon dioxide using continuous-flow isotope-ratio mass spectrometry, *Rapid Communications in Mass Spectrometry V.* 20, pp. 200-208.
- Fisher R. E., Sriskantharajah S., Lowry D., Lanoisellé M., Fowler C. M. R., James R. H., Hermansen O., Lund Myhre C., Stohl A., Greinert J., Nisbet-Jones P. B. R., Mienert J., and Nisbet E. G. (2011).

Arctic methane sources: Isotopic evidence for atmospheric inputs, *Geophys. Res. Lett.*, 38, L21803, doi:10.1029/2011GL049319.

Myhre G., Shindell D., Bréon F.-M., Collins W., Fuglestedt J., Huang J., Koch D., Lamarque J.-F., Lee D., Mendoza B., Nakajima T., Robock A., Stephens G., Takemura T., and Zhang H. (2013). Anthropogenic and natural radiative forcing, in: *Climate Change 2013: the Physical Science Basis. Contribution of Working Group I to the Fifth Assessment Report of the Intergovernmental Panel on Climate Change*, edited by: Stocker, T. F., Qin, D., Plattner, G.-K., Tignor, M., Allen, S. K., Boschung, J., Nauels, A., Xia, Y., Bex, V., and Midgley, P. M., Cambridge University Press, Cambridge, UK, New York, NY, USA, pp. 659–740.

Pataki D. E., Ehleringer J. R., Flanagan L. B., Yakir D., Bowling D. R., Still C. J., Buchmann N., Kaplan J. O., and Berry J. A. (2003). The application and interpretation of Keeling plots in terrestrial carbon cycle research, *Global Biogeochem. Cycles*, 17, 1022, doi:10.1029/2001GB001850, 1.

Quay P., Stutsman J., Wilbur D., Snover A., Dlugokencky E. J., and Brown T. (1999). The isotopic composition of atmospheric CH₄. *Glob. Biogeochem. Cy.*, 13, pp. 445–461.

Rigby M., Manning A. J., and Prinn R. G. (2012). The value of high-frequency, high-precision methane isotopologue measurements for source and sink estimation, *J. Geophys. Res: Atmos.*, 117(D12), doi:10.1029/2011JD017384.

Shakhova N., Semiletov I., Sergienko V., Lobkovsky L., Yusupov V., Salyuk A., Salomatin A., Chernykh D., Kosmach D., Panteleev G., Nicolovsky D., Samarkin V., Joye S., Charkin A., Dudarev O., Meluzov A., Gustafsson O. (2015). The East Siberian Arctic Shelf: towards further assessment of permafrost-related methane fluxes and role of sea ice. *Phil. Trans. R. Soc. A* 373: 20140451. <http://dx.doi.org/10.1098/rsta.2014.0451>.

Shakhova N., Semiletov I., Leifer I., Sergienko V., Salyuk A., Kosmach D., Chernykh D., Stubbs C., Nicolovsky D., Tumskoy V., Gustafsson O. (2014). Ebullition and storm-induced methane release from the East Siberian Arctic Shelf. *Nature Geoscience*, Vol. 7, pp. 64–70.

Shakhova N., Semiletov I., Leifer I., Salyuk A., Rekan P., and Kosmach D. (2010). Geochemical and geophysical evidence of methane release over the East Siberian Arctic Shelf, *J. Geophys. Res.*, 115, C08007, doi:10.1029/2009JC005602.

Skorokhod A.I., Pankratova N.V., Belikov I.B., Thompson R. L., Novigatsky A. N., Golitsyn G. S. (2016). Observations of atmospheric methane and its stable isotope ratio ($\delta^{13}\text{C}$) over the Russian Arctic seas from ship cruises in the summer and autumn of 2015, *Dokl. Earth Sc.* 470: 1081. doi:10.1134/S1028334X16100160.

Thornton B. F., Geibel M. C., Crill P. M., Humborg C., and Mörth C.-M. (2016). Methane fluxes from the sea to the atmosphere across the Siberian shelf seas, *Geophys. Res. Lett.*, 43, DOI: 10.1002/2016GL068977.

Warwick N. J., Cain M. L., Fisher R., France J. L., Lowry D., Michel S. E., Nisbet E. G., Vaughn B. H., White J. W. C., and Pyle J. A. (2016). Using $\delta^{13}\text{C}\text{-CH}_4$ and $\delta\text{D}\text{-CH}_4$ to constrain Arctic methane emissions. *Atmos. Chem. Phys. Discuss.*, doi:10.5194/acp-2016-408.



Natalia V. Pankratova currently works as Scientific Researcher in the Laboratory of Atmospheric Gaseous Species at the A.M. Obukhov Institute of Atmospheric Physics RAS. The focus area of her interest is atmospheric chemistry, atmospheric compositions, and methane cycle. In 2002 she graduated from Department of Meteorology and climatology of Geographical Faculty of Lomonosov Moscow State University. She received her PhD in 2014. In 2015 and 2016 took part in two ship cruises providing shipborne measurements of greenhouse and reactive gases in the lower atmosphere over the Arctic, Northern Atlantic and Northern Pacific.

Stanislav Myslenkov^{1,2,3*}, Alisa Medvedeva², Victor Arkhipkin¹, Margarita Markina^{1,2}, Galina Surkova¹, Aleksey Krylov¹, Sergey Dobrolyubov¹, Sergey Zilitinkevich^{1,4}, Peter Koltermann¹

¹ Lomonosov Moscow State University, Moscow, Russia

² P.P. Shirshov Institute of Oceanology, Russian Academy of Sciences, Moscow, Russia

³ Hydrometeorological Research Centre of the Russian Federation, Marine forecast division

⁴ Finnish Meteorological Institute, Helsinki, Finland

* **Corresponding author:** stasocean@gmail.com

LONG-TERM STATISTICS OF STORMS IN THE BALTIC, BARENTS AND WHITE SEAS AND THEIR FUTURE CLIMATE PROJECTIONS

ABSTRACT. The numerical model simulations of storm activity in the White, Baltic and Barents Seas were analyzed for the period from 1979 to 2015. In this paper the storm number of these seas was calculated. The connections of wind wave climate with indices of large-scale atmospheric circulation such as NAO, AO and SCAND were estimated. Also, the future changes of wind wave climate were analysed.

KEY WORDS: wind waves, storm, climate change, SWAN, reanalysis, Baltic Sea, Barents Sea, White Sea, significant wave height, trend, storminess, model, future change, NAO, AO, SCAND, large-scale atmospheric circulation

CITATION: Stanislav Myslenkov, Alisa Medvedeva, Victor Arkhipkin, Margarita Markina, Galina Surkova, Aleksey Krylov, Sergey Dobrolyubov, Sergey Zilitinkevich, Peter Koltermann (2018) Long-term Statistics of Storms in the Baltic, Barents and White Seas and Their Future Climate Projections. *Geography, Environment, Sustainability*, Vol.11, No 1, p. 93-112

DOI-10.24057/2071-9388-2018-11-1-93-112

INTRODUCTION

Wind waves are an important component of climate system and study of their interannual variability helps to understand current climate changes and to assess wave impact in the future. The study of the storminess in the Baltic, Barents and White

Seas have great importance for shipping, constructing on coasts and shelf, oil and gas field development. In this paper, a new approach estimating climate changes has been implemented. We counted a number of storms using significant wave height threshold in three neighbor seas and estimated the connection of storminess

with indices of large-scale atmospheric circulation.

The wave conditions in the Baltic Sea were investigated in several studies (Kriezi and Broman, 2008; Lopatukhin et al. 2006; Medvedeva et al. 2015; Sommere, 2008; Zaitseva-Pärnaste, 2009). Different wave models and wind forcing have been used in these papers. The results of wave simulations have been estimated by comparing with buoy measurements and wave sensors (Kriezi and Broman, 2008; Medvedeva et al. 2016). There are many interesting papers about wave hindcast and climate in the Barents and White Seas (Arkhipkin et al. 2015; Korablina et al. 2016; Lopatukhin et al. 2003; Myslenkov et al. 2016; Reistad et al. 2011). Stopa et al. (2016) presented wave climate and hindcast based on altimeter data set and investigation of wave trend in the Arctic region from 1992 to 2014. The decrease of the sea ice extent in the Arctic Ocean over the last years is described in Mokhov (2013). The altimeter data and model results show that the reduction of the sea ice coverage causes a growth of wave heights instead of the increasing wind speeds. However, regional trends are influenced by large-scale interannual climate oscillations like the North Atlantic Oscillation (NAO) and Pacific Decadal Oscillation (Stopa et al. 2016).

The wind and wave climate in the Arctic region based on altimeter measurements were presented by Liu et al. (2016). Trend analysis shows a clear spatial (regional) and temporal (interannual) variability in wave height and wind speed. Wave heights in the Chukchi, Beaufort (near northern Alaska) and Laptev Seas increase at 0.1–0.3 m per decade. These trends have been found statistically significant at the 90% level. The trends of wave heights in the Greenland and Barents Seas, on the contrary, are weak and not statistically significant. In the Barents and Kara Seas, winds and waves increased between 1996 and 2006. Large-scale atmospheric circulation variations such as the Arctic Oscillation (AO) and the Arctic dipole anomaly have a clear impact on the variation of winds and waves in the

Atlantic sector (Liu et al. 2016). Wang (2001) investigated wave heights in the Northern hemisphere and related atmospheric circulation regimes.

In order to take adequate precautions and to reduce risks and damages from the storm the information about the time of occurrence and magnitude of such events is required. This sort of research has been done for other basins of the World Ocean e.g. North Atlantic (De León and Soares, 2015; Rusu et al. 2015). There are a limited number of studies devoted to storm number, their interannual variability and their connection with global atmospheric circulation in the Baltic, Barents and White Seas, so these subject still remains challenging (Korablina et al. 2016; Medvedeva et al. 2015). Our paper focuses mainly on the storm statistics in the Baltic, Barents and White Seas and their connection with large-scale atmosphere circulation indices. The aim of this paper was to compare storm interannual variability in these three neighbor seas and to reveal common and different from each other features and also to assess the connection of storms with indices of large-scale atmospheric circulation.

MATERIALS AND METHODS

In order to estimate decadal and interannual changes of the wind wave fields the SWAN, short from Simulating WAVes Nearshore, (Booij et al. 1999) and WaveWatch III (Tolman 2009) numerical wave models were used. These models are state-of-the-art and are widely applied for reconstruction of wave fields and such parameters as significant wave heights (in this paper it was considered as mean of 1/3 of the highest waves), periods, lengths, swell heights and energy transport with different spatial and temporal resolutions by solving the energy balance equation (1) in spectral dimensions (Myslenkov et al. 2016; Reistad et al. 2011; Stopa et al. 2016).

For the Baltic and the White Seas the third-generation spectral wind wave model SWAN (version 41.01) has been

implemented in order to obtain wind wave parameters. As a wind forcing we used 10-m wind from Climate Forecast System Reanalysis from the National Centers for Environmental Prediction (NCEP/CFSR) with a spatial resolution $0.3^\circ \times 0.3^\circ$ and a time step 1 hour (Saha et al. 2010) for the period from 1979 to 2010. Starting from 2011, we used NCEP/CFSv2 (Saha et al. 2014), which is the extension of NCEP/CFSR; it has a spatial resolution $\sim 0.205^\circ \times 0.204^\circ$ and a time step of 1 hour. The accuracy of the obtained wave parameters is high and it has been estimated by using measurements of the wave parameters (Medvedeva et al. 2016). Accuracy of the model was estimated for the same period, basin and data as in present paper, see details in (Medvedeva et al. 2016): in average R was 0.96, $Bias$ 0.05, $RMSE$ 0.29 and scatter index 0.18.

For the Barents Sea, the spectral model WaveWatch III version 4.18 has been implemented with an unstructured grid covering the North Atlantic basin and Arctic seas (Fig. 1). "ST1" parametrization has been used for energy input and dissipation. This scheme is based on the same equations that the SWAN configuration used in this study. "DIA" scheme has been implemented for non-linear wave interactions (Hasselmann and Hasselmann, 1985). In addition, WaveWatch allows involving ice coverage. "IC0" scheme has been used for wave energy attenuation in the ice where wave energy reduces exponentially in grid points with ice concentrations between 25% and 75%, otherwise grid points are considered to be open water (<25%) or land (>75%). In WaveWatch III simulations in the Barents Sea we used wind forcing fields and ice concentration from NCEP/CFSR reanalysis from 1979 to 2010 (Saha et al. 2010). This model showed a good agreement with measurements for these regions (Stopa et al. 2016; Tolman 2009). In the White Sea storm statistics was calculated only for days without ice fields. For the Baltic Sea, we didn't exclude any data because Baltic Proper and South-eastern basin usually are not covered by ice.

Calculations have been performed using unstructured grids for the Barents and the White Seas with a spatial resolution 10–20 km in the central and open parts of the seas and 200–500 m in the coastal zones. The unstructured grid for the Barents Sea included the North Atlantic region from the Equator to the North Pole with a spatial resolution $\sim 1^\circ$ (Fig. 1). The grid for the Baltic Sea was rectangular and had a resolution $0.05^\circ \times 0.05^\circ$. The computational grid was created on the basis of the General Bathymetric Chart of the Oceans (GEBCO) with a spatial resolution of one nautical mile for the deep sea. Data from high-resolution navigation maps were used for the bathymetry in coastal zones.

The model description

The SWAN model is a third-generation spectral wind wave model developed by Delft University of Technology in the Netherlands (Booij et al. 1999) which is traditionally applied for shallow water areas. WaveWatch III has been developed in many research groups, predominantly by the United States' National Oceanic and Atmospheric Administration (NOAA). Based on the same energy balance equation, WaveWatch III is more developed and has more different formulations for the wind input and the whitecapping. It incorporates state-of-the-art formulations for the deep water processes of wave generation, dissipation and the quadruplet wave-wave interactions used by the WAM model (Komen et al. 1994).

The processes included are wind input, whitecapping, bottom friction, depth-induced wave breaking, dissipation due to vegetation, mud or turbulence, obstacle transmission, nonlinear wave-wave interactions (quadruplets and triads) and wave-induced set-up (2).

All information about the sea surface is contained in the wave variance spectrum or energy density $E(\sigma, \theta)$, distributing wave energy over (radian) frequencies σ (as observed in a frame of reference moving with current velocity) and propagation directions θ (the direction normal to the

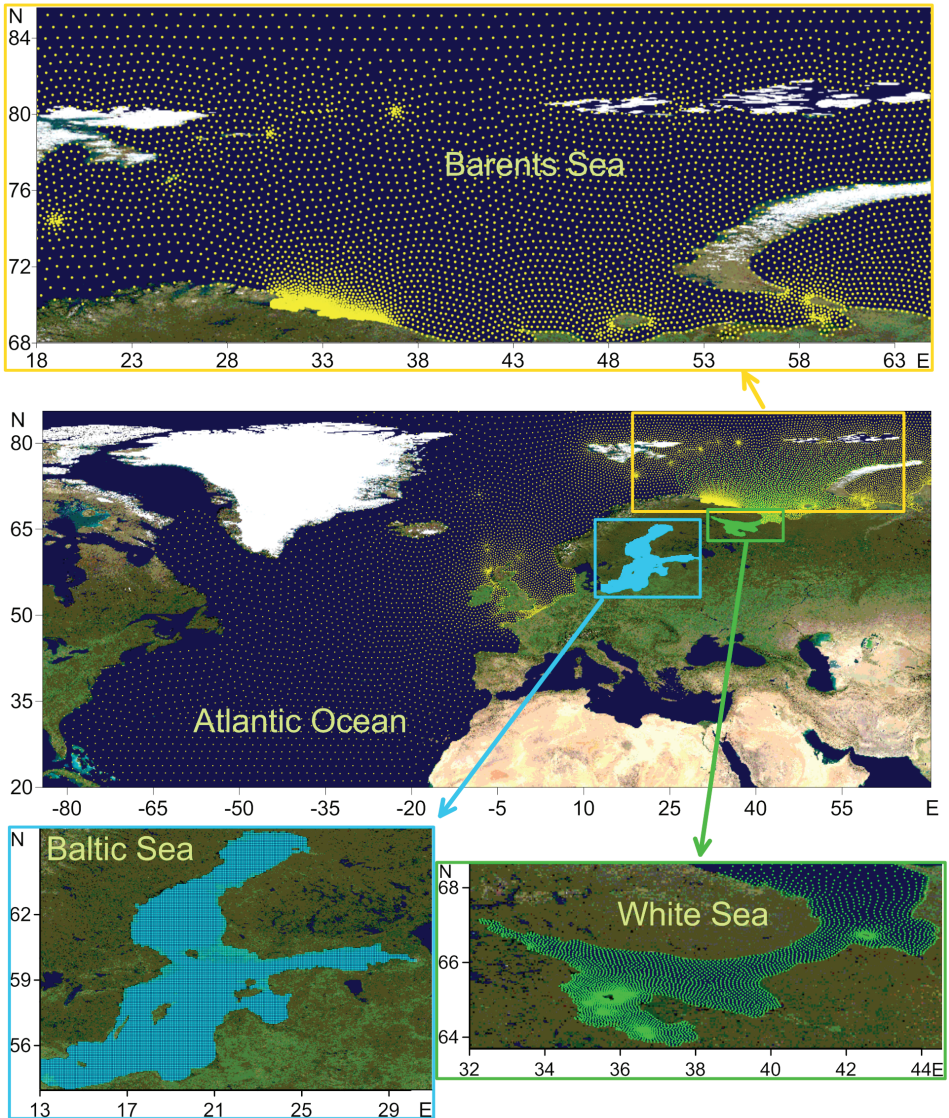


Fig. 1. The computational grids for the Barents, White and a Baltic Seas

wave crest of each spectral component). The action density is defined as $N = E/\sigma$ and is conserved during propagation along its wave characteristic in the presence of ambient current, whereas energy density E is not.

The evolution of the action density N is governed by the action balance equation, which reads (Komen et al. 1994):

$$\frac{\partial N}{\partial t} + \nabla_x \cdot \left[(\vec{c}_g + \vec{U}) N \right] + \frac{\partial c_\sigma N}{\partial \sigma} + \frac{\partial c_\theta N}{\partial \theta} = \frac{Stot}{\sigma} \quad (1)$$

The left-hand side is the kinematic part of this equation. The second term denotes the propagation of wave energy in two-dimensional geographical $\sim x^2$ -space, with the group velocity $\sim c_g = \partial \sigma / \partial \sim k$ following from the dispersion relation $\sigma^2 = g |\sim k| \tanh(|\sim k| d)$ where $\sim \vec{k}$ is the wave number vector and d is the water depth. The third term represents the effect of shifting of the radian frequency due to variations in depth and mean currents. The fourth term represents depth-induced and current-induced refraction.

The quantities C_{σ} and C_{θ} are the propagation velocities in spectral space (σ, θ) . The right-hand side contains S_{tot} which is the non-conservative source/sink term that represents all physical processes, which generate, dissipate, or redistribute wave energy. In shallow water, six processes contribute to S_{tot} :

$$S_{tot} = S_{in} + S_{nl3} + S_{nl4} + S_{ds,w} + S_{ds,b} + S_{ds,br} \quad (2)$$

These terms denote, respectively, wave growth by the wind, nonlinear transfer of wave energy through three-wave and four-wave interactions and wave decay due to whitecapping, bottom friction, and depth-induced wave breaking.

The model output and storm count

The significant wave heights, periods and wavelengths were reconstructed with wave models for the period from 1979 to 2010 years with a time step of 3 hours for the White and Barents Seas, and for the Baltic Sea – until 2015 with the same time step. Since 2011 year we start to use new version of reanalysis for the Baltic Sea, but the results for the White and Barents Seas in this paper limited by 2010 year, because the calculations with new reanalysis in progress. The main results of wind wave climate investigations (more detailed information about the applied methods, validation and other technical details) for each Sea was presented in recent publications (Arkhipkin et al. 2015; Kislov et al. 2016; Korablina et al. 2016; Medvedeva et al. 2015. 2016; Myslenkov et al. 2015a,b, 2016; Surkova et al. 2013).

All situations when H_s exceeded the chosen threshold (from 2 to 10 meters) were considered as a storm. The number of storm situations with different significant wave heights was calculated for every year from 1979 to 2010 and respectively 2015. For example, if H_s in one grid node is higher than 4 meters then it was considered as the start of a storm with criteria $H_s \geq 4$ m. An event is considered to be finished when the H_s in all nodes was less than the chosen threshold. When the H_s reached

the level of 4 meters next time it was considered as another next storm event. A storm with $H_s \geq 10$ meters is taken into account for each other of the lower criteria from 2 to 10 m and it was included in all these selections. This method of the storm count has some inaccuracy, firstly, when two events happen directly one after

another and, secondly, when in the sea under investigation there are two storms in different parts of the sea. Nevertheless, these cases are not very frequent.

RESULTS AND DISCUSSION

Storm number and trends

In the Baltic Sea during 37 years the number of storms with $H_s \geq 2$ m amounts to 2559, approximately 70 per year, with criteria 3 m – 1285, 4 m – 1107, 5 m – 649. These results indicate that about a half of all storm situations have a significant wave height of more than three meters (Fig. 2).

Typical periods of intensification and relaxation of wind waves are 10–12 years for the Baltic Sea, see Soomere and Räämet (2014). According to the obtained running average of storm number, there is a 10-year period of intensification/weakening of the storm activity. For various parts of the Baltic Sea, there is a discrepancy between the trends of the ten-year increase or decrease. Notably, that the rapid changes of intensification or weakening of wave activity can happen during one decade (Soomere et al. 2008; Broman et al. 2006). In figure 2, the maximum of $H_s \geq 2$ m was observed in 1983, the local minima are in 1984, 1996 and 2006. For $H_s \geq 3$ m, the local maxima are in 1983, 1990, 1995 and 2008 years.

There is no significant tendency in storm number in the Baltic Sea with $H_s \geq 2$ m. However, for criteria $H_s \geq 4$ m we found a statistically significant negative trend, it amounts -0.17. For storms with $H_s \geq 3$ m the linear trend of the decrease can be observed in figure 2, but it's not statistically

significant. For 37 years (1979–2015) the maximum computed significant wave height amounts to 8.5 m, wavelength – 130 m, wave period – 10 s.

In the Barents Sea, wind wave conditions are significantly more severe. Four meters were taken as the lowest H_s threshold for the Barents Sea to calculate storm number, the standard deviation of wave height is about 3 meters for this sea, and thus 4 meters is the lowest level when we can distinguish storm events from noise. Storm number with $H_s \geq 4$ meters in the Barents Sea is of the same order as storm number with $H_s \geq 2$ meters in the Baltic having about 80 storms per a year. The maximum of storms with $H_s \geq 4$ m was observed in 2005 (Fig. 2). For $H_s \geq 4$ m, local maximum was identified in 2005. The storms with $H_s \geq 5$ m were registered 40–60 times per a year with local increases in 1989, 1992, 1995 and 2003. For $H_s \geq 6$ m, there is a local maximum of storms in 1991. For $H_s \geq 7$ m, the maximum was identified in 1990. There is no significant trend in the Barents Sea detected for the entire period. However, if we divide the period from 1979 to 2010 into 3 segments, we can clearly identify 3 different linear trends for $H_s \geq 6$ m (Fig. 2a). From 1979 to 1991 the quantity of storms increases, from 1992 to 2002 it decreases and then not great augmentation again occurs. Thus for the Barents Sea, the same period as in the Baltic Sea about 10–12 years was identified. For 32 years (1979–2010) the maximum computed significant wave height is 16 m (at the west boundary, 25°E). The same analysis was carried out for the White Sea. In the central open part of the White Sea, the number of storms with $H_s \geq 2$ m is about 20 times per a year for the ice-free period (Fig. 2). As for storms with $H_s \geq 3$ m, they occurred only 5–6 times per year. Interannual variability of the number of storms in the White Sea is less determined than in the Barents, but for $H_s \geq 2$ m there is a maximum in 1995 and a minimum in 1999. Since 1999, the storm number increases, but positive trend in storminess isn't significant. For $H_s \geq 3$ m, there are two maxima in 1986 and 1994, two minima in 1985 and 1999.

In the White Sea, the following features of the wave climate are observed: the maximum of number of storms in the autumn and winter months, a significant spatial and temporal heterogeneity of the properties of wind wave fields, where each part of the sea such as Onega Bay, Basin, Gorlo, and Voronka has their own determined wave mode.

In addition, the relations of storm number between different Seas was studied. It is interesting that the highest significant correlation (0.56) was discovered between the storm number, discussed above, of the Barents storms with $H_s \geq 7$ m and Baltic storms with $H_s \geq 4$ m, which have statistically significant negative trend. These events occur about 20 times per a year. For others Baltic storms with $H_s \geq 3, 5$ m and Barents events with $H_s \geq 5, 6, 8$ m R was also approximately 0.5. We can make a supposition that it reflects the connection of these processes and its common origin. For more severe Barents storms with upper thresholds 9 and 10 m the link $R = 0.52$ m is observed with the White Sea storms with $H_s \geq 3$ m level (about 5 times per a year), however this connection is reflected only on scales of greater wave heights and isn't observed with the Baltic Sea. All other correlation coefficients are small. So high correlation is not observed between White and Baltic Seas at all. And for events with $H_s \geq 2$ m it was not revealed too.

The relations of storm number with atmospheric indices. In order to study the connection with the global atmospheric circulation, 3 indices North-Atlantic Oscillation (NAO), Arctic Oscillation (AO), Scandinavian Index (SCAND) have been considered. The correlation coefficient (R) was calculated between these indices and the max H_s , the results are presented in table 1.

We will regard as the state of the atmosphere with a positive value of the NAO index as the positive phase of the oscillation and when the value is below zero – as negative (<http://www.cpc.ncep.noaa.gov/> 2017). In the positive phase of the oscillation, the Icelandic minimum and

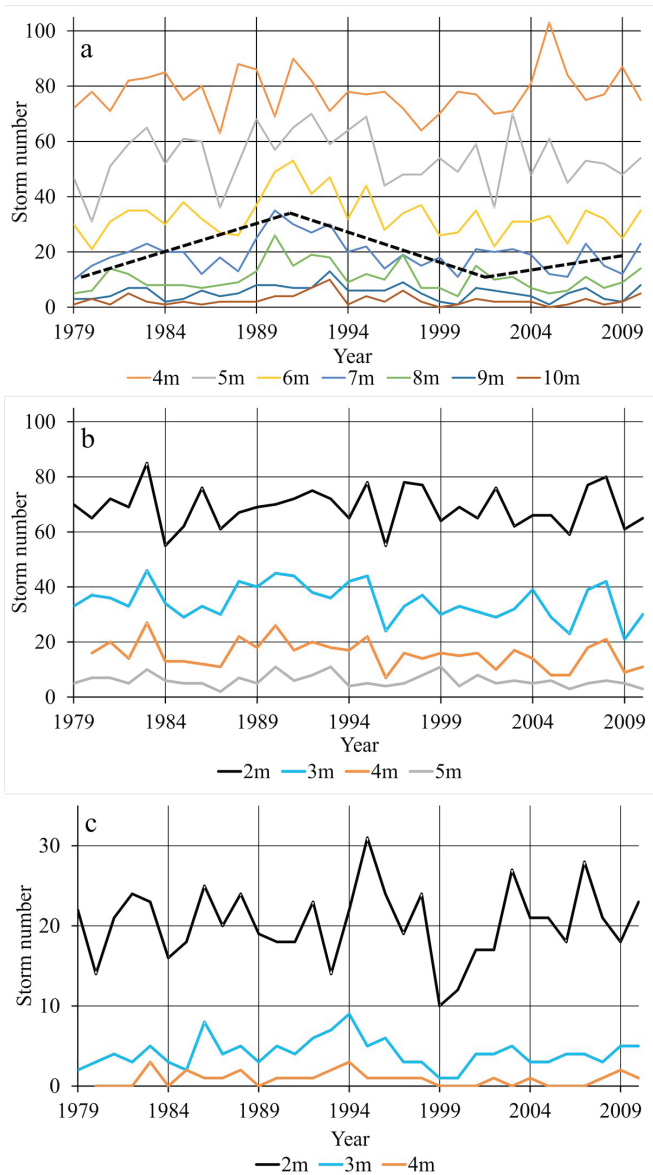


Fig. 2. The number of storms with the different H_s for the Barents (a), Baltic (b) and White Seas (c)

the Azores maximum are well developed, the pressure gradients between them are increased, the zonal circulation is strengthened. In the negative phase, there is a weakening of the zonal transport and an intensification of the meridional processes.

The AO is a large-scale mode of climate variability also referred to as the Northern Hemisphere annular mode (<http://www.cpc.ncep.noaa.gov/> 2017).

The AO is a climate pattern characterized by winds circulating counterclockwise around the Arctic at around 55°N latitude. When the AO is in its positive phase, a belt of strong winds circulating around the North Pole acts to confine colder air across Polar Regions. This belt of winds becomes weaker and more distorted in the negative phase of the AO, which allows an easier southward penetration of colder, arctic air

Table 1. The coefficient of correlation R between mean annual storm number with different H_s threshold for the Baltic, White and Barents Seas and mean annual indices of large-scale atmospheric circulation. Bold font indicates significant R

Baltic Sea				White Sea				Barents Sea			
$H_s \geq$	NAO	AO	SCAND	$H_s \geq$	NAO	AO	SCAND	$H_s \geq$	NAO	AO	SCAND
2 m	0.12	0.32	-0.59	2 m	-0.07	-0.02	-0.29	4 m	0.12	0.09	0.16
3 m	0.42	0.49	-0.47	3 m	0.18	0.2	0.06	5 m	0.44	0.45	-0.24
4 m	0.35	0.45	-0.52					6 m	0.27	0.35	-0.33
5 m	0.28	0.36	-0.32					7 m	0.35	0.47	-0.23
2 m (by NCAR)	0.31	0.46	-0.48					8 m	0.21	0.42	-0.19
								9 m	0.18	0.36	0.11
								10 m	0.03	0.11	-0.02

masses and increased storminess into the mid-latitudes.

The Scandinavia pattern SCAND consists of a primary circulation center over Scandinavia, with weaker centers of opposite sign over Western Europe and eastern Russia/ western Mongolia. The Scandinavia pattern has been previously referred to as the Eurasia-1 pattern by (Barnston and Livezey 1987). The positive phase of this pattern is associated with positive height anomalies, sometimes reflecting major blocking anticyclones, over Scandinavia and western Russia, while the negative phase of the pattern is associated with negative height anomalies in these regions. The positive phase of the Scandinavia pattern is associated with below-average temperatures across central Russia and also over western Europe. It is also associated with above-average precipitation across central and southern Europe and below-average precipitation across Scandinavia.

Correlation analysis of the mean annual number of the storm and mean annual indices of atmospheric circulation is presented in table 1. It showed that connection of storm number in the Barents Sea R about 0.5 is only with AO, for $H_s \geq 5$ m (0.45) and $H_s \geq 7$ m (0.49). However, if we consider not annual but

winter averaged monthly index AO (DJFM) and monthly values of storm number, then, in the Barents Sea, the connections between a number of storms and AO on decadal scales is reflected better. The highest correlation coefficient between AO index (averaged from December to March) R (0.6) was obtained for storms with $H_s \geq 7$ m (Fig. 3a), and for $H_s \geq 8$ m with AO it amounts to 0.57. With SCAND pattern the link isn't observed.

For the White Sea, the relations between a number of storms and AO, NAO indices are weak (Fig. 3c, d). Maximum $R = 0.26$ and other coefficients are less. The liaison between storm number in the Barents and White Seas and SCAND pattern is weak and it was not revealed.

For the Baltic Sea the connection of storm number is mostly pronounced with SCAND. The highest correlation is -0.59 for $H_s \geq 2$ m (Table 1). Also R with AO reaches 0.45-0.49 for different thresholds. Summarizing this section, we can say that the connection with indices of global atmospheric circulation is mostly developed for the Baltic Sea with SCAND pattern, less with AO. Secondly, it is reflected in the Barents Sea with AO. For the White Sea such link was not revealed.

Fig. 3 (e, f) shows good correspondence for the Baltic Sea annual storm number and NAO, AO indices. However, maximum R amounts 0.49 for the storm number with $H_s \geq 3$ m and it was revealed with AO. For events with $H_s \geq 4$ m, it amounts 0.45. With NAO the connection is not obvious. As for SCAND pattern, it is worth noting that R is the highest but it is negative about -0.59 for $H_s \geq 2$ m, -0.52 for $H_s \geq 4$ m, and -0.47 for $H_s \geq 3$ m (Table 1). It means that the increase in storm number over the Baltic Sea corresponds to the negative phase of the Scandinavian pattern associated with negative height anomalies in this region.

The connections between a number of storms with positive and negative NAO, AO and SCAND phases are shown in fig. 4. It shows that there is no positive or negative significant trend in a number of storms with $H_s \geq 2$ m. For comparison, (Medvedeva et al. 2015) showed a similar trend, but the simulations were based

on other reanalysis data NCEP/NCAR (Kalnay et al. 1996). They had a longer time coverage from 1948 to 2010 but less accuracy of the modeled results and errors are twice as high. Previous versions of the reanalysis data have shown an increase in storm activity and an obvious 20-year periodicity. In figure 3, we noted the decrease of stronger storms shown by linear trends. There is only one trend corresponding to $H_s \geq 4$ m, which is statistically significant by Fisher criteria. To compare with the previous version of the reanalysis (NCAR) the coefficient R with AO is lower and amounts to 0.46 (with CFSR 0.49). With NAO and SCAND NCAR reanalysis shows worse correlation.

The relations of maximum H_s and storm number with atmospheric indices for regions of the Baltic Sea

The commonly accepted reasons behind the possible increase in the Baltic Sea

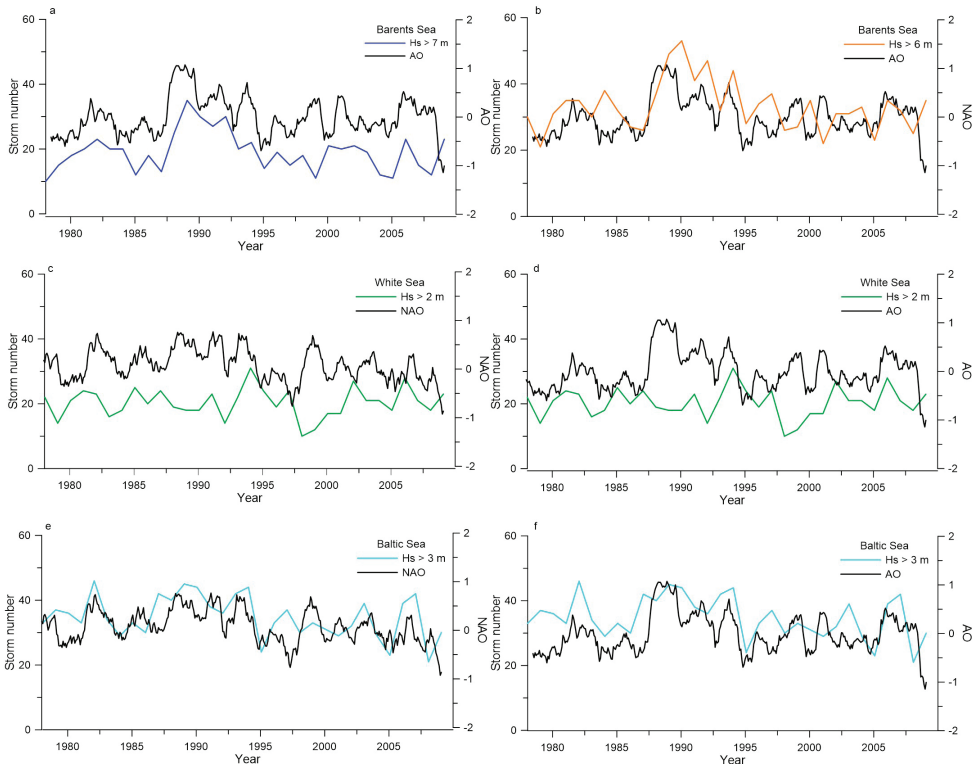


Fig. 3. Connections between indices AO, NAO and the number of storms in the Barents (a, b), White (c, d) and Baltic Seas (e, f). Indices are presented by running average with 13 months values

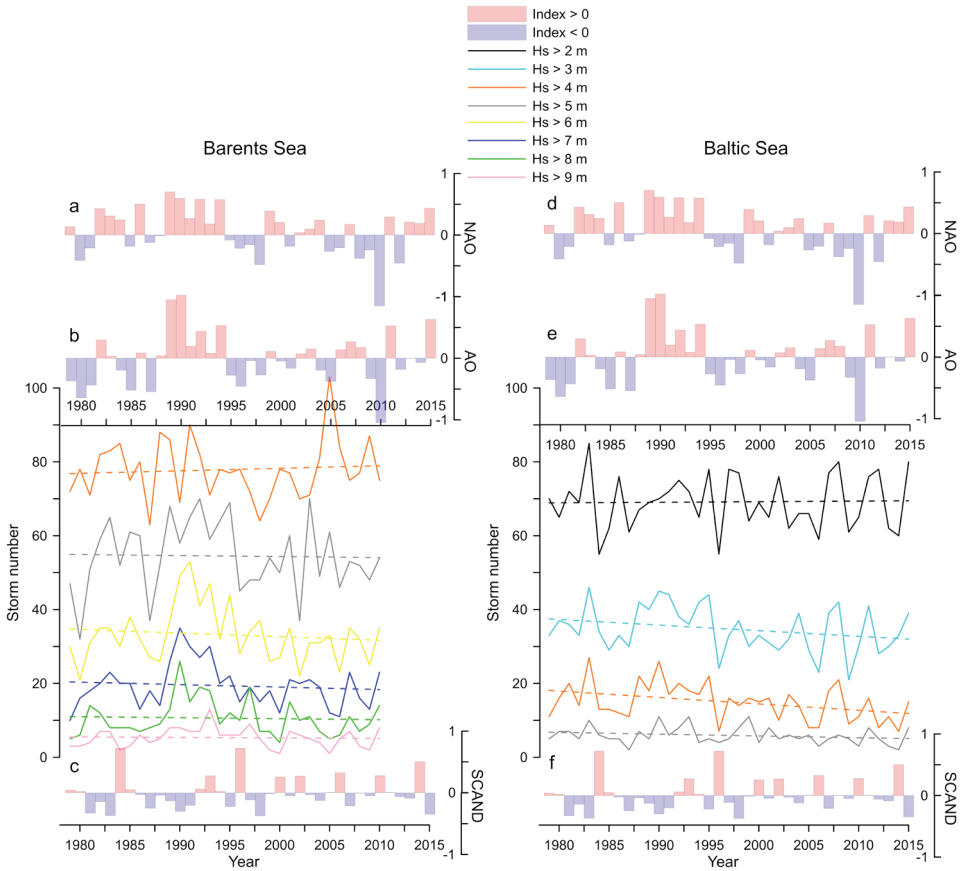


Fig. 4. Storm number with different H_s threshold for the Barents (a-c) and Baltic (d-f) Seas with the NAO, AO, SCAND indices. The dashed line represents linear trends

wave heights are 1) a reduction of sea ice in northern parts of the sea and 2) an increase in the wind speed (Hünicke et al. 2015). Both these reasons should lead to a spatially inhomogeneous increase in the wave heights, first of all in seasonally ice-covered northern part of the Sea and along the eastern segments of the basin where the predominant south-westerly and north-north-westerly winds usually create the severest wave conditions. Analysis of Kudryavtseva and Soomere (2017) reveals an unexpected strong meridional pattern of changes: the wave heights have increased in the western offshore of the sea and have decreased (or exhibit no changes) along the eastern nearshore. It is, therefore, unlikely that a discernable increase in the wind speed has occurred in this region. This among other things means that a greater level

of storms and swells (Bertin et al. 2013) may only characterize some parts of the North Atlantic. This is consistent with the conclusion that the basin-wide average geostrophic wind speed has not increased over the entire Baltic Sea (Soomere and Räämet, 2014).

In this paper the entire Baltic Sea was divided into 5 areas (Fig. 5): the South-Eastern Baltic (I), the Gulf of Bothnia (II), the Gulf of Finland (III), the Gulf of Riga (IV) and the Baltic Proper (V) (Fig. 5) and the maximum H_s was identified for each part for every month (2200 values in all). As maximum H_s , we considered maximum value registered in this area for a selected period (for example the maximum value of H_s in one node in the Gulf of Finland in January 1990). Then for every month of this period from January to December, the

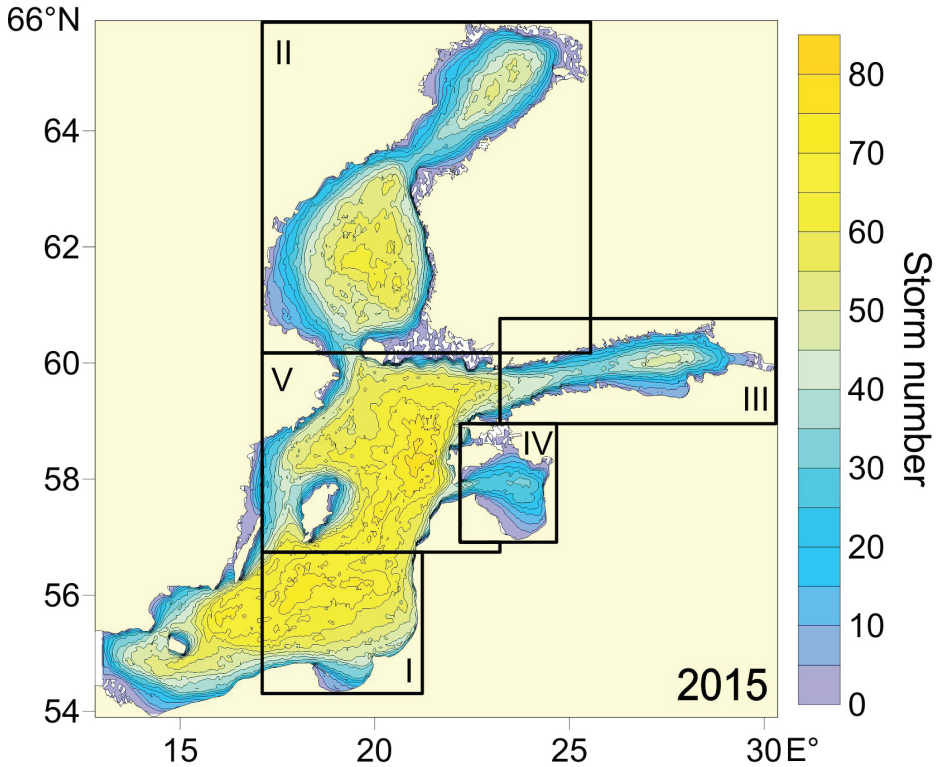


Fig. 5. Map of the yearly distribution of the storm numbers in every node in 2015 with 5 areas in which trends of max H_s and storm number were estimated: I – the Southeastern Baltic (in rectangular from Slupsk to Liepaja), II – the Gulf of Bothnia (including the Bothnian Bay and the Bothnian Sea), III – the Gulf of Finland, IV – the Gulf of Riga, V – the Baltic Proper

maximum H_s was selected (444 values in all).

For the Baltic Sea in the cold season, the field variability connected to the NAO is most pronounced. If we take into account only the period from December to March (with $R \geq 0.5$), the connection of max H_s is more significant with AO, slightly less significant with NAO and negative (-0.4; -0.5) with SCAND (Table 2).

We observe a positive high correlation coefficient of ≥ 0.5 with the NAO index for five months: January, February, March and April, and for the Baltic Proper for November. For all other months, it has a low value close to the zero or negative. The highest value of $R = 0.7$ was observed for December in the Gulf of Finland (Fig. 6, Table 2). It is evident from the figures 3, 4, that every increase of

the H_s in the Gulf of Finland corresponds to the positive phase of the NAO and AO indices. It is obvious that with positive NAO the number of deep cyclones over the North Atlantic region increases and maximum H_s increase too. Negative NAO phase in most cases coincides with the H_s decrease.

The AO index $R \geq 0.5$ was identified for the winter period (plus April), the maximum value equals 0.64 for the Southeastern part of the Baltic Sea for January. In the spring-autumn period, the link is not obvious.

All coefficients R with the SCAND are negative. Notably, for January, February, April, and September with $R \leq -0.5$, i.e. the H_s increases with the negative phase of the index. The highest values of R -0.67, -0.65 are found in the Southeastern part of the Baltic Sea.

Table 2. Correlation coefficient *R* calculated between the value of max *H_s* (for a month) and monthly indices of large-scale atmosphere circulation (NAO, AO, SCAND). The bold font indicates significant *R*

Month	1	2	3	11	12	
NAO	0.47	0.29	0.57	-0.05	0.59	Southeastern Baltic
	0.18	0.53	0.55	-0.01	0.43	Gulf of Bothnia
	0.36	0.54	0.55	-0.04	0.70	Gulf of Finland
	0.44	0.49	0.49	0.11	0.65	Gulf of Riga
	0.52	0.38	0.57	0.55	0.60	Baltic Proper
AO	0.64	0.54	0.51	0.27	0.44	Southeastern Baltic
	0.17	0.49	0.47	0.07	0.49	Gulf of Bothnia
	0.57	0.55	0.58	0.21	0.56	Gulf of Finland
	0.50	0.57	0.55	0.30	0.50	Gulf of Riga
	0.56	0.55	0.50	0.49	0.58	Baltic Proper
SCAND	-0.67	-0.65	-0.40	-0.45	-0.37	Southeastern Baltic
	-0.19	-0.45	-0.21	-0.45	-0.31	Gulf of Bothnia
	-0.41	-0.57	-0.31	-0.43	-0.28	Gulf of Finland
	-0.42	-0.46	-0.39	-0.39	-0.27	Gulf of Riga
	-0.60	-0.58	-0.35	-0.32	-0.35	Baltic Proper

From the geographical perspective the highest *R* was noted in the Gulf of Finland (Fig. 6, Table 2) as with NAO, so with AO. For this area, the maximum value for NAO corresponds to December (*R* = 0.7) and for AO in March (0.68). Thus, with such complex configuration of the Baltic Sea, the NAO and AO indices have the most influence on the Gulf of Finland and secondly on the Baltic Proper. The lowest *R* coefficients were observed for the Gulf of Bothnia. It is worth noting, that in the last decade from 2005 to 2015 the storm number with *H_s* ≥ 2, 3, 4 m increases in the entrance of the Gulf of Finland. This conclusion is based on obtained results and on analysis of maps of maximum *H_s* distribution (constructed for every month for every year). In addition, it propagates deeper to the east, so it reflects the displacement of the trajectories of cyclones, which have moved 5° to the north. It changes the length of the wave fetch and promotes wave penetration into the Gulf of Finland.

As for storm number in separate parts of the sea (Table 3), the highest *R* is noted in the Baltic Proper with AO for *H_s* ≥ 3 m and *R* equals 0.62. For storm events with *H_s* ≥ 4 m, the situation is the same: the correlation for the Baltic Proper is stronger 0.54.

Summarizing, the connection between significant wave height and indices is stronger in the Baltic Proper and it was observed in more months than in any other part of the sea, th Baltic Proper is on the second place. If we consider the absolute value of correlation, in the Gulf of Finland *R* amounts 0.7 in the December.

As for seasonal variability of correlation – the connection is more determined from November to March with a maximum in the February.

If we take into account, storm number separately calculated for parts of the Baltic then in the Baltic Proper *R* is higher.

Table 3. The correlation coefficient between the number of storms and indices of atmospheric circulation in different parts of the Baltic Sea. The bold font shows significant $R \geq 0.5$

<i>R</i>	NAO	AO	SCAND
<i>H_s ≥ 2 m</i>			
Southeastern Baltic	0.08	0.23	-0.56
Gulf of Bothnia	0.26	0.41	-0.50
Gulf of Finland	0.32	0.43	-0.19
Gulf of Riga	0.43	0.54	-0.26
Baltic Proper	0.17	0.35	-0.61
<i>H_s ≥ 3 m</i>			
Southeastern Baltic	0.41	0.46	-0.48
Gulf of Bothnia	0.32	0.48	-0.47
Gulf of Finland	0.51	0.55	-0.39
Gulf of Riga	0.46	0.45	-0.25
Baltic Proper	0.42	0.62	-0.49
<i>H_s ≥ 4 m</i>			
Southeastern Baltic	0.28	0.33	-0.16
Gulf of Bothnia	0.33	0.35	-0.17
Gulf of Finland	0.40	0.41	-0.27
Baltic Proper	0.43	0.54	-0.37

Future changes

The climate projection of weather pattern accompanying extreme winds over the Barents and Baltic Seas is carried out with the database of CMIP5 models ensemble runs (RCP8.5 scenario), see Moss et al. 2008; Taylor et al. 2012. According to this scenario, the global surface air temperature will be 3.5-4°C higher than in 1961-1990. The key idea relies upon the “environment – to circulation” method (Huth et al. 2008). It is based on the assumption that extreme weather phenomena (local or mesoscale) are connected through physical mechanisms with large-scale (synoptic) events. Then it is possible to make projections indirectly, studying configuration and intensity of sea level atmospheric pressure (SLP) fields which are supposed to be the determining factor of the wind speed and thus of wind waves. In this way, there is no need to run

a wave model for the future climate, but to look into the climate projection for the fields of SLP, which are associated with storm situations in the modern climate.

Due to cyclonic activity in high latitudes, strong winds and stormwind waves are frequently observed there all year round, especially, in the cold season. For the severe and specific climate of the Barents and Baltic Seas, it is complicated to adequately observe directly the atmosphere and ocean and even to use information from satellites. In this case, weather and climate models are of great value to understanding the present atmosphere-ocean interaction processes and their physical mechanisms. Earth system modeling is an important instrument for future climate projection of extreme weather events, which should help to identify and manage the risks of extreme events (Field et al. 2012).

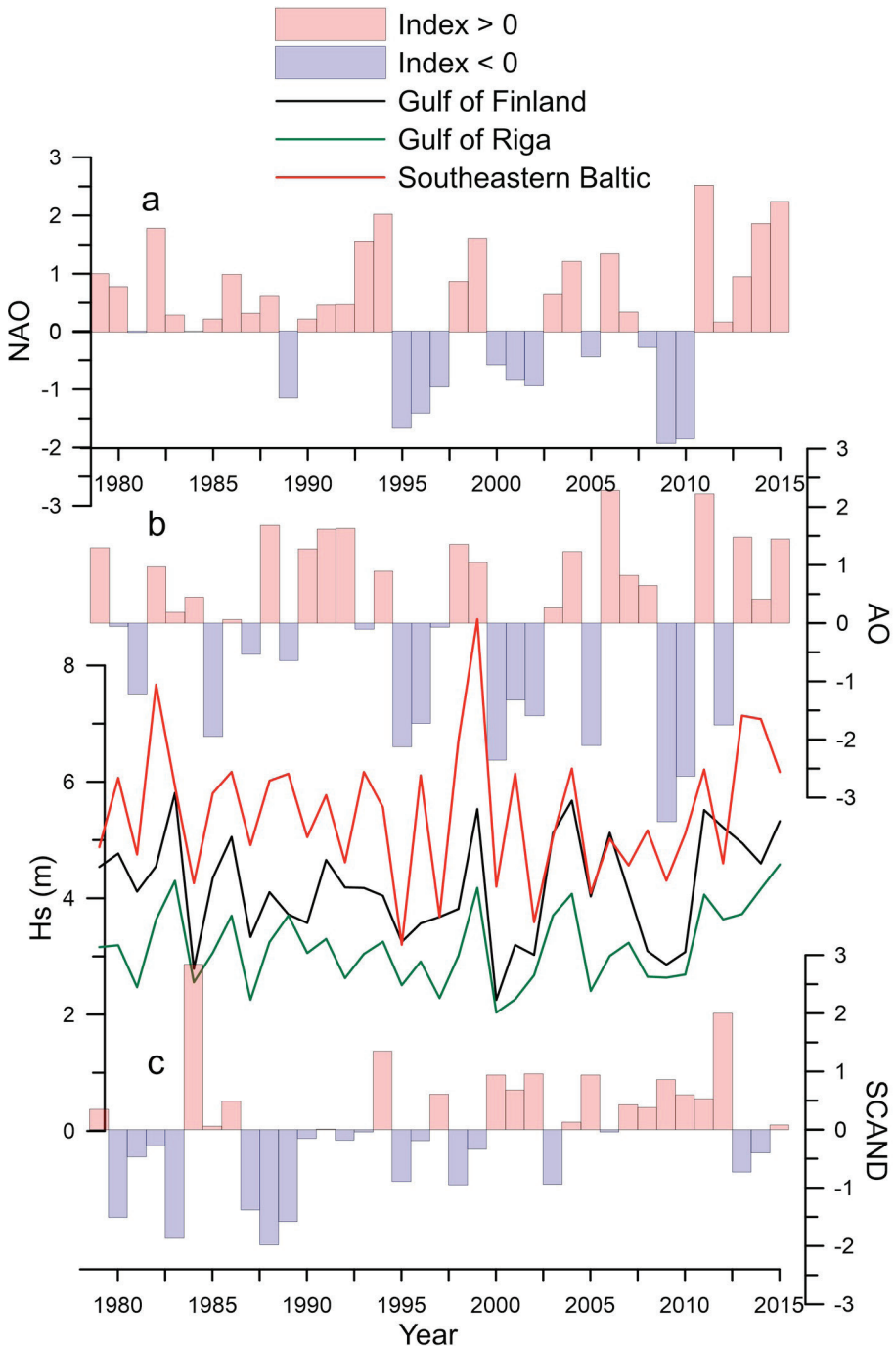


Fig. 6. Storm number with different H_s threshold for the Barents (a-c) and Baltic (d-f) Seas with the NAO, AO, SCAND indices. The dashed line represents linear trends Interannual variability of maximum significant wave heights in the Gulf of Finland (black line), Baltic Proper (red line) and Gulf of Riga (green line) for December from 1979 to 2015 with 3 indices of large-scale atmospheric circulation; NAO (a), AO (b), SCAND (c).

To make a projection of extreme events in the future we applied the original method described in Surkova et al. (2013), Surkova and Krylov (2017). We used two approaches to get the calendar of these events for the last decades. For the Baltic Sea, a calendar of storms was derived from results of experiments of the wave model SWAN for 1948–2011. We choose such days when the modeled H_s was 4 m or higher (the government standard of general requirements for safety in emergencies specifies waves with a height of 4 m or more in the coastal zone and 6 m or more in the open sea as hazardous ones). For the Barents Sea, we considered a day as an extreme event when the wind speed was higher than the value of its 99th percentile. We found 364 events for the Baltic Sea (1950–2010) and 240 events for the Barents Sea (1981–2010).

Based on these calendars, a catalog of atmospheric SLP fields was prepared for each sea. The data used was the one of NCEP/NCAR reanalysis (Kalnay et al. 1996) for the Baltic Sea, and ERA-Interim for the Barents Sea (Dee et al. 2011). Every storm SLP field from reanalysis then was compared with everyday models SLPs of 1950–2005 period for every climate model (24 CMIP5 models for the Baltic Sea and

27 models for the Barents Sea). When for the present climate the SLP from the climate model had a coefficient of spatial correlation R more than the critical one R_c and the same spatial variance as the storm field it was taken into account. It was found that when $R_c \geq 0.97$ –0.98 (individually calculated for each model) the number of storm events simulated by the model is as many as in the storm calendar.

Then analogs of “storm SLP fields” and their frequency were investigated for the climate models results for an RCP8.5 CMIP5 experiment for 2006–2100. For this period the days were chosen when the correlation of modeled SLP and storm SLP from reanalysis was higher than R_c .

The results show (Fig. 7) that the frequency of extreme weather events connected with high wind speed and wind waves can shift towards higher values over the Baltic and Barents Seas according to most climate models in the case of the increasing global warming under scenario RCP8.5.

CONCLUSIONS

The numerical model simulations of storm activity in the White, Baltic and Barents Seas were analyzed. From 1979 to 2015

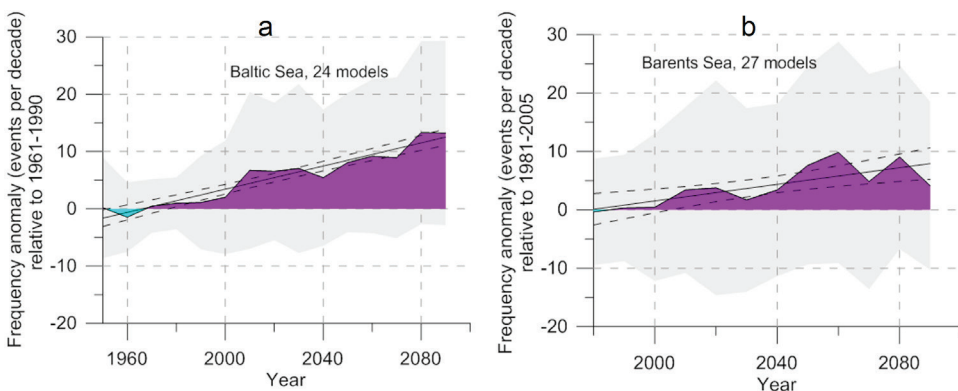


Fig. 7. Frequency anomaly (events per decade) of SLP patterns forcing high wind waves over the Baltic Sea (a) and high wind speed over the Barents Sea (b). The number of CMIP5 models used to calculate the multi-model mean is indicated on graphs. The CMIP5 multi-model mean is given by the light and dark blue filling. The trend is a straight solid line, its significance at the 5% level is shown by the dashed lines. Multi-model ensemble range is indicated by grey shaded bands (within 3-sigma limits)

the number of storms with different H_s threshold was calculated. High interannual variability is observed for all studied seas. The storm conditions in the Barents Sea is significantly more severe in comparison with the other considered seas. The storm number with $H_s \geq 2$ m in the Baltic is comparable with storm number with $H_s \geq 4$ m in the Barents Sea: an average 80 per year. The number of storms in the White Sea is four times lower: ~20 per a year with $H_s \geq 2$ m. In the Barents Sea, the most severe storms have threshold $H_s \geq 10$ m, which even doesn't occur in the Baltic and White Seas. For the Baltic, the considered limit was 5 m (5-7 per a year) and for the White Sea – only 4 m (2-3 per a year).

There is no significant trend of storm number in the Baltic, Barents and White Seas detected for the entire period. For the Barents and Baltic Seas the variability period about 10–12 years was identified. In the Baltic and Barents Seas, the small-scale increase of the number of storms was found in 1992–1994 years. It corresponds to the high positive NAO and AO and significant negative SCAND values. For the White Sea, the positive NAO phase in contrary corresponds to the decrease of the storm number. On average, the connection with global atmospheric circulation is stronger ($R \geq 0.5$) for the Baltic Sea, then for the other two seas. The most pronounced liaison for the Baltic is with SCAND pattern, for the Barents – with AO. The connection with AO index is clearer than with NAO for all three seas. Notably, that for stronger storms with $H_s \geq 4$ m in the Baltic the significant negative linear trend was identified. It is interesting that the number of these events is connected

with Barents storms with H_s threshold 7 m and correlation between them is 0.56. Also correlation of number of stronger storms in the Barents Sea ($H_s \geq 8, 9$ m) and storm number of the White Sea ($H_s \geq 3$ m) is significant (0.52). It reflects the common origin of these events.

According to the RCP8.5 scenario, in the second part of the XXI century the number of storm events will rise in the Baltic and Barents Seas.

ACKNOWLEDGMENTS

The results of part 1 (Storm number and trends) were obtained in the framework of the state assignment of FASO Russia (theme No. 0149-2018-0015). The results of part 2 (The relations of storm number with atmospheric indices) were obtained within the Russian Science Foundation grant (project No.14-50-00095). The results of part 3 (The relations of maximum H_s and storm number with atmospheric indices for regions of the Baltic Sea) were obtained within the Russian Foundation for Basic Research grant (project No. 16-35-00338). The results of part 4 (Future changes) were obtained within the Russian Science Foundation grant (project No. 14-37-00038).

«S. Myslenkov and S. Zilitinkevich acknowledge support from the Academy of Finland projects ABBA No. 280700 (2014-2017); S. Zilitinkevich acknowledges support from the Academy of Finland project ClimEco No. 314 798/799 (2018-2020) and RSF project No. 15-17-20009 (2015-2018)». ■

REFERENCES

Arkhipkin V., Dobrolyubov S., Myslenkov S., and Korablina A. (2015). The Wave Climate of the White Sea, Changing Climate and Socio-Economic Potential of the Russian Arctic. In: S. Sokratov, ed., 1st ed. Moscow: Liga-Vent, pp.48-58 (in Russian with English summary).

Barnston A. and Livezey R. (1987). Classification, seasonality, and persistence of low-frequency atmospheric circulation patterns. *Monthly weather review*, 115(6), pp. 1083-1126.

Bertin X., Prouteau E., and Letetrel C. (2013). A significant increase in wave height in the North Atlantic Ocean over the 20th century. *Global and Planetary Change*, 106, pp. 77-83.

Booij N., Ris R., and Holthuijsen L. (1999). A Third-Generation Wave Model for Coastal Regions. 1. Model Description and Validation. *Journal of geophysical research: Oceans*, 104(C4), pp.7649-7666.

Broman B., Hammarklint T., Rannat K., Soomere T., and Valdmann, A. (2006). Trends and extremes of wave fields in the north-eastern part of the Baltic Proper. *Oceanologia*, 48(S), pp.165-184.

Dee D., Uppala S., Simmons A., Berrisford P., Poli P., Kobayashi S., ..., and Bechtold P. (2011). The ERA-Interim reanalysis: configuration and performance of the data assimilation system, *QJ Roy. Meteor. Soc.*, 137, pp. 553–597.

De León, S., and Soares, C. (2015). Hindcast of the Hércules winter storm in the North Atlantic. *Natural Hazards*, 78(3), pp.1883-1897.

Field C., Barros V., Stocker T., Qin D., Dokken D., and Ebi K. (2012). IPCC 2012. Managing the risks of extreme events and disasters to advance climate change adaptation. A special report of the intergovernmental panel on climate change. Cambridge University Press. Cambridge: Cambridge University Press.

Hasselmann S. and Hasselmann K. (1985). Computations and parameterizations of the nonlinear energy transfer in a gravity-wave spectrum. Part I: A new method for efficient computations of the exact nonlinear transfer integral. *Journal of Physical Oceanography*, 15(11), pp.1369-1377.

National Weather Service Climate Prediction Center (2017). [online] Available at: <http://www.cpc.ncep.noaa.gov/> [Accessed 01 Nov. 2017].

Hünicke B., Zorita E., Soomere T., Madsen K. S., Johansson M., and Suursaar Ü. (2015). Recent change—Sea level and wind waves. In *Second Assessment of Climate Change for the Baltic Sea Basin* (pp. 155-185). Springer, Cham.

Huth R., Beck C., Philipp A., Demuzere M., Ustrnul Z., Cahynová M., Kyselý J., and Tveito O. (2008). Classifications of Atmospheric Circulation Patterns Recent Advances and Applications. *Trends and Directions in Climate Research*, Ann. N.Y. Acad. Sci., 1146(1), pp.105-152. DOI: 10.1196/annals.1446.019.

Kalnay E., Kanamitsu M., Kistler R., Collins W., Deaven D., Gandin L., ..., and Zhu Y. (1996). The NCEP/NCAR 40-year reanalysis project. *Bulletin of the American meteorological Society*, 77(3), pp. 437-471.

Kislov A., Surkova G., and Arkhipkin V. (2016). Occurrence Frequency of Storm Wind Waves in the Baltic, Black, and Caspian Seas under Changing Climate Conditions. *Russian Meteorology and Hydrology*, 41(2), pp.121-129 (in Russian).

Komen G., Cavaleri L., Donelan M., Hasselmann K., Hasselmann S., and Janssen P. (1994). *Dynamics and modeling of ocean waves*. Cambridge: Cambridge University Press.

Korablina A., Arkhipkin V., Dobrolyubov S., and Myslenkov S. (2016). Modeling storm surges and wave climate in the White and Barents Seas. In Saint-Petersburg, Russia: EMECS 11 – Sea Coasts XXVI Joint Conference «Managing Risks to Coastal Regions and Communities in a Changing World», 2016, pp.184-194. DOI: 10.21610/conferencearticle_58b4317442aca

Kriezi E. and Broman B. (2008). Past and future wave climate in the Baltic Sea produced by the SWAN model with forcing from the regional climate model RCA of the Rossby Centre. In US/EU-Baltic International Symposium, 2008 IEEE/ OES, pp. 1-7.

Kudryavtseva N. and Soomere T. (2017). Satellite altimetry reveals spatial patterns of variations in the Baltic Sea wave climate. arXiv preprint arXiv:1705.01307.

Liu Q., Babanin A., Zieger S., Young I., and Guan C. (2016). Wind and Wave Climate in the Arctic Ocean as Observed by Altimeters. *Journal of Climate*, 29(22), pp.7957-7975.

Lopatukhin L., Buhanovskij A., Degtyarev A., and Rozhkov V. (2003). Reference data of wind and waves climate of the Barents, Okhotsk, and Caspian Seas. Russian Maritime Register of Shipping, Saint-Petersburg: SPB (in Russian).

Lopatukhin L., Buhanovskij A., Ivanov S., and Chernysheva E. (2006). Reference data on the regime of wind and waves of the Baltic, Northern, Black, Azov and Mediterranean Seas. Russian Maritime Register of Shipping. Saint-Petersburg: SPB (in Russian).

Medvedeva A., Arkhipkin V., Myslenkov S., and Zilitinkevich S. (2015). Wave climate of the Baltic Sea following the results of the SWAN spectral model application. *Moscow University Bulletin. Series 5. Geography* (1), pp.12-22 (in Russian with English summary).

Medvedeva A., Myslenkov S., Medvedev I., Arkhipkin V., Krechik V., and Dobrolyubov S. (2016). Numerical Modeling of the Wind Waves in the Baltic Sea using the Rectangular and Unstructured Grids and the Reanalysis NCEP/CFR. *Proceedings of the Hydrometeorological Research Center of the Russian Federation* (362), pp. 37-54 (in Russian with English summary).

Mokhov I., Semenov V., Khon V., and Pogarsky F. (2013). Change of sea ice content in the Arctic and the associated climatic effects, detection and simulation. *Led i Sneg*, 53(2), pp. 53-62.

Moss R., Babiker W., Brinkman S., Calvo E., Carter T., Edmonds J., ... and Jones R. N. (2008). *Towards New Scenarios for the Analysis of Emissions: Climate Change, Impacts and Response Strategies*.

Myslenkov S., Arkhipkin V., and Koltermann K.P. (2015a). Evaluation of swell height in the Barents and White Seas. *Moscow University Bulletin. Series 5. Geography* (5), pp. 59-66 (in Russian with English summary).

Myslenkov S., Platonov V., Toropov P., and Shestakova A. (2015b). Simulation of storm waves in the Barents Sea. *Moscow University Bulletin. Series 5. Geography* (6), pp.65-75 (in Russian with English summary).

Myslenkov S.A., Golubkin P.A. and Zabolotskikh E.V. (2016). Evaluation of wave model in the Barents Sea under winter cyclone conditions. *Moscow University Bulletin. Series 5. Geography* (6), pp.26-32 (in Russian with English summary).

Reistad M., Breivik O., Haakenstad H., Aarnes O. J., Furevik B. R., and Bidlot J. R. (2011). A high-resolution hindcast of wind and waves for the North Sea, the Norwegian Sea, and the Barents Sea. *Journal of Geophysical Research: Oceans*, 116(C5).

Rusu L., de León S., and Soares C. (2015). Numerical modeling of the North Atlantic storms affecting the West Iberian coast. *Maritime Technology and Engineering*, 978-1.

Saha S. et al. (2010). The NCEP climate forecast system reanalysis. *Bull. Am. Meteorol. Soc.*, 91(8), pp.1015-1057.

Saha S. et al. (2014). The NCEP Climate Forecast System Version 2. *J. Climate*. 27, pp. 2185-2208. DOI: 10.1175/JCLI-D-12-00823.1.

Soomere T. and Räämet A. (2014). Decadal changes in the Baltic Sea wave heights. *Journal of Marine Systems*, 129, pp. 86-95.

Soomere T., Behrens A., Tuomi L. and Nielsen J. (2008). Wave conditions in the Baltic Proper and in the Gulf of Finland during windstorm Gudrun. *Natural Hazards & Earth System Sci.*, 8(1), pp.37-46.

Stocker T. (Ed.). (2014). *Climate change 2013: the physical science basis: Working Group I contribution to the Fifth assessment report of the Intergovernmental Panel on Climate Change*. Cambridge University Press.

Stopa J., Arduin F., and Girard-Arduin F. (2016). Wave climate in the Arctic 1992-2014: seasonality and trends. *Cryosphere*, 10(4), pp.1605-1629.

Surkova G. (2015 October). Climate projection of storm weather patterns, In: Özhan, E. (Ed.). *Proceedings of the Twelfth International Conference on the Mediterranean Coastal Environment MEDCOAST 15*, Varna, Bulgaria, pp.531-540.

Surkova G., Arkhipkin V., and Kislov A. (2013). Atmospheric circulation and storm events in the Black Sea and Caspian Sea. *Central European Journal of Geosciences*, 5(4), pp.548-559. DOI : 10.2478/s13533-012-0150-7.

Surkova G. and Krylov A. (2017) Extremely Strong Winds And Weather Patterns // *Proceedings of the Thirteenth International Conference on the Mediterranean Coastal Environment MEDCOAST 17*. Turkey.

Taylor K. E., Stouffer R. J., and Meehl G. A. (2012). An overview of CMIP5 and the experiment design. *Bulletin of the American Meteorological Society*, 93(4), pp.485-498

Tolman H. L. (2009). User manual and system documentation of {WAVEWATCH-III} Version 3.14. US: Department of Commerce, National Oceanic and Atmospheric Administration, National Weather Service, National Centers for Environmental Prediction.

Wang X. L. and Swail V. R. (2001). Changes of extreme wave heights in Northern Hemisphere oceans and related atmospheric circulation regimes. *Journal of Climate*, 14(10), pp.2204-2221. DOI:10.1175/1520-0442(2001)014<2204:coewhi>2.0.co;2.

Zaitseva-Pärnaste I., Suursaar Ü., Kullas T., Lapimaa S., and Soomere T. (2009). Seasonal and long-term variations of wave conditions in the northern Baltic Sea. *J. Coast. Res.* SI(56) pp.277-281.



Stanislav A. Myslenkov is a Senior Researcher at the Department of Oceanology, Faculty of Geography, Lomonosov Moscow State University, Russia. He received the PhD in 2017. Research interests are wind waves, wave energy, ocean currents, experimental oceanography.

**Natalia Shabanova^{1*}, Stanislav Ogorodov¹, Pavel Shabanov²,
Alisa Baranskaya¹**

¹Faculty of Geography, Lomonosov Moscow State University, Moscow, Russia

²Shirshov Institute of Oceanology, Moscow, Russia

* **Corresponding author:** Nat.Volobuyeva@gmail.com

HYDROMETEOROLOGICAL FORCING OF WESTERN RUSSIAN ARCTIC COASTAL DYNAMICS: XX-CENTURY HISTORY AND CURRENT STATE

ABSTRACT. The Arctic coasts in permafrost regions are currently quickly retreating, being extremely vulnerable to the ongoing environmental changes. While the spatial variability of their retreat rates is determined by local geomorphological and cryolithological aspects, their temporal evolution is governed mainly by hydrometeorological factors, namely, wave action coupled to thermoabrasion (thermodenudation), are active during ice-free period. We define the combined wave and thermal action as “hydrometeorological stress”, and analyze its components and evolution, confirming it by known natural and remote sensing observations of coastal retreat rates. We estimated changes in the main hydrometeorological factors in the XX and XXI centuries for several sites on the coasts of the Kara and Barents Seas basing on observation and ERA reanalysis data. The term of hydrometeorological forcing is intended as an increment of the hydrometeorological stress, occurring because of changes of the hydrometeorological factors. Our results show that the current thermodenudation forcing amounts 15-50% of the 1979-1988 mean level and thermoabrasion forcing is equal to 35-130%. We detected 1989 (1993) – 1997 and 2005 – 2013 as periods of extreme hydrometeorological stress, as far as both thermodenudation and thermoabrasion were in a positive phase. It was also revealed that the hydrometeorological stress of the recent 10 years was apparently unprecedentedly high at the Barents-Kara region: the previous Arctic warming of the 1930-40s caused high thermoabrasion rates due to longer ice-free period despite cold summer temperatures, while, the latest ongoing warming shows previously unseen simultaneous increase in both thermodenudation and thermoabrasion.

KEY WORDS: western Russian Arctic, climate change, hydrometeorological factors, hydrometeorological stress, hydrometeorological forcing, coastal dynamics

CITATION: Natalia Shabanova, Stanislav Ogorodov, Pavel Shabanov, Alisa Baranskaya (2018) Hydrometeorological Forcing of Western Russian Arctic Coastal Dynamics: XX-Century History and Current State. *Geography, Environment, Sustainability*, Vol.11, No 1, p. 113-129
DOI-10.24057/2071-9388-2018-11-1-113-129

INTRODUCTION

At the beginning of the century, awareness has risen that changes in coastal systems are forced by large-scale processes and act over relatively long (decadal) timescales (Hanson et al. 2003). The persisting climate change allowed to trace changes in coastal dynamics caused by evolving hydrometeorological conditions. Such changes were described at arctic coasts with permafrost (Grigoriev et al. 2006, Günter et al. 2015, Jones et al. 2009, Rachold et al. 2005, Vasiliev et al. 2011, Ogorodov et al. 2016) and others summarized in (Lantuit et al. 2013) and tropical coasts (e.g., Livingston, 2014). One of the most intriguing topics is the behavior of Arctic coasts, as in most cases they are composed by continuous permafrost and contain ground ice; therefore, they may dramatically react to temperature growth. Indeed, in the last 15-20 years, increase of coastal retreat rates relatively to previous average values have been recorded in different Arctic regions (Günter et al. 2015, Jones et al. 2009, Vasiliev et al. 2011, Grigoriev et al. 2006, Vergun et al. 2013). Such increase might have been caused by the latest warming, more precisely, by the latest climate change, as not only temperature has been growing, but the whole land-ocean-atmosphere system has been changing, including winds and sea ice conditions, which, in their turn, influence sea coasts. Still, tracing the hydrometeorological effect on Arctic coastal dynamics is a difficult task, as studies of coastal dynamics are subject to several major challenges.

Challenges in studies of coastal dynamics: lack of observation data

The coasts of Russian Arctic (contrarily to the European Arctic and most part of the Canadian and US Arctic) are remote and difficult to access. They are rarely visited, the main purpose being oil and gas infrastructure construction and operation. Research activity in field is usually limited to short time periods. Fieldwork timeframes are determined by engineering and production requirements and are difficult to adjust to scientific tasks. Therefore, coastal dynamics observations are irregular both spatially

and temporally: coasts are observed in different months (not at the end of ice-free period, as preferable), sometimes not every year, with varying methods which are hard to compare. There is in fact no regular network for coastal observations, as polar hydrometeorological stations are not authorized to conduct coastal retreat rate measurements. Hydrometeorological data produced by these stations is hard to process for several reasons. Firstly, the network of stations is extremely scarce, the resolution ranging from 100 to 500 km. Secondly, the network of stations with long-term observations (not less than about 30 years, Fig. 1) is even more scarce. Thirdly, there are lots of temporal gaps due to a variety of reasons, referred both to data operation problems and periods with no observations, caused, in turn, by both economical and natural reasons (insufficient funding, understaff, fires and severe weather conditions). Finally, some of the data (like ice and sea level data) are of hard access, as they are of special usage according to regulations of the Russian Federation. The only way to obtain reliable and complete characterization of hydrometeorological conditions is to use modelling data, like reanalyses.

In coastal retreat rate studies, satellite imagery provides both good spatial and temporal coverage, however, it also faces several issues: 1) old-data imagery are of low resolution (7-10 m) and do not allow to detect the coastline with sufficient accuracy; 2) there is a problem in detecting the coastline itself (the position of the cliff edge, usually designated as the coastline, can in many cases be hard to recognize); 3) unfavorable weather conditions like sea ice and clouds make interpretation impossible.

In situ sediment transport measurements (like, for example, acoustic backscatter measurements of suspended sediment transport) are not used in the Russian Arctic. Estimations of changes in the coastal dynamics are usually based on measuring the position of the cliff edge in field at numerous cross-sections referenced to the State geodetic network or using remote

sensing data. Coastal retreat rates depend greatly on local geocryological, (ice content, presence of ice bodies), lithological (grain size, texture) geomorphological (height of the coastal bluff, etc.) conditions. At different sections they vary by the scales of 1-10 m. Therefore, it is challenging to combine annual in situ measurements with estimations of coastal dynamics on a long-term scale. As reported in (Aagard et al. 2004): «A significant problem in current coastal research is the understanding of linkages between morphological phenomena occurring on different temporal and spatial scales. Morphodynamic processes in the nearshore typically exhibit nonlinear behavior and consequently, phenomena which occur on short temporal (event) scales as, e.g. observed during field experiments have generally been difficult to upscale to provide an understanding of the long-term behavior of the coast on the time scale of seasons or decades».

Considering difficulties in direct observations of coastal destruction, one of the promising approaches is assessing not the retreat rates themselves, but the driving climatic factors of coastal dynamics. Such factors are easier to characterize, as data on hydrometeorological conditions can be obtained for much longer time periods and larger spatial extent, as they don't depend on high-resolution imagery availability and fieldwork measurements. In the present study, we aim to characterize and estimate the climatic-induced potential of coastal dynamics, determined as the quantitative expression of hydrometeorological impact on coasts. The mentioned potential varies from year to year and the coasts may experience it completely or not depending on their inner factors (grain texture, ice content, etc.). In this way, research of coastal dynamics obtains a way forward through estimation of its factors and their variability.

Hydrometeorological factors of the Arctic coastal dynamics

Coastal dynamics of the Russian Arctic are determined by two related processes. Ground ice in permafrost melts due to heat energy coming to the cliff from warm

air and sea water. This process is called thermodenudation. After the sediments melt, they are removed by direct wave action, which is called abrasion. The interaction of these two processes, when permafrost simultaneously thaws and is carried away by waves is called thermoabrasion, being the main mechanism of destruction for most of the retreating coasts in the cryolithozone. The intensity of thermoabrasion therefore depends on two main hydrometeorological parameters: temperature and wind-wave energy.

The thermal factor regulates the amount of heat, due to which permafrost exposed in the coastal cliffs, melts. It generally depends on air and water temperature, and the number of days with positive temperature, during which the processes of thawing are active.

The wind-wave energy, determining the intensity of mechanical abrasion, depends on a greater number of environmental conditions. Because most waves in the Russian Arctic seas are wind-generated, wind conditions play a crucial role in the wave energy flux formation. Wind speed, wind direction and frequency are therefore important parameters. It has been shown, for instance, that storms provide the largest contribution to the total amount of wind-wave energy (Popov, Sovershaev, 1982). Because during most of the year the Arctic seas are covered by ice, waves can execute their mechanical action only in the relatively short ice-free period. Consequently, the yearly wave energy flux providing abrasion is determined by the ice-free period duration. In its turn, the ice-free period duration depends on the Arctic sea ice cover conditions, likely related to global temperature and local (regional) weather conditions (wind directions and heat transfer). The length of the wave fetch is also important, and it generally also depends on the extent of the ice cover, as, during the summer, distance from the sea ice rim to a certain coastal point can change every day. In this way, Coastal dynamics depends on hydrometeorological processes of different scales, from global to local.

Climate change of the latest decades results in changes of all described conditions: wind, ice and thermal. In the present study, we aim to estimate thermal and wave-energetic impact on coastal retreat rates at several key areas of the Yamal Peninsula characterized by different permafrost and lithologic conditions. By doing this, we will be able to assess the importance of each of the mentioned hydrometeorological factor and quantify their impact on the retreat rates for a better understanding of coastal dynamics and their evolution through time.

Hydrometeorological stress and hydrometeorological forcing

The retreat rate Rr of an Arctic thermoabrasional coast composed by permafrost is determined by a combination of hydrometeorological forces, called here hydrometeorological stress or potential F :

$$Rr = \gamma F(f_1, f_2, \dots, f_N) = \gamma F(T, WE(n, p, x), \dots) \quad (1)$$

$$[\gamma] = m / J \quad (2)$$

where f_1, f_2, \dots, f_N are CD (coastal dynamics) hydrometeorological factors, including air temperature T , wind-wave energy WE depending, in its turn, on the ice-free period duration n , wave fetch x and shoreward storm frequency p . Here, γ is a parameter of sensitivity. It is equal to 0 for rocky coasts or coasts with no permafrost, and is apposite numeric value for frozen sediments, depending on their ice content (the greater the ice content is – the higher is γ). For specific local conditions (for example, the areas which contain ice bodies like ice wedges or tabular ground ice), γ may be extraordinarily high as such types of coasts may dramatically react to HM (hydrometeorological) forcing. Today, quantitative estimation of this sensitivity parameter remains subject to future studies. We use γ for quantitative description of the different reaction of coastal areas to hydrometeorological forcing, as their behavior shows great spatial variability: in the same year, some coasts retreat significantly when others may stay almost stable.

The hydrometeorological stress (potential) consists of two parts: 1) mechanical part, being the energy, coming to the coast from shoreward waves and called the wind-energetic potential of coastal dynamics, – and 2) thermal part, being the energy transmitted to the coasts from the atmosphere (CD thermal potential).

Hydrometeorological forcing is an increment of the hydrometeorological stress (potential), appearing due to changes of hydrometeorological factors. It can be divided into CD thermal forcing (F_T), caused by changes in temperature conditions, and CD mechanical forcing (F_{WE}), caused by wind-wave energy changes.

In the present study, we introduce the term «coastal dynamics hydrometeorological forcing» on the analogy of the radiative forcing used in climatology and IPCC reports (IPCC, 2001; Myhre et al. 1998). The increment Δf_i in i factor of coastal dynamics provokes coastal dynamics ΔF_i hydrometeorological forcing Δf_i , which, in its turn, leads to coastal retreat rate change ΔRr_i , associated with this factor with the specific sensitivity to this factor γ_i :

$$\Delta f_i \rightarrow \Delta F_i \rightarrow \Delta Rr_i \quad (3)$$

$$\Delta Rr_i = \gamma_i \Delta F_i \quad (4)$$

$$\Delta Rr = \sum_i^N \gamma_i \Delta F_i \quad (5)$$

CD hydrometeorological stress, as well as coastal retreat rate, is always positive for coasts composed by permafrost and can be characterized, for example, by its mean value during a certain period of interest. In these terms, hydrometeorological forcing is considered as a deviation of the current HM stress from the mean value, resulting in changing coastal retreat rates.

CD hydrometeorological stress is close to the term of “environmental forcing” used in literature (Forbes, 2011; Günter, 2013 et al.; Lantuit et al., 2013). Still, we use namely the term «hydrometeorological stress» in the present study, attempting, first of all, not to mix it with the term “forcing”.

widely used in climate change research and, secondly, aiming to emphasize the hydrometeorological aspect of the object under investigation.

RESEARCH AREA

In the present study, we focus on the western and central Russian Arctic coasts. We are continuing and extending previous work done for Pechora Sea coasts (Varandey area) and Western Yamal coasts (Marresalya area) and Western Yamal coasts (Marresalya and Baydaratskaya Bay areas) (Vergun et al. 2013; Ogorodov et al. 2016). To be able to compare measured monitoring data to the results of hydrometeorologic factors' estimations, we mostly took sites with long-term field monitoring data showing natural observations on coastal retreat rates, mostly gathered by the Laboratory of geocology of the North, MSU since the 1980s until present.

We also expand the research area over the northern part of the Barents-Kara region, adding Frantz-Joseph Land and several Kara Sea islands (Belyi and Vize islands) (Fig. 1).

MATERIALS AND METHODS

Estimation of the thermal potential of thermodenudation

The thermal potential of thermodenudation is estimated by the air thawing and freezing indexes (I_{at} and I_{af} , respectively) showing the number of positive/negative °C-days per year (Andersland and Ladanyi, 2004). A similar parameter called degree days thawing was used in Günter et al. 2015. These indexes are the evaluations of the annual amount of heat added to or extracted from the ground and permafrost during warm and cold periods, respectively. For their calculation, we used both observation and reanalysis data since 1979. It is assumed that I_{at} can be reliably calculated if there are observations for 90% of summer days (June–September). The same applies for winter temperatures: we need not less than 218 (of 243) daily means for January–May and October–December. Several tests with years of complete data (1979–2013) showed that in the case of missing data, the underestimation of the values of I_{at} and I_{af} is approximately equal to the percentage of missing days. This allows

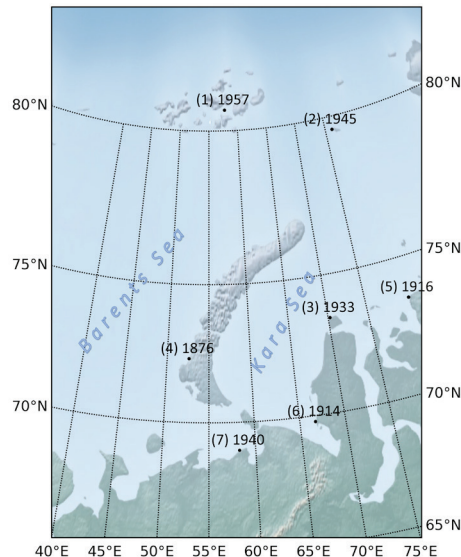


Fig. 1. Research area and hydrometeorological long-term observation stations (the year when observations started indicated in green): (from North to South) 1) Krenkelya Hydrometeorological Observatory (Heiss island); 2) Vize Island; 3) Popova station (Belyi Island); 4) Malyie Karmakuly (Novaya Zemlya arch.); 5) Dikson island; 6) Marresalya (Western Yamal); 7) Varandey (Pechora Sea coast)

us to reconstruct I_{af} and I_{af} for the years with missing data by dividing the accumulated value by the percentage of present daily means.

Along with observational data, ERA Interim (Dee et al. 2011) and ERA 20C reanalyses (Poli et al. 2016) were used. Reanalysis data were compared to observational data (Table 1). Mean I_{af} differences amount 15-16% (relatively to mean values) for both reanalyses. I_{af} means differ by 16% for ERA Interim and 27% for ERA 20C. Reanalyses samples are corrected for these errors. The root mean square error of corrected samples and observational data does not exceed 12% for I_{af} , and the correlation coefficient amounts 0.87-0.89. The variance of the observational data is by 20-30% higher than for reanalyses' data.

For I_{af} the RMSE (root mean square error) is much lower compared to the summer temperatures and amounts 4-5% of the mean value. Correlation between reanalyses and observations reaches 0.94-0.96. The observation variance is by 8% lower than the variance of the values reproduced by ERA.

Ice-free period duration assessment

Daily sea ice concentration data were analyzed using the 12.5 km resolution product of Norwegian and Danish meteorological Institutes (EUMETSAT, 2014), following the study by Günter et al. 2015, where another 25 km resolution product of NASA was used with application to Buor Khaya Bay. With its help, open water days (OWD), which are equivalent to the ice-free period duration (IFP), were calculated for the period of 1979-2014 (35 years).

All sea ice concentration satellite products are affected by large uncertainties over low sea ice concentrations and open water in coastal zone. Nevertheless, it appeared possible to detect the start and end dates of ice-free period. In the Barents-Kara region, the start of the ice-free period and the freeze-up are usually expressed in abrupt changes on the annual curve

of sea ice concentration. These changes can be objectively detected. The ice-free period duration, derived from satellite data by the described method, was compared to observational data for Varandey and Marresalya stations. The accuracy of the method is 12 days on the average (5 days at the beginning of the period and 7 days for the freeze-up). In three of the 35 cases it reached 40-55 days which can be considered as a large uncertainty. Despite that, the interannual variability features and trends are similar for both observational and satellite data. In this way, although the described data and methodology should be used with care for precise detection of the ice-free period duration, it shows good results for revealing long-term trends and general features of the main factors of coastal dynamics evolution.

The assessment of coastal dynamics' wind-wave-energetic potential: Popov-Sovershaev method

The wave energy (WE), tentatively called «wave-energy flux», was calculated according to the Popov-Sovershaev method (Popov and Sovershaev, 1982, Ogorodov, 2002). The method is based on the wave processes theory and applies correlations between wind speed and parameters of wind-induced waves. WE is expressed as the mass of water coming to the coastline per ice-free season (tons/yr). In the Popov-Sovershaev method, the wave energy flux (tons/yr) is proportional to the wind speed (V) to the power of three, to the ice-free period duration (n), wave fetch (x) and frequency of wave-generating winds (p).

For deep-water conditions, when the sea floor does not affect wave formation, the wave energy flux per second (for 1 m of wave front) at the outer coastal zone

$$WE = 3 \times 10^{-6} V^3 x \quad (6)$$

boundary is calculated using the equation: where V is the real wind speed of a chosen direction measured by anemometer at 10 m above sea level [m/s], x is wave fetch [km] along the current wind direction. The dimension of the coefficient corresponds

Table 1. Comparison of the ERA Interim and 20C reanalyses' data with observational data for the three stations in the Kara and Barents Seas: means, variances, systematic deviations (SD), RMSE (root mean square error) values of corrected to SD (standard deviation) values and correlation coefficients. A) Air thawing index I_{at} ; B) air freezing index I_{af}

Station	Mean values			SD – systematic deviation			Variance values			RMSE of SD-corrected			Correlation coefficient	
	Obs	Interim	Clim	Int-Obs	Clim-Obs	Obs	Interim	Clim	Int-Obs	Clim-Obs	Int-Obs	Clim-Obs	Int-Obs	Clim-Obs
Marre-salva	mo	mi	mc	mi-mo	mc-mo	do	di	dc	ri	rc	ci	cc		
	672	780	577	108	-95	155	136	108	56	76	0.95	0.89		
Popova				<i>0,16*</i>	<i>0,14*</i>				<i>0,08*</i>	<i>0,11*</i>				
	413	329	457	-84	44	104	74	88	59	50	0.82	0.87		
Varan-dey				<i>0,20*</i>	<i>0,11*</i>				<i>0,14*</i>	<i>0,12*</i>				
	874	977	691	102	-183	186	153	139	83	100	0.89	0.84		
Mean				<i>0,12*</i>	<i>0,21*</i>				<i>0,10*</i>	<i>0,12*</i>				
	653	695	575	42	-78	148	121	112	66.7	75.9	0.89	0.87		
			0.16*	0.15*					0.11*	0.12*				

* proportion of observation mean value (mo)

Station	Mean values			SD – systematic deviation			Variance values			RMSE of SD-corrected			Correlation coefficient	
	Obs	Interim	Clim	Int-Obs	Clim-Obs	Obs	Interim	Clim	Int-Obs	Clim-Obs	Int-Obs	Clim-Obs	Int-Obs	Clim-Obs
Marre-salva	mo	mi	mc	mi-mo	mc-mo	do	di	dc	ri	rc	ci	cc		
	-3283	-3606	-3951	-323	-667	427	494	467	155	131	0.95	0.96		
Popova				<i>0,10*</i>	<i>0,20*</i>				<i>0,05*</i>	<i>0,04*</i>				
	-3818	-3419	-4305	399	-487	400	397	415	85	166	0.98	0.91		
Varan-dey				<i>0,10*</i>	<i>0,13*</i>				<i>0,02*</i>	<i>0,04*</i>				
	-2605	-3334	-3891	-730	-1286	398	441	441	113	135	0.97	0.95		
Mean				<i>0,28*</i>	<i>0,49*</i>				<i>0,04*</i>	<i>0,05*</i>				
	-3235	-3453	-4048	-217	-813	408	443	441	118	144	0.96	0.94		
			0.16*	0.27*					0.04*	0.05*				

* proportion of observation mean value (mo)

to the dimensions of p/g , where w is density [t/m^3], and g is gravitational acceleration [m/s^2]. Thus, WE has dimension of tons per second:

$$\frac{t}{m^3} \cdot \frac{s^2}{m} \cdot \frac{m^3}{s^3} \cdot m = \frac{t}{s} \quad (7)$$

For the whole ice-free period, the wave energy flux is equivalent to the water mass coming to the coast expressed in tons.

Wave directions, wave fetches and depths were obtained from digital elevation model ETOPO1 (Amante and Eakins, 2009). The frequency of wave-generating winds was calculated for the time of the ice-free period. For wind data, ERA Interim reanalysis was used. The Popov–Sovershaev method is based on wave processes theory, and applies correlations between wind speed and parameters of wind-induced waves. Wind speeds from 6 m/s and higher were used, as it had been shown in (Popov and Sovershaev, 1982) that the effect of weaker winds (velocities <6 m/s) is negligible for geomorphological coastal studies. The ice-free period duration was determined with the help of satellite imagery data, as shown in 2.2.

Objective periodization: residual-mass curve method

The residual mass curve method was used to detect periods of increased and decreased hydrometeorological stress. The RM-curve method provides the relative intensity of the parameter to its long-term mean value. The RM-curve method is commonly used in hydrology. Modular coefficients are calculated as the relation of current annual value X_i to the long-term mean value :

$$K_i = \frac{X_i}{\bar{X}} \quad (8)$$

The deviation of K_i from one is positive if the current value is higher than the mean value and negative if it is lower than the mean. If K_i are positive for several subsequent years, the accumulating K_i will result in the growth of the sum $\sum_i K_i$ (ascending branch of the $\sum_i K_i$ curve).

When the period of low values begins, the curve starts to descend. The bend of the curve gives evidence of the end or beginning of the period with high or low values. To compare temperature and wave-energy curves anomalies $(X_i/\bar{X}-1)$ can be divided by the variation coefficient C_v with the purpose to equalize the scales of fluctuations:

$$X_{-N_i} = \frac{X_i/\bar{X}-1}{C_v} = \frac{X_i - \bar{X}}{\delta} \quad (9)$$

where δ is the standard deviation and " N_i " in X_{-N_i} means "normalized by standard deviation". The RM-curve values are calculated through accumulation:

$$X_{-RM_i} = \sum_i X_{-N_i} \quad (10)$$

This method has limitations related to the dependence of result on the mean values of the studied parameters. The method is suitable for cyclic processes where the oscillation magnitude is constant during several periods of oscillation. If the oscillation with the outstanding magnitude occurs, the mean value moves much higher/lower than the usual value. In such case, it is harder for the deviation $X_i - \bar{X}$ to reach positive/negative values and the determination of high-value/low-value period becomes difficult. However, the ascending/descending branch of the RM-curve does not occur in this case, the derivative of the curve noticeably changes if there are the up-trend/down-trend values in the original series and the high/low-value period may be detected using the RM-curve derivative analysis.

RESULTS

The retreat of the Arctic coasts in the XX century

In the last years, many reviews of coastal erosion rates in the Arctic appeared (Lantuit et al. 2013, etc.). For comparison with the variability of hydrometeorological parameters, we collected literature data covering long time intervals (Table 2),

allowing to divide it into periods, similarly to the large-scale oscillations of the coastal dynamics' hydrometeorological factors.

In the Arctic, coastal retreat rates were increasing and decreasing at different times in different regions. Generally speaking, periods of heightened erosion rates occurred from about 1985 to 1995 and from 2002 to present; low values were noted from about 1995 to 2002. In the recent years, some of the coasts experienced accelerated erosion. The Kara Sea coasts also started retreating faster, as it was noticed during field monitoring and with the help of remote sensing data in the Varandey area (Pechora Sea), and on the coasts of the Baydaratskaya bay, Kara Sea (Ogorodov et al. 2016). In the Kharasavey region, the years 2006-2016 are characterized by 1.5-3 times higher retreat rates compared to 1964-2006 mean (Belova et al. 2017). At Muostakh island (Laptev Sea), the 2010-2012 mean coastal retreat rate reached 4.1 ± 2.0 m/year, which is 2.3 times faster than the historical (1951-2012) mean (Günter et al. 2015).

Both authors notice that the highest acceleration is observed at sites with high ground ice content in the frozen sediments and underline the role of thermodenudation.

It is also remarkable that in the Eastern Siberian Seas the period of 1935-45 was characterized by high retreat rates

(Grigoriev et al. 2006). For other Arctic seas, there is little known about this period as observations were not yet conducted on a regular basis back in the 1930s-1940s. We will further suggest an explanation to the increased coastal retreat rates at that time.

Evolution of the hydrometeorological stress in 1979-2015

Thermal stress evolution

The process of thermodenudation is determined by thermal conditions, above all, by summer temperatures, leading to thawing of the permafrost. The XX-century evolution of I_{at} gives evidence that the latest warming of the 1990s-2000s was high, but comparable to previous increases of the 1950-60s and 1920s (Fig.2A). 1922, 1923 and 1924 in sense of I_{at} are still record warm.

An unusual aspect of the current warming is that since the 1980s, both summer and winter temperatures have evolved in-phase, which had never been observed before. The latest warming is often compared to the previous great Arctic warming of 1930-40s which was expressed in the rise of the mean annual temperatures. Some stations' historical maximums are still related to the period of 1940-1945, and the current warming has not still managed to break these records. However, the analysis of the air freezing and air thawing indexes shows that the warming of 1930-40s is provided

Table 2. Coastal erosion rates in different Arctic regions and periods (XX-XXI cent.): literature data

Reference	Region	Method	Erosion rates, m/year (averaged for the indicated periods)				
Jones, 2009	Alaska, Beaufort Sea	Satellite images		1955-79 6.8	1979-2002 8.7		2002-07 13.6
Vasiliev, 2011	Western Yamal, Kara Sea	Direct field observations		1978-81 ~1.2	1988-1992 1.7-3.5	1997-2002 ~1	2006-10 ~2.5
Grigoriev, 2006	Eastern Siberian Seas	Literature sources and others	~1935-45 ~6-7	~1955-65 ~3	~1985-1995 ~5-6	The beg. of 2000s ~2	

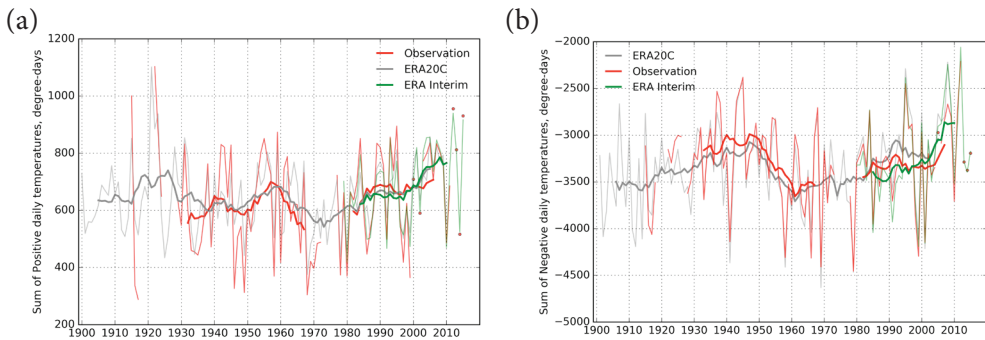


Fig. 2. Air thawing (I_{at}) – a – and air freezing (I_{af}) – b – indexes at Marresalya station calculated using observational and reanalyzes' data. Bold lines show 11-year running mean values' evolution

by increased winter temperatures only (Fig. 2B), while summer temperatures were close to low values. Consequently, it is reasonable to expect higher thermodenudation potential to be more likely related to the 1950-60s, rather than to 1930-40 as previously expected.

The current thermodenudation potential is therefore unprecised as it is provided by both high I_{at} , provoking weaker freezing in winter, and I_{af} , making the ice melt effectively in summer.

Within the latest 35 years, generally characterized by positive trends in I_{af} and I_{at} (on the average 17.3 and 5.7 degree-days per year respectively, see table 3), there were periods of heightened and decreased values of these two parameters. Residual mass curve analyses for 11 stations showed that 1988 – 1994 and 2004 – 2014 may be considered as I_{at} and I_{af} positive-phase, and 1995 – 2003 as a negative phase (Belova et al. 2017, Shabanova, Channellier, 2013).

Ice free period extension

The median value of the ice-free period duration in the Barents-Kara region increased by about 30 days (43% per 35 years) (Fig. 3). Such prolongation occurred, above all, due to earlier ice melt (by about 19 days). This agrees well with the results by (Günter et al. 2015) obtained for the Laptev Sea: the Buor Khaya Bay cleared up by 10 days earlier in 2010-2012 compared to 1992-2012 mean, and froze up by 5 days later only.

Similarly, to I_{at} and I_{af} , the ice-free period duration evolution has three main features: 1) positive trend; 2) relatively low values in 1996-1999; 3) extremely high values after 2004. It is remarkable that the scatter of IFPD in different locations may reach 160-170 days for the same year; however, scatter disappears when negative and positive phases occur: in 1998-99 and 2009-2010 it was equal to 20 – 55 days. This gives evidence of the large scale of processes leading to the described IFPD evolution.

The most considerable changes of IFPD happened around Franz-Josef Land, where IFPD for some years was close to 10 days and in 2008 – 2013 was consistently higher than 70. For Franz-Joseph Land, the IFPD extension amounts 300-700%. It means that the coasts of these islands, previously almost unexposed to waves, now experience the action of thermoabrasion during at least two months every year. This inevitably leads to activation coastal erosion, marked in the natural observations of the recent years (Romanenko et al. 2015). Some field works were conducted here in 2012-2015. The benchmarks installed in 2012 allowed to reveal for the first time ever the coastal retreat rates for Aldger Island. It amounts to 1.7 m/year. Here the thermoabrasion is of great importance as it threatens lots of historical monuments of the archipelago with extinction or damage, thus impeding the activity of the national park «Russian Arctic».

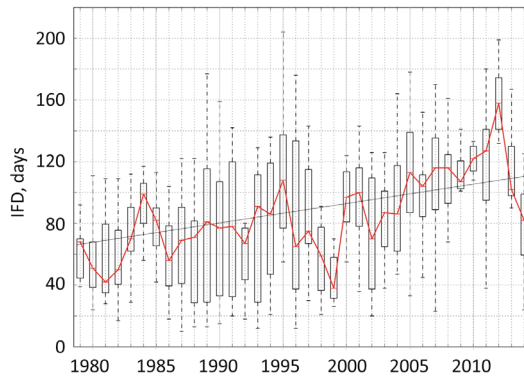


Fig. 3. Ice-free period duration at 11 stations of Barents-Kara region determined using EUMETSAT (EUMETSAT, 2014) satellite data product. “Boxes” show 25 and 75% quantiles, whiskers – the highest and the lowest values. The red line indicates the median evolution, the black line shows the trend of the median value

Marresalya ice observation data, available from 1929, reveal the IFPD maximum corresponding to the warming of 1930-1940s and the positive trend of 1985-2012. The period of 1960-1984 is characterized by a negative phase of IFPD.

Wave energy stress evolution

The wave-energy flux evolution partly follows the IFPD evolution as they are in linear dependence (Fig. 4). The difference occurs due to wave-dangerous wind frequency evolution. It appeared that NW winds frequency fluctuates similarly to I_{at} , reaching a local minimum in 1996 – 2002 and local maximums in 1988 – 1995 and 2003-2013, respectively. This gives the evidence that western coasts experience

more intense wave-energy forcing compared to coasts with other orientation. Western coasts are characterized by positive WE trends: Marresalya’s WE trend is significant at 0.05 significance level (see Table 3), while other coasts and all-stations-mean trends are positive, but insignificant even at 0.1 level.

In terms of mean values, the WE flux has increased by 70% compared to 1979 – 1988 mean. This increase is less than the within-sample variance, that is why the trend can’t be considered significant.

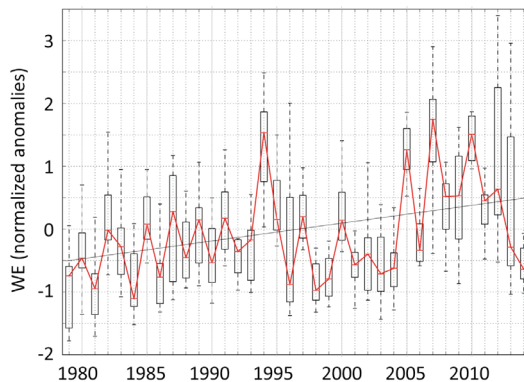


Fig. 4. Wave energy flux evolution at 11 stations of the Barents-Kara region expressed in anomalies divided by standard deviation. “Boxes” show 25 and 75% quantiles, whiskers – the highest and the lowest values. The red line indicates the median evolution, the black line shows the trend of the median value

Total hydrometeorological stress evolution

For the general estimation of the total hydrometeorological stress evolution, both thermoabrasional and thermodenudational potentials were analyzed. They have similar evolution with maximums in 1989 (1993) – 1997 and 2005–2013, respectively. The 1998 – 2004 period is characterized by low values of both potentials. The anomalies of both parameters normalized by standard deviation were summed to calculate total (combined wave-energetic and thermal) stress, equal to the overall hydrometeorological stress of coastal dynamics. Its evolution in 1979 – 2015 and periodization is shown in Figure 5.

It has been revealed that up to 2014 the total stress has increased by about 100% if compared to the 1979 – 2014 mean value. Trends' characteristics of both thermodenudation, thermoabrasion and total HM stress are presented in Table 3.

DISCUSSION

During the last 35 years, total hydrometeorological stress has increased by about 100% for Yamal, Pechora Sea and Franz-Josef land regions. At that thermodenudation forcing amounts 15-50% of 1979-1988 mean level and thermoabrasion forcing is equal to 35-130%. The last one, however, cannot be considered significant in terms of statistics.

Table 3. Characteristics of hydrometeorological forces' trends at the Kara and Barents Seas stations based on data from 1979 – 2015. Trends which are significant at 0.01 level are marked by bold italics, at 0.05 level by italics

HM factor	Trend characteristic	Popova	Marresalya	Varandey	Mean
Air thawing index (I_{at})	Trend (°C-days/year)	5.5	4.3	7.3	5.7
	37-year increment (% of 1979 - 1988 mean value)	53	15	36	35
	37-year increment (% of 1979 - 2014 variance)	1.7	1	1.4	1.4
	p-value	0.0016	0.074	0.0116	0.028
Air freezing index (I_{af})	Trend (°C-days/year)	23.9	13.5	13.9	17.1
	37-year increment (% of 1979 - 1988 mean value)	22	26	19	22
	37-year increment (% of 1979 - 2014 variance)	1.7	1.1	1.2	1.33
	p-value	0.0016	0.073	0.031	0.035
Wave energy flux (WE)	Trend (tons/year)	4455	10763	8499	7906
	37-year increment (% of 1979 - 1988 mean value)	37	129	44	70
	37-year increment (% of 1979 - 2014 variance)	0.56	1.4	0.84	0.93
	p-value	0.34	0.014	0.16	0.17

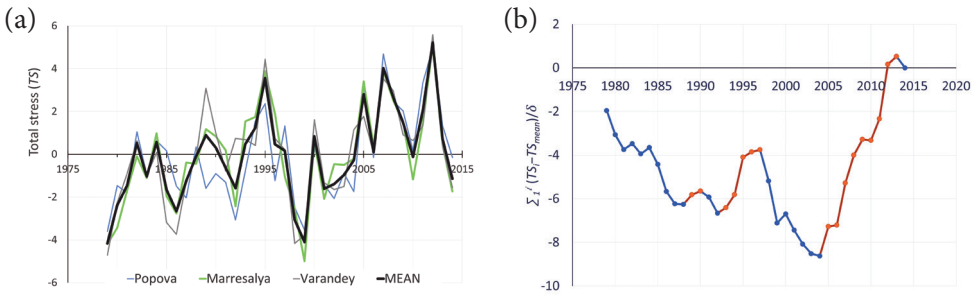


Fig. 5. a) Total hydrometeorological (combined wave energetic and temperature) stress at the Popova, Marresalya and Varandey coasts. b) Residual mass curve for the total stress, averaged among Popova, Marresalya, Varandey. Red dots and lines indicate ascending branches of RM-curve, blue dots and lines show descending branches

Still, all the thermoabrasion (wave energy) components, including the ice-free period duration and storms frequency demonstrate the same evolution as thermodenudation. Consequently, the periods of 1989 (1993) – 1997 and 2005 – 2013 are characterized by extreme hydrometeorological stress, as far as both thermodenudation and thermoabrasion processes were in a positive phase. In 1979 – 1988 and 1998 – 2004, both thermoabrasion and thermodenudation were in a negative phase. Scarce data on coastal retreat rates' evolution derived from literature and natural observations, confirm these trends in the evolution of the hydrometeorological factors.

Generally, the fact that the ice-free period duration (IFPD) extension is followed by local temperature growth, is logical and can be easily predicted. It is also inevitable, that in this case, the wave energy flux increases as well, being a linear function of the IFPD. The new and unexpected result is that temperature and IFPD growth is accompanied by wave-dangerous winds frequency increase, provoking the record-breaking hydrometeorological stress for west-oriented coasts. Moreover, although, in theory, a link between summer temperatures and the ice-free period duration can be expected, our results are showing that during the XX century (at least, starting from the 1920-s), there was apparently no period when both summer temperatures (being is crucial for thermodenudation) and the ice-free period duration (important for thermoabrasion) simultaneously increased, the only exception being recent 15-year

period. The Arctic warming of the 1930-40s was characterized by warm winters and long ice-free period, while summer temperatures were close to the local minimum. The local maximum of summer temperatures was observed in the 1950s, when there were less open water days. Contrarily to the warming of the 1930-40s, the current warming is expressed in both summer and winter temperatures increase together with the ice-free period growth. Figure 6 shows that before 1968, the IFPD and were negatively correlated and every year after 1967, positive linear linkage grew. Since 1989, the correlation coefficient exceeds 0.39, which is significant at 0.01 level. Since 2007, it has exceeded 0.65, which is statistically significant and means that in 1967 – 2007 (and after that), the IFPD and are linearly linked to each other to a considerable degree.

The mentioned facts lead to a disputable conclusion that as the latest warming differs from the previous one in its parameters and evolution, it should be caused by other reasons and mechanisms. Such idea may serve as indirect support to the anthropogenic explanation of the current warming. The conception also supposes that the latest warming "switched on" all the hydrometeorological forces of Arctic coastal dynamic (thermal, sea ice, winds), while previously (at least in XX century) they were "switched on" optionally and not simultaneously.

High hydrometeorological stress of the recent years is visibly expressed in an

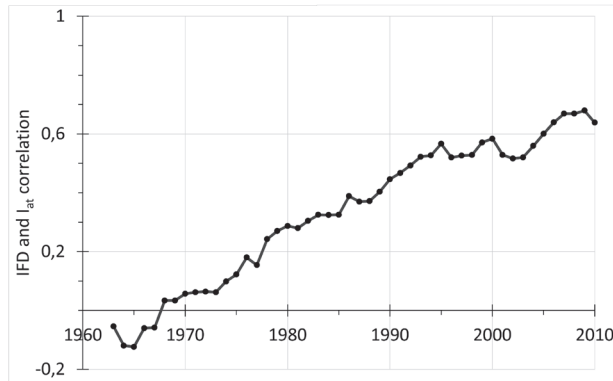


Fig. 6. Evolution of the correlation coefficient between the Air Thawing index (I_{at}) and the ice-free period duration (IFPD) at Marresalya station. The value for every year expresses the correlation of the samples over the previous 40 years (for example, in 2010 – for the period 1971-2010). This can be interpreted like a 40-year-running correlation coefficient

increase of the coastal retreat rates through the whole Arctic basin (Jones et al. 2009; Vasiliev et al. 2011; Günter et al. 2015; Belova et al. 2017). The intensification of thermodenudation process is confirmed by temperature data. The highest acceleration in coastal retreat is observed at the sites with ice-rich permafrost, which underlines the role of the thermodenudation process. The western coasts experience the highest HM forcing, as their thermoabrasion intensification occurs due not only to the IFPD prolongation, but also to an increase of wave-dangerous winds' frequency. Coasts of all orientation experience thermoabrasion and thermodenudation intensification due to climate change.

CONCLUSION

In this study the term of hydrometeorological forcing as distinct to hydrometeorological stress was intended and used for the assessment of the current Arctic coastal dynamics' state. Hydrometeorological stress sizes up the level of HM factors' exposure to coasts. HM forcing is an increment of HM stress appearing to change of coastal dynamics' HM factors'.

Annual sum of daily positive temperatures is used to assess thermodenudation forcing. Thermoabrasion forcing is determined through wave-energy flux calculation. Both thermodenudation and thermoabrasion factors evolution from 1979 to 2015 was

analyzed together with ice-free period duration and wave-dangerous winds' directions frequency.

The variety of data is used in the study. Both observation and reanalysis data are used for thermal condition description. ERA Interim describes the "modern" period of 1979-2015 and ERA 20C was brought in to cover the whole XX-century (1900 – 2010). It is shown that ERA reanalyzes data are suitable for long-term interannual and interdecadal evolution of temperatures over the Barents and Kara regions. ERA Interim reanalysis wind data were also used for wave energy flux calculation.

We brought in the satellite data product (EUMETSAT, 2014) to determine the ice-free period start and end dates and duration and ETOPO1 digital elevation model for wave-energy flux calculation.

We revealed that thermodenudation forcing amounts 15-50% of the 1979-1988 mean level and thermoabrasion forcing is equal to 35-130%. The periods of 1989 (1993) – 1997 and 2005 – 2013 are characterized by extreme hydrometeorological stress, as far as both thermodenudation and thermoabrasion were in a positive phase. In 1979 – 1988 and 1998 – 2004, both thermodenudation and thermoabrasion were in a negative phase. Data on coastal retreat rates' evolution derived from literature and natural observations,

confirm these trends in the evolution of the hydrometeorological factors. It was also revealed that the hydrometeorological stress of the recent 10 years was apparently unprecedentedly high at the Barents-Kara region: the previous Arctic warming of the 1930-40s caused high thermoabrasion rates due to longer ice-free period despite cold summer temperatures, while, the latest ongoing warming shows previously unseen simultaneous increase in both thermodenudation and thermoabrasion. To obtain more details on the evolution, characteristics and mechanisms of the hydrometeorological forcing in different parts of the Russian Arctic, more detailed

data on coastal retreat rates are required. As field monitoring and remote sensing data analysis are quickly evolving, there is good perspective of revealing the nature and possible development of the current climate change and its impact on the vulnerable Arctic coasts.

ACKNOWLEDGEMENTS

The work was executed with the financial support of the Russian Science Foundation Project No. 16-17-00034. ■

REFERENCES

- Aagaard T., Davidson-Arnott R., Greenwood B., Nielsen J. (2004). Sediment supply from shoreface to dunes: linking sediment transport measurements and long-term morphological evolution. *Geomorphology*, 60, pp. 205-224. DOI: 10.1016/j.geomorph.2003.08.002.
- Amante C. and Eakins B.W. (2009). ETOPO1 1 Arc-Minute Global Relief Model: Procedures, Data Sources and Analysis. NOAA Technical Memorandum NESDIS NGDC-24. National Geophysical Data Center, NOAA. DOI: 10.7289/V5C8276M [Assessed 15 October 2016].
- Andersland O.B. and Ladanyi B. (2004). *Frozen Ground Engineering*. 2nd Edition. Hoboken, New Jersey: John Wiley & Sons.
- Belova N.G., Shabanova N.N., Ogorodov S.A., Kamalov A.M., Kuznetsov D.E., Baranskaya A.V., Novikova A.V. (2017). Dynamics of thermoerosional coasts of Kara Sea on the example of the Cape Kharasavey area, (Western Yamal). *Earth's Cryosphere*, V. XXI, №6, pp. 85-96. DOI: 10.21782/KZ1560-7496-2017-6(85-96).
- Dee D.P., Uppala S.M., Simmons A.J., Berrisford P., Poli P., Kobayashi S., Andrae U., Balmaseda M.A., Balsamo G., Bauer P., Bechtold P., Beljaars A.C.M., van den Berg L., Bidlot J., Bormann N., Delsol C., Dragani R., Fuentes M., Geer A.J., Haimberger L., Healy S.B., Hersbach H., Hólm E.V., Isaksen L., Kållberg P., Köhler M., Matricardi M., McNally A.P., Monge-Sanz B.M., Morcrette J.-J., Park B.-K., Peubey C., de Rosnay P., Tavolato C., Thépaut J.-N. and Vitart F. (2011). The ERA-Interim reanalysis: configuration and performance of the data assimilation system. *Q.J.R. Meteorological Society*, 137, pp. 553–597. DOI: 10.1002/qj.828.
- EUMETSAT Ocean and Sea Ice Satellite Application Facility. Global sea ice concentration reprocessing dataset 1978-2015, (v1.2). (2015). Norwegian and Danish Meteorological Institutes. [online] Available at: <http://osisaf.met.no> [Accessed 20 October 2016].
- Forbes D.L. (editor). (2011). *State of the Arctic Coast 2010 – Scientific Review and Outlook*. International Arctic Science Committee, Land-Ocean Interactions in the Coastal Zone, Arctic Monitoring and Assessment Programme, International Permafrost Association. Geesthacht, Germany: HelmholtzZentrum.

Grigoriev M.N., Razumov S.O., Kunitskiy V.V., Spector V.B. (2006). Eastern Russian Arctic seas coastal dynamics: main factors, laws and tendencies. *Earth's Cryosphere*, № 4, pp. 74–95.

Günther F., Overduin P.P., Yakshina I.A., Opel T., Baranskaya A.V. and Grigoriev M.N. (2015). Observing Muostakh disappear: permafrost thaw subsidence and erosion of a ground-ice-rich island in response to arctic summer warming and sea ice reduction. *The Cryosphere*, 9 (1), pp. 151-178. DOI: 10.5194/tc-9-151-2015.

Hanson H., Aarninkhof S., Capobianco M., Jiménez J.A., Larson M., Nicholls R.J., Plant N.G., Southgate H.N., Steetzel H.J., Stive M.J.F. and H.J. de Vriend. (2003). Modelling of Coastal Evolution on Yearly to Decadal Time Scales. *Journal of Coastal Research*, Vol. 19, No. 4, pp. 790-811.

IPCC 2001: Climate Change 2001: The Scientific Basis. Contribution of Working Group I to the Third Assessment Report of the Intergovernmental Panel on Climate Change [Houghton J.T., Y. Ding, D.J. Griggs, M. Noguer, P.J. van der Linden, X. Dai, K. Maskell and C.A. Johnson (eds.)]. (2001). Cambridge University Press, Cambridge, United Kingdom and New York, NY, USA, 881pp.

Jones B.M., Arp C.D., Jorgenson M.T., Hinkel K.M., Schmutz J.A., Flint P.L. Increase in the rate and uniformity of coastline erosion in Arctic Alaska. *Geophysical Research Letters*, 36, L03503. DOI: 10.1029/2008GL036205

Myhre et al. (1998). New estimates of radiative forcing due to well mixed greenhouse gases. *Geophysical Research Letters*, Vol. 25, No. 14, pp. 2715–2718.

Lantuit H., Overduin P.P., Wetterich S. (2013). Recent Progress Regarding Permafrost Coasts. *Permafrost and Periglacial Processes*, 24, pp. 120–130. DOI:10.1002/ppp.1777.

Livingston R.J. (2014). *Climate Change and Coastal Ecosystems: Long-Term Effects of Climate and Nutrient Loading on Trophic Organization*. New York: CRC Press.

Ogorodov S.A. (2002). Application of wind-energetic method of Popov-Sovershaev for investigation of coastal dynamics in the Arctic. *Ber. Polarforsch. Meeresrosch.*, pp. 37-42.

Ogorodov S.A., Baranskaya A.V., Belova N.G., Kamalov A.M., Kuznetsov D.E., Overduin P.P., Shabanova N.N., Vergun A.P. (2016). Coastal dynamics of the Pechora and Kara seas under changing climatic conditions and human disturbances. *Geography, environment, sustainability*, v.9, №3, pp. 53-73.

Poli P., Hersbach H., Dee D.P., Berrisford P., Simmons A.J., Vitart F., Laloyaux P., Tan D.H., Peubey C., Thépaut J., Trémolet Y., Hólm E.V., Bonavita M., Isaksen L. and Fisher M. (2016). ERA-20C: An Atmospheric Reanalysis of the Twentieth Century. *Journal of Climate*, 29, pp. 4083–4097.

Popov B.A., Sovershaev V.A. (1982). Some features of the coastal dynamics in the Asian Arctic, *Geography questions*, 119. *Sea coasts*. Moscow, Mysl', pp. 105–116 (in Russian).

Rachold V., Are F.E., Atkinson E.D., Cherkashov G. and Solomon S.M. (2005). Arctic Coastal Dynamic (ACD). *Geo-Mat Letters* (25), pp. 63-203.

Romanenko F.A., Shilovtseva O.A., Shabanova N.N., Kononova N.K. (2015). Arctic climate change, natural hazards and Franz-Jozef Land relief dynamics, Changing climate and socio-economical potential of Russian Arctic under edition of Sokratov S.A. V.1, Moscow, Liga-Vent, pp.58-73 (in Russian).

Shabanova N.N., Channellier C.C. (2013). Climate change on the Yamal Peninsula and its impact on the exogenous processes. Society of Petroleum Engineers - SPE Arctic and Extreme Environments Conference and Exhibition, AEE 2013, V 3, pp. 70-81

Vasiliev A.A., Shirokov R.S., Oblogov G.E. and I.D. Streletskaia. (2011). Coastal Dynamics of the Western Yamal. Earth's Cryosphere, v. XV, №4, pp. 63-65.

Vergun A.P., Baranskaya A.V., Belova N.G., Kamalov A.M., Kokin O.V., Kuznetsov D.E., Shabanova N.N., Ogorodov S.A. (2013). Coastal Dynamics Monitoring at the Barents and Kara Seas. Society of Petroleum Engineers - SPE Arctic and Extreme Environments Conference and Exhibition, AEE 2013

Received on November 20th, 2017

Accepted on March 1st, 2018



Natalia N. Shabanova graduated from the Geographical Faculty of Moscow State University in 2011. Her area of interests lies in the meteorology and climatology of the Polar regions, especially Barents and Kara Seas. She focuses on hydrometeorological factors of coastal dynamics and its evolution within climate change.

**Alexander Mahura^{1*}, Iraxte Gonzalez-Aparicio², Roman Nuterman³,
Alexander Baklanov⁴**

¹ Institute for Atmospheric and Earth System Research (INAR) / Physics, Faculty of Science, University of Helsinki (UHEL)

² European Commission, DG-Joint Research Centre (EC, DG-JRC), Energy, Transport and Climate Directorate

³ University of Copenhagen (UCPH), Niels Bohr Institute

⁴ World Meteorological Organization (WMO), Research Department

* **Corresponding author:** alexander.mahura@helsinki.fi

SEASONAL IMPACT ANALYSIS ON POPULATION DUE TO CONTINUOUS SULPHUR EMISSIONS FROM SEVERONIKEL SMELTERS OF THE KOLA PENINSULA

ABSTRACT. This study is devoted to investigation of total deposition and loading patterns for population of the North-West Russia and Scandinavian countries due to continuous emissions (following “mild emission scenario”) of sulphates from the Cu-Ni smelters (Severonikel enterprise, Murmansk region, Russia). The Lagrangian long-range dispersion model (Danish Emergency Response Model for Atmosphere) was run in a long-term mode to simulate atmospheric transport, dispersion and deposition over the Northern Hemispheric’s domain north of 10°N, and results were integrated and analyzed in the GIS environment. Analysis was performed on annual and seasonal scales, including depositions, impact on urban areas and calculating individual and collective loadings on population in selected regions of Russia and Scandinavian countries.

It was found that wet deposition dominates, and it is higher in winter. The North-West Russia is more influenced by the Severonikel emissions compared with the Scandinavian countries. Among urban areas, the Russian cities of Murmansk (due to its proximity to the source) and Arkhangelsk (due to dominating atmospheric flows) are under the highest impact. The yearly individual loadings on population are the largest (up to 120 kg/person) for the Murmansk region; lower (15 kg/person) for territories of the northern Norway, and the smallest (less than 5 kg/person) for the eastern Finland, Karelia Republic, and Arkhangelsk region. These loadings have distinct seasonal variability with a largest contribution during winter-spring for Russia, spring – for Norway, and autumn – for Finland and Sweden; and the lowest during summer (i.e. less than 10 and 1 kg/person for the Russia and Scandinavian countries, respectively). The yearly collective loadings for population living on the impacted territories in Russia, Finland, Norway, and Sweden are 2628, 140.4, 13, and 10.7 tonnes, respectively.

KEY WORDS: atmospheric transport, dispersion and deposition modelling, sulphates, GIS analysis; individual and collective loadings

CITATION: Alexander Mahura, I. Gonzalez-Aparicio, Roman Nuterman, Alexander Baklanov (2018) Seasonal Impact Analysis On Population Due To Continuous Sulphur Emissions From Severonikel Smelters Of The Kola Peninsula. *Geography, Environment, Sustainability*, Vol.11, No 1, p. 130-144
DOI-10.24057/2071-9388-2018-11-1-130-144

INTRODUCTION

During the last decades the enterprises of various risks (nuclear, chemical, biological, etc.) are under permanent and critical view from the society. There is a number of important questions addressed as they are important because they are related to environmental issues and people's life. What are the potential impacts on the environment and on humans? Which geographical regions, countries, population groups etc. are under the largest influence when continuous emissions or accidental releases are taken place at different risk objects? Answers on such questions are, first of all, directly linked with investigation of atmospheric transport and deposition of pollution as well as estimation of their effects on population and environment.

Large Russian industrial major enterprises such as the Norilsk Nickel, Pechenganikel and Severonikel are sources of continuous emissions (www.nornickel.com, www.kolagmk.ru). The two latter are located on the Kola Peninsula. Information about environmental and pollution situation in the Murmansk region of Russia is provided through annual state reports. A series of studies was performed as a part of the Russian state scientific-research programmes, Kola Science Center of the Russian Academy of Sciences projects, Arctic Monitoring and Assessment Programme activities, and others.

Many field campaigns taking meteorological and pollution measurements, soil and water samples were conducted in surroundings of the sources (Golubeva et al. 2010, Hansen et al. 2017). In addition, local and remote

continuous monitoring is carried out in order to evaluate influence on various ecosystems and people (Berglen et al. 2016, Reimann et al. 1999, Lappalainen et al. 2007).

Analysis of forest ecosystems of the Kola Peninsula, Karaban and Gutarsky (1995) revealed that within a 30-40 km radius from the emission sources the impact is the largest. Moreover, level of damage varies depending on a type of a forest (Gutarsky et al. 1997) and area of the forest decline is expanding (Hagner and Rigina, 1998). Microbial communities in polluted soils showed significant decrease in biomass and growth rate (Blagodatskaya et al. 2008). Following the smelters production and amount of toxic loading produced, Moiseenko et al. (2006) found that water ecosystem (the Imandra Lake near Severonikel) strongly affects a human's health. Higher altitude lakes in Khibiny mountains showed both contributions: from the local smelters and due to transboundary pollution (Dauvalter et al. 2003). Modelling of concentration and deposition patterns resulted from continuous and accidental releases (radionuclides, gaseous chemical species and aerosols) from potential sources of nuclear and chemical risks was performed in Mahura et al. (2006ab, 2007, 2008) and proved to be a reliable approach.

In this study, the influence of continuous emissions of pollutants (on example of sulphates) on population is evaluated taking into account available meteorological and emission data for the year 2000. For that long-term modelling of concentration and deposition patterns, their integration into the GIS environment and further analysis were performed. Results of analysis of temporal

and spatial variability of deposition patterns on annual and seasonal scales, impact on the most populated urban areas, individual and collective loadings on the population living within different geographical territories (with a focus on selected Russian regions and Scandinavian countries) are presented in this paper.

MATERIALS AND METHODS

Pollution from Cu-Ni Smelters

There are several major locations in the Russian Arctic associated with large amounts of sulphur dioxide (SO₂) and heavy metals emissions. These are known as Cu-Ni smelters having the largest environmental and health impacts. These are three Russian enterprises: Norilsk Nickel (Krasnoyarsk Krai), Pechenganickel (cities of Zapolyarny and Nikel, Murmansk region) and Severonikel (city of Monchegorsk, Murmansk region). Following the Kola Mining and Metallurgical Company (see more news at www.kolagmk.ru) activities and technological changes a substantial reduction of emissions was performed in recent years. For example, at the beginning of the last decade (year of 2000), the SO₂ emissions from the Severonikel and Pechenganickel enterprises reached 45300 and 151200 tonnes, respectively (Ekimov et al. 2001). Thus, calculated emission intensities of the Monchegorsk smelters are $1.433 \cdot 10^9$ µg/sec. In this study, hereafter, an analysis of impact due to the Severonikel smelters is based on the defined above intensities and considering so-called the "mild scenario" (i.e. about 31.6 thou. tonnes per year corresponding to about 86.4 tonnes per day). Such scenario was chosen according to dominating tendencies in reduction of emissions. Although not the entire released amount of SO₂ can be converted following chemical transformations into sulphates (SO₄⁻²) during long-range atmospheric transport, it was assumed that it occurred at maximal level (i.e. 82%; IPCC, 2001) in order to obtain the highest estimates for analysed parameters. I.e. we assumed that 82% of emitted SO₂ were converted to SO₄⁻², and then as aerosols were transported, dispersed and deposited.

Long-Term Modelling of Continuous Emissions

The modeling of atmospheric transport, dispersion and deposition of different pollutants is essential input for estimation of possible consequences on different scales ranging from hemispheric, regional, subregional, and transboundary to mesoscale and local scales. Generated model output is crucial for multi-level assessment of risk, vulnerability, impact, short- and long-term consequences for environment and population, which is living near-by or remotely from the sources of possible accidental releases and continuous emissions.

In this study, the long-term modeling of atmospheric transport, dispersion and deposition of pollution resulted from continuous emissions from the Severonikel Cu-Ni smelters was performed employing the Lagrangian-type Danish Emergency Response Model for Atmosphere (DERMA; Sorensen, 1998; Baklanov et al. 2008) in a long-term mode. The probabilistic approach, sensitivity of the model to meteorology and diffusion parameters, deposition processes, and other parameterizations are also described in more details by Baklanov and Mahura (2004), Sorensen (1998), Baklanov and Sørensen (2001). The European Centre for Medium-Range Weather Forecast (ECMWF) data archives were used as input meteorological 3D fields for the year 2000. The meteorological data are given at 1 x 1 degree resolution at every 6 hour time interval and covering the Northern Hemisphere starting 10°N. Only the emissions of sulphates were taken into account, although heavy metals are also linked with emissions from the smelters. The metals are mostly will be deposited at shorter distances from the sources, and hence, will have more influence on a local scale. As more detailed information about a technological cycle of the Severonikel production chain and hence, corresponding diurnal cycle of emissions, were not available on a daily basis, for the model runs it was assumed that the continuous emissions occurred daily at the constant rate (see Section @Pollution from Cu-Ni Smelters). Then, for each run, the

pollution plume originated near the source was transported through the atmosphere (as well as dispersed and deposited due to dry and wet deposition processes) during following 10 days. It should be noted that in general, levels of pollution can vary significantly depending on dominating meteorological conditions both within the boundary layer as well as free troposphere, and the most highest levels of pollution are generally observed in a vicinity of the sources.

The generated model output included: the air concentration, the time integrated air concentration (TIAC), the dry deposition (DD) and the wet deposition (WD) (see Fig. 1). Note that such output - if it is summed over a long period of time (for example: month, season, year) or if it is averaged over a short period of time (for example: day, period of accidental release) - can represent possible short- and long-term

effects and probabilistic characteristics of industrial pollution. In general, based on such available output, the geographical boundaries of potential influence due to continuous (or accidental) atmospheric releases of pollutants from different sources can be identified and possible impacts can be evaluated. An example of simulated summary and average TIAC, DD and WD patterns during 10 days of the atmospheric transport, dispersion and deposition for the month of April are shown in Fig. 1.

GIS Integration of Dispersion Modelling Results

The results of the long-term dispersion modelling were integrated into the Geographical Information System (GIS; ArcGIS geospatial processing software; www.gis.com) environment (Fig. 2) in order to assess the impact on population due to continuous anthropogenic emissions

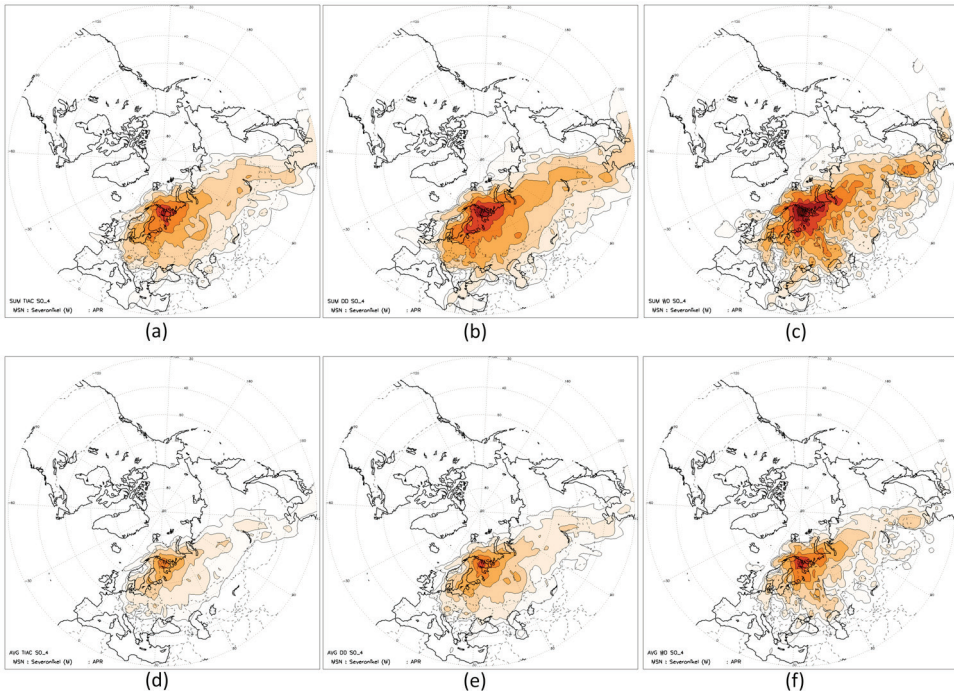


Fig. 1. Spatial patterns of the (abc) summary and (def) average - (ad) time integrated air concentration (TIAC), (be) dry (DD) and (cf) wet (WD) deposition - patterns during April due to continuous emissions of sulphates from the Severonikel smelters (deposition and concentration isolines are shown starting from the lowest $1e-2 \mu\text{g}/\text{m}^2$ and $1e-2 \mu\text{g}/\text{m}^3$, respectively; Δ MSN – location of the plant on the Kola Peninsula)

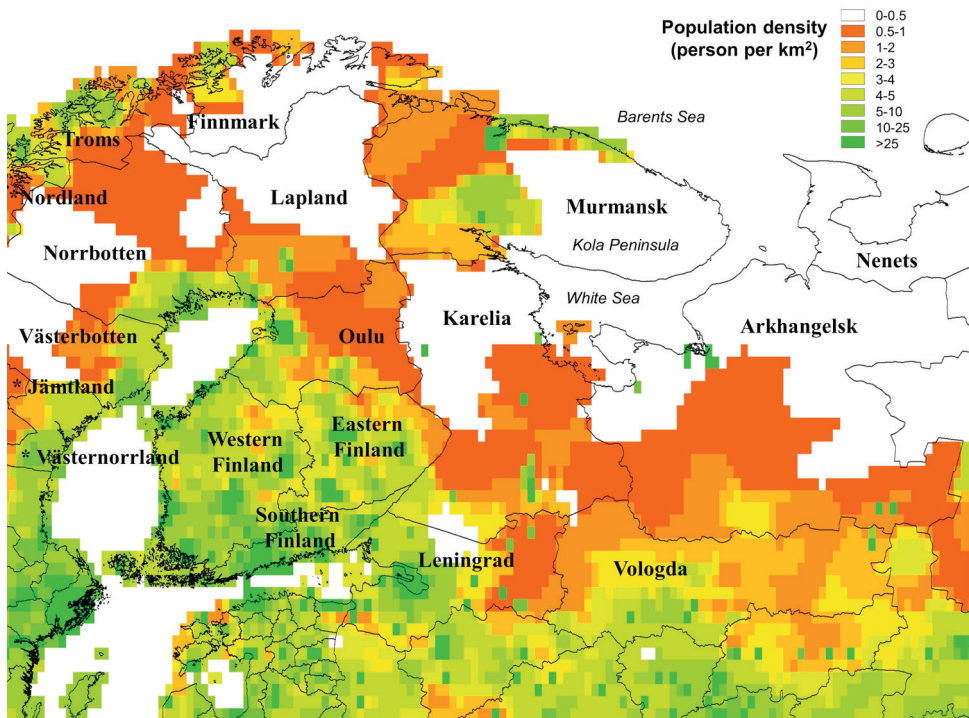
from the Severonikel smelters. For that, the ArcMap component of ArcGIS was applied. Note that ArcMap was used to geospatially view, edit, create, and analyze the integrated modelling data through exploring these results and creating maps. Moreover, note that the same coordinate system is required to work in ArcMap with different data-frames and layers. In particular, all data were converted into the Geographical Coordinate System GCS-WGS-1984. The WGS-1984 (World Geodetic Survey 1984) is a standard definition of a global reference system for a geospatial information, and is the reference system for the Global Positioning System (GPS).

At first, the countries and administrative units (regions/ oblast, provinces, counties) boundaries and population density of the European countries and Russia were loaded (see Fig. 2a; with interpolated population data). Data about administrative boundaries of the Russian regions (including Murmansk region) were extracted at gis-lab.info. Data about boundaries of the European countries and administrative units were downloaded from www.diva-gis.org. Data about the

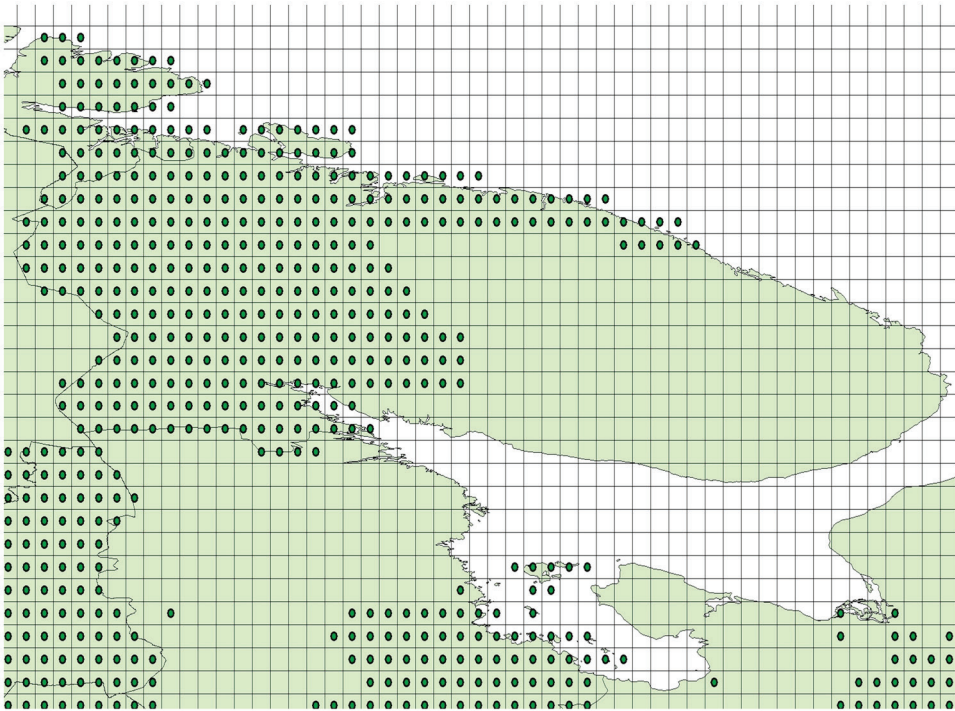
population density were obtained from the Center for International Earth Science Information Network (CIESIN; www.ciesin.org).

At second, the header (with information on number of grid points along latitude and longitude, south-west corner of modelling domain, and attribute for missing values) was added to the dispersion modelling output file, and it was needed for obtaining further information about spatial resolution and location. Then, the file was converted into the same GCS-WGS-1984 coordinate system.

At third, the raster centroids (centers of grid cells) were used to create the vector grid. For that, integrated raster data were converted into points and polygons. Because centroids were generated at regular grid, the Hawth tool (www.spatial ecology.com) was used to create a vector grid, where the resolution could be changed, in particular, increased. For a case of non-regular grid see González-Aparicio et al. (2010). The attribute table was used to transfer data from raster to vector grid based on spatial location. Subsequently,



(a)



(b)

Fig. 2. (a) Geographical boundaries of administrative units (regions, provinces, counties, etc.) and population density (in persons per km²), and (b) Example of extracted geographical region with overlapped layers of the total deposition, administrative boundaries and population density in order to calculate the impact on population exposed to emissions

new layers were created for different attributes taking into account grid cells with deposition greater than zero.

Finally, the overlapping (Fig. 2b) of the deposition layer with the administrative boundaries was performed in order to calculate the total deposition for selected regions and counties. The similar procedure (but in addition using the population density layer) was carried out to calculate the impact on population exposed to emissions. And then, these final results in a vector grid were converted into a raster format to visualise different levels of impact.

RESULTS AND DISCUSSIONS

Monthly Variability of Deposition

The simulation results on the Northern Hemispheric scale showed that a substantial value of deposition was observed not only

over the Kola Peninsula, but also on the regional scale. This includes contribution to Arctic regions (e.g. Arctic haze), transboundary atmospheric pollution transport between North-West Russia and Nordic countries, as well as to other geographical regions/ countries. As seen in Fig. 3, in particular, such influence is observed faraway on the Pacific region countries (Japan, China, and Korea). Due to irregularities of precipitation patterns, the isolated areas of the wet deposition is observed even along the western seashore of the North American continent (e.g. Canada and USA).

The supplementary materials – i.e. the animated web-based atlas of the modelled month-to-month variability of the averaged and summary TIAC, DD and WD patterns is available and plotted for the geographical domain covering the Northern Hemisphere

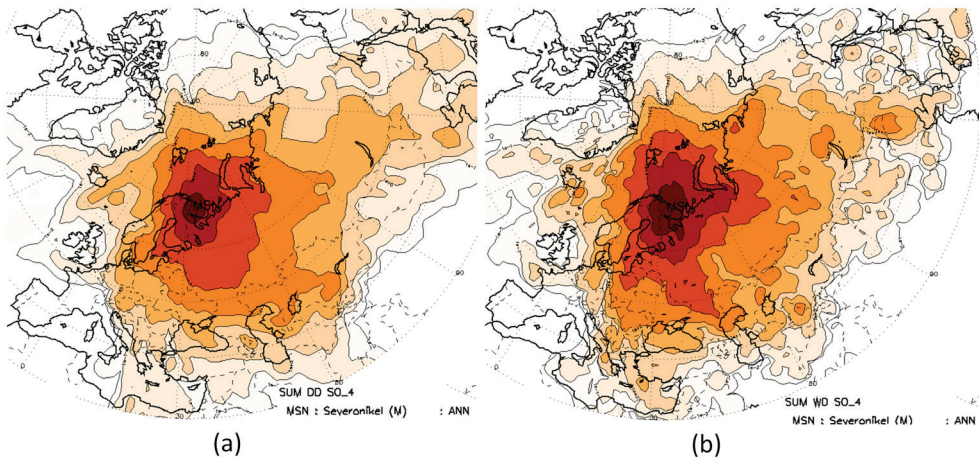


Fig. 3. Spatial patterns of the yearly (2000) summary (a) dry and (b) wet deposition due to continuous emissions of sulphates from the Severonikel smelters (isolines are shown starting from the lowest $1e-2 \mu\text{g}/\text{m}^2$; ΔMSN – location of the plant on the Kola Peninsula)

north of 30°N .

The simulated concentration and deposition fields allowed evaluating the spatial and temporal variability of resulted patterns on different scales. It has been found that for the “mild scenario emissions” (i.e. approx. 31.6 thou. tonnes), for the Severonikel smelters, the annual average daily dry deposition (DD) value is about 6 t. The highest average DD (10 t) is in September, and the lowest – less than 3 t – in April. The annual average daily wet deposition (WD) is about 23 t, and a strong month-to-month variability is seen compared with dry deposition (Fig. 4a). The highest average WD (more than 50 t) is in February although with the largest variability, and the lowest – about 6 t – in July. The WD is higher in magnitude and has more monthly variability compared with DD, and hence, WD is dominating in total deposition.

There are also differences in the total amount deposited from daily releases of the smelters (Fig. 4b). On an annual scale, on average, 33% of emitted amount could be deposited on the surface during 10 days of atmospheric transport from the sources. The highest deposited amount of 65% is observed in February and the lowest of 14% – in July. In general, during January–May the deposited amount is almost twice larger compared with June–October, but in November–December – it is close to the

annual average. Such identified pattern depends on dominated synoptic and large scale atmospheric transport as well as meso-scale circulation patterns over the Northern Hemisphere domain. Moreover, a larger amount of precipitation (and hence, the wet deposition) is taking place during winter and spring compared to summer and autumn months.

Regional Distribution of Deposition Patterns

A summary for total (as a sum of dry and wet) deposition characteristics for selected territories of the North-West Russia and Scandinavian countries is shown in Table 1. It includes analysis for total deposition (average and maximum) taking into account areas of grid cells enclosed by administrative boundaries of the selected regions/oblast, provinces and counties of selected countries. As seen, for the Murmansk region, where the source of emissions is located, on average, the deposition can reach up to $28 \mu\text{g}/\text{m}^2$ (with minimum of $14 \mu\text{g}/\text{m}^2$, and maximum of $122 \mu\text{g}/\text{m}^2$). The second most polluted Russian region is the Republic of Karelia followed by the Arkhangelsk region with average depositions, which are more than order of magnitude smaller compared with the Murmansk region. Among Finnish provinces, Lapland is the most polluted, and level of pollution is comparable with

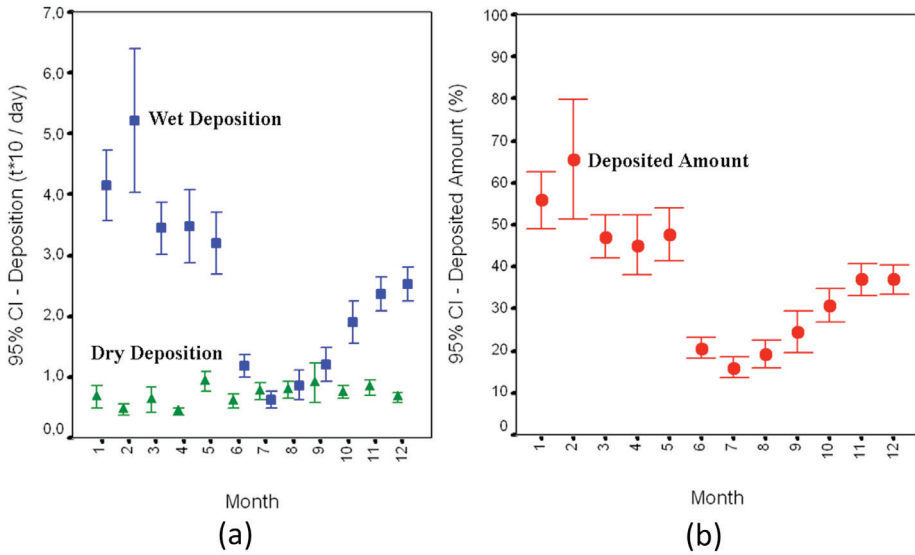


Fig. 4. Month-to-month variability at 95% confidence interval of averaged dry and wet deposition patterns (in tonnes per day) and (b) deposited amount (in %) resulted from the Severonikel continuous emissions

Karelia. The Swedish Norrbotten province has the highest deposition in the country. The Norwegian Finnmark county has also the largest deposition level, mostly due to its proximity to the source.

The analysis of the seasonal variability of the averaged total deposition (thereafter, ATD) showed, that for all Finnish provinces (except, Southern Finland) ATD is higher in autumn and it is the lowest in summer months. For the Norwegian counties, ATD is also higher in autumn (similarly for Finland and Sweden), but it is the lowest during winter. For the Russian regions considered, ATD is higher in spring; except, for the Arkhangelsk and Nenets regions (which are located easterly of the Kola Peninsula). Here, it is observed in autumn, similarly to the Scandinavian countries. The lower values of ATD are observed in summer and winter.

For the maximum total deposition (thereafter, MTD), on a seasonal cycle, it was found that for Finland, the MTD is the largest for the northern territories (Lapland province) in spring, for the southern territories (Southern Finland) – in winter, and for the rest (Oulu, Eastern and Western Finland provinces) – in autumn. The MTD is the lowest for all Finnish provinces in summer. For the Norwegian counties considered, the MTD is the largest

in spring (Finnmark) and autumn (Troms and Nordland); and MTD is the lowest – in winter and summer. For the Russian regions in focus, the largest maxima are linked with spring time, but for the easterly located regions (Arkhangelsk and Nenets) – in autumn. The lower maxima are more characteristic for summer compared with winter. For Sweden, the largest maxima are observed for all counties in autumn.

Individual and Collective Loadings on Population

Although sulphur deposition has ecological impacts, and first of all, on water and terrestrial ecosystems, in our study, the sulphates deposition effects on population were considered through contamination of the urban areas (e.g. those grid cells with a population fraction presented). Possible direct health effects on population might occur when the wet deposition process occurs with acidic pollutants in acid precipitation. Possible indirect effects might occur when the underlying urban surface (with soils and ground/surface waters) is contaminated due to both dry and wet deposition processes. In our study, these effects are combined through the loadings on the population.

Table 1. Regional distribution of total deposition (annual and seasonal) of sulphates due to continuous emissions of the Severonikel smelters

Country	Region/ County/ Province	Total Deposition ($\mu\text{g}/\text{m}^2$)									
		Spring		Summer		Fall		Winter		Year	
Statistics		Avg	Max	Avg	Max	Avg	Max	Avg	Max	Avg	Max
Finland											
	Lapland	623	2263	230	571	940	2219	392	2117	2185	7170
	Oulu	282	792	61	180	802	1344	297	594	1442	2910
	Eastern Finland	70	122	21	38	316	698	160	354	567	1200
	Western Finland	30	40	8	17	131	573	37	64	205	640
	Southern Finland	42	73	9	18	48	105	85	137	183	332
Norway											
	Finnmark	826	3218	307	760	909	2242	197	889	2239	6730
	Troms	26	49	40	91	126	235	10	29	202	403
	NordLand	4	11	3	11	18	31	3	7	28	50
Russia											
	Murmansk	11228	56495	2279	7849	4369	11124	10406	46667	28282	122000
	Karelia	581	2181	198	611	542	1476	447	1677	1768	5050
	Arkhangelsk	112	578	115	1185	282	1651	42	148	551	3030
	Nenets	161	376	11	36	249	702	21	193	442	1250
	Vologda	107	391	26	216	66	243	15	47	214	864
	Leningrad	83	221	19	45	28	67	66	102	196	309
Sweden											
	Norrbotnen	16	67	19	75	92	268	11	65	138	397
	Vesterbotten	2	7	1	2	15	31	12	29	30	69

The estimation of deposited amounts of sulphates with respect to population (thereafter, the loadings) for selected regions of Russia and Scandinavian countries was performed. At first, the yearly and seasonal deposition for the population density (in $\mu\text{g}\cdot\text{m}^{-2}$ / $\text{person}\cdot\text{km}^{-2}$) was calculated. At second, the yearly and seasonal individual loadings (in kg / person) were evaluated. At third, yearly collective loadings (in kg) for the entire population residing within the administrative boundaries of the studied regions/ counties/ provinces were also evaluated.

As seen in Fig. 5-6, for population residing in the central and northern territories (in urban settlements) of the Kola Peninsula the yearly individual loading can be more than 40 kg/person and up to 120 kg/person for most populated urban areas (located not far from the source of emissions) of the Murmansk region. For bordering territories with the Murmansk region such loadings are less than 5 kg/person for territories of the eastern Finland, Karelia Republic, and Arkhangelsk region; and not greater than 15 kg/person – for the northern Norway. There is also seasonal variability in

loadings, but it is less pronounced for the Scandinavian countries compared with the Russian regions. In particular, for all regions considered the loadings are the lowest in summer, i.e. less than 10 kg/person for Russia, and less than 1 kg/person for three considered Scandinavian countries. For the Russian regions the percentage contribution into the yearly individual loading is higher during winter-spring (in sum 85%) period compared with summer-autumn (15%). For Norway, such contribution is the largest in spring (34%) and the lowest – in summer (18%). For Finland, it is similar during all seasons, except autumn (32%). For Sweden, the contribution is similar during winter-spring period, the largest - in autumn (41%) and the smallest - in summer (11%). Such results are also in good correspondence with dominated deposition, and especially wet deposition, patterns in the studied geographical area.

During a year, about 33% of emissions (which is equivalent to 10.4 thousand tonnes for

the mild scenario emissions) were deposited on the underlying surface. But only a part of this process occurred over populated areas, the rest took place over non-populated territories including northern seas' aquatoria. In total, only 2792 tonnes (i.e. 27%, or less than 1/3) were deposited over the populated areas of the studied countries.

For the entire population residing on the territory of the Murmansk region the yearly collective loading is 2403 tonnes. Taking into account the total population of this region (according to 2002 Census – 892534 inhabitants), an average value of such loading is about 2.7 kg/person. Among all Russian regions, the Karelia Republic and Arkhangelsk region have the second largest loadings – 83 and 77 t, respectively. For the populated territories of bordering countries with the Murmansk region, the collective loading is 140.4 t for the entire Finland (with the largest contribution of 70.6 t from the Oulu province). For Sweden, this loading is about 10.7 t with the largest contribution

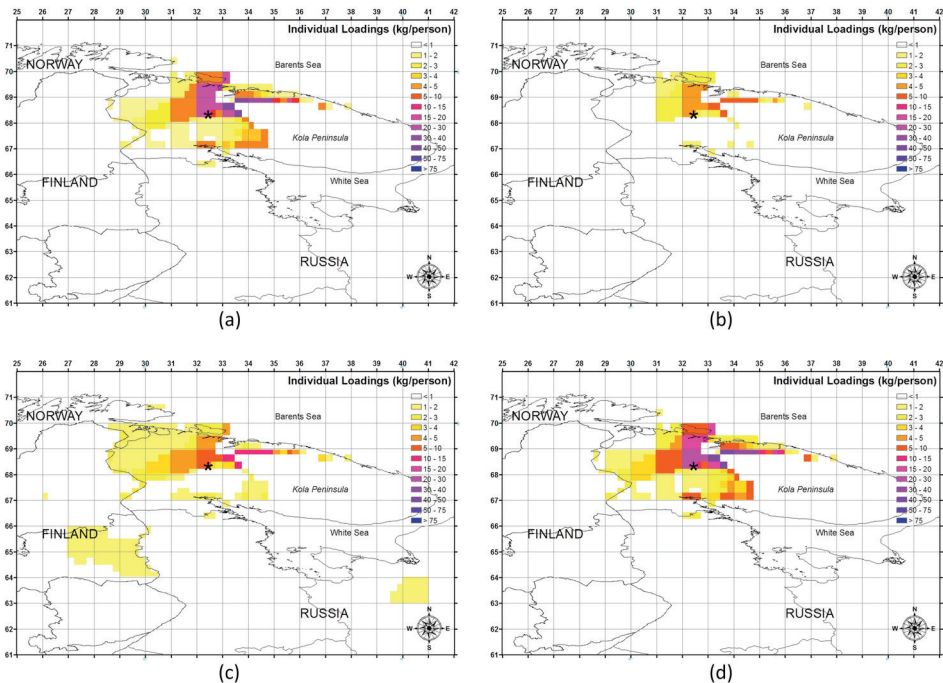


Fig. 5. Seasonal individual loadings for population (in kg/person) from deposited sulphates resulted from the Severonikel smelters continuous emissions (mild scenario; * - location of the Severonikel plant on the Kola Peninsula): (a) spring, (b) summer, (c) autumn, and (d) winter

(9.2 t or 87%) from the Norbotten county. For the northern Norway (Troms, Finnmark, and Nordland counties) it is about 13 t.

Note that the estimated magnitude of concentration and deposition patterns have limitations due to uncertainties in the modeling (based on lower horizontal resolution, boundary meteorological conditions, etc.) that would limit the magnitudes of the concentrations and deposition results. On a perspective, the online integrated meteorology-chemistry-aerosols Enviro-HIRLAM (Environment – High Resolution Limited Area Model) modelling system (Baklanov et al. 2017) in a downscaling chain (with running consequently at 15-5-2 km horizontal resolutions) is planned to be used for the domain of the North-West Russia and Scandinavian countries. Both the meteorological and atmospheric composition (including deposition patterns) at the same selected resolutions will be simulated, which will allow more in depth evaluation of loadings not only for population (associated with urban areas) but also with other ecosystems (such as

forest, soils, lakes, etc.) of the studied region in focus.

CONCLUSION

In this study, the investigation of impact on population due to continuous emissions of sulphates from the Severonikel Cu-Ni smelters (city of Monchegorsk, Murmansk region, Russia) was performed employing the Lagrangian long-range transport model DERMA in a long-term simulation mode and applying GIS tools for integrating and analysis of the dispersion modeling results.

It was found that over the model domain (covering Northern Hemisphere starting at 10°N) on annual scale, daily dry deposition is about 6 t with the highest (10 t) - in September. The wet deposition is 23 t (maximum 50 t - in February), and it is dominating in the total deposition. On average, about 33% of the emissions could be deposited on the surface during 10 days of the atmospheric transport from the smelters with the highest (65%) and lowest (14%) deposited amounts observed in February and July, respectively.

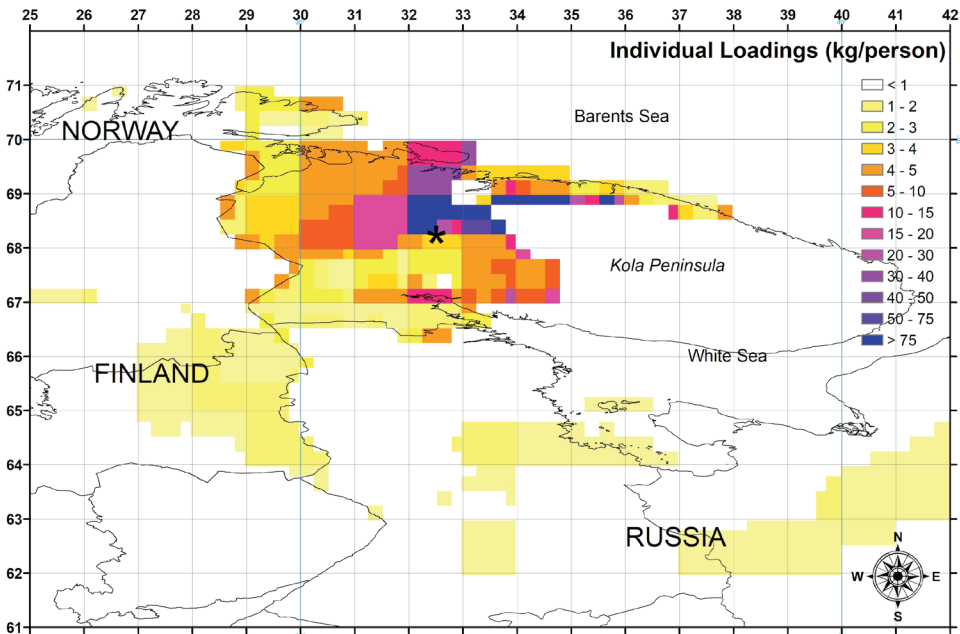


Fig. 6. Yearly individual loadings for population (in kg/person) from deposited sulphates resulted from the Severonikel smelters continuous emissions (mild scenario, * - location of the Severonikel plant on the Kola Peninsula)

The Murmansk region of Russia, where the smelters are located, is the most impacted, followed by the Karelia Republic and Arkhangelsk region (with the total deposition more than order of magnitude lower compared with the Murmansk region). Among administrative units of the Scandinavian countries, Lapland (Finland), Norrbotten (Sweden) and Finnmark (Norway) have the highest depositions. On average, it is higher in autumn for all three Scandinavian countries; and lower in summer (for Finland) and winter (for Norway). For the Russian regions, on average, deposition is higher in spring (except, the Arkhangelsk and Nenets regions), and it is lower in summer and winter.

The maximum total deposition is observed for the northern, central, and southern territories of Finland in spring, autumn and winter, respectively. For Sweden, it occurs in autumn. For the northernmost part of Norway it takes place in spring, and for other territories – in autumn. For Russia, the largest maxima are linked with spring and autumn for the territories southerly and easterly of the Severonikel smelters, respectively.

The yearly individual loading can be up to 120 kg/person for the most populated urban areas of the Murmansk region. For bordering territories with this region such loadings are less than 5 kg/person for territories of the eastern Finland, Karelia Republic, and Arkhangelsk region; and not greater than 15 kg/person – for the Finnmark county of Norway. There exists seasonal variability (with lowest loadings in summer), which is less pronounced for the Scandinavian countries. The percentage contribution into such loading is higher in winter-spring for Russia (in sum 85%), in spring for Norway (34%), in autumn for Finland and Sweden (32 and 41%, respectively). The yearly collective loading is the highest (2403 tonnes) for the

Murmansk region. Both the Karelia Republic and Arkhangelsk region have the second largest loadings (83 and 77 t). For populated territories of the bordering countries with the Murmansk region such loadings are 140.4, 13, and 10.7 t for Finland, Norway and Sweden, correspondingly.

The results of this study are applicable for (i) evaluation of risks, vulnerability, and short- and long-term consequences due to airborne pollution on population, environment, and ecosystems; (ii) complex human health impact assessments taking into account social, economic, and other factors; (iii) support of decision-makers, adjustment of legislation at regional levels, control pollution exceedances; planning preventive measures, mitigation scenarios, etc.

ACKNOWLEDGEMENTS

This research received financial support from several projects including the Pan-Eurasian EXperiment (PEEX; www.atm.helsinki.fi/peex) Programme, NordForsk CRAICC-PEEX (CRyosphere-Atmosphere Interactions in a Changing Arctic Climate) and CRUCIAL-PEEX (Critical steps in understanding land surface – atmosphere interactions: from improved knowledge to socioeconomic solution) projects, and the FP6 EC Enviro-RISKS project (Enviro-RISKS - Man-induced Environmental Risks: Monitoring, Management and Remediation of Man-made Changes in Siberia; project.risks.scert.ru). The simulations were performed at CRAY-XC30 HPC supercomputer, and the ECMWF meteorological data archives were used in this study. Thanks to Drs. J.H. Sorensen (Danish Meteorological Institute, Copenhagen, Denmark) and O. Rigina (Kola Science Center, Apatity, Russia) for useful discussions. Thank you to anonymous reviewers for constructive and useful comments and suggestions to the manuscript. ■

REFERENCES

- Baklanov A. and Mahura A. (2004). Assessment of possible airborne impact from risk sites: methodology for probabilistic atmospheric studies, *Atmospheric Chemistry and Physics*, 4, pp. 485-495.
- Baklanov A. and Sørensen J. (2001). Parameterisation of radionuclide deposition in atmospheric long-range transport modelling. *Physics and Chemistry of the Earth: (B)*, 26(10), pp. 787-799.
- Baklanov A., Sørensen J., and Mahura A. (2008). Methodology for Probabilistic Atmospheric Studies using Long-Term Dispersion Modelling. *Environ. Model Assess.*, 13, pp. 541-552.
- Baklanov A., Korsholm U.S., Nuterman R., Mahura A., Nielsen K.P., Sass B.H., Rasmussen A., Zakey A., Kaas E., Kurganskiy A., Sørensen J., and González-Aparicio I. (2017). Enviro-HIRLAM online integrated meteorology–chemistry modelling system: strategy, methodology, developments and applications (v7.2), *Geosci. Model Dev.*, 10, pp. 2971-2999.
- Berglen T.F., Dauge F., Andersen E., Nilsson L.O., Svendby T.M., Tønnesen D., Vadset M. and Våler R.L. (2016). Air Quality Monitoring in the Border Areas of Norway and Russia-Progress Report April 2015–March 2016. NILU-Norsk Institut for Luftforskning; Kjeller, Norway: 2016-16. p. 112
- Blagodatskaya E.V., Pampura T.V., Bogomolova I.N., Koptsik G.N. and Lukina N.V. (2008). Effect of emissions from a Copper-Nickel Smelter on soil microbial communities in forest biogeocenoses of the Kola Peninsula. *Ecology*, 35 (2), pp. 202-210.
- Dauvalter V., Moiseenko T., and Kagan L. (2003). Global Change in Respect to Tendency to Acidification of Subarctic Mountain Lakes. *Advances in Global Change Research*, 9(2), pp. 187-194.
- Ekimov S.V., Samodova I.V., Petrov I.M., Troitsky V.V., and Burstein M.A. (2001). Russian smelter emissions, «Mining Journal», London, November 23, p 393.
- Golubeva N.I., Burtseva L.V., and Ginzburg V.A. (2010). Heavy metals in the atmospheric precipitation on the Barents Sea coast. *Russ. Meteorol. Hydrol.* 35: 333.
- González-Aparicio I., Nuterman R., Korsholm U.S., Mahura A., Acero J.A., Hidalgo J., and Baklanov A. (2010). Land-Use Database Processing Approach for Meso-Scale Urban NWP Model Initialization. DMI Scientific Report 10-02, 34 p. ISBN: 978-87-7478-593-4.
- Gutarsky M.L., Karaban R. T., and Nazarov I.M. (1997). On the Assessment of Sulphur Deposition on Forests Growing Over the Areas of Industrial Impact. *Environmental Monitoring and Assessment*, 48(2), pp. 125-137.
- Hagner O. and Rigina O. (1998). Detection of Forest Decline in Monchegorsk Area. *Remote Sensing of Environment*, 63 (1), 1998, pp. 11-23
- Hansen M. D., Nøst T. H., Heimstad E. S., Evenset A., Dudarev A.A., Rautio A., Myllynen P., Dushkina E.V., Jagodic M., Christensen G.N., Anda E.E., Brustad M. and Sandanger T.M. (2017). The Impact of a Nickel-Copper Smelter on Concentrations of Toxic Elements in Local Wild Food from the Norwegian, Finnish, and Russian Border Regions. *International Journal of Environmental Research and Public Health*, 14(7), 694.

IPCC (2001). *Aerosols, their Direct and Indirect Effects*// IPCC, 2001: *Climate Change 2001: The Scientific Basis. Contribution of Working Group I to the Third Assessment Report of the Intergovernmental Panel on Climate Change*. Cambridge University Press, Cambridge, United Kingdom and New York, NY, USA, 302 p.

Karaban R. T. and M. L. Gutarsky (1995). Studies of precipitation contamination levels over the north-western forests of Russia subject to emissions from the two nickel smelters. *Water, Air, & Soil Pollution*, 85(4), pp. 2071-2076.

Lappalainen A., Tammi J. and Puro-Tahvanainen A. (2007). The effects of nickel smelters on water quality and littoral fish species composition in small watercourses in the border area of Finland, Norway and Russia. *Boreal Environ. Res.* (12), pp. 455-466.

Mahura A., Baklanov A. and Sørensen J.H. (2006a). Influence of long-range and long-term continuous and accidental anthropogenic emissions from Eurasian sources on Greenland environment. *Proceedings of the International Conference «The Greenlandic Environment: Pollution and Solutions»*, 21-23 Feb 2006, Sisimiut in Greenland, pp. 15-22.

Mahura A., Baklanov A., Sorensen J.H. and Tridvornov A. (2006b). Long-term modelling for estimation of man-induced environmental risks. *Abstracts of the European Geosciences Union (EGU) General Assembly, 2-7 April 2006, Vienna, Austria, EGU06-A-03781*.

Mahura A., Baklanov A., Sørensen J.H., Svetlov A. and Koshkin V. (2007). Assessment of Long-Range Transport and Deposition from Cu-Ni Smelters of Russian North. In *«Air, Water and Soil Quality Modelling for Risk and Impact Assessment»*, Security Through Science, Series C - Environmental Security. Eds. A. Ebel, T. Davitashvili, Springer Elsevier Publishers, pp. 115-124.

Mahura A., Baklanov A. and Sørensen J.H. (2008). *Enviro-RISKS: Overview of Applications for Short- and Long-Term Modelling and Assessment for Atmospheric Pollutants*. *Abstracts of the International Conference on Environmental Observations, Modelling and Information Systems, ENVIROMIS-2008, 28 June – 5 July 2008, Tomsk, Russia, p.106*.

Moiseenko T.I., Voinov A.A, Megorsky V.V., Gashkina N.A., Kudriavtseva L.P., Vandish O.I., Sharov A.N., Sharova Yu. and Koroleva I.N. (2006). Ecosystem and human health assessment to define environmental management strategies: The case of long-term human impacts on an Arctic lake. *Sci. Total Environ.*, 369(1-3), pp. 1-20.

Reimann C., Halleraker J.H., Kashulina G. and Bogatyrev I. (1999). Comparison of plant and precipitation chemistry in catchments with different levels of pollution on the Kola Peninsula, Russia. *Sci. Total Environ.*, 243, pp.169-191.

Sørensen J.H. (1998). Sensitivity of the DERMA long-range Gaussian dispersion model to meteorological input and diffusion parameters. *Atmospheric Environment*, 32 (24), pp. 4195-4206.

project.risks.scert.ru (2017). Official Website of the FP6 EC Enviro-RISKS project (*Enviro-RISKS - Man-induced Environmental Risks: Monitoring, Management and Remediation of Man-made Changes in Siberia*). [online] Available at: <http://project.risks.scert.ru/> [Accessed 11 Mar 2017].

www.atm.helsinki.fi/peex (2017). Official Website of the Pan-Eurasian EXperiment (PEEX) programme. [online] Available at: <https://www.atm.helsinki.fi/peex> [Accessed 11 Mar 2017].

www.nornickel.com (2017). Official Website of the Public Joint Stock Company "Mining and Metallurgical Company "NORILSK NICKEL" [online] Available at: www.nornickel.com [Accessed 11 Mar 2017].

www.kolagmk.ru (2017). Official Website of the Kola Mining and Metallurgical Company (Kola MMC) [online] Available at: <http://www.kolagmk.ru> [Accessed 11 Mar 2017] (in Russian).

www.gis.com (2017). Official Website of the ArcGIS geospatial processing software [online] Available at: <http://www.gis.com> [Accessed 11 Mar 2017].

gis-lab.info (2017). Website of the GIS-LAB independent online resource specializing in GIS and remote sensing [online] Available at: <http://gis-lab.info/projects/osm-export.html> [Accessed 11 Mar 2017] (in Russian).

www.diva-gis.org (2017). Website of the DIVA-GIS free computer program and data archives for mapping and geographic data analysis in GIS. [online] Available at: <http://www.diva-gis.org/Data> [Accessed 11 Mar 2017].

www.ciesin.org (2017). Website of the Center for International Earth Science Information Network with data and information products and resources [online] Available at: <http://www.ciesin.org/data.html> [Accessed 11 Mar 2017].

www.spatalecolology.com (2017). Website of the Hawth's analysis tools for ArcGIS [online] Available at: <http://www.spatalecolology.com/htools> [Accessed 11 Mar 2017].

Received on November 27th, 2017

Accepted on March 1st, 2018



Alexander Mahura, PhD (Phys&Math., Atm.Sci.), MSc (Env. Mod., Atm.Sci.), BSc. (Atm.Sci.); more than 25 years of research experience; fields of research are modelling of atmospheric processes and transport of pollutants (including radionuclides) on local-meso-regional-hemispheric scales, on-line integrated meteorology-chemistry-aerosols modelling at regional-urban scales, impact of urban areas on meteorology and atmospheric composition, atmospheric chemistry, atmospheric boundary layer processes, environmental impact and risk assessment, fine-scale road weather forecasting, birch pollen modelling, numerical weather prediction, statistics; consulting/co-advising students BSc/MSc/PhD on relevant research projects/theses; co-author of over 300 sci.-tech. publications, incl. 5 books and about 50 peer-reviewed papers.

**Sergey N. Bobylev¹, Olga Yu.Chereshnya¹, Markku Kulmala²,
Hanna K. Lappalainen^{3,4,5}, Tuukka Petäjä^{3,5}, Svetlana V. Solov'eva¹,
Vladimir S. Tikunov^{1*}, Veli-Pekka Tynkkynen⁶**

¹ Moscow State University, Russia

² Institute for Atmospheric and Earth System Research, University of Helsinki, Helsinki, Finland

³ University of Helsinki, Finland

⁴ Finnish meteorological Institute, Finland

⁵ Tyumen State University, Russia

⁶ Aleksanteri Institute, Department of Social Research, University of Helsinki, Helsinki, Finland

***Corresponding author:** vstikunov@yandex.ru

INDICATORS FOR DIGITALIZATION OF SUSTAINABLE DEVELOPMENT GOALS IN PEEEX PROGRAM

ABSTRACT. This article describes the Pan-Eurasian Experiment (PEEX) program and indicators for monitoring of implementation and digitalization of Sustainable Development Goals (SDG) in Russia, especially environmental goals. The authors considered the possibility of integration and identification of the methodological approaches of the socio-economic research to environmental sciences. Paper gives insights into the international framework of the United Nations, addresses several relevant indicators to be monitored in a Russian perspective and summarizes shortly the status of the monitoring activities and provide an overview on the main tasks for the upcoming years to reach the sustainable development goals established by the United Nations. The tasks to which the Goals divided are considered in detail. The indicators of Russian statistics that can be used to monitor the implementation of these tasks are determined. It is shown, that more detailed regional analysis and new data is needed in order to quantify the feedbackloops.

KEY WORDS: sustainable development goals, Pan Eurasian Experiment, digitization

CITATION: Sergey N. Bobylev, Olga Yu.Chereshnya, Markku Kulmala, Hanna K. Lappalainen, Tuukka Petäjä, Svetlana V. Solov'eva, Vladimir S. Tikunov, Veli-Pekka Tynkkynen (2018) Indicators for digitalization of sustainable development goals in PEEEX Program. Geography, Environment, Sustainability, Vol.11, No 1, p. 145-156
DOI-10.24057/2071-9388-2018-11-1-145-156

INTRODUCTION

The Pan-Eurasian Experiment (PEEX) program, initiated in 2012, is motivated by the environmental Grand Challenges for the Arctic – boreal regions. The program is especially designed for practical solutions in the field of climate change and air quality (Kulmala, 2015, Kulmala et al. 2015, 2016, Lappalainen et al. 2014, 2016). The research agenda addresses the complexity of the different types of feedbacks between land atmosphere – ocean and society interfaces and continuum (Lappalainen et al. 2016).

At the moment, the main focus of the research program is on quantifying the so-called COntinental Biosphere-Aerosol-Cloud-Climate (COBACC) feedback hypothesis relevant to the changing climate of the Northern Eurasian boreal (taiga) forest regions. The COBACC has two major overlapping loops (Kulmala et al. 2013) boosted by the increased atmospheric CO₂ levels and air temperature. The increased CO₂ and temperature effects ecosystem gross primary production (GPP), increase the amount of emitted biogenic volatile organic compounds (BVOC) and consequently increases the secondary organic aerosol (SOA) formation. The SOA formation contributes increase the share of diffuse solar radiation and number concentration of cloud condensation nuclei in the atmosphere and increase further the cloud droplet number concentration. The increasing CO₂ and consequent increase in average temperature is influenced by the anthropogenic activities and emissions. The COBACC feedback loop suppresses global warming. It can provide a broad framework to connect the human activities, continental biosphere, and changing climate conditions (Kulmala et al. 2014).

The near-future challenge in implementing the PEEX research agenda is to achieve a successful integration and identification of the methodological approaches of the socio-economic research to environmental sciences (Lappalainen et al. 2015). The first step in this task is to establish a researchers' network in the field of natural sciences and socio-economic sciences and initiate

research collaboration between socio-economics and environmental sciences. Here we give insights into the international framework of the United Nations, address several relevant indicators to be monitored in a Russian perspectives and summarize shortly the status of the monitoring activities and provide an overview on the main tasks for the upcoming years to reach the sustainable development goals established by the United Nations.

International frameworks and the sustainable development challenge

The society as a whole need to respond to and cope with the interconnected Grand Challenges. In September 2015, the General Assembly of United Nations adopted the 2030 Agenda for Sustainable Development. This agenda includes 17 Sustainable Development Goals (SDGs) that emphasizes a holistic approach to achieving sustainable development for all. At present, it is clear that comprehensive data in a digital form is the key factor to gauge the socio-economic development in a sustainable manner and taking into account the state of the environment. Digitization of various directions of socio-eco-economic transformations is one of the most important tasks for the transition of the world society towards sustainable development. The concept of sustainable development in recent decades has become widespread as a basic approach to assessing the prospects for the development of society and the state of the environment, as well as the effectiveness of resource management. It is a paradigm of the development of mankind in the 21st century. This approach is clearly constituted in the UN conceptual documents of recent years. Since 2015, there has been a sharp increase in theoretical and practical interest in the measurement of sustainability, which was largely due to the decisions of the United Nations Conference in September 2015, at which the Sustainable Development Goals (SDGs) (Table 1) were adopted for the period 2016-2030. The document is supported by all countries. Along with the formulation of the Goals themselves, relevant tasks and quantitative indicators were proposed. In fact, the process of sustainable development

is being digitized, which allows us to monitor and correct them. All UN members intend to develop their own SDGs systems.

Currently, the environmental statistics relevant to SDGs have the largest number of gaps compared to the other social and economic statistics. This situation is observed all over the world. This is explained by quite understandable problems: the colossal complexity of natural interrelations; the difficulty of complete assessing the consequences of the anthropogenic impact

on the environment; the challenge of modern science in digitization and adequate quantitative reflection of natural patterns; high costs of obtaining the vast majority of environmental indicators. In this regard, great opportunities are provided by scientific and technological progress, radical technological changes in the field of monitoring the state of the environment, the development of the most complex models reflecting natural transformations. As an example, the European Commission has made significant investment on developing the European

Table 1. Sustainable development goals (SDG) adopted in the United Nations 2030 agenda for sustainable development

Sustainable Development Goals	
Goal 1.	End poverty in all its forms everywhere
Goal 2.	End hunger, achieve food security and improved nutrition and promote sustainable agriculture
Goal 3.	Ensure healthy lives and promote well-being for all at all ages
Goal 4.	Ensure inclusive and equitable quality education and promote lifelong learning opportunities for all
Goal 5.	Achieve gender equality and empower all women and girls
Goal 6.	Ensure availability and sustainable management of water and sanitation for all
Goal 7.	Ensure access to affordable, reliable, sustainable and modern energy for all
Goal 8.	Promote sustained, inclusive and sustainable economic growth, full and productive employment and decent work for all
Goal 9.	Build resilient infrastructure, promote inclusive and sustainable industrialization and foster innovation
Goal 10.	Reduce inequality within and among countries
Goal 11.	Make cities and human settlements inclusive, safe, resilient and sustainable
Goal 12.	Ensure sustainable consumption and production patterns
Goal 13.	Take urgent action to combat climate change and its impacts
Goal 14.	Conserve and sustainably use the oceans, seas and marine resources for sustainable development
Goal 15.	Protect, restore and promote sustainable use of terrestrial ecosystems, sustainably manage forests, combat desertification, and halt and reverse land degradation and halt biodiversity loss
Goal 16.	Promote peaceful and inclusive societies for sustainable development, provide access to justice for all and build effective, accountable and inclusive institutions at all levels
Goal 17.	Strengthen the means of implementation and revitalize the Global Partnership for Sustainable Development

environmental research infrastructures and established “The European Strategy Forum on Research Infrastructures” (ESFRI) in 2002. The ESFRI has a key role in policy-making on research infrastructures in Europe. The European Commission and ESFRI encourage Member States and Associated Countries to develop national roadmaps for research infrastructures (RIs). These roadmaps are vital blueprints which enable countries to set national priorities and to earmark funds for both national and pan-European RIs (ec.europa.eu/research/infrastructures/index_en.cfm?pg=esfri). The ICOS (Integrated Carbon Observation System), ACTRIS (European Research Infrastructure for the observation of Aerosol, Clouds, and Trace gases) and LTER (Long-Term Ecosystem Research) are the most relevant European infrastructures for the PEEC Program. PEEC has also promoted the environmental monitoring system based on SMEAR (Stations Measuring the Earth Surface – Atmosphere Relations, Kulmala, 2018) which integrates ICOS, ACTIS and LTER measurement concepts and data formats.

Part of the data relevant to the UN sustainable development goals will have to be obtained from alternative in addition to the official statistics system, in particular, based on scientific research and observations. However, it should be borne in mind that the use of alternative sources presents certain problems, since the data may not be of sufficient quality, and the source of information may be unstable. In this regard, it is necessary to use more big data, as well as geospatial, satellite, GIS data. In addition to expanding the array of environmental data, it is necessary to integrate them with the data of the Digital Economy and the Digital Society. Economic and social development data pools needs to connect to the environmental data analysis, in particular, with such fundamental and complex natural processes as climate change, loss and degradation of ecosystems and their services, etc. The Institute of Remote Sensing and Digital Earth, Chinese Academy of Sciences (RADI/CAS) has been actively launching the new Digital Belt and Road (DBAR) Program, which could be focusing on

the monitoring of environmental change including urbanization in the Belt and Road region. In addition to data analysis based on multidisciplinary data pools the facilitating the collaboration between science and government decision-making, DBAR could also enhance scientific practice for environmental change in the Belt and Road region, the transport corridors and their footprint areas across the Eurasian regions.

Russian perspectives and the UN Sustainable Development Goals (SDGs)

Specialized hydrometeorological support is one of the most important activities in the effective use of information resources for the digitization of environmental monitoring. Potential and prospects for digitalization can be illustrated by the example of the activity of such a structure as Rosgidromet, which provides a significant part of environmental information for the Russian economy and society based on the environmental monitoring. At present, Russia incurs significant economic losses from hazardous natural phenomena. Only in 2015, 973 such phenomena were recorded on the territory of the country, of which 412 caused significant damage; 140 of them were observed in the waters of the seas in the areas of responsibility of the Russian Federation. (Roshydromet, 2016) There was a clear trend of a rapid increase in the number of dangerous phenomena which lead to various significant socio-economic damage - an average increase of 7-8% per year. In general, the annual damage from hazardous phenomena is estimated by a huge amount of 0.5-1% of the Russian GDP.

In this regard, the timely submission of the hydrometeorological information together with comprehensive data on the status of the environment e.g. via SMEAR observation concept in a timely manner and to the extent it provides significant benefits to society and a wide range of economic sectors and activities. According to the estimates of the Administration of Hydrometeorological Service in 2015, the economic effect of using such information amounted to 32.8 billion rubles. (State report..., 2016.) The bulk of the overall

economic effect (70%) accounts for two types of economic activity: «Production and distribution of electricity, gas and water» and «Transport and communications.»

The modern monitoring network allows obtaining large data sets for three natural environments: air, water resources of the land and the shelves of the seas. Observations of atmospheric air pollution are carried out by Roshydromet at 636 posts in 229 cities. Observations of surface waters of the land are carried out at 1725 stations for hydrochemical indicators and at 263 points for hydrobiological indicators. Observations of the marine environment by hydrochemical indicators are carried out at 292 stations in the shelf regions of Russia. At 1,266 stations, radioactive contamination of the environment is monitoring.

Achievements in the relevant fields related to environmental protection are of great importance from the point of view of forming the infrastructure of the digitalization of society and economy, scientific and technological achievements in the relevant fields related to environmental protection are of great importance. Based on these achievements in the Roshydromet system, only 145 patents or certificates of registration of intellectual property objects were received in Rospatent in 2015 (including 10 inventions, 3 utility models, 27 for databases, 105 for software).

Space monitoring and interaction with foreign partners is of particular importance today. Now the state territorially distributed space monitoring system of Roshydromet in the European (Moscow-Obninsk-Dolgoprudny), Siberian (Novosibirsk) and Far-Eastern (Khabarovsk) centres of FGBU «Research Center» Planeta «, acting as a unified information system, regularly received and processed data from 17 foreign and 7 domestic remote-sensing satellites. The satellite remote sensing observation capacity should be matched with a network of ground-based observation sites that provide the ground-truth and calibration services for the remote sensed data.

As an example of important environmental indicators for the digital economy and

society, consider possible indicators for some SDGs and their environmental goals, based on available official Russian statistics and research, mainly on Roshydromet data. Table 2 highlights four such goals (SDGs № 11, 13, 14, 15) related to the formation of sustainable cities, combating climate change, preserving ocean and marine resources, and terrestrial ecosystems. We will use the approach of highlighting key indicators (key/core indicators).

At SDG № 11 about the formation of sustainable cities, the important task is to reduce the environmental impact on urban residents. According to medical experts, particulates with a diameter less than 10 and 2.5 microns (PM10 and PM2.5) represent one of the main threats to public health as a result of environmental pollution. Currently, in Russia, correct estimates for this indicator are available only in Moscow - 39 $\mu\text{g}/\text{m}^3$, which is an average for the world's cities. For comparison, the maximum PM10 concentrations in the world megacities were recorded in Beijing - 116 $\mu\text{g}/\text{m}^3$, Istanbul - 51 $\mu\text{g}/\text{m}^3$, Mexico - 44 $\mu\text{g}/\text{m}^3$ and Hong Kong - 44.5 $\mu\text{g}/\text{m}^3$. The minimum indicators for PM10 are fixed in the following European capitals: Stockholm - 19 $\mu\text{g}/\text{m}^3$, Paris - 21 $\mu\text{g}/\text{m}^3$ and London - 22 $\mu\text{g}/\text{m}^3$.

However, to address the sustainable development goals in a more detailed level, the monitoring of air quality and health effects should be developed with a comprehensive approach (e.g. Kulmala, 2015) as the negative health effects are not only limited to the aerosol mass concentration. Specifically, aerosol number concentration in the ultra-fine size range (below 100 nm in diameter) has been identified to be even more harmful (e.g. Kim et al. 2015) than the larger PM2.5 particles that typically do not penetrate deep into the lungs or the blood circulation (Hussein et al. 2013). The long-term observations should be incorporated as part of a measurement network (Hari et al. 2016) and operated in connection with detailed emission analysis frameworks (Crippa et al. 2015).

SDG № 11 includes also social and cultural aspects of sustainability, therefore data

on particle emissions is able to tell only a limited story how inclusive and resilient society is. Thus, it is better to add indicators on social cohesion and equity issues vis-à-vis the environmental change, for example, differences in socio-economic wellbeing between groups of people; the divide between the very rich and very poor; distribution of health problems caused by the environmental change among the population. A resilient society is such where the effects of environmental problems do not disproportionately burden people in a lesser socio-economic position. These groups protected from the environmental problems caused by economic activities that are benefitting well-off groups.

SDG № 13 is aimed at providing measures to combat global climate change (IPCC, 2013). For Russia, climate issues are becoming more relevant as awareness of significant negative consequences increases (e.g. Schuur et al. 2015). This is largely due to the increase in the number of natural disasters and dangerous natural phenomena. Climatic changes occur much faster than in the Arctic countries of the world: taking into account the data for 2016, the average annual temperature in the territory of the Russian Federation is growing more than 2.5 times faster than the global temperature, at a rate of 0.43 °C during the last 10 years. Especially rapid growth is observed in the polar region, where the growth rate reaches 0.8C for 10 years. (Revich, 2011). In the future, as a result of warming, the risks associated with economic and social objects located

in the permafrost zone (which is spread over two-thirds of the Russian territory) sharply increase. According to World Bank experts (2009), Russia can become the most vulnerable country in Eastern Europe and Central Asia in the process of global climate change. In several decades, the total damage from climate change for the Russian economy could reach \$ 10 billion, which will be caused by an increase in the number of natural disasters and disasters on its territory. The country's territory is located in different climatic zones, therefore the list of hydrometeorological phenomena causing natural disasters in its regions is very large. The greater part of the country needs, to one degree or another, protection against dangerous natural phenomena. The melting of permafrost can lead to catastrophes in the energy sector, infrastructure, settlements. In the zone of potential climate, problems are the main objects of the energy sector and productive agricultural regions.

In climatic goal № 13, there are two important tasks (Table 2) for national sustainable development policies. For the first task, the key indicator is the number of people affected by natural disasters. Unfortunately, Russia does not have comprehensive statistics on the number of such victims. Nevertheless, the number of them is undoubtedly great. This is evidenced by medical studies that determined the additional mortality in the country as a result of anomalous heat waves in the summer of 2010. This year, a prolonged wave of heat in 2010 led to 58 thousand additional deaths among 60 million people

Table 2. Selected indicators in the environmental objectives of sustainable development

Sustainable Development Goals	Task	Indicator	Value
Goal 11. Make cities and human settlements inclusive, safe, resilient and sustainable	11.6. By 2030, reduce the adverse per capita environmental impact of cities, including by paying special attention to air quality and municipal and other waste management	11.6.2. Annual mean levels of fine particulate matter (e.g. PM2.5 and PM10) in cities (population weighted)	Data only for Moscow - 39µg/m ³

Goal 13. Take urgent action to combat climate change and its impacts	13.1. increase resistance and adaptability to dangerous climate events and natural disasters in all countries;	13.1.2. Number of deaths, missing persons and persons affected by disaster per 100,000 people	additional deaths caused by climatic disaster 96,7 (prolonged wave of heat in 2010 year)
	13.2 Integrate climate change measures into national policies, strategies and planning	13.2.1 Integrated policy/strategy/plan which increases countries' ability to adapt to the adverse impacts of climate change, and foster climate resilience and low greenhouse gas emissions development in a manner that does not threaten food production 13.2.(+). Greenhouse gas emissions and its trend	2651,2 million tons of CO ₂ -equivalent in Russia
Goal 14. Conserve and sustainably use the oceans, seas and marine resources for sustainable development	14.1. By 2025, prevent and significantly reduce marine pollution of all kinds, in particular from land-based activities, including marine debris and nutrient pollution	14.1.1. basic substances that pollute marine ecosystems (proposed by the authors for Russia in connection with the availability of Roshydromet data on marine pollution)	- petroleum hydrocarbons - pesticides - biogenic substances - heavy metals
Goal 15. Protect, restore and promote sustainable use of terrestrial ecosystems, sustainably manage forests, combat desertification, and halt and reverse land degradation and halt biodiversity loss	15.1. By 2020, ensure the conservation, restoration and sustainable use of terrestrial and inland freshwater ecosystems and their services, in particular forests, wetlands, mountains and drylands, in line with obligations under international agreements	15.1.1. Forest area as a proportion of total land area 15.1.(+) Share of protected areas	47% of Russia 12% of Russia (208 mln.ha)

in the European region of Russia. (Revich, 2011) This phenomenon was 'natural', but the estimate is that such occasions will become more frequent as the climate changes. As an indicator for SDG № 13 per 100 thousand of the population, this will amount to 96.7 people. (Table 2). Overall, the indicators for the development of climate relevant parameters (such as greenhouse gas and aerosol concentrations) should be incorporated with the comprehensive observation networks along with the meteorological variables.

For the second task, incorporate climate change response measures into national policies, strategies, and planning, the authors propose an indicator of greenhouse gas emissions. The emission trend, would be much more informative, showing are Russia's emissions increasing or falling. In comparison with 1990, the aggregate greenhouse gas emissions decreased by 45.8%, taking into account the absorbing capacity of ecosystems, and by 30% - without taking into account the volume of absorption. As of the end of 2015, the emissions amounted to 2132.5 million tons of CO₂-eq, respectively, and 2,651 million tons of CO₂-equivalent. (Table 3).

The SDGN^o 14 on the conservation of oceans and seas for sustainable development is difficult for quantitative identification of indicators. Nevertheless, the potential for providing the necessary data is available. Information hydrometeorological support of oceanic and marine activities in Russia

is carried out with the help of the Unified System for the World Ocean (ESIMO). In the activity of ESIMO, 31 organizations of twelve ministries and departments of Russia, as well as a number of commercial organizations. Automated workstations for ESIMO users are supported in 24 regional offices of the Ministry of Emergency Situations of Russia, the State Marine Emergency and Rescue Coordination Service of the Russian Federation, the Ministry of Transport of the Russian Federation, the Situation Centers of the Ministry of Emergencies of Russia, the Ministry of Natural Resources of Russia, Roshydromet, the Department of Shipbuilding Industry and Marine Equipment, and Roskosmos. ESIMO is actively using spatial data and services to assess the situation in the seas of Russia and the World Ocean based on the widespread use of GIS technologies. The electronic sea atlas ESIMO contains more than 6000 information layers with data in the field of hydrometeorology, physics of the sea, pollution of the marine environment, marine geology, geophysics and others. The total amount of information resources ESIMO is more than 15 terabytes. About 30% of the resources are updated from a few minutes to a day.

As indicators for SDG № 14, the data on which provides Russian statistics, there are four: oil carbohydrates, pesticides, nutrients, heavy metals (Table 2). In general, in coastal marine areas, the quality of seawater changed from «clean» to «moderately polluted». Almost everywhere reduction of oil hydrocarbons and pesticides was noted. Priority pollutants

Table 3. Greenhouse gas emissions in Russia (Bulletin Main indicators of environmental protection, Rosstat 2017)

	1990	2011	2012	2013	2014	2015
Total Incl.:	3363,32	2284,29	2295,05	2643,1	2648,9	2651,2
carbondioxide (CO ₂)	2505.36	1648.13	1656.77	1666.6	1671.6	1670.8
methane (CH ₄)	593.40	506.76	502.55	856.6	859.1	864.1
nitrousoxide (N ₂ O)	223.27	116.95	115.95	89.9	90.2	90.4
hydrofluorocarbons (HFC)	28.41	9.41	11.34	21.5	24.1	21.2
perfluorocarbons (PFC)	11.68	2.54	2.47	3.4	3.1	3.6
sulfurhexafluoride (SF ₆)	1.20	0.51	5.97	4.9	0.8	1.1

in the bottom surface layers are biogenic substances and heavy metals, their content is lower or at the level of MPC. The dirtiest sea water in the Russian shelf is the sea in the north of the Caspian Sea. The long-term observational capacity should be extended to uptake of greenhouse gases to the ecosystems via photosynthesis and emission inventories should be obtained for the utilization of gas and oil, including black carbon emissions due to flaring. The problem thus far has been that overall emissions trends in the Russian hydrocarbon industry have not been either known or are not accurate. It is well known that thousands of smaller oil spills take place in production and pipelines. The estimates range from one to five per cent of production, that is a minimum of 5 million tonnes of oil spilled to the environment. Here, satellite data, big data and other data using versatile methods should be applied to unfold real volumes of spilled oil.

SDG № 15 is related to the conservation of terrestrial ecosystems. Within the framework of this Goal, for task 15.1, the specific weight of the area covered by forests in the total area (indicator 15.1.1 in Table 2) is the main indicator. The terrestrial ecosystems can provide adaptation processes by greenhouse gas uptake and secondary biogenic aerosol production (Kulmala et al. 2014). The observational facility should be able to determine these feedback mechanisms and provide insights into their optimization. A fairly simple indicator is related, nevertheless, with the need to implement high-quality monitoring, satellite observations, a large-scale monitoring network. In particular, this is due to significant fluctuations in some areas of forest area as a result of fires, pest damage, mass felling, including illegal, etc. Sometimes, for example, large areas of forest fires can differ several times according to ground and satellite observations. Now the proportion of forests in the country is 47% (these data differ from some international databases, in particular, FAO and the World Bank). (State report ..., 2016.) More forests only in Brazil - 58%. In general, ten countries with the largest forest potential account for about 67% of the world's forests. Russia's share is leading on the planet - 20% of

the total forest area; Brazil's share is 12%, Canada - 9, the United States - 8, China - 5%. Much more interesting figures would be the ones depicting how the quality of Russia's ecosystems is changing, for the better or for worse and what is the share of original, untouched ecosystems in Russia. For this purpose, can be used indicator of the share of protected areas. The share of protected areas of federal, regional and local significance without marine areas amounted in 2015 to 12% of the country's territory, 208.6 million hectares. This indicator has some deficiencies. For example, regional proportions of adequate protected territories size are different due to a large spectrum of ecosystem patterns in Russia; many protected areas in industrial regions are situated within impact zones and their ecosystems experience anthropogenic transformation. But now it is the most approximate indicators from the available statistics.

CONCLUSION

In order to meet the UN Sustainable Development Goals (SDGs) in, which are also integral aspects, especially the SDGs No 11, 13, 15, 17, of the PEEC program we a roadmap for strengthening the Russian contribution to international frameworks. The recent analysis and statics of the SDG relevant indicator in Russia demonstrates the economic losses from hazardous natural phenomena and the state of the greenhouse gas emission in general. More detailed regional analysis and new data is needed in order to quantify the feedback loops such as COBACC.

The PEEC program provides a platform for coordinating the socio-economic research with the natural sciences in Russia and to analyze and quantify the feedbacks between anthropogenic and other society (human) activities and land – atmospheric – ocean systems. Roshydromet is significant player in providing the atmospheric and hydrological observations in Russia, Furthermore, the Roshydromet coordinates and facilitates a significant research infrastructure (in situ observation network). This is addressing great synergy between

Roshyderomet and PEEX Program.

Russian Federation (unique project identifier RFMEFI58317X0061) and with the financial support of Russian Foundation for Basic Research (RFBR) (project №18-05-00236). ■

ACKNOWLEDGEMENT

The studies were conducted with the financial support of the state represented by the Ministry of Education and Science of the

REFERENCES

Alekseychik P., Lappalainen H.K., Petäjä T., Zaitseva N., Heimann H., Laurila T., Lihavainen H., Asmi E., Arshinov M., Shevchenko V., Makshtas A., Dubtsov S., Mikhailov E., Lapshina E., Kirpotin S., Kurbatova Yu., Ding A., Guo H., Park S., Lavric J.V, Reum F., Panov A., Prokushkin A., and Kulmala M. (2016). Ground-based station network in Arctic and Subarctic Eurasia: an overview. *J. Geography Environment Sustainability*, 2, pp. 75-88.

Arneeth A., Harrison S. P., Tsigaridis K., Menon S., Bartlein P. J., Feichter H., Korhola A., Kulmala M., O'Donnell D., Schurgers G., Sorvari S., Vesala T., and Zaehle S. (2010). Terrestrial biogeochemical feedbacks in the climate system: from past to future. *Nat. Geosci.*, 3, pp. 525–532, 2010.

Baklanov A. (2017). Overview of the European framework for online integrated air quality and meteorology modelling (EuMetChem). *Atmospheric Chemistry and Physics*, doi:10.5194/acp-special_issue370-preface, 2017.

Bulletin Main indicators of environmental protection (2017). Rosstat.

Crippa M., Janssens-Maenhout G., Dentener F., Guizzardi D., Sindelarova K., Muntean M., Van Dingenen R. and Granier C. (2015). Forty years of improvements in European air quality: regional policy-industry interactions with global impacts. *Atmos. Chem. Phys.* 15, pp. 3825-3841.

Duch B. J., Groh S. E., and Allen D. E. (2001). *The Power of Problem-Based Learning*. Stylus Publishing, Sterling, VA, U.S.A., 2001.

Environmental Protection in Russia (2016). Rosstat.

Hari P. and Kulmala M.: Stations for Measuring Ecosystem – Atmosphere Relations (SMEAR II). *Boreal Environ. Res.*, 10, 315–322, 2005.

Hari P., Andreae M. O., Kabat P., and Kulmala M. (2009). A comprehensive network of measuring stations to monitor climate change. *Boreal Environ. Res.*, 14, pp. 442–446, 2009.

Hari P., Petäjä T., Bäck J., Kerminen V-M., Lappalainen H.K., Vihma T., Laurila T., Viisanen Y., Vesala T., and Kulmala M. (2016). Conceptual design of a measurement network of the global change. *Atmos. Chem. Phys.*, 16, pp. 1017-1028, <http://www.atmos-chem-phys.net/16/1017/2016/>, doi:10.5194/acp-16-1017-2016.

Hussein T., Löndahl J., Paasonen P., Koivisto A.J., Petäjä T., Hämeri K., and Kulmala M. (2013). Modeling regional deposited dose of submicron aerosol particles. *Sci. Tot. Environ.*, pp. 458-460, 140-149.

Junninen H., Lauri A., Keronen P., Aalto P., Hiltunen V., Hari P. and Kulmala M. (2009). Smart-SMEAR: on-line data exploration and visualization tool for SMEAR stations. *Boreal Environ. Res.* 14, pp. 447–457, 2009.

Kim K.-H., Kabir E., Kabir S. (2015). A review on the human health impact of airborne particulate matter. *Environ. International*, 74, 136-143.

Kulmala M. (2015). China's choking cocktail. *Nature*, 526, pp. 497–499.

Kulmala M., Nieminen T., Nikandrova A., Lehtipalo K., Manninen H.E., Kajos M.K., Kolari P., Lauri A., Petaja T., Krejci R., Hansson H.C., Swietlicki E., Lindroth A., Christensen T.R., Arneth A., Hari P., Back J., Vesala T., Kerminen V.-M. (2014). CO₂-induced terrestrial climate feedback mechanism: From carbon sink to aerosol source and back. *Boreal. Env. Res.* 19, Suppl. B, p. 122.

Kulmala M. (2018). Build a global Earth observatory, *Nature* (in press).

Kulmala M., Lappalainen H.K., Petäjä T., Kerminen V.-M., Viisanen Y., Matvienko G., Melnikov V., Baklanov A., Bondur V., Kasimov, N., and Zilitinkevich S. (2016). Pan-Eurasian Experiment (PEEX) Program: Grant Challenges in the Arctic-boreal context *J. Geography Environment Sustainability*, 2, pp. 5–18, DOI:http://dx.doi.org/10.15356/2071-9388_02v09_2016_01, 2016.

Kulmala M., Lappalainen H.K., Petäjä T., Kurten T., Kerminen V.-M., Viisanen Y., Hari P., Bondur V., Kasimov N., Kotlyakov V., Matvienko G., Baklanov A., Guo H., Ding A., Hansson H.-C., and Zilitinkevich S., (2015). Introduction: The Pan-Eurasian Experiment (PEEX) – multi-disciplinary, multi-scale and multi-component research and capacity building initiative *Atmos. Chem. Phys.*, 15, 13085-13096, 2015 doi:10.5194/acp-15-13085-2015.

Lappalainen H.K., Kulmala M., and Zilitinkevich S. (editors) (2015). Pan-Eurasian Experiment (PEEX) Science Plan. Helsinki 2015. ISBN 978-951-51-0587-5 (printed).

Lappalainen H.K., Petäjä T., Kujansuu J., Kerminen V., Shvidenko A., Bäck J., Vesala T., Vihma T., De Leeuw G., Lauri A., Ruuskanen T., Lapshin V.B., Zaitseva N., Glezer O., Arshinov M., Spracklen D.V., Arnold S.R., Juhola S., Lihavainen H., Viisanen Y., Chubarova N., Chalov S., Filatov N., Skorokhod A., Elansky N., Dyukarev E., Esau I., Hari P., Kotlyakov V., Kasimov N., Bondur V., Matvienko G., Baklanov A., Mareev E., Troitskaya Y., Ding A., Guo H., Zilitinkevich S., and Kulmala M. (2014). Pan Eurasian Experiment (PEEX) - A research initiative meeting the Grand Challenges of the changing environment of the Northern Pan-Eurasian arctic-boreal areas. *GEOGRAPHY, ENVIRONMENT, SUSTAINABILITY*, 2014; 7(2):13-48. DOI:10.24057/2071-9388-2014-7-2-13-48.

Nordic Climate Change Research (2009). NordForsk Policy Briefs 2009-8. Mandag Morgen, 2009.

On the activities of Roshydromet in 2015 and tasks for 2016 (final report) (draft) (2016). MNR, Roshydromet. Moscow.

Revich B.A. (2011). Waves of heat, air quality and mortality in the European part of Russia in the summer of 2010: the results of the preliminary assessment. *Human Ecology*, 7.

Schuur E.A.G., McGuire A.D., Schädel C., Grosse G., Harden J.W., Hayes D.J., Hugelius G., Koven C.D., Kuhry P., Lawrence D.M., Natali S.M., Olefeldt D., Romanovsky V.E., Schaefer K., Turetsky M.R., Treat C.C. and Vonk J.E. (2015). Climate change and the permafrost carbon feedback. *Nature* 520, pp. 171–179.

State report «On the state and on the protection of the environment of the Russian Federation in 2015» (2016). Moscow: Ministry of Natural Resources of Russia; NIA-Nature.

Received on December 20th, 2017

Accepted on March 1st, 2018



Vladimir S. Tikunov is Professor, D.Sc. in Geography, Head of the Integrated Mapping Laboratory, MSU Faculty of Geography, and Director of the Center of the World Data System for Geography. He is Professor Emeritus of the Lomonosov Moscow State University. He lectured at a number of national and international universities. He has led a number of Russian and international projects. His work has been used in many thematic maps and atlases: National Atlas of Russia (Editor-in-Chief of Vol. 3), National Atlas of the Arctic, Environmental Atlas of Russia, Atlas of Socio-Economic Development of Russia, Atlas of the Khanty-Mansi Autonomous District – Yugra, etc. He is a recipient of the D.N. Anuchin Award for his work in mathematical cartographic modeling. He is also a recipient of the Award in Science and Technology of the Russian Federation Government for the development of environmental and natural-resources atlases of Russia. He was Vice-President and, currently, is Chairman of the Commission on GI for Sustainability of the International Cartographic Association. He has been a member of the editorial boards of 14 Russian and international journals. Since 1994 he has been organizing annual international conferences InterCarto-InterGIS that take place both in Russia and abroad. He published over 500 scientific works, including 21 monographs, textbooks, and manuals in 28 countries of the world and in 14 languages.

**Svetlana M. Malkhazova¹, Varvara A. Mironova^{1*}, Dmitry S. Orlov^{1,2},
Olga S. Adishcheva¹**

¹Department of Biogeography, Faculty of Geography, Lomonosov Moscow State University

²Institute for Atmospheric and Earth System Research, Faculty of Science, University of Helsinki, Finland

*Corresponding author; mironova.va@gmail.com

INFLUENCE OF CLIMATIC FACTOR ON NATURALLY DETERMINED DISEASES IN A REGIONAL CONTEXT

ABSTRACT. The spread of almost all diseases caused by living pathogens is determined primarily by environmental conditions. These pathogens like any other biological objects are the components of the certain natural ecosystems. An essential part of any medico-geographical assessment is the search for links between the spread of diseases and factors of the geographical environment. The role of factors that affect the spread of the natural diseases is unequal. The climatic factor is deemed one of the main determinants for the spread of naturally-determined diseases. This factor manifests itself at all levels of territorial differentiation. The goal of these studies was to identify the natural and climatic suitability of the certain territory for spread of diseases in order to assess the possible influence of the climatic factor on the medico-geographical situation in the context of the regional environment. The objectives are to estimate the role of climatic and weather parameters in the functioning of natural foci in Russia; to assess the natural and climatic suitability of the territory for spread of diseases; and to identify the climatic preconditions of spread of particular climate-dependent infections. In this study, on the example of several climate-dependent diseases different approaches to medico-geographical assessment have been implemented and number of new methodological solutions have been proposed.

KEY WORDS: Medical geography, naturally-determined diseases, climatic factor

CITATION: Svetlana M. Malkhazova, Varvara A. Mironova, Dmitry S. Orlov, Olga S. Adishcheva (2018) Influence of Climatic Factor on Naturally Determined Diseases in a Regional Context. *Geography, Environment, Sustainability*, Vol.11, No 1, p. 157-170
DOI-10.24057/2071-9388-2018-11-1-157-170

INTRODUCTION

The spread of almost all diseases caused by living pathogens is determined primarily by environmental conditions. Their parasitic systems like any other biological objects are integral components of ecosystems, thus their spatial distribution and dynamics are influenced by various natural factors (Malkhazova 2001).

An essential part of any medico-geographical assessment is search for links between spread of diseases and factors of the geographical environment. These factors are considered as preconditions of infectious diseases as postulated by a concept developed and substantiated by the Russian scholars in the middle of 20th century. Although existence of a disease in reality is determined by a nature and a structure of a geosystem as a whole, only one of the natural components usually turns to be the direct cause of the spread of certain disease. Therefore, depending on the research tasks, it is possible to consider both the landscapes and their individual components as disease preconditions.

The role of factors affecting spread of natural diseases is different. The climatic factor is deemed one of the main determinants for spread of naturally-determined diseases. This factor manifests itself at all levels of territorial differentiation. At its highest (national) level it determines the latitudinal zoning which, in turn, defines the conditions for the existence of disease hosts and vectors and, ultimately, the foci of diseases. At the regional level the effect of climate conditions manifests itself in parameters of weather such as average monthly temperature, precipitation levels, snow cover height, duration of the frost-free period, etc. Climate characteristics are especially crucial for poikilothermic animals like arthropods and for the pathogens that spend part of their life cycles inside them.

Atmospheric temperature defines the heat supply of a region which has a significant influence on pathogen hosts and vectors affecting the pathogen's survival in vectors and in the environment. It also determines

existence of disease vector populations that have a thermal optimum and threshold temperatures above and below which they cannot survive. Important parameters are also the sum of active temperatures (i.e. the sum of temperatures during a period with the annual daily temperatures above 10°C) (Isaev 2001) and the sum of effective temperatures, or growing degree days (GDDs) (i.e. the number of temperature degrees above a certain threshold temperature below which an organism cannot survive). The sum of active temperatures characterizes the heat supply of an ecosystem, whereas GDDs reflect warmth needs of a particular biological species. These parameters are mostly used in relation to plants, but, in fact, they characterize warmth necessities of any poikilothermic organisms, including pathogens and vectors (Podolsky 1967). Other meteorological indices (minimum temperature, maximum temperature, etc.) can play a significant role, especially on the local level.

Precipitation determine availability and characteristics of water bodies where vectors breed (primarily mosquitoes, horseflies, etc.). Water bodies also serve as habitats for hydrophilic species that carry natural focal infections like tularemia or leptospirosis.

Over the recent years, the team at the Department of Biogeography of the Faculty of Geography of the Lomonosov Moscow State University conducted the research with the aim to assess the changes in distribution of naturally-determined diseases and the role of climatic factor in their development. The goal of these studies was to identify the natural and climatic suitability of the certain territory for spread of diseases in order to assess the possible influence of the climatic factor on the medico-geographical situation in the context of the regional environment. The objectives are to estimate the role of climatic and weather parameters in the functioning of natural foci in Russia; to assess the natural and climatic suitability of the territory for spread of diseases; and to identify the climatic preconditions of spread of particular climate-dependent infections.

Below we consider the results of a study of the climatic factor effect on spread of certain important naturally-determined diseases in Russia with different transmission mechanisms.

MATERIALS AND METHODS

To identify the natural and climatic suitability of the territory for the spread of diseases, three model infections were chosen: tularemia (as of the most important widespread natural focal disease), West Nile fever (as one of the most important emergent vector-borne disease with expanding nosoarea), and vivax malaria (as one of the most important natural endemic anthroponosis).

Statistical data on population morbidity rates in 1997-2015 was provided by The Federal Service for Surveillance on Consumer Rights Protection and Human Wellbeing (Rospotrebnadzor) and Moscow branch of the federal anti-plague agency "Rospotrebnadzor Anti-Plague Center". The data on the tularemia pathogen culture isolation from environmental sources was considered for the period 1941- 2015, climatic data for assessment of favorability of climatic conditions for malaria reintroduction was considered for the period of 51 years (1965-2015). A numerous literature sources (Lvov and Lebedev 1974; Lvov and Ilyichev 1979; Lvov 1989; Tran et al. 2014, etc.), cartographic materials

(Geographical Atlas, 1982; Atlas of the USSR, 1983; National Atlas of Russia, 2007; Medico-geographical Atlas... 2017), Department of Biogeography's archive data served as information sources throughout our research. Data processing was carried out using Microsoft Excel, MapInfo Professional 11.0. and ArcGIS 10.1 software. To calculate meteorological characteristics, mean daily air temperature and precipitation data obtained from open online databases (<http://www.worldclim.org>; www.meteo.ru) was used.

The overall algorithm implemented in the study consisted in, with the use of morbidity rates data, evaluating spread of considered infections, and then, with the use of meteorological parameters, assessing the effect of climate on the naturally determined diseases distribution (Fig. 1). Specific approaches and methodologies were chosen based on the disease peculiarities, territorial level of research and data availability.

RESULTS AND DISCUSSION

Tularemia

Tularemia (rabbit disease) is a highly infectious bacterial disease caused by a hazard class A pathogen, Francisella tularensis. Tularemia can spread through arthropod bites, infected water or dust, or by handling sick animals. The impact

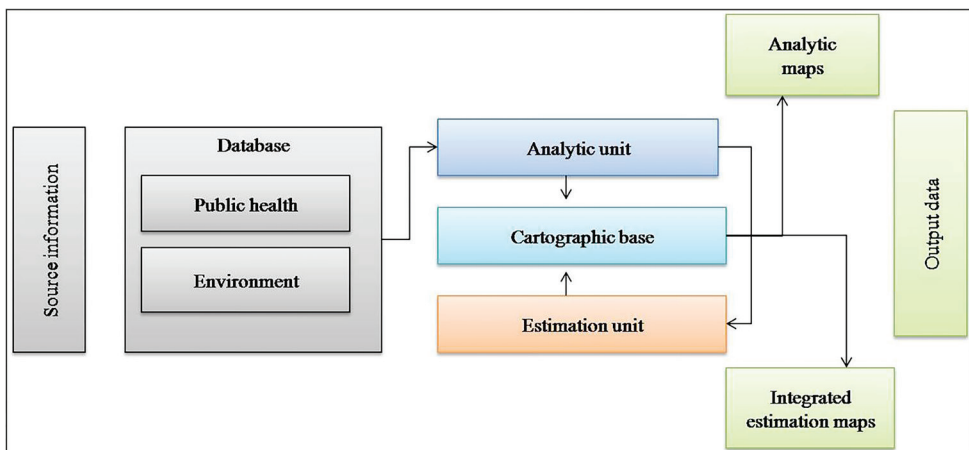


Fig. 1. The algorithm for the assessment of the state of population health
Results and discussion

of climate change is likely to have an effect on tularemia transmission patterns in highly endemic areas because a large majority of cases transmitted to humans by blood-feeding arthropods occur during the summer season and is linked to increased temperatures (Rydén et al. 2009; Meshcheryakova et al. 2014). Therefore, high temperature for a long period accompanied by low rainfall and low humidity may affect the vector's biology and initiate a tularemia outbreak.

In recent years, on an average of 100 to 500 tularemia cases were reported annually in the Russian Federation. There are active natural foci of tularemia on endemic areas as evidenced by the results of isolation of the pathogen cultures from rodents, arthropods, environmental objects, including water samples from open reservoirs. Tularemia manifests itself primarily as a sporadic disease in Russia. At the same time, there were vector-borne outbreaks that occurred in 2005 in the Central Federal District with more than 800 people affected and in the Khanty-Mansiysk Autonomous Okrug in 2013 with more than 1,000 individuals involved. Over the past decade, about 2,000 tularemia cases have been reported in the Russian Federation, the most of them occurred in the European territory of Russia. The spread of tularemia is uneven due to variations in natural (primarily climatic) conditions in focal area.

To identify peculiarities of tularemia distribution on areas with various climatic conditions, three key regions with different climate types were selected: Murmansk Oblast, Moscow Oblast, Krasnodar Krai (including the Republic of Adygea), and a series of maps was created. Using the GIS package MapInfo Professional 11.0, we marked on the raster regional climatic maps the sites of cases of human infection with tularemia (red dots) and sites of cases of isolating of the tularemia pathogens (blue dots). Climate types were considered in accordance with B.P. Alisov's classification (Atlas... 1983).

Tularemia morbidity rate in Murmansk Oblast is very low and occurs only as

sporadic cases. From 1997 to 2015 only eight cases of tularemia were reported. Pathogen cultures from environment objects were also quite rarely isolated. All locations of human infection and pathogen culture isolation were confined to the northern and central regions of the Oblast with varied mean annual air temperatures but with the same amount of precipitation from 500 to 600 mm per year.

According to climatic zoning of Russia (National Atlas.. 2007) tularemia foci are dispersed over the territories of both Atlantic province of the subarctic climatic belt (moderately cold, wet, the total solar radiation is 2,700 MJ/m² per year, the sum of air temperatures above 10°C is 200°C, the average annual precipitation and evaporation sum is more than 200 mm) and in the Atlantic-Arctic province of the temperate belt (moderately warm, excessively wet, the total solar radiation is 3150-3350 MJ/m² per year, the sum of air temperatures above 10°C is 800-1400°C, the average annual precipitation and evaporation sum is more than 200 mm). In general, Murmansk Oblast can be attributed as the area unfavorable for the existence of tularemia foci. Rare cases of human disease and isolated pathogen cultures were associated with unusual weather conditions (for example, extremely high summer temperatures).

Tularemia morbidity in Moscow Oblast has been registered since 1941 and to date, the presence of tularemia natural foci of three types has been reliably confirmed in 36 administrative districts within the said region: floodplain and swamp, field and meadow and forest foci. Tularemia foci activity is confirmed by registered autochthonous morbidity, isolation of the pathogen cultures from rodents, bloodsucking arthropods, snow-covered nests and from the natural water bodies. From 1965 through 2013, 226 cultures of tularemia microbe were isolated, 96 of them from small mammals. The highest number of cultures (25%) was isolated in the field and meadow stations from common voles. The number of water voles in recent decades has decreased significantly, most

likely due to the ongoing changes in biocenoses (Demidova et al. 2015). One of the factors that determine the circulation of the tularemia pathogen in the natural foci of Moscow Oblast are ixodid ticks that are considered vectors and long-term natural reservoirs of this infection, both in epizootic and interepizootic periods.

The locations where cases of human tularemia infection were recorded are evenly distributed throughout the territory of the region (Fig.2).

On the basis of the data obtained, the regionalization of Moscow Oblast according to the degree of epidemic danger was carried out (Fig. 3). Points were assigned to each administrative district with the following indicators: the number of tularemia cases (1-3 points); the number of years of disease cases registration (1-3

points); the number of isolated tularemia pathogen cultures from environmental sources (1-3 points); the number of years with pathogen reporting (1-3 points); presence of settlements with infected humans near the pathogen isolation sites (1-3 points). On the basis of this scoring, all districts of the Moscow Oblast were divided into three groups: areas with high epidemic hazard (11-15 points), areas with moderate epidemic hazard (6-10 points), and areas with low epidemic hazard (0-5 points).

In Krasnodar Krai and the Republic of Adygea (Fig. 4), epizootics among rodents and disease cases among humans were periodically reported. Natural foci of tularemia were found within 35 districts of Krasnodar Krai and 7 districts of the Republic of Adygea. The most epizootologically important are two landscapes: the plain-steppe and piedmont in which human

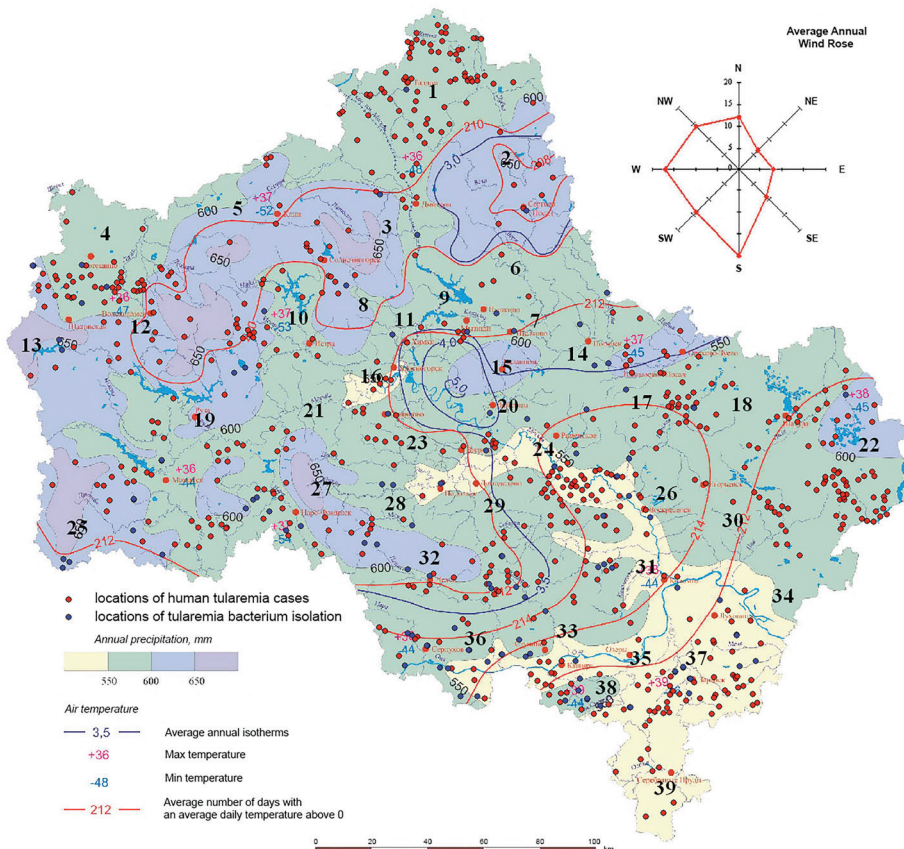


Fig. 2. Climatic characteristics of Moscow region and tularemia cases distribution

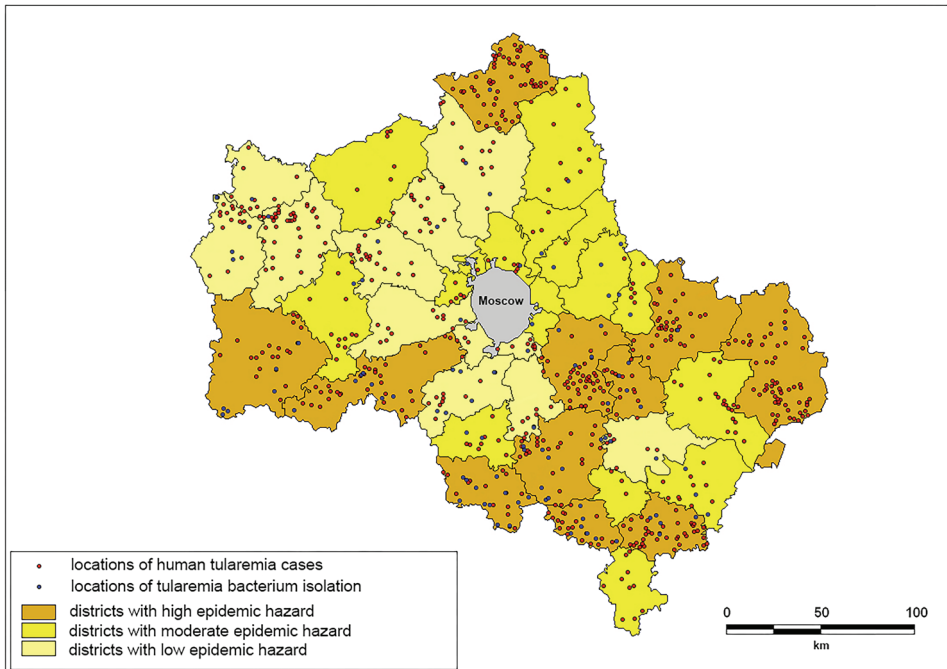


Fig. 3. Regionalization of Moscow Oblast according to the degree of tularemia epidemic risk

disease cases were reported for decades and pathogens were isolated from rodents and ticks. There are 28 species of rodents which are the main nutrient sources of ixodid ticks in this region. This factor plays a leading role in the maintaining of tularemia natural foci. Sporadic human cases and the isolation of the pathogen cultures have been reported from 1997 to 2015. All cases were unevenly distributed throughout the region concentrating in the plain-steppe and piedmont regions of the Atlantic-continent Southern European climatic province of the temperate belt with average annual precipitation of 500-800 mm (very warm, not sufficiently moist, the total solar radiation is 4600-5050 MJ/m² per year, the sum of air temperatures above 10°C is 2600-3200°C, the average annual precipitation and evaporation sum is -200 – -400 mm). In the south of Krasnodar Krai, tularemia was not reported in areas with an average annual precipitation of 800 mm or more.

Thus, natural foci of tularemia are common in different climatic zones of Russia and are confined to various landscapes. The conditions of human infection,

seasonality, magnitude of morbidity and other epidemiological features of tularemia infection vary significantly in areas with natural foci of one type or another. Apparently, the areas with a moderate climate are the optimal for this infection. In the arctic, subarctic, subtropical belts, tularemia occurs within intrazonal landscapes.

West Nile fever

West Nile fever (WNF) is a natural focal arboviral emergent infectious disease caused by West Nile virus (WNV). WNV was first isolated in 1937 from a feverish patient in the West Nile province in northern Uganda, which gave its name. After 60 years, the disease was revealed on 5 continents, so the virus became the most common arbovirus in the world. The main components of WNF natural focus are hosts (predominantly birds), vectors (predominantly blood-sucking mosquitoes) and the pathogen itself (WNV). The two most significant natural factors in WNF's epidemiology are climatic and biotic (availability of suitable vectors and hosts). WNV transmission on

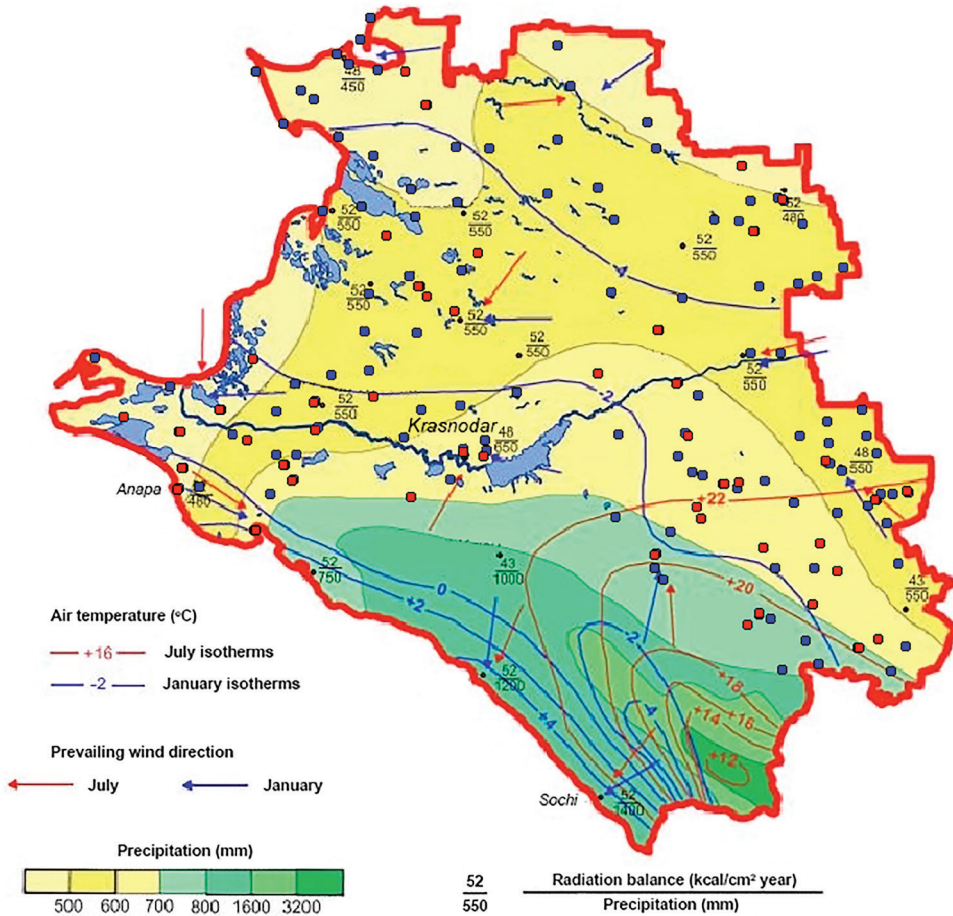


Fig. 4. Climatic characteristics of Krasnodar Krai and the Republic of Adygea and tularemia cases distribution

its own depends on a complex interaction of different factors, related to virus, birds, mosquitoes, humans, and weather, that contribute to epidemic/epizootic spread of the infection. The reproduction of WNV in infected mosquitoes increases along with temperature rise (Kilpatrick et al. 2008). An increase in temperature in the 18–30°C range shortens the gonotrophic period of mosquitoes encouraging mosquito activity (increasing the frequency of mosquito's bloodmeals) (Paz et al. 2008). It was shown that extrinsic incubation period (EIP) of the virus in an American mosquito species *Cx. tarsalis* decreased from 30 days at 18°C to 10 days at 26°C (Reisen et al. 2006). Supposedly, this results in intensifying WNV transmission which may accelerate at high temperatures. It was estimated for American strains of WNV that the temperature threshold for virus

developing in a mosquito is 14.3°C, and the EIP required for its transmission is 109°C/day (Reisen et al. 2006; Hartley et al. 2012).

It was long believed that the northern border of WNV's nosogenic territory in Russia more or less coincides with the 16°C July isotherm, meaning that the majority of Russia's territory is at risk (Lvov et al. 1989). Unfortunately, an accurate data on EIP duration and the threshold temperatures for WNV strains occurring in Russia and its populations of *Culex* mosquitoes is not available but juxtaposition of results of several Russian studies with estimation of Reisen et al. (2006) confirms acceptability of these figures for Russian strains (Platonov et al. 2014; Safronov et al. 2014). Cold winter months lower the likelihood of an outbreak during the following summer (Platonov et al. 2014).

The first case of human disease with the WNV in Russia was detected in the Astrakhan Oblast in 1997. By 2017, 20 regions (mainly located in the south of the European part of Russia, the Southern Urals and the south of Western Siberia) are already affected by the arbovirus. Currently, WNV cases are registered in most years in the Astrakhan, Volgograd and Rostov oblasts. In this area, the most suitable climatic and biotic conditions for the pathogen occur (continuously high temperatures and the presence of a large number of birds in the aquatic complexes and wetlands). More than 2400 cases of the disease were registered during 20 years. The biggest amount of cases (more than 100 yearly) occurred in 1999, 2007, 2010, 2012 and 2016.

For the purpose to determine the northern limit of the possible spread of WNV in regions with continental climate we relied on the results of the study in other globe regions and on the estimates for the territory of Russia (Lvov et al. 1989; Reisen et al. 2006; Kilpatrick et al. 2008; Adishcheva et al. 2016) and took as the border the July isotherm at 14°C, and the duration of the period with temperatures above 10°C for 135 days. In more humid, maritime climate,

the nosoreal is limited by the sum of the effective temperatures above 10°C, which must be at least 2000°C. The potential nosoreal of the WNV was ascertained by imposing these indicators on the administrative map of Russia chosen as a basis for the convenience for counting the number of regions in which the natural and climatic conditions allow the transmission of the virus.

The analysis shows (Fig. 5) that about 60 regions of the Russian Federation are located on the area of WNF potential outbreak risk. The main WNF natural foci in Russia saturated in the lowlands of the Volga and Don rivers but, since its introduction in Russia, WNF has moved significantly eastward and northward in just two decades. Overall, the disease was reported in 21 Russian regions from 1997 to 2015. Most WNF cases in Russia occur in the summer beginning in mid-July. Outbreaks in Russia's southern regions are first of all linked with favourable climate conditions (average July temperatures far exceed 16°C, which allows for the rapid accumulation of virus in mosquitoes' salivary glands) and the presence of hosts and vectors. Therefore, with the climate warming, the

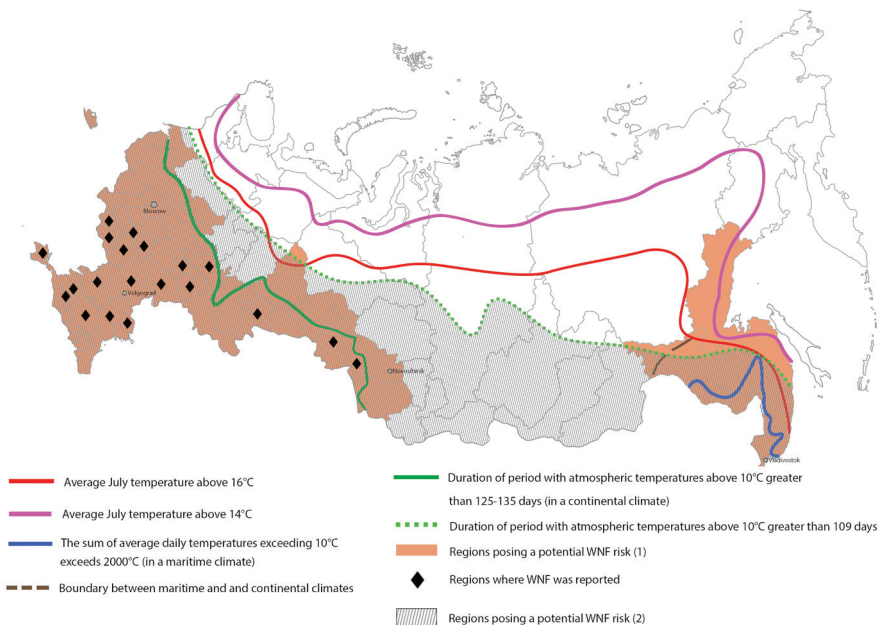


Fig. 5. WNF potential risk areas

range of suitable climatic conditions is possible to expand which may increase the geographical range of mosquitoes and, correspondingly, the range of WNF in Russia.

Vivax malaria

There are four species of malaria that infect humans. Each of them induce one of four different diseases, each with specific clinical features and epidemiology. In the pre-elimination era malaria was endemic in most of Europe. In the middle of 20th century all species of malaria were eliminated on the territory of the USSR, and since then, short-living episodes of autochthonous transmission following importation of *P. vivax* have been documented in a number of European countries, but Russia was the most affected. More than 500 autochthonous cases were recorded in European Russia from 1997 to 2010. Autochthonous malaria cases were reported in 24 of 50 regions of European Russia. After 2004 local malaria transmission dramatically decreased due to less favorable weather conditions after 2002 and interruption of the importation of malaria from Tajikistan and Azerbaijan due to improvement of malariological situation in these countries.

From the point of view of possible transmission re-introduction, vivax malaria represents a reliable model because it was highly endemic in European Russia in the past and, unlike other malaria species, could easily re-introduce itself in previously endemic areas after elimination (Mironova 2006; WHO 2010).

During the last half of the 20th century the suitability of climatic conditions for vivax malaria transmission improved on the entire territory of European Russia but this trend manifested itself differently in various parts of the potential nosoarea. We estimated the changes in favorability of climatic conditions for vivax malaria transmission in different parts of European Russia.

To assess the role of climate change trends in reemergence of vivax malaria in European Russia we investigated the variations in favorability of weather conditions in

different parts of European Russia in order to assess their role in malaria reintroduction. Summer temperatures have been analyzed for 5 geographical points of various climatic zones in European Russia for 51 years up to 2015 (Fig.6). The analysis was based on Moshkovsky's method (Moshkovsky and Rashina 1950), that allows to assess elements of malaria season.

Required sum of temperatures above the base temperature for *Plasmodium vivax* is 105 degree-days

The formula for calculating of daily effective temperature for *P. vivax* parasite is

$$E = T_a - T_b, \text{ at } T_a > T_l, \text{ where:}$$

E – effective temperature (a sum of temperatures gained by a parasite during one day)

T_a – daily average temperature

T_b – base temperature (14,5°C)

T_l – Lower threshold of development (+16°C)

The effective temperatures are summarized for the whole season starting from the date of beginning of the period of effective infectivity (e.g. the date of a stable transition of daily average temperatures through the threshold of +16°C) till the date of the last effective infection of mosquito.

Each summer season was classified upon its favorability to vivax malaria transmission into several groups, from “absolutely unfavorable” to “particularly favorable”, according to the previously elaborated methodology (Mironova 2006). The structure of malaria epidemic season and the correspondence of its parts is discussed in details in our work dedicated to the method of prognosis of vivax malaria potential spread using climate modeling data (Malkhazova et al. 2018).

The territory of European Russia was tentatively divided into three latitudinal parts. The trends in the evolution of the malariological situation were examined in each of them.

Northern part of possible malaria nosogenic territory.

During the period under review, the occurrence of secondary malaria cases (that

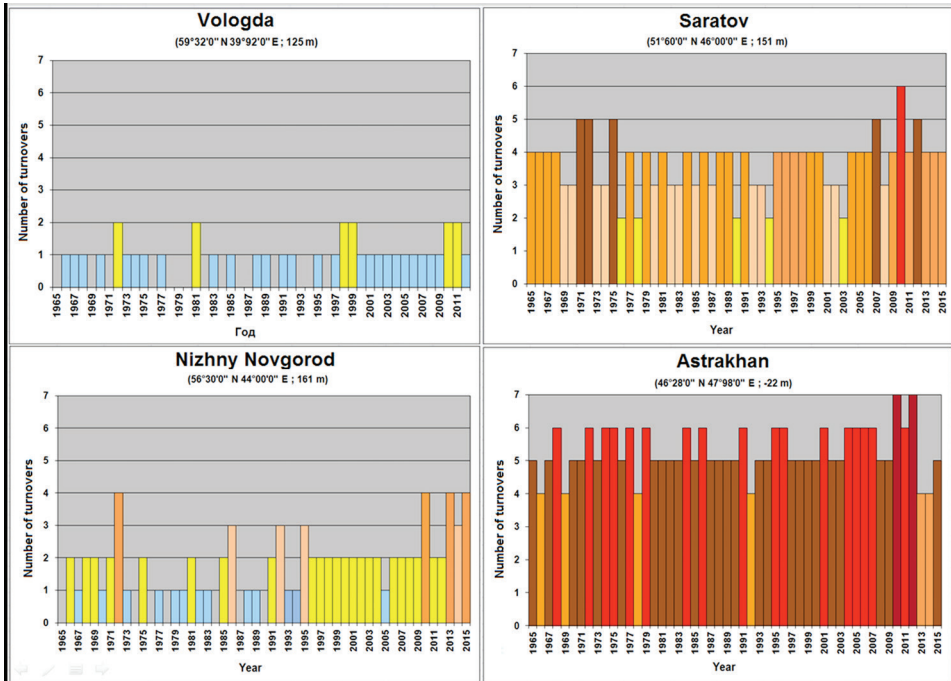


Fig. 6. Vivax malaria epidemic seasons in different parts of European Russia

is, ephemeral transmission) in Arkhangelsk was possible in less than half of the seasons and only three times – (in 1972, 1974 and 2010) third generation cases could occur from secondary cases. The remaining seasons were absolutely unfavorable, meaning that maturation of sporozoites in mosquitoes was impossible. From 1991 to 1997, the amount of warmth needed to transmit malaria by mosquitoes was not reached. The situation has changed slightly since 1998 and the main distinguishing feature of this period was a significantly smaller number of absolutely unfavorable seasons.

Mean annual sum of air temperatures above 10°C in Arkhangelsk is about 1200°C. In the years when the transmission of vivax malaria was possible, the average annual sum of the effective temperatures (above the threshold value of +16°C) was only 182.8°/days. Given that the minimum amount of effective temperatures for a vivax is 105°/days, we can say that in general this region is unfavorable for the spread of malaria and the climatic changes of the past few decades have affected only by a slight increase in the number of seasons when an ephemeral transmission is possible.

The meteorological situation in Vologda (see Fig. 6) is similar to the situation described above in Arkhangelsk. It differs only in a larger number of seasons during which only ephemeral transmission from imported cases is possible (i.e. the unfavorable seasons). It is noteworthy that absolutely unfavorable seasons have not been noted after 1997 which fact, it may be supposed, is due to the increase in the heat supply in this region. However, the number of days with an average daily air temperature above + 16°C is negligible.

Despite the fact that, according to our calculations, the probability of local transmission of vivax malaria in Arkhangelsk and Vologda is estimated as extremely low, we can state the presence of a tendency to a certain increase in favorability of climatic conditions in the northern periphery of the potential nosoareal of malaria. If these trends persist in these territories, it is possible to talk about the probable occurrence of autochthonous cases under appropriate conditions, at least in certain years.

Central part of possible malaria nosogenic territory.

The considered period of 1965-2015 in Nizhny Novgorod (see Fig. 6) can be quite clearly divided into two intervals, before and after 1995. During the first period, the number of favorable epidemic seasons was insignificant and unfavorable and absolutely unfavorable seasons prevailed. After 1995, the transmission of vivax malaria became possible annually in this region. There were conditions favorable for occurrence of cases of the second and third generation and after 2010 there were three very favorable seasons (2010, 2013 and 2015) during which cases of the fourth generation could occur, i.e. there were opportunities for epidemic outbreaks in presence of infected individuals. We previously observed the similar situation in Moscow region (Mironova 2006).

Southern part of possible malaria nosogenic territory.

The climatic conditions of Saratov (see Fig. 6) have always been very favorable for malaria transmission. However, there is a trend to an increase in the number of infection turnovers during the season, starting from mid-1990s. If before 1995, the seasons with four possible turnovers alternated with seasons with only three or even two, then after 1995 there were almost no seasons with less than four turnovers of the infection.

In Astrakhan (see Fig. 6), considering the region's fair heat supply, absolutely all seasons were very favorable for the transmission of vivax malaria differing only in the number of infection turnovers. Since the mid-1990s, however, the trend towards an increase in the number of turnovers during one epidemic season is fairly evident (despite two relatively unfavorable seasons of 2013 and 2014 when only four infections were possible).

As demonstrated by the calculations, throughout the European territory of Russia (ETR), one can note an increase in the degree of favorability of the climate conditions for the transmission of malaria. There is a trend

in the north of the ETR towards an increase in number of seasons favorable for malaria transmission. At the same time there is an increase in the number of possible turnovers during one season in the southern regions. This conclusion corresponds to our previous estimations made for Moscow region (Mironova 2006) and to modeling implemented for European Russia as a whole (Malkhazova et al. 2018).

Besides the favorable climatic conditions, the presence of infection (infected persons) and an effective vector is crucial for spread of malaria. Therefore, the favorable climate conditions themselves do not certainly produce autochthonous malaria cases. We can speak only about the existence of climatic preconditions which can be realized in local transmission in the presence of necessary members of malaria parasitic system.

CONCLUSIONS

The climatic factor is deemed one of the main determinants for the spread of naturally determined diseases.

An essential part of any medico-geographical assessment is the search for links between the spread of diseases and factors of the geographical environment. A medico-geographical analysis allows for establishing the relationships between diseases and natural factors and differentiate territories upon epidemiological hazard levels.

The analysis showed that natural foci of tularemia are common in different climatic zones of Russia and are confined to various landscapes but the conditions of human infection (seasonality, morbidity rates and other epidemiological features) of tularemia infection vary significantly. The conditions of different climatic zones are not equal for existence of tularemia natural foci. In European Russia, the most favorable for tularemia infection are the areas with a moderate type of climate – (temperate belt), Atlantic-continent European region (total solar radiation - 3350-4200 MJ/m² per year, the sum of air temperatures above

10°C - 1600-2400°C, average annual the sum of precipitation and evaporation - 200 - -100 mm). In the Arctic, subarctic, subtropical climatic belts, tularemia occurs mainly within the intrazonal landscapes, such as floodplains and deltas of rivers, coasts of lakes and swamps.

Outbreaks of West Nile fever in Russia are primarily linked with favorable climate conditions (average July temperatures far exceed 16°C which allows for the rapid accumulation of virus in mosquitoes' salivary glands) and the presence of viral hosts and vectors. The analysis shows that about 60 constituent entities of the Russian Federation are located on WNF outbreak risk area. The main WNF natural focal area in Russia have been evolved in the lowlands of the Volga and Don rivers but, since its introduction in Russia, WNF has moved significantly eastward and northward in just two decades.

During the recent decades, the suitability of climatic conditions for vivax malaria transmission improved on the entire territory of European Russia but this trend manifested itself differently in various parts of the potential nosoarea. In general, the possibility of autochthonous malaria transmission is estimated as extremely low at its northern periphery but it can be noted that there is a tendency towards a rising number of favorable malaria transmission seasons. If this trend remains stable on these territories, we can talk about the possibility of local cases occurrence in the presence of an infection source. In the central and southern parts of the potential nosoarea, the climate

suitability improved due to a more favorable combination of temperatures during summers. The changes are more apparent in central parts of European Russia. With regard to southern part of European Russia, the climatic changes evidence in that in some seasons the number of possible transmission turnovers exceeded 7 for the first time in the past 50 years.

Regional and global environmental changes, first and foremost, the global warming, may complicate the modern medico-geographical situation. With the climate warming, the range of suitable climatic conditions is possible to expand, which may increase the geographical ranges of naturally-determined diseases in Russia. All this called for a focused research in order to assess possible alterations.

ACKNOWLEDGEMENTS

This study has been supported by the Grant program from Russian Science Foundation (RSF) (Project No.17-77-20070) "An initial assessment and projection of the bioclimatic comfort in Russian cities in XXI century against the context of climate change" and by the Grant program from Russian Foundation for Basic Research (RFBR) (Project No. 16-05-00827 A) "Regional trends of urban mortality in Russia: environmental health assessment and mapping". Research on tularemia was supported by the Russian Science Foundation (RSF) (Project no. 14-50-00029) "Scientific Fundamentals of the Creation of a National Depository Bank of Living Systems". ■

REFERENCES

- Adishcheva O.S., Malkhazova S.M., Orlov D.S. (2016). Distribution of West Nile Fever in Russia. *MSU Vestnik. Series 5. Geography*. 4: pp. 48-55. (in Russian).
- Demidova T.N., Popov V.P., Polukhina A.N., Orlov D.S., Mescheryakova I.S., and Mikhailova T.V. (2015). Epizootic and epidemic manifestation of natural foci of tularemia in Moscow region (1965-2013). *Journal of microbiology, epidemiology and immunobiology*, (2), pp. 24-31. (in Russian).
- Gvozdetsky N.A. (Eds) (1983). *Atlas of the USSR*. Moscow: Main department of geodesy and cartography. P. 100. (in Russian).

Hartley D.M., Barker C.M., Le Menach A., Niu T., Gaff H.D., and Reisen W.K. (2012). Effects of temperature on emergence and seasonality of West Nile virus in California. *The American journal of tropical medicine and hygiene*, 86(5), pp. 884-894.

Isaev A.A. (2001). *Ecological climatology*. – M.: Science World, 456 p. (in Russian).

Kilpatrick A.M., Meola M.A., Moudy R.M., and Kramer L.D. (2008). Temperature, viral genetics, and the transmission of West Nile virus by *Culex pipiens* mosquitoes. *PLoS pathogens*, 4(6), e1000092.

Kolosova L.N. (eds) (1982). *Geographical Atlas for secondary school teachers*. 4th edition. Moscow: Main department of geodesy and cartography. P. 143. (in Russian).

Lvov D.K. and Ilyichev V.D. (1979). Bird migration and pathogen transfer (ecologico-geographical relations of birds with infectious pathogens). Moscow. Science. 270 p. (in Russian).

Lvov D.K. and Lebedev A.D. (1974) *Arboviruses ecology*. Moscow: Medicine. 182 p. (in Russian).

Lvov D.K., Klimenko S.M. and Gaydamovich S.Ya. (1989) *Arboviruses and arboviral infections*. Moscow: Medicine. 336 p. (in Russian).

Malkhazova S.M. (2001). *Medico-geographical Analysis of the Territories: Mapping, Assessment, Forecast*. Moscow: Science World. 239 p. (in Russian).

Malkhazova S.M., Shartova N.V., and Mironova V.A. (2018). Epidemiological Consequences of Climate Change (with Special Reference to Malaria in Russia). In *Climate Change and Air Pollution*. Springer, Cham, pp. 151-164.

Medico-geographical Atlas of Russia «Natural Focal Diseases». 2nd Edition / Vatlina T.V., Kotova T.V., Malkhazova S.M., Mironova V.A., Orlov D.S., Pestina P.V., Rummyantsev V.Yu., Ryabova N.V., Soldatov M.S., Shartova N.V. / edited by S.M. Malkhazova. M.: Faculty of geography, 2017. 216 p.

Meshcheryakova I.S., Dobrovolskiy A.A., Demidova T.N., Kormilitsyna M.I., and Mikhailova T.V. (2014). Transmissible Epidemic Outbreak of Tularemia in Khanty-Mansiysk City in 2013. *Epidemiology and Vaccination*, 5 (78), pp.14-20 (in Russian).

Mironova V.A. (2006). Climate change trends and malaria in Moscow region. Moscow: *Medical parasitology and parasitic diseases*. Vol. 4, pp. 20-25 (in Russian).

Moshkovsky S.D. and Rashina M.G. (Eds) (1951). *Epidemiology and Medical Parasitology for Entomologists*. Moscow: Medgiz. 455 p. (in Russian).

Paz S., and Albersheim I. (2008). Influence of warming tendency on *Culex pipiens* population abundance and on the probability of West Nile Fever outbreaks (Israeli case study: 2001–2005). *EcoHealth*, 5(1), 40-48.

Platonov A.E., Tolpin V.A., Gridneva K.A., Titkov A.V., Platonova O.V., Kolyasnikova N.M., ... and Rezza G. (2014). The incidence of West Nile disease in Russia in relation to climatic and environmental factors. *International journal of environmental research and public health*, 11(2), pp. 1211-1232.

Podolsky A.S. (1967). New developments in phenological forecasting. Moscow: Kolos, 232 p. (in Russian).

Reisen W.K., Fang Y., Lothrop H.D., Martinez V.M., Wilson J., O'Connor P, ... and Brault A.C. (2006). Overwintering of West Nile virus in southern California. *Journal of medical entomology*, 43(2), pp. 344-355.

Rydén P., Sjöstedt A., and Johansson A. (2009). Effects of climate change on tularaemia disease activity in Sweden. *Global health action*, 2(1), 2063 p.

Safronov V.A., Smolenskij V.Ju., Smeljanskij V.P., Savchenko S.T., Razdorskij A.S. and Toporkov V.P. (2014). Assessment of epidemic manifestations of the West Nile fever in the Volgograd region depending on the climatic conditions. Moscow: *Problems of virology*, 59(6), pp. 42-26 (in Russian).

Dumnov A.D., Kirsanov A.A., Kiseleva E.A., Lipiyainen K.L., Rybalsky N.G., Snakin V.V., ... and Gribchenko Yu.N. (2007). *The National Atlas of Russia*. Nature. Vol.2. P. 495 (in Russian).

Tran A., Sudre B., Paz S., Rossi M., Desbrosse A., Chevalier V., and Semenza J. C. (2014). Environmental predictors of West Nile fever risk in Europe. *International journal of health geographics*, 13(1), 26.

World Health Organization (2010). Practical guidelines on malaria elimination for countries of the WHO European Region. In *Practical guidelines on malaria elimination for countries of the WHO European Region*. Geneva, WHO, 109 p. (in Russian).

Received on February 1st, 2018

Accepted on March 1st, 2018



Svetlana M. Malkhazova is Doctor of Geographical Sciences, Professor, Head of the Department of Biogeography, Faculty of Geography, Lomonosov Moscow State University. Her main research interests relate to biogeography, ecology, and medical geography. She is the author of over 250 scientific publications, including 10 books, several textbooks, and medical and environmental atlases.

Lassi Heininen^{1,2*}

¹ International Institute for Applied System Analysis, IIASA

² University of Lapland, Finland

*Corresponding author; lassi.heininen@ulapland.fi

ARCTIC GEOPOLITICS FROM CLASSICAL TO CRITICAL APPROACH – IMPORTANCE OF IMMATERIAL FACTORS

ABSTRACT. Despite different perceptions, discourses and approaches, the post-Cold War Arctic is with a high geopolitical stability based on institutional, international cooperation started by the Arctic states and supported by Arctic indigenous peoples, non-governmental organizations and sub-national governments. As a result, there are neither armed conflicts nor serious disputes on national borders. Behind the high geopolitical stability are on the one hand, common interests of the Arctic states to decrease military tension and increase political stability by causing a transformation from confrontation to environmental cooperation. On the other hand, there are certain features of Arctic geopolitics as prerequisites for a transformation, such as firm state sovereignty, high degree of legal certainty, and flexibility in agenda setting. When assessing a state of Arctic geopolitics and IR of the post-Cold War era, there is an ambivalence on how 'geopolitics' is defined. Behind are the dualism of military presence based on the nuclear weapons' systems and the high stability based on international, institutional cooperation between the eight Arctic states. As well as, that there are two major competing discourses: first, the Arctic as a 'zone of peace' and exceptional in world politics, and second, that there is a race of resources and the consequent emerging conflicts in the Arctic. In addition, there are fresh reminders that Arctic geopolitics is impacted by (grand) environmental challenges and 'wicked problems', in particular climate change; and that new multi-dimensional dynamics has made Arctic geopolitics global. The article aims to draw up a holistic picture of the post-Cold War Arctic, and discuss what might be special features of Arctic geopolitics in globalization. The article examines and discusses the transformation of approach from classical geopolitics to critical geopolitics by applying main approaches of geopolitics to the Arctic/Arctic geopolitics.

KEY WORDS: Geopolitics, the Arctic, Critical, post-Cold War, World politic

CITATION: Lassi Heininen (2018) Arctic Geopolitics from classical to critical approach – importance of immaterial factors. *Geography, Environment, Sustainability*, Vol.11, No 1, p. 171-186
DOI-10.24057/2071-9388-2018-11-1-171-186

INTRODUCTION

The ultimate aim, or 'arts', of 'Politics' is said to make possible to happen. This requires contest and (political) fight, which is done through, and by, a speech act and rhetoric. They, as well as texts, construct geopolitics, too (Moisio 2003). For example, the phrase to call the Arctic as a "zone of peace" by President Mikhail Gorbachev (1987) has influenced the reality and Arctic geopolitics. There are also other visions or perceptions concerning of the Arctic region, such as "Homeland", "Land of discovery", "Storehouse of resources", "Theater for military", "Environmental linchpin", "Scientific Arctic" by the Arctic Human Development Report (AHDR 2004). Correspondingly, among the imaginaries, or external and internal images, to cross borders are "Terra nullius", "Frozen ocean", "Indigenous statehood", "Resource frontier", "Nature reserve" by Contesting the Arctic (Steinberg et al. 2015). Finally, statements like "What happens in the Arctic, doesn't stay there!", indicate, even manifest, that the Arctic is been globalized (Heininen and Finger, 2017), and the global Arctic has become a barometer for global environmental and climate change.

As an analysis of different perceptions, the Arctic Human Development Report 2004 (Heininen 2004) recognized and defined the following as the main themes/trends of the early-21st century's Arctic geopolitics and IR: increasing circumpolar cooperation by indigenous peoples and sub-national governments; region-building with states as major actors; and a new kind of relations between the Arctic and rest of world. They are still relevant, though the context is been slightly changed, in particular the last one has become more important and strategic.

Popular geopolitics is more than written text. This is seen, when media does not only report about the Arctic but also influence how big audience is reading and interpreting Arctic geopolitics. For example, when a Russian long-range strategic bomber (Tupolev 95 "Bear") is seen flying pass (in international air space), or a military exercise is happening - though the question is about routine patrolling and activities by armies

-, the slogan or headline that "geopolitics is back!" may occur. Or, that in the Arctic there is a 'race' for resources and consequent emerging conflicts, as "*The Battle for the North Pole*" (Traufetter, 2008) media headline indicates. The interpretation of a return of geopolitics, particularly after the Russian expedition to the bottom of the North Pole in 2007, is not only media headlines, wretched slogans or misleading rhetoric. It was/is along to the mainstream interpretation of geopolitics, as well as that of new realism of IR as a traditional understanding of politics, which for example directed the European Union's attention to the Arctic (Raspotnik, 2016). Unlike, indigenous peoples' issues, in particular raised by their organizations, such as identities, land use, self-determination, or knowledge-creation and the interplay between science and politics as responses to security challenges of climate change, are mostly been interpreted to deal with 'governance', not geopolitics. Although dealing with values and aims, and bringing in other actors, they are along to critical approach of geopolitics.

Behind is that at the early-21st Arctic geopolitics and international century relations (IR) have been influenced by two major discourses (Heininen, 2010): The dominating discourse says that the Arctic of the early-21st century is with a high geopolitical stability based on established intergovernmental cooperation, the Arctic as a 'zone of peace' (Heininen 2016; Zagorski 2017; Byers 2017; NGP Yearbook 2011, 2012). As a counter-argument, there is another discourse saying that a race of resources and the consequent emerging conflicts, or even a new 'cold war', has started in the Arctic (Borgerson 2008; Traufetter 2008). Further, that the Arctic is like any other region of the world, and therefore it cannot be isolated from international politics (Käpylä and Mikkola 2015). In the literature of Arctic geopolitics & IR there are several contributions concentrating on the one hand, on different images and perceptions of the Arctic, Arctic governance, Arctic & Northern indigenous peoples and identities (Raspotnik 2016; Steinberg et al. eds. 2015; Powell and Dodds eds. 2014), and on the other hand, on (state) sovereignty,

international law and treaties, national policies, institutional points of view and international institutions, such as the Arctic Council (Murray and Nuttall eds. 2014; Yearbook of Polar Law 2013; Heininen 2011). In addition, there are a few fresh reminders: First, that 'the environment matters', i.e. Arctic geopolitics, as well as security, is impacted by (grand) environmental challenges, in particular long-range pollution (e.g. nuclear wastes) and rapid climate change (Hoogensen Gjörv et al. eds. 2013). Second, that globalization and its new geo-physical and socio-economic dynamics affect the Arctic region, and followed from that the new multi-dimensional dynamics has made Arctic geopolitics global (Keil and Knecht eds. 2017; Heininen and Southcott, eds. 2010), and the globalized Arctic has worldwide implications to the Earth (System) (Heininen and Finger 2017).

The aim of this article is to draw up a holistic picture of the post-Cold War Arctic, and discuss what might be special features of Arctic geopolitics in globalization. The article examines and discusses the transformation of approach from classical geopolitics to critical geopolitics by applying main approaches of geopolitics to the Arctic/Arctic geopolitics. Before applying geopolitics to the post-Cold War Arctic, I will examine and discuss the main schools of thought of geopolitics and their factors, in particular the approach shift from classical to critical geopolitics.

MATERIALS AND METHODS

When assessing a state of Arctic geopolitics and IR of the post-Cold War era, there is an ambivalence on how 'geopolitics' is defined, and what approach to use. Behind is the dualism of on the one hand, military presence based on the nuclear weapons' systems of the two superpowers – this is according to classical geopolitics and emphasizing physical space, power, technology and a state -, and on the other hand, high geopolitical stability based on international, institutional cooperation between, and concern on state of the environment by, the eight Arctic states – this indicates critical approach of geopolitics and emphasizes an importance of other

factors, such as quality of the environment, knowledge, and that there are several actors. The both parts of the dualism are correct, and thus, facts. Therefore, it is needed to ask: Does the current Arctic geopolitics go along to the mainstream understanding (classical) of geopolitics, or along to critical approach based on the transformation from classical to critical geopolitics? Or, is the current state (of Arctic geopolitics) some sort of hybrid, which includes aspects from the both approach?

To answer to these questions I apply the main schools of thought of geopolitics – classical, new and critical -, and their factors, to the Arctic and Arctic geopolitics of the post-Cold War period. Here factors (of geopolitics) play important role, as well as who are the actors, in particular important are values and aims of actors, their relations with theories and facts, and in particular how to change the facts to reach the values and aims. Final, I define and discuss common interests between the Arctic states, as well as special features of Arctic geopolitics, which made possible the transformation of the post-Cold War geopolitics from confrontation to high stability.

The used method here is critical approach of geopolitics. It is analytical and goes beyond classical geopolitics and traditional or positivist interpretation of international politics by drawing up a holistic picture on the issue area and having an unorthodox approach of IR. The critical approach, as critical social science in general, aims to take into consideration, in addition of general criteria of science (including criticism), values and aims/goals, and their relations with theories and facts, the interrelations between theories, facts, values and aims/goals, and final, how to change the facts to reach the values and aims/goals (Harle 2003). This is much according to the original idea of 'politics' to make possible to happen. If you value peace, and aim to have a peaceful situation, you choose theories, methods and means accordingly. Therefore, you cannot lean alone on factors, such as physical space, natural resources and power/force, which are determined with aims/goals like natural laws. You also need actors, in whose interest

peace is, people(s), civil society and other non-state and non-(security)political elitist actors. Behind is philosophy that to maintain peace is never passive and needs actors with interests, including values and aims to change facts to reach the values.

RESULTS

Despite different perceptions, discourses and approaches, the post-Cold War Arctic is with a high geopolitical stability based on institutional, international cooperation started by the Arctic states and supported by Arctic non-state actors, such as Arctic indigenous peoples, non-governmental organizations and sub-national governments. As a result, there are neither armed conflicts nor serious disputes on national borders. Instead, there is functional cooperation on several fields, and a dialogue between the Arctic states and other local actors, and between Arctic actors and those from outside of the region. The high stability, as well as cooperation, is firmly stated, even demonstrated, by the eight Arctic states with the first preamble of the joint ministerial meeting declarations of the Arctic Council: "Reaffirming the commitment to maintain peace, stability and constructive cooperation in the Arctic." (e.g., Iqaluit Declaration 2015; Fairbanks Declaration 2017), as well as by the five littoral states of the Arctic Ocean (Ilulissat Declaration 2008). The stability seems to have a solid foundation and be resilient, since it has been managed to maintain in spite of recent turbulent times in international politics and uncommon instabilities in world politics, and it has already passed, for far, a few tests (Clifford 2017; Heininen 2016; Heininen et al. 2014).

Behind the high geopolitical stability are on the one hand, common interests of the Arctic states to decrease military tension and increase political stability by causing a transformation from the confrontation of the Cold War period to functional environmental cooperation, and on the other hand, certain features of Arctic geopolitics as prerequisites for a transformation. Though there is a need for further research (Heininen forthcoming), among already known, discussed and analyzed common interests between the Arctic states are): First, to decrease

military tension and increase political stability between the former rivals, as the ultimate aim for confidence-building. Second, to start transboundary and functional (expert and scientific) cooperation for environmental protection and assessment, which could be expanded onto other fields. Third, to allow modern region-building with states as major actors, such as the establishment of the Arctic Council. Fourth, to support and encourage circumpolar inter-regional cooperation between Arctic indigenous peoples, sub-national governments and other non-state (local and regional) actors, which will correspondingly support environmental protection and region-building lead by states; Fifth, based on the history of exploration to maintain and enhance the Arctic as a 'laboratory'/'workshop' of international scientific research (Toyama Statement 2016), including to allow the scientific community to reach higher position of influence "within the Arctic Council's subgovernmental policymaking environment than at the domestic level" (Forbis and Hayhoe 2018). Final, to enhance and develop sustainable and long-term business relations and economic development in the Arctic, much prioritized by the Arctic states' national policies and strategies and according to the mission of the Arctic Economic Council.

These common interests and high stability would not be there in the post-Cold War Arctic without a joint understanding within the Arctic states of the value and importance of the high stability, and that the stability built on confidence (which is correspondingly based on cooperation) would be beneficial for all the parties (Heininen 2016; Byers 2017). This understanding, or 'Arctic consensus' (Zagorski 2017), is there even to that extend that there is rational thinking within the Arctic states how much each of them would lose, if anyone of them would damage the cooperation. Behind is 'spillover', the main idea of the process of functional cooperation that as states "become more embedded in an integration process, the benefits of cooperation and the costs of withdrawing from cooperative ventures increase." (Lamy et al. 2013). The short history of the post-Cold War Arctic supports this assertion by the theory of functionalism.

Correspondingly, before this cooperation started in the Arctic region there were a few features of Arctic geopolitics, as well as those of Arctic security, which can be interpreted to be preconditions for the current state of high geopolitical stability. They made functional cooperation (for environmental protection) possible and promoted the manmade trans-boundary cooperation, and thus also made the transformation possible in the first place. Later they put the Arctic states' governments carefully to consider the risk and costs if they would lose the high stability. Thus, they created opportunities for the Arctic states to recognize common interests and understand the benefits of them, and at the same time these features were strengthened. Among the features as preconditions for international cooperation and high geopolitical are: First, global nuclear deterrence of the two superpowers - the Soviet Union and the USA - as the original nature of the military and a legacy of the Cold War period. Second, that in the Arctic there were/are neither (armed) conflicts nor serious disputes on state sovereignty or disagreements of national borders between the Arctic states. Third, instead there was/is a high degree of international legal certainty in the Arctic, in particular meaning the UNCLOS and the legally-binding agreements under the auspices of the Arctic Council. Fourth, there were devolution and other soft ways of (the Nordic model of) governance, which were renewed and promoted by innovative legal and political arrangements (The Arctic Yearbook 2017; AHDR 2004). Final, the Arctic states have separated issue areas by leaving issues of 'high' politics out of the joint agenda of the Arctic Council (also Byers 2017), in particular that "the Arctic Council should not deal with matters related to military security" (a well-known foot-note in the Ottawa Declaration 1996). As a result, the agenda setting in the post-Cold War Arctic is flexible.

Following the common interests and the geopolitical features as prerequisites, it is possible - as well as there is a need for further research (Heininen forth-coming) - to recognize several special features of the post-post Cold War Arctic as potential new themes of Arctic geopolitics of the 2010s. The first special feature is that Arctic geopolitics

(consisting of traditional and new several factors of geopolitics), as well as Arctic security (including aspects of traditional, environmental and human security), are tightly connected with the environment. Following from this, geopolitics and security in the Arctic context are combined with each other, as the second feature. The third feature of Arctic geopolitics is 'exceptionalism', i.e. the high geopolitical stability of the post-Cold War Arctic based on the institutional cooperation between the Arctic states, and supported by the Arctic Council observer countries, makes the Arctic region exceptional in world politics and IR. Finally, the Arctic is globalized, and thus, the globalized Arctic can be interpreted as a new geopolitical context, which can be interpreted as a potential asset to reformulate a state of world politics with 'uncommon instability' (Heininen 2016).

DISCUSSION

From classical to critical geopolitics

Geopolitics is one of the so-called grand theories used in several disciplines, such as (Political) Geography, Strategic studies and IR. It deals with 'Geography', 'Politics' and 'Technology' with an emphasis on the interrelationships between them. 'Classical geopolitics', the original school of thoughts on geopolitics, as well as its sub-theories, is traditionally interpreted to deal with 'physical space', including natural resources, 'power' and a 'state'. In the focus, are the strategic value and control of a physical space, and the power and hegemony connected with a state (Dougherty and Pfaltzgraff, 1990). Here a 'state' refers to the institution of a nation / unified state as a political and administrative entity, or 'polity', as well as the unified state system. 'Power' means both 'might' of, and brute force by, a state, which is, if needed, guaranteed by "unilateral, national(istic), competitive, military power" (Newcombe 1986). In addition, 'technology' plays a relevant role here, as the technology models of geopolitics did in the Cold War Arctic emphasizing the importance of advanced (arms) technology (e.g., airplane, missile and submarine) (Heininen 1991).

Among implementations are the above-mentioned technology models, which emphasize the strategic importance, even determination of technology. They are interpreted to be the ultimate precondition – if advanced military technology allowed it to happen, it happened - for the militarization of the Arctic in the 2nd World War and the Cold War (Heininen 1991). The resources models emphasize the strategic importance of natural resources and potential race and emerging conflicts related to their utilization (Dalby 2002), as the other discourse of Arctic geopolitics states. Final, the so-called “Great Game” vision emphasizes the geostrategic importance of Central Asia very high and followed from this, even as determined, there was the hegemony competition of the major powers in the 19th and 20th centuries and partly still at the early-21st century.

These models/visions, as well as geopolitics in general, have largely been applied, as well as misused, in politics within the last hundred years. For example, the Nazi Germany used geopolitics, in particular geopolitical thinking interpreted by Friedrich Ratzel and Karl Haushofer, for its power politics and as an excuse to occupy new territories and resources, ‘Lebensraum’ (Dougherty and Pfaltzgraff 1990). This much ruined the reputation of geopolitics for decades, and was the reason why geopolitics became almost a taboo in science after the 2nd World War. Research on geopolitics was not, however, totally forgotten in the Cold War period, but applied in security and strategic studies, in particular dealing with the maritime strategies of the Soviet Union and the USA in the High North and Arctic waters (e.g. Posen 1987; Miller 1986), as well as arms control and disarmament in the Arctic (Heininen 1991). It was also applied in environmental studies by broadening the scope, for example with an ecological perspective (Dougherty and Pfaltzgraff, 1990). The environment was interpreted to be a geopolitical treat, when states collapse as a result of the explosion of demographic and environmental forces, that the degradation of natural environment causes migration, growth of urban areas, and the consequent disintegration and ethnic conflicts (Kaplan 2002).

Among major (sub)theories of classical geopolitics are the Heartland theory, the Seapower theory and that of Rimland: According to the Heartland theory of Mackinder (e.g. 1904), Russia can be interpreted, or even determined, to control the world, since it controls East Europe and the landmass of Eurasia (the ‘Heartland’). It is good to remember that at the time the Arctic Ocean was totally ice-covered and thus, made the huge landmass of Eurasia even bigger. Mahan’s Seapower theory (e.g. Mahan 1918) much challenges the Heartland theory and states that who controls, at least, two of the world oceans and has open access into two oceans, controls the world, as did the British Empire and the USA later (interestingly, the Arctic Ocean was neither taken into consideration nor defined as an ocean at the time). Not surprisingly, the USA still much emphasizes the freedom of seas, which is one of the reasons for the USA not to ratify the UNCLOS. Correspondingly, Spykman criticized Mackinder’s Heartland theory for overestimating the potential of the Heartland’s land mass (Dougherty and Pfaltzgraff 1990), and his Rimland theory (Spykman 1944) emphasizes the strategic importance of the ‘Inner Crescent’, i.e. the rimland between the heartland and the oceans from the Mediterranean to China. Spykman’s theory was a foundation for George Kennan’s ‘policy of containment’ of the Soviet Union, but it has not been applied to the Arctic region consisting of an ocean and two rimlands.

Based on these major theories geopolitics is much to study the spatialization of international politics by major powers and hegemonic states, which understands geopolitics to be concerned “the geography of international politics”, especially the relationship between the physical environment and the conduct of foreign policy (Tuathail and Agnew, 1992). Due to the narrow thinking of classical approach, importance of real issues and challenges, such as the environment, people(s) and climate change, were underestimated or neglected. This much sounds like power politics, or what is understood as ‘Realpolitik’, a traditional understanding of international politics and practice of diplomacy “based

on the assessment of power, territory, and material interests, with little concern on ethical realities" (Lamy et al. 2013).

Classical geopolitics was challenged in the 1990s by new and critical approaches that re-conceptualized the traditional definitions and interpretations. In the background was on the one hand, that classical geopolitics interpreted geopolitics as a determined dogma. Geopolitics and its traditional interpretations were not deeply analyzed but more copied from natural sciences, as a state "was seen as a living organism that occupies and that grows, contracts, and eventually dies", or at least as an aggregate-organism (Dougherty and Pfaltzgraff 1990). For example, not to consider the Arctic Ocean as an ocean, but only determined by sea ice, does not take into consideration changes in a nature, i.e. climate change, and that those changes, when they are rapid, have societal impacts and influence politics and policy-making. On the other hand, there was a shift in mindset and cultures due to globalization, as well as change in security premises due to pollution and the consequent environmental awakening, and their impacts to policy-shaping and policy-making.

Behind were also indicators of a transition into other kinds of more globalized systems, such as economic integration making 'geo-economics' strategic, regional or city states as new influential actors (with different interests as nation states), and later the social and economic systems based on the digital world developed with the internet (here the internet as a virtual reality can be seen as an emerging geopolitical space (Vuori, 2017)). These approaches made geopolitics a discursive practice by which to represent international politics as a 'world' characterized by particular types of places, peoples and dramas (Tuathail and Agnew, 1992). Geopolitics was (re)defined as human action not determined, since people give the meaning for 'geo' in social and political activities, they are actors, not 'geo' per se. Following from this, geopolitics could also be defined as a contest or fight, where the relation between geopolitical discourse and geopolitical rhetoric is important (Moisio, 2003).

All in all, redefinition of geopolitics occupied more room with new discourses, and 'new' and 'critical' schools of thought of geopolitics were established. It was the 1990s, when geopolitics had some sort of renaissance in research. For example, 'new geopolitics' as a school of thoughts is keenly related with the growing importance of 'Economics' per se, and economic integration, when after the end of the Cold War period economics took over geopolitics (Ohmae, 1995). Economic integration became more important in international politics and foreign policy, when national economies were not any more strictly regulated by states, influenced by new theories of economics, such as 'New liberalism', but opened for international markets run by trans-national financial and other companies.

The importance of geo-economics could also be seen in the 1990s among the Arctic states, when after the end of the Cold War the Nordic countries, first joined the European Economic Area (EEA) in 1994, and in 1995 Finland and Sweden joined the ECs / EU (Denmark had joined in 1973). As well as, when Canada and the USA, together with Mexico, established the North America Free Trade Area (NAFTA) in 1996. Or, when the Arctic states showed more interest towards economic activities in the Arctic by establishing joint ventures between Western and Russian companies dealing with exploitation of hydrocarbons in the Russian Arctic, and thus going beyond the geopolitical barriers of the Cold War. For example, there were several negotiations between Russian companies (e.g. Gazprom, Rosneft) and Western companies (e.g. Norsk Hydro, Conoco Inc., Total S.A., Neste Oy) about joint exploitation of oil and gas drilling ventures. The best known of them the Shtokman gas field "became a flagship name for Russian oil and gas development in offshore Arctic conditions. "This flagship status was related to the desire of the state to find new sources of economic stability..." (Goes, 2018). So, when internationally the Shtokman case was seen from the point of view of geo-economics and a part of new liberalism, nationally in Russia it was seen as a strategic resource base which

provides the means for the socio-economic development of the country.

These new discourses and approaches challenged, as well as problematized, the traditional approaches of geopolitics by having a general understanding that, in addition of physical space, technology and state power, there exit other factors, which deal with values, aims/goals and other immaterial things, as well as interrelations between different factors. Among them are 'social space', 'identity/ies' and 'knowledge', which come together with people(s), indicating that there are other actors as a state (Moisio 2003; Jukarainen 1999). As well as 'cooperation' and 'peace' as means how to change the existing facts and reach your aims. As a result, in addition of more traditional factors, new (immaterial and soft) factors, as well as new actors, were also recognized relevant to geopolitics, and that they - i.e. values and aims, their relations with theories and facts and their interrelations - should be taken into consideration, in particular how to change the facts to reach the values and aims.

Recent changes of Arctic geopolitics

Based on classical approach of geopolitics (e.g., the technology and resources models, etc..) and its major factors (e.g., physical space, power connected with a state) for the Arctic states – either the eight Arctic states (A8), or the five littoral states of the Arctic Ocean (A5) – sovereignty, power over resources and resource governance, and economic interests are still important. They do, however, also take into consideration fundamental changes in the Arctic and Arctic geopolitics due to globalization and global impacts, such as climate change, within the Arctic region. Indeed, climate change, and long-range pollution earlier, have clearly shown, even manifested, the strategic importance of the environment, and that it has become an important (new) geopolitical factor as a value with aims to change it (either via mitigation or adaptation) (Heininen 2013). One of the weaknesses of the traditional approach of geopolitics is a lack to recognize the environment as a value, and that quality

Table 1. Differences between 'Classical' and 'Critical' Geopolitics and Their Factors

'Classical' geopolitics:	'Critical' geopolitics:
<p>Traditional and narrow interpretation of 'Geo' + 'Politics';</p> <p>Reflects exploration, state sovereignty, hegemony and force;</p> <p>Factors: physical space + natural resources technology, power/force by the state (e.g. the Resource models and Technology models)</p> <p>Critical how power transformation happens: 12 times of 16 a war has occurred when a rising power defeat (Allison, 2017).</p>	<p>Goes beyond 'Realpolitik' and challenges mainstream thinking;</p> <p>Reflects sophisticated power and recognizes knowledge as power;</p> <p>Factors: in addition those of classical geopolitics identity/ies, images, knowledge, 'politicization' of physical space (the environment), and in addition of the state several actors (including people(s) and civil society).</p> <p>From classical geopolitics to critical geopolitics indicates and reflects the movement from determined, disciplinary theories towards different discourses and interpretations ('politicization' of physical space), from power politics to knowledge (wicked problems), from centralized to subsidiarity (devolution), from national to local and global (globalism), and from material to immaterial (digitalization).</p>

(of the environment) matters, in addition of interpreting the environment only as physical space with natural resources. The irony here is that geopolitics is defined as one of the major environmental theories (Dougherty and Pfaltzgraff 1990).

Unlike, critical geopolitics recognizes new factors, such as identities, knowledge, stability, as well as takes into consideration other actors, indigenous and other peoples, civil societies and sub-national governments, as well as their interests, are in focus. Based on that it is needed to have a more holistic and multi-dimensional approach and solid description of the twenty-first century's globalized Arctic region. Further, the multi-dimensional and multi-functional nature of Arctic geopolitics includes, for example, that there are more sophisticated factors and several actors with their identities have taken into consideration. Further, that identity matters and much deals with livelihoods, and that pollution impacts heavily and kills thousands, and that climate change threatens peoples' traditional livelihoods. This approach refers to critical geopolitics including the following aspects: first, to take into consideration rapid climate change and long-range pollution which together with an increase in extractive industries create a real wicked problem in the Arctic; second, based on the COP 21 Paris Agreement and the related pressure to reduce CO₂ emissions, freeze new investments in (offshore) oil and gas drilling (e.g. Shell's decision to withdraw from the Beaufort Sea) and develop renewable energy resources in the Arctic; third, to (re)define who are relevant (international) actors and stakeholders in Arctic geopolitics and regional (resource) development, and in particular what is the position of the Arctic states and state-related actors there.

Controversial or not, those traditional factors of geopolitics - physical space, natural resources, technology and power of a state - are still present and relevant in the Arctic and Arctic geopolitics: The Arctic is a geographical region with a unique ecosystem, large marine nature and ice covered seas. The Arctic is (still) interpreted as a resource storehouse due to its rich

natural resources, such as hydrocarbons and other minerals (USGS 2008), fishes and other marine animals, forests. Though it might sound as a cliché, this is the de facto reason for mass-scale utilization of resources, and that resource exploitation has been emphasized in the national strategies and policies of all Arctic states. Following from this, it is justified to argue that the resource models are still relevant and applied in the Arctic. The technology models are also relevant, though not emphasized in the national strategies. The heavy military structures, mostly nuclear weapon systems of Russia and the USA, are deployed in the region due to their global deterrence (Wezeman 2012), which is also a reason for no real nuclear disarmament, yet, in the Arctic.

Unlike, critical geopolitics recognizes several factors, and that there are several actors, which influence Arctic geopolitics. One of the new factors is an 'actor' per se, i.e. the fact that there are other actors as a/the 'state', people(s) and civil societies, and Indigenous peoples without their own state (Abele and Rodon 2007). The agent-based modeling emphasizes the importance of actors but forgets the importance of their interests, though actors always come with interests, and interests much deal with values. Indeed, the post-Cold War Arctic geopolitics is influenced by an increasingly dense network of transnational actors, including Indigenous peoples (organizations) energetically emphasizing their cultural and political identities and redefining sovereignty (Inuit Declaration 2009), sub-national governments in charge of regional development seeking collaboration both within and beyond national borders, NGOs with concerns and ambitions to shape the discourse, and academic communities producing knowledge, thus shaping our understanding of the region.

Closely related with (Indigenous) peoples and civil societies (geographical) knowledge is a format of power, which is relevant, and should take into consideration (Moisio, 2003). The more critical factor climate change, in particular its global nature, has become, the more important format

of power, or influence, knowledge on climate and the environment has become. Therefore, in Arctic research traditional or indigenous environmental knowledge (TEK) has already some time been recognized by Western science (Toyama Statement, 2016; Agreement of Science Cooperation, 2017). Following from this, power does not, any more, mean only 'hard' power, political or economic power and military force, and more importantly, there is influence, which can be transferred into power. Though the air is, every-now-and-then, full of mis- and disinformation, conspiracy theories, manipulation and falsification, and these are not only phenomena of the era of the internet and social media, power based on influence is more based on knowledge and communications. Finally, to have identity, knowledge and other immaterial values as geopolitical factors, as well as indigenous peoples as actors, there is a growing concern on a state (quality) of the environment and that of climate. As critical approaches of geopolitics, this means to politicize a physical space. Indeed, the post-Cold War Arctic is been highly politicized, though not re-militarized, by more soft and sophisticated

ways than was the militarization in the Cold War.

If in the 2nd WW geopolitics was misused, in the Arctic of the 2010s it is often misunderstood, in particular in media reports and also by policy-makers, and understood narrowly to mean traditional approach (classical) geopolitics. Fortunately, so far this has come with less harmful consequences causing mostly misinformation and confusion, though it has put the established international Arctic cooperation into a test. Actually, geopolitics influences, or the influence is seen in, the post-Cold War Arctic by several and different ways: from the presence of the nuclear weapon systems (as a legacy of classical geopolitics of the Cold War), and an emphasis on sovereignty by the littoral states of the Arctic Ocean (as a legacy of state and state power) to responses of non-state actors on a state of the environment (as an example of politicization of the Arctic region) and those of governments to new security threats (as an evidence of a shift in security premises) due to impacts of long-range pollution and global warming, as well as to growing global

Table 2. Major Stages of Arctic Geopolitics

Cold War's geopolitics:	Transition period's (1980s-1990s) geopolitics:	Post-Cold War's geopolitics:
<p>Dominated by militarization: the military (the nuclear weapon systems); technology, state hegemony and power game = mostly based on classical geopolitics.</p>	<p>Dominated by environmental degradation and transboundary cooperation: long-range pollution, nuclear accidents and growing concern on the environment; international cooperation on environmental protection and research; self-consciousness and circumpolar cooperation by Indigenous peoples = based on new and more critical approaches of geopolitics.</p>	<p>Dominated by climate change and hype of exploitation: pollution & rapid climate change (e.g. food safety); hype of mass-scale exploitation and increase of economic activities ('geoeconomics'); importance of state sovereignty and energy security; high geopolitical stability and firm transboundary cooperation (exceptional); scientific and traditional knowledge (on climate and environment) as a new format of power = based on critical geopolitics and globalism.</p>

interest towards, and influence in, the Arctic (as critical approaches of geopolitics).

In contrast to traditional approach, a comprehensive description with holistic approach of the twenty-first century's Arctic geopolitics includes comprehensive coverage of the approaches of both classical (Cold war) and critical (post-Cold war) geopolitics, i.e. "the history and identity of a 'geopolitical' Arctic and the contemporary triangle of Arctic geopolitics: rights, interests and responsibilities" (Raspotnik, 2016). For example, to (re)place the Arctic within the context of global multi-dimensional change, and explore worldwide implications would give a chance to define the global Arctic as a new geopolitical context. A state of Arctic geopolitics at the post-Cold War era is much with this kind of comprehensive approach including identities, rights and responsibilities, as well as (traditional) knowledge and stability-building (Heininen 2016).

CONCLUSIONS

At the early-21st century the Arctic region plays a key role in the global ecosystem and bio-geophysical processes that are heavily impacted by climate change and other global changes, and are closely integrated with current global economics and related energy security dynamics, as they relate to world politics. Long-range pollution was the first trigger, which caused a change in security premises and a paradigm shift, and made environmental protection as the first field of functional cooperation between the eight Arctic states. It was followed by the rapid warming of Arctic climate. These were wake-up calls to the Arctic states of growing concern on a state of the environment by non-state actors, such as indigenous peoples, (I)NGOs, scientists and scholars to start environmental cooperation. These were behind the first special feature of Arctic geopolitics from the point of view of critical approach of geopolitics.

Followed from the functional cooperation for environmental protection by the Arctic states, there was a significant change in

Arctic geopolitics from the confrontation of the Cold War period to transboundary cooperation at the 21st century. Due to this institutionalized Arctic cooperation there is high geopolitical stability and the region is neither overtly plagued by military conflicts nor disarmament, though the nuclear weapon systems of Russia and the USA are still been deployed there. International Arctic cooperation, under the auspices of the Arctic Council and between the Arctic states and the Arctic Council observer countries continues, so far, after passing a few tests of growing tension between Russia and the West, as well as the consequent sanctions and counter-sanctions. This exceptionalism is another special feature of Arctic geopolitics (from the point of view of critical approach of geopolitics).

Behind are on the one hand, common interests starting from the ultimate aim to decrease military tension and increase political stability using functional cooperation on environmental protection, due to pollution (in particular nuclear safety), and region-building as the main means. On the other hand, certain features of the Arctic were prerequisites for stability-building, such as the original global nature of the military, firm state sovereignty, high degree of legal certainty, and separation of certain issue areas, in particular that military-security, on the agenda of the Arctic Council. Followed from this, first conclusion of this article is that the high Arctic geopolitical stability is conscious and manmade (by the Arctic states). It also seems to be resilient, since it has passed a few tests, and big geopolitical changes, such as the self-governing status of Greenland, could be executed in a calm and peaceful manner with full agreement of a state and sub-national government.

Another conclusion, as well as a scientific finding, is that based on the common interests and the preconditions there are certain (existing or emerging) features of Arctic geopolitics: First, that geopolitics and security are tightly connected with the environment, and second that geopolitics and security are been combined with each other in the Arctic context. The third feature of Arctic geopolitics is that the Arctic is

globalized. The final one is that the high geopolitical stability, as a common interest of the Arctic states and their joint efforts to maintain it, makes the globalized, stable Arctic region exceptional in world politics and IR. This can be interpreted as a potential asset to (re)formulate world politics of turbulent times and with 'uncommon instability' and IR. These special features can

be interpreted as new themes, or trends, of the post-post Cold War's Arctic geopolitics. When to interpret them as trends, there is an opportunity for a paradigm shift in approaches of geopolitics, if to aim to change the facts in order to reach the values, i.e. how to understand politics and power and make peaceful transformation to happen. ■

REFERENCES

Abele F. and Rodon T. (2007). "Inuit Diplomacy in the Global Era: The Strengths of Multilateral Internationalism." *Canadian Foreign Policy*, (13)3 (2007), pp. 45-63.

Ackren M. (2014). "Greenlandic Paradiplomatic Relations." *Security and Sovereignty in the North Atlantic*. Basingstoke: Palgrave Macmillan, Palgrave Pivot, 42-61.

AHDR (2004). *Arctic Human Development Report, AHDR 2004*. Akureyri: Stefansson Arctic Institute.

The Agreement on Enhancing International Arctic Scientific Cooperation (2017). Signed on 11 May 2017 by the Arctic States.

Allison G. (2017). High stakes: Can Trump and Xi avoid war and strike a North Korea deal? *TIME*, April 17, 2017, pp. 8-9.

The Arctic Yearbook 2017 – "Change and Innovation in the Arctic: Policy, Society & Environment." Eds. by L. Heininen, H. Exner-Pirot & J. Plouffe. [online] Thematic Network on Geopolitics and Security, and Northern Research Forum. Available at: <http://www.arcticyearbook.com>

The Arctic Yearbook 2015 "Arctic Governance and Governing." Eds. by L. Heininen, H. Exner-Pirot and J. Plouffe. [online] Thematic Network on Geopolitics and Security, and Northern Research Forum. Available at: <http://www.arcticyearbook.com>

Borgerson S.G. (2008). "Arctic Meltdown: The Economic and Security Implications of Global Warming". *Foreign Affairs*, March/April 2008.

Byers M. (2017). Crises and international cooperation: an Arctic case study. *International Relations 2017*, Vol. 31(4) 375-402.

Byers M. (2013). *International Law and the Arctic*. Cambridge, UK: Cambridge Studies in International and Comparative Law.

Clifford R. (2017). How has cooperation in the Arctic survived Western-Russian geopolitical tension? Available at: <http://pagebuilder.arctic.arcpublishing.com/pb/voices/analysis/2017/01/04/how-has-cooperation-in-the-arctic-survived-western-russian-geopolitical-tension/>

Dalby S. (2002). "Environmental Security." *Borderlines*, Volume 20. Minneapolis: University of Minnesota Press.

Dougherty J.E. and Pfaltzgraff R.L. Jr. (1990). *Contending Theories of International Relations. A Comprehensive Survey*. Third Edition. USA: Harper Collins Publishers.

Fairbanks Declaration (2017). Fairbanks Declaration On the Occasion of the Tenth Ministerial Meeting of the Arctic Council. (mimeo)

Forbis R.Jr. and Hayhoe K. (2018). "Does Arctic Governance hold the key to achieving climate policy targets?" *Environmental Research Letters* 13 [online] (2018) 020201 Available at: <https://doi.org/10.1088/1748-9326/aaa359>

Goes M. (2018). An interview in a phone by L. Heininen in 8 March 2018. Personal notes.

Gorbachev M. (1987). The Speech in Murmansk at the ceremonial meeting of the occasion of the presentation of the Order of Lenin and the Glod Star Medal to the city of Murmansk, October 1, 1987. Moscow: Novosti Press Agency.

Harle V. (2003). "Onko kriittinen geopolitiikka kriittistä tiedettä? Muuttuva geopolitiikka. Eds. by V. Harle and S. Moisio. Tampere: Gaudeamus, pp. 17-35.

Heininen L. (forth-coming). "Special Features of Arctic Geopolitics – a potential asset for world politics?" *GlobalArctic Handbook*. Eds. by M. Finger & L. Heininen. Springer. (will be published in autumn 2018)

Heininen L. (2016). "Security of the Global Arctic in Transformation – Changes in Problem Definition of Security". *Future Security of the Global Arctic. State Policy, Economic Security and Climate*. Ed. by Lassi Heininen. Basingstoke: Palgrave Macmillan, Palgrave Pivot, 2016, pp. 12-34.

Heininen L. (2014). "Northern Geopolitics: Actors, Interests and Processes in the circumpolar Arctic." *Polar Geopolitics: Knowledges, Resources and Legal Regimes*. Edited by Richard C. Powell and Klaus Dodds. Edward Elgar: Cheltenham, UK and Northampton, Massachusetts, 2014, pp. 241-258.

Heininen L. (2013). "'Politicization' of the Environment: Environmental Politics and Security in the Circumpolar North." *The Fast-Changing Arctic: Rethinking Arctic Security for a warmer World*. Edited by Barry Scott Zellen. Calgary: University of Calgary Press, pp. 35-55.

Heininen, L. (2011). "Arctic Strategies and Policies - Inventory and Comparative Study." Akureyri: The Northern Research Forum & The University of Lapland. August 2011.

Heininen L. (2010). "Pohjoiset alueet muutoksessa – geopolitiittinen näkökulma (The High North in a Change – Geopolitical point of view)." *Politiikka 1 / 2010*, pp. 5-19.

Heininen L. (2004). "Circumpolar International Relations and Geopolitics." In: AHDR (Arctic Human Development Report) 2004. Akureyri: Stefansson Arctic Institute, pp. 207-225.

Heininen L. (1991). "Sotilaallisen läsnäolon ympäristöriskit Arktiksessa - Kohti Arktiksen säätelyjärjestelmää." Tampere Peace Research Institute. Research Report No. 43. Tampere: Tampereen yliopisto.

Heininen L. and Finger M. (2017). "The 'Global Arctic' as a New Geopolitical Context and Method." *Journal of Borderlands Studies*, 2017. [online] Available at: <https://doi.org/10.1080/08865655.2017.1315605> (downloaded at 05:37 04 December 2017)

Heininen L. and Southcott C., ed. (2010). *The Circumpolar North and Globalization*. Fairbanks: University of Alaska Press.

Heininen L., Sergunin A. and Yarovoy G. (2014). "Russian Strategies in the Arctic: Avoiding a New Cold War." The Valdai Discussion Club, Grantees Report. Moscow, Russia, September 2014. Available at: www.valdaiclub.com. Accessed on 22nd of October 2014.

Hoogensen Gjörv G., Bazely D.R., Goloviznina M. and Tanentzap A.J., eds. (2013). *Environmental and Human Security in the Arctic*. Tonbridge, Kent: Routledge and Eartscan from Routledge.

Inuit Declaration (2009). *A Circumpolar Inuit Declaration on Sovereignty in the Arctic*. adopted by the Inuit Circumpolar Council.

The Ilulissat Declaration (2008). *Arctic Ocean Conference – Ilulissat, Greenland, 27-29 May 2008*. (mimeo)

Iqaluit Declaration (2015). *On the occasion of the Ninth Ministerial Meeting of the Arctic Council*. Iqaluit, Canada, 24 April 2015. (mimeo)

Jukarainen P. (1999). "Norden is Dead - Long Live the Eastwards Faced Euro-North. Geopolitical Re-making of Norden in a Nordic Journal." *Cooperation and Conflict*, vol. 34(4), pp. 355-382. SAGE Publications.

Kaplan R.D. (2002). *The Coming Anarchy. Shattering the Dreams of the Post Cold War*. USA: Random House.

Keil K. and Knecht S., ed. (2017). *Governing Arctic Change. Global Perspectives*. London: Palgrave Macmillan.

Käpylä J. and Mikkola H. (2015). *On Arctic Exceptionalism. Critical reflections in the light of the Arctic Sunrise case and the crisis in Ukraine*. The Finnish Institute of International Affairs, FIIA Working Paper, April 2015.

Lamy S.L., Baylis J., Smith S., Owens P. (2013). *Introduction to Global Politics*. New York, Oxford: Oxford University Press. Second Edition.

Mackinder H.J. (1904). *The Geographical Pivot of History*. *The Geographical Journal*, Vol. XXIII. No. 4, April 1904, pp. 421-444.

Mahan A.T. (1918). *The Influence of Sea Power upon History 1660-1783*. Boston.

Miller S. (1986). *The Maritime Strategy and Geopolitics in the High North*. September 1986. (mimeo)

Moisio S. (2003). "Geopolitiikka kamppailuna". *Muuttuva geopolitiikka*. Eds. by V. Harle & S. Moisio. Tampere: Gaudeamus, pp. 93-109.

Murray R.W. and Nuttall A.D., ed. (2014). *International Relations and the Arctic. Understanding Policy and Governance*. Amherst, New York: Cambria Press.

Newcombe H. (1986). "Collective Security, Common Security and Alternative Security: A Conceptual Comparison." *Peace Research Reviews*, 10(3), pp. 1-8, 95-99.

NGP Yearbook 2011, "Sustainable Development in the Arctic region though peace and stability" (2012). *Nordia Geographical Publications, Volume 40: 4*. 2012. Tornio: Geographical Society of Northern Finland.

Ohmae K. (1995). *The End of the Nation State. The Rise of Regional Economics*. New York: The Free Press.

Ottawa Declaration (1996). Declaration on the Establishment of the Arctic Council. Ottawa, Canada – September 19, 1996. (mimeo)

Posen B. (1987). U.S. Maritime Strategy: a dangerous game. *Bulletin of Atomic Scientists*, Vol. 43. No. 7, September 1987, pp. 24-29.

Powell R.C. and Dodds K., ed. (2014) *Polar Geopolitics: Knowledges, Resources and Legal Regimes*. Cheltenham, UK and Northampton, Massachusetts: Edward Elgar.

Raspotnik A. (2016). *The European Union and its Northern Frontier: European Geopolitics and its Arctic Context*. PhD. Universität zu Köln, Deutschland.

Spykman N.J. (1938). Geography and Foreign Policy I. *The American Political Science Review*, Vol. 32, Issue 1.

Spykman N.J. (1944). *The Geography of Peace*. New York.

Steinberg P.E., Tasch J. and Gerhardt H., ed. (2015). *Contesting the Arctic, Politics and imaginaries in the Circumpolar North*. London: I.B. Tauris Publishers.

Toyama Conference Statement (2015). *Integrating Arctic Research: A Roadmap for the Future*. ASSW 2015 in Toyama, 30 April 2015. (mimeo)

Traufetter G. (2008). *The Battle for the North Pole. Melting Ice Brings Competition for Resources*. *Der Spiegel*, 19 September 2008.

Tuathail G.O. and Agnew J. (1992). "Geopolitics and discourse: practical geopolitical reasoning in American foreign policy." *Political Geography*, Volume 11, Issue 2, March 1992, pp. 190-204.

USGS (2008). 'Circum-Arctic Resource Appraisal: Estimates of Undiscovered Oil and Gas North of the Arctic Circle.' US Geological Survey Fact Sheet 2008-3049. July 2008, <http://www.eurasiareview.com>

Vuori A. (2017). "The emerging political space of the internet: Geopolitics in the digital world." Research Plan for a PhD studies (September 2017). University of Lapland. (mimeo)

Wezeman S.T. (2012). *Military Capabilities in the Arctic*. SIPRI Background Paper, March 2012.

The Yearbook of Polar Law Volume 5, 2013 (2013). Edited by G. Alfredsson, T. Koivurova and A. Stepien. Leiden-Boston: Martinus Nijhoff Publishers.

Zagorski A. (2017). "Arctic Consensus." *The Arctic Herald, Information & Analytical Journal*, 1(20). 2017, pp. 42-47.



Dr. Lassi Heininen is a Professor of Arctic Politics at University of Lapland (Finland) and Senior Research Scholar (associate) at IIASA (Austria). His research fields include IR, Geopolitics, Security Studies, Environmental Politics, Arctic Studies. Prof. Heininen teaches and lectures regularly abroad, and supervises MA and PhD students from different countries. Among his other recent academic positions are Visiting Professor at University of Akureyri (Iceland), Adjunct Professor at Trent University (Canada), Director of International Summer School in Karelia at Petrozavodsk State University (Russia), Holder of Foreign Experts Professorship at Tongji University (China). He is also Head of (UARctic-NRF) Thematic Network on Geopolitics and Security.

SPECIAL PEEEX SCIENCE CONFERENCE ISSUE

This special issue of the journal *Geography, Environment, Sustainability* includes the publications presented at the 3rd Pan-Eurasian Experiment (PEEX) Science Conference which was held on September, 19-22nd, 2017, in Moscow, Russia. The conference was hosted by Lomonosov Moscow State University, Faculty of Geography. More than 150 participants from 12 countries (Finland, China, Norway, Germany, Denmark, etc) took part in this event.

The Pan-Eurasian Experiment (PEEX) Program (www.atm.helsinki.fi/peex/) is an international, multi-disciplinary, multiscale bottom-up initiative (Kulmala et al. 2015, 2016; Lappalainen et al. 2016, 2017). The main scientific mission of the PEEEX Program is to understand large-scale feedbacks and interactions between the land-atmosphere-ocean continuum in the changing climate of northern high latitude and in China (Lappalainen et al. 2016). The Program was developed for integrating observational and modeling framework to identify different climate forcing and feedback mechanisms in the northern parts of the Earth system, and therefore enable more reliable predictions of future regional and global climate. Besides climate change–air quality issues, the PEEEX Program aims to provide a continuum from deep scientific understanding to socio-economic solutions (Kulmala et al. 2015).

Within the above scientific framework, the program of the 3rd PEEEX Science Conference included 23 sessions on various topics, such as urban air quality, the phenomenon of «heat Islands» in cities, natural hazards, environmental change and human health, arctic aerosols, remote sensing research and education. Altogether 181 abstracts were submitted; of which 113 (63%) represented atmospheric sciences, 24 (13%) ocean sciences, and 44 (24%) socio-economic disciplines, including political and epidemiological sciences, research infrastructures (12; 7%), and university science oriented education (5; 3%) (Lappalainen et al. 2018; this issue).

This issue of the journal contains 13 papers concerning different PEEEX scientific topics. The issue is opened by an overview of the first 5 years of the PEEEX Program operation and its future prospects (Lappalainen et al.). In the Section “Geography” Grigoriev and Frolova discuss some phenomena of the terrestrial water storage change and its impact on water balance over European part of Russia. The presentation of the National Atlas of the Arctic as a set of geographic, ecological, economic, historical-ethnographic, cultural, and social features is given by Kasimov et al. The Arctic topic is also concerned in the paper devoted to the problems of permafrost dynamics in the coastal zone of eastern-Asian sector of the Arctic (Pizhankova) as well as in the paper “Western Russian arctic coastal dynamics hydrometeorological forcing in XX-century and current state (Shabanova et al.). In the “Environment” Section two papers are devoted to evaluating methane emissions from thermokarst lakes in the southern tundra of Western Siberia (Kazantsev et al.) and from the Siberian Arctic Shelf (Pankratova et al.). The aerosol radiative and temperature effects in clear-sky conditions are discussed in (Chubarova et al.) using COSMO model. The Myslenkov et al. paper concerns long-term statistics of storms in the Baltic, Barents and White seas as well as

future climate projections for the Baltic sea. The role of PEEEX program and indicators for digitalization of sustainable development goals especially in the environmental field are discussed by Bobylev et al. in the "Sustainability" Section. Two papers of this issue are devoted to human health: "The human health effects due to continuous emissions from Severonikel smelters of the Kola Peninsula by Alexander Mahura et al. and "Influence of climatic factor on naturally determined diseases in a regional context" by Malkhazova et al. The Lassi Heininen paper concerns some aspects of the Arctic geopolitics from classical to critical approach. A few other papers, which had been presented at the 3-rd PEEEX Science Conference, will be published in the next issues of GES journal. ■

REFERENCES

Kulmala M., Lappalainen H.K., Petäjä T., Kerminen V-M., Viisanen Y., Matvienko G., Melnikov V., Baklanov A., Bondur V., Kasimov N., and Zilitinkevich S. (2016). Pan-Eurasian Experiment (PEEX) Program: Grant Challenges in the Arctic-boreal context. *J. Geography Environment Sustainability*, 2, pp. 5–18, DOI:http://dx.doi.org/10.15356/2071-9388_02v09_2016_01.

Kulmala M., Lappalainen H.K., Petäjä T., Kurten T., Kerminen V-M., Viisanen Y., Hari P., Bondur V., Kasimov N., Kotlyakov V., Matvienko G., Baklanov A., Guo H., Ding A., Hansson H-C., and Zilitinkevich S. (2015). Introduction: The Pan-Eurasian Experiment (PEEX) – multi-disciplinary, multi-scale and multi-component research and capacity building initiative. *Atmos. Chem. Phys.*, 15, 13085-13096, doi:10.5194/acp-15-13085-2015.

Lappalainen H.K., Petäjä T., Kujansuu J., Kerminen V-M., Shvidenko A., Bäck J., Vesala T., Vihma T., De Leeuw G., Lauri A., Ruuskanen T., Lapshin V.B., Zaitseva N., Glezer O., Arshinov M., Spracklen D.V., Arnold S.R., Juhola S., Lihavainen H., Viisanen Y., Chubarova N., Chalov S., Filatov N., Skorokhod A., Elansky N., Dyukarev E., Esau I., Hari P., Kotlyakov V., Kasimov N., Bondur V., Matvienko G., Baklanov A., Mareev E., Troitskaya Y., Ding A., Guo H., Zilitinkevich S., and Kulmalas M. (2014). Pan Eurasian Experiment (PEEX) - A research initiative meeting the Grand Challenges of the changing environment of the Northern Pan-Eurasian arctic-boreal areas. *Geography, Environment, Sustainability*, 2017, 7(2):13-48.

Lappalainen H.K., Kerminen V.M., Petäjä T., Kurten T., Baklanov A., Shvidenko A., Bäck J., Vihma T., Alekseychik P., Arnold S., Arshinov M., Asmi E., Belan B., Bobylev L., Chalov S., Cheng Y., Chubarova N., de Leeuw G., Ding A., Dobrolyubov S.A., Dubtsov S., Dyukare E., Elansky N., Eleftheriadis K., Esau I., Filatov N., Flint M., Fu C., Glezer O., Gliko A., Heiman M., Holtslag A.A., Hörrak U., Janhunen J., Juhola S., Järvi L., Järvinen H., Kanukhina A., Konstantinov P., Kotlyakov V., Kieloaho A.J., Komarov A.S., Kujansuu J., Kukkone I., Kyrö E., Laaksonen A., Laurila T., Lihavainen H., Lisitz A., Mahur A., Makshtas A., Mareev E., Mazon S., Matishov D., Melnikov V., Mikhailov E., Moisseev D., Nigmatulin R., Noe S.M., Ojala A., Pihlatie M., Popovicheva O., Pumpanen J., Regerand T., Repina I., Shcherbinin A., Shevchenko V., Sipilä M., Skorokhod A., Spracklen D.V., Su H., Subetto D.A., Sun J., Terzhevik A.Y., Timofeyev Y., Troitskaya Y., Tynkkynen V.P., Kharuk V.I., Zaytseva N., Zhang J., Viisanen Y., Vesala T., Hari P., Hansson H.C., Matvienko G.G., Kasimov N.S., Guo H., Bondur V., Zilitinkevich S., Kulmala M. Pan-Eurasian Experiment (PEEX): Towards holistic understanding of the feedbacks and interactions in the land-atmosphere-ocean-society continuum in the Northern Eurasian region. *Atmospheric Chemistry and Physics, European Geophysical Society (Germany)*, 2016, 16, c. 14421-14461

Lappalainen H.K., Altimir N., Kerminen V-M., Petäjä T., Makkonen R., Alekseychik P., Zaytseva N., Bashmakova I., Kujansuu J., Lauri A., Haapanala P., Mazon S., Borisova A., Konstantinov P., Chalov S., Laurila T., Asmi E., Lihavainen H., Bäck J., Arshinov M., Mahura A., Arnold S., Vihma T., Uotila P., de Leeuw G., Kukkonen I., Malkhazova S., Tynkkynen V.-P., Fedorova I., Hansson H.-C., Dobrolyubov S., Melnikov V., Matvienko G., Baklanov A., Viisanen Y., Kasimov N., Guo H., Bondur V., Zilitinkevich S. and Kulmala M. An overview of the first 5 years in operation and future prospects. This issue.

AUTHOR GUIDELINES

1. Authors are encouraged to submit high-quality, original work: scientific papers according to the scope of the Journal, reviews (only solicited) and brief articles.
2. Papers are accepted in English. Either British or American English spelling and punctuation may be used.
3. All authors of an article are asked to indicate their names (with one forename in full for each author, other forenames being given as initials followed by the surname) and the name and full postal address (including postal code) of the affiliation where the work was done. If there is more than one institution involved in the work, authors' names should be linked to the appropriate institutions by the use of 1, 2, 3 etc superscript. Telephone and fax numbers and e-mail addresses of the authors could be published as well. One author should be identified as a Corresponding Author. The e-mail address of the corresponding author will be published, unless requested otherwise.

EXAMPLE:

Ivan I. Ivanov¹, Anton A. Petrov^{1*}, David H. Smith²

¹University/Organization name, Street, City, ZIP-code, Country

²University/Organization name, Street, City, ZIP-code, Country

* **Corresponding author:** example@example.com

4. The GES Journal style is to include information about the author(s) of an article. Therefore we encourage the authors to submit their portrait photos and short CVs (up to 100 words).
5. Article structure should contain further sections:
 - Abstract.
 - Keywords (Immediately after the abstract, provide a maximum of 6 keywords, avoiding general and plural terms and multiple concepts (avoid, for example, 'and', 'of'). Be sparing with abbreviations: only abbreviations firmly established in the field may be eligible. These keywords will be used for indexing purposes.).
 - Introduction (State the objectives of the work and provide an adequate background, avoiding a detailed literature survey or a summary of the results.).
 - Material and methods (Provide sufficient details to allow the work to be reproduced by an independent researcher. Methods that are already published should be summarized, and indicated by a reference. If quoting directly from a previously published method, use quotation marks and also cite the source. Any modifications to existing methods should also be described.
 - Results (Results should be clear and concise.).
 - Discussion (This should explore the significance of the results of the work, not repeat them. A combined Results and Discussion section is often appropriate. Avoid extensive citations and discussion of published literature.).
 - Conclusions (The main conclusions of the study may be presented in a short Conclusions section, which may stand alone or form a subsection of a Discussion or Results and Discussion section.).
 - Acknowledgements (List here those individuals who provided help during the research and funds which provided financial support of your research.).
 - References (Make a list of references according to guidance provided below).
 - Appendices (If there is more than one appendix, they should be identified as A, B, etc.

Formulae and equations in appendices should be given separate numbering: Eq. (A.1), Eq. (A.2), etc.; in a subsequent appendix, Eq. (B.1) and so on. Similarly for tables and figures: Table A.1; Fig. A.1, etc.).

6. Sections and sub-sections shouldn't be numbered, but divided into sub-levels. If you would like to refer to a particular section, name it without any numbers (for example: see "Materials and methods")

7. Math equations should be submitted as editable text and not as images (use appropriate tool in text editor). Present simple formulae in line with normal text where possible and use the solidus (/) instead of a horizontal line for small fractional terms, e.g., X/Y. In principle, variables are to be presented in italics. Number consecutively any equations that have to be displayed separately from the text (if referred to explicitly in the text).

8. Figures and figure captions. Number the illustrations according to their sequence in the text. Regardless of the application used, when your figure is finalized, please 'save as' or convert the images to one of the following formats: TIFF, JPG. Supply files that are optimized for screen use. **The resolution should be at least 300 dpi.** Besides inserting figures into your manuscript, you must also upload appropriate files during paper submission. Ensure that each illustration has a caption. A caption should comprise a brief title (not on the figure itself) and a description of the illustration beginning from "Fig. 1..." (note: no any dots in the end of the capture!). Keep text in the illustrations themselves to a minimum but explain all symbols and abbreviations used.

Example of referring to the figure in text: (Fig. 1)

Example of figure caption: Fig. 1. The distribution of the family Monimiaceae

9. Tables. Please submit tables as editable text and not as images. Tables can be placed either next to the relevant text in the article, or on separate page(s) at the end. Number tables consecutively in accordance with their appearance in the text, place table caption above the table body and place any table notes below the body. Be sparing in the use of tables and ensure that the data presented in them do not duplicate results described elsewhere in the article. Please avoid using vertical rules and shading in table cells.

Example of table caption: Table 1. Case studies and used methods

10. The optimum size of a manuscript is about 3,000–5,000 words. Under the decision (or request) of the Editorial Board methodological and problem articles or reviews up to 8,000–10,000 words long can be accepted.

11. To facilitate the editorial assessment and reviewing process authors should submit "full" electronic version of their manuscript with embedded figures of "screen" quality as a **PDF or DOC file.**

12. We encourage authors to list three potential expert reviewers in their field. The Editorial Board will view these names as suggestions only.

13. Original reviews of submitted manuscripts remain deposited for 3 years.

SCIENTIFIC AND PRACTICAL PEER-REVIEWED JOURNAL “GEOGRAPHY, ENVIRONMENT, SUSTAINABILITY”

No. 01 (v. 11) 2018

FOUNDERS OF THE MAGAZINE: Russian Geographical Society, Faculty of Geography, Lomonosov Moscow State University and Institute of Geography of the Russian Academy of Sciences

The magazine is published with financial support of the Russian Geographical Society.

The magazine is registered in Federal service on supervision of observance of the legislation in sphere of mass communications and protection of a cultural heritage. The certificate of registration: ПИ № ФС77-67752, 2016, December 21.

PUBLISHER

Russian Geographical Society
Moscow, 109012 Russia
Novaya ploshchad, 10, korp. 2
Phone 8-800-700-18-45
E-mail: press@rgo.ru
www.rgo.ru/en

EDITORIAL OFFICE

Lomonosov Moscow State University
Moscow 119991 Russia
Leninskie Gory,
Faculty of Geography, 1806a
Phone 7-495-9391552
Fax 7-495-9391552
E-mail: ges-journal@geogr.msu.ru
www.ges.rgo.ru

DESIGN & PRINTING

Agency «CONNECT»
Moscow, 117452,
Artekovskaya str., 9, korp. 1
Phone: +7 (495) 955-91-53
E-mail: info@connect-adv.ru

Sent into print 30.03.2018
Order N gi118

Format 70 ½ 100 cm/16
15,76 p. sh.
Digital print
Circulation 95 ex.